Ilze Apine

ORCID 0000-0001-9425-7568

Magnetic resonance enterography in the diagnosis of Crohn's disease using diffusion-weighted imaging with background body signal suppression (DWIBS) sequence

Doctoral Thesis for obtaining a doctoral degree (*PhD*)

Sector – Clinical Medicine

Sub-Sector – Radiology

Supervisor of the Doctoral Thesis:

Dr. med., Dr. habil. med. Professor **Gaida Krūmiņa,** Rīga Stradiņš University

Scientific Advisor:

Dr. med. Professor **Juris Pokrotnieks,** Rīga Stradiņš University

Riga, 2020

Anotācija

Promocijas darbā "Magnētiskās rezonanses enterogrāfija (MRE) Krona slimības diagnosticēšanā, izmantojot difūzijas uzsvērto attēlu ar ķermeņa fona signāla nomākšanas (*diffusion-weighted imaging with background body signal suppression – DWIBS*) sekvenci", tiek apskatīta Krona slimības (KS) diagnosticēšana un terminālā ileīta aktivitātes novērtēšana, izmantojot uzsvērto attēlu ar ķermeņa fona signāla nomākšanas (*DWIBS*) sekvenci.

Darba mērķis bija izvērtēt *DWIBS* sekvences iespējamās priekšrocības Krona slimības magnētiskās rezonanses diagnostikā bez iepriekšējas pacienta zarnu trakta sagatavošanas un *ileum* terminālajā cilpā lokalizētas KS aktivitātes noteikšanā. Darbā ir iekļauti dati, kas iegūti no 106 pieaugušiem pacientiem bez klīniskām, laboratoriskām un radioloģiskām iekaisīgas zarnu slimības pazīmēm, kā arī no 5 pieaugušiem pacientiem un 12 bērniem ar pierādītu *ileum* terminālajā cilpā lokalizētu KS.

Darbā analizēti līdz šim nepietiekami pētītie difūzijas uzsvērto attēlu (*Diffusion-Weighted Imaging – DWI*) aspekti – difūzijas ierobežojuma kvantitatīvs novērtējums zarnu sieniņās bez iepriekšējas tievo un resno zarnu sagatavošanas, kā arī KS skartas zarnas sieniņu difūzijas ierobežojuma kvantitatīva noteikšana, izmantojot šķietamo difūziju koeficientu (*Apparent diffusion coefficient – ADC*). Pētījuma mērķis bija novērtēt *DWIBS* sekvences iespējamās priekšrocības un ieguvumus, izmantojot neselektīvo tauku signāla nomākšanas tehniku *STIR* (*Short T1 inversion recovery* – inversijas atjaunošanās ar īsu T1 laiku), to salīdzinot ar klasisko *DWI* sekvenci ar selektīvo tauku slāpēšanas tehnoloģiju *SPIR* (*Spectral pre-saturation with inversion recovery* – spektrālā piesātināšana ar inversijas atjaunošanos).

Pētījumā klasiskajai *DWI* sekvencei ar selektīvo *SPIR* tehniku salīdzinājumā ar *DWIBS* sekvenci tika konstatēti statistiski nozīmīgi labāki rezultāti. Rezultāti parādīja, ka, neraugoties uz uzlabotu izšķirtspēju un kvalitatīvi labāku iekaisīgi izmainīto zonu attēlojumu, *DWIBS* sekvence nav piemērota ne kvantitatīvai KS diagnosticēšanai bez pacienta iepriekšējas sagatavošanas, ne slimības aktivitātes izvērtējumam. Pētījumā arī tika konstatēts, ka arī klasiskās *DWI* sekvences *ADC* vērtību mērījumi nav piemēroti KS kvantitatīvai izvērtēšanai pacientiem bez iepriekšējas zarnu trakta sagatavošanas ar hiperosmolāru perorālu kontrastvielu.

Pētījuma ietvaros tika izstrādāti ieteikumi par *DWI* sekvenču tauku supresijas tehnikas izvēli *ileum* terminālajā cilpā lokalizētas KS aktivitātes izvērtēšanā, kā arī par *ADC* mērījumu piemērotību KS kvantitatīvai diagnostikai, veicot MRE izmeklējumus bez iepriekšējas pacienta zarnu trakta sagatavošanas.

Annotation

The Doctoral Thesis “Magnetic resonance enterography in diagnosis of Crohn’s disease using diffusion-weighted imaging with background body signal suppression (DWIBS) sequence” deals with diagnosis of terminal ileitis and evaluation of activity using the DWIBS sequence.

The aim of the Thesis is to evaluate possible advantages of DWIBS sequences in diagnosis of Crohn’s Disease (CD), without prior preparation of the bowel and evaluation of the activity of CD localised in the terminal *ileum*. The Thesis includes data gathered from 106 adult patients without any clinical, laboratory-based or radiological evidence of the inflammatory bowel disease, as well as 5 adult patients and 12 children with proven CD localised in the terminal *ileum*.

The dissertation analyses the hitherto insufficiently studied aspects of diffusion-weighted imaging (DWI) (quantitative evaluation of diffusion restriction in bowel walls of patients without prior preparation of small and large intestines), as well as the application of quantitative evaluation of diffusion restriction in CD using apparent diffusion coefficients (ADC). The scope of the research was to estimate potential advantages and benefits of the DWIBS sequence using the non-selective fat suppression technique STIR (inversion recovery with a short T1 time) over the conventional DWI sequence with the spectrally selective fat suppression technique SPIR (spectral pre-saturation with inversion recovery).

The study found that the performance of the DWIBS sequence statistically significantly lags behind the conventional DWI sequence with the spectrally selective SPIR fat signal suppression technique. The results showed that despite improved resolution and qualitatively better representation of inflamed areas, the DWIBS sequence is not reliable for both quantitative diagnosis of CD without prior preparation of the patient and evaluation of disease activity using ADC measurements.

Within the framework of the research, recommendations have been developed on the choice of fat suppression technique for DWI sequences for evaluating activity of Crohn’s disease, located in the terminal ileum, as well as on the suitability of ADC measurements for quantitative diagnosis of CD by MRE without prior preparation of the patient's intestinal tract.

Content

Abbreviations

ADC – Apparent diffusion coefficient

ADC-DWIBS – ADC based on DWIBS fat suppression technique

CA – Contrast agent

CD – Crohn's disease

CDEIS – Crohn's disease endoscopic index of severity

CHESS – (Chemical shift selective fat suppression)

CI – Confidence interval

CNR – Contrast-to-noise ratio

DWI – Diffusion-weighted imaging

DWI_{SPIR} – DWI with SPIR fat suppression technique

ADC-DWI_{SPIR} – ADC based on DWI_{SPIR}

ADC-DWIBS – ADC based on DWIBS

DWI-MaRIA – Magnetic resonance index of activity based on DWI

DWIBS – Diffusion-weighted imaging with background body signal suppression

ECCO – European Chron's and Colitis Organisation

ESGAR – European Society of Gastrointestinal and Abdominal Radiologists

Gd – Gadolinium

IBD – Inflammatory bowel disease

IR – Inversion recovery

i/v – intravenous

MaRIA – Magnetic resonance index of activity

MR – Magnetic resonance

MRE – Magnetic resonance enterography

MRI – Magnetic resonance imaging

RCE – Relative contrast enhancement

RF – Radiofrequency

ROI – Region of interest

SD – Standard deviation

SD-*post*Gd – Standard deviation in the T1 weighted images after gadolinium contrast administration

SD-*pre*Gd – Standard deviation in the T1 weighted images before gadolinium contrast administration

SI – Signal intensity

SNR – Signal-to-noise ratio

SPAIR – Spectral attenuated inversion recovery

SPIR – Spectral pre-saturation with inversion recovery

STIR – short T1 inversion recovery

TI – Inversion time

WSI – Wall signal intensity

WSI-*post*Gd – Wall signal intensity after gadolinium contrast administration

WSI-*pre*Gd – Wall signal intensity before gadolinium contrast administration

Introduction

Topicality, novelty and practical implications of the study

Crohn's disease (CD) is a chronic idiopathic inflammatory bowel disease which can affect any part of the digestive tract, and is characterised by unpredictable periods of exacerbation and remission (Gajendran et al., 2018). Globally, the incidence of CD has increased markedly in both paediatric and adult patients over the past 50 years (Molodecky et al., 2012; Barnes and Kappelman, 2018). Although mortality from CD is relatively low, several manifestations of CD, such as chronic inflammation, fistulae, stricture, and abscess formation, impair patients' quality of life. As a result of CD progression, up to 80 % of cases require surgical resection of the inflamed intestinal zone, and in more than 10 % of cases a stoma is required (Cosnes et al., 2011). The progression of CD can be prevented only by an active therapeutic approach (Dulai et al., 2015; Torres et al., 2020), based on both timely primary diagnosis of the pathology and dynamic follow-up. Today, there is still no common "gold standard" in diagnosis of inflammatory bowel disease (IBD), and CD is diagnosed by combining endoscopic, histological, radiological examinations and/or laboratory tests (Panes et al., 2013; Tontini et al., 2015).

In diagnosis of CD, the method of choice is videocolonoscopy with morphological analysis of tissue specimen. However, its initial diagnosis and follow-up can be complicated, as this method allows visualisation of only a limited part of the small intestine and selective evaluation of mucosa. With the help of video capsule endoscopy in the case of non-obstructive mucosa CD, the entire length of the small intestine can be assessed (Wang et al., 2013); however, this method does not allow obtaining tissue samples for morphological analysis. Relying solely on endoscopic imaging techniques may lead to incomplete diagnosis of full-scale changes, especially due to strong regenerative capacity of the intestinal mucosa (Okamoto, 2011; Shimizu et al., 2019) and the possible presence of inflamed or fibrotically altered subcutaneous mucosa, as well as deeper localised tissues (Sankey et al., 1993; Surawicz et al., 1994; Martin et al., 2012; Magro et al., 2013; Gajendran et al., 2018). Endoscopic examination methods do not always provide an objective picture of the depth and extent of inflammation in CD; however, accurate assessment of changes is very important. In cases of newly diagnosed CD, it is important to start appropriate treatment in time, and in pre-diagnosed cases it is important to make objective judgements about the effectiveness of treatments and prescribe the right medication. For this purpose, a method of visual diagnostics is needed, which provides relief to the intestinal wall and allows evaluation of any transmural changes.

Due to the high resolution of MR, excellent soft tissue contrast, and the designed dynamic post-contrast series, magnetic resonance imaging (MRI) is the most optimal and promising method for assessment of intestinal wall pathologies without exposing patients to potentially carcinogenic ionising radiation (Martin et al., 2012; Masselli and Gualdi, 2012; Smith et al., 2012). In 2019, cross-sectional imaging methods, including magnetic resonance enterography (MRE), have been recognised for the first time as an alternative to endoscopy for assessment of CD activity in guidelines issued by the *ECCO* (*European Chron's and Colitis Organisation*) and *ESGAR* (*European Society of Gastrointestinal and Abdominal Radiologists*) (Maaser et al., 2019). According to the *ECCO-ESGAR* guidelines on imaging methods for assessment of CD, in intestinal MRI, the T1 dynamic series with intravenous (i/v) gadolinium (Gd)-containing contrast agent (CA) is mandatory (Panes et al., 2013), being the basis of the only validated magnetic resonance activity index MaRIA (Magnetic resonance index of activity*)*. However, multiple administrations of Gd CA have been associated with the development of serious complications such as systemic nephrogenic fibrosis (Schlaudecker and Bernheisel, 2009), as well as the formation of Gd deposits in the basal ganglia and soft tissues of the brain (Gibby W. and A., 2004; Daram S. and B., 2005; Koreishi A., Nazarian R., Saenz A., Klepeis V., McDonald A., Farris A., Colvin R., Duncan L., Mandal R., 2009; Gulani et al., 2017; Quattrocchi and van der Molen, 2017). Thus, it is important to design and develop solutions for clinical abdominal radiology that would replace the administration of i/v Gd-containing CA during MRI scanning.

With the development of magnetic resonance (MR) technologies, diffusion-weighted imaging (DWI) sequences have been an indispensable part of the MRE protocol over the last decade (Choi et al., 2016; Dohan et al., 2016). In the DWI sequence, the tissue contrast is based on differences in movements of water molecules in different tissues (Chilla et al., 2015). DWI images highlight normal hypercellular tissues and provide information on tissues with diffusion limitation, i.e., inflammatory changes, including abscesses, and benign and malignant formations (Luna, 2012). The DWI sequence is able to identify pathological changes before they appear in conventional MR images (Baliyan et al., 2016). Studies show that limited diffusion in the intestinal wall correlates with areas of active disease in histological preparations (Anupindi et al., 2013). DWI is a useful sequence for both identification of inflammatory bowel segments and evaluation of inflammatory activity and treatment efficacy (Stanescu-Siegmund et al., 2017). The sensitivity of DWI sequences to differentiate inflammatory changes, outperforms the T1 dynamic series with i/v administration of Gd CA (Oto et al., 2011; Neubauer et al., 2013; Sirin et al., 2015). Thus, it can be assumed that in CD diagnosis, the DWI sequence is more informative than the T1 post-contrast series. It more realistically reflects the actual

extent of the inflammatory process and has the potential to replace i/v administration of CA, not only in the initial diagnosis of CD, but also when evaluating inflammatory activity in pre-diagnosed CD (Buisson et al., 2013; Hordonneau et al., 2014) using DWI-based MaRIA, called Clermont score. The diffusion restriction found in DWI images can be assessed both qualitatively and quantitatively, using the apparent diffusion coefficient (ADC) expressed in mm^2/s. ADC values for inflamed intestinal walls have been shown to be $0.8–2.4 \times 10^{-3}$ mm^2/s lower than unchanged intestinal wall ADC values (Dohan et al., 2016). Although the addition of a DWI sequence to a range of traditional MRE protocols increases the overall sensitivity and specificity of the method (Kim et al., 2015), the specificity of the DWI sequence, when used alone, is low at 39–61 % (Qi et al., 2015; Choi et al., 2016). To date, there is no single MRE algorithm for patients with suspected IBD, including DWI sequences.

DWI image acquisition is complex and based on difficult physical processes that result in various image distortions (Sánchez-González and Lafuente-Martínez J., 2012; Drake-Pérez et al., 2018). To prevent them, DWI protocols incorporate one of the fat signal suppression techniques (Javier Sánchez-González, 2012). They can suppress the resonant signal from fat, both selectively and non-selectively. Selective fat signal, or spectral, suppression (hereinafter – spectrally selective fat suppression) techniques, suppress only the fat resonant frequency spectrum. Examples of spectrally selective fat suppression techniques, are CHESS (Chemical shift selective fat suppression), SPAIR (Spectral attenuated inversion recovery) and SPIR (Spectral pre-saturation with inversion recovery) (Del Grande et al., 2014; Indrati, 2017). A disadvantage of spectrally selective fat suppression techniques are the artifacts caused by magnetic field heterogeneity (Del Grande et al., 2014; Moore et al., 2014).

One of the newest and most clinically relevant derivatives of the DWI sequence is DWIBS – diffusion-weighted imaging with background body signal suppression. It was developed in 2004 by a research team at Tokai University School of Medicine, led by Taro Takahara, in order to examine oncology patients and obtain whole-body images to identify tumour recurrences and metastases (Takahara et al., 2004). It is currently widely used in diagnosis of inflammatory changes, abscesses, intravascular thrombi, as well as in visualisation of peripheral nerves (Kwee et al., 2009). The DWIBS sequence includes the non-selective fat suppression technique STIR (Short T1 inversion recovery). Unlike spectrally selective fat suppression based on suppression of the fat resonant frequency spectrum, STIR technique is based on the differences between the T1 relaxation times of fat and water protons, as scanning suppresses the signal from the fat tissue with short T1 time, similar to the fat tissue (Horger, 2007). The DWIBS sequence is intended for scanning with the patient breathing freely. In order to compensate for movements, it allows for the simultaneous excitation of multiple scan slices,

and the reading of signals over a long period of time (Takahara et al., 2004). DWI with the non-selective STIR fat suppression technique provides a sustained and homogeneous fat suppression in large areas of the body (Takahara et al., 2004; Moore et al., 2014), including sites located on the periphery of the body (Del Grande et al., 2014), providing higher contrast-to-noise ratio (CNR) (Kwee et al., 2009). The non-selectivity of the STIR technique may be a disadvantage in cases where tissues contain other substances with short T1 time, such as methaemoglobin, mucus-containing and viscous substrate, protein, and melanin (Del Grande et al., 2014). Another disadvantage of STIR fat suppression is the reduced signal-to-noise ratio (SNR) with partial loss of proton signal during inversion (Kwee et al., 2008b), which causes noise in the images. There is also literary data on the analysis of ADC values based on DWI with STIR fat suppression. The sequence of DWI with STIR has been shown to be superior to DWI with spectrally selective fat suppression in the diagnosis of malignant and benign breast processes (Stadlbauer et al., 2009). It has also been reported that ADC values of the DWIBS sequence are not affected by motility (Stone et al., 2012), which could be an important factor in the study of peristaltic intestines.

Similarly to the conventional DWI with spectrally selective fat suppression (hereinafter – conventional DWI), the DWIBS sequences can very accurately differentiate the intestinal sections affected by CD, and despite the noise in the images, DWIBS images can more accurately visualise small structures such as lymph nodes, and the intestinal wall contours are sharper (Fig. 1). Judging by the ability of the conventional DWI sequence to diagnose inflammatory processes in the intestinal wall with high sensitivity, and considering the advantages of the DWIBS sequence (increased CNR), this sequence could be promising in the diagnostics of CD. However, there is no literary data on its use in patients with CD, and comparison with conventional DWI sequences so far.

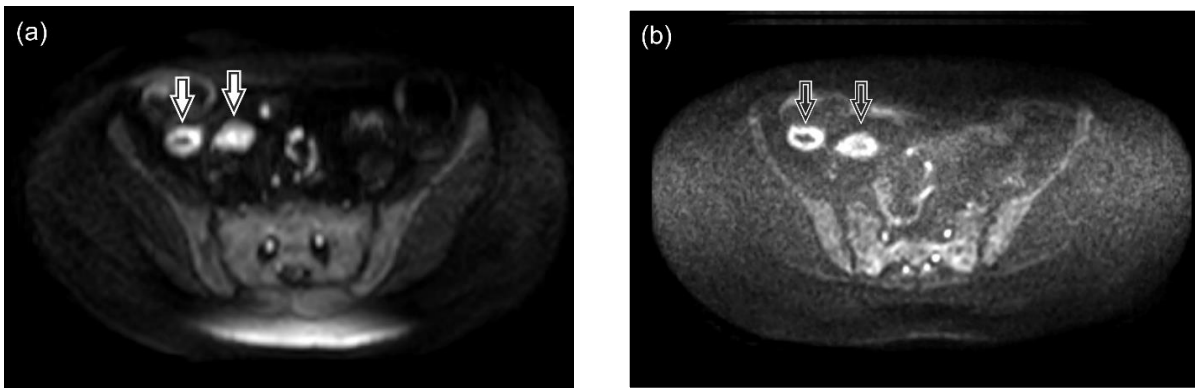

Figure 1. **Tracking images of the conventional DWI sequence with the spectrally selective SPIR fat suppression technique (a) and DWIBS (b) with a b value of 800 s/mm^2 in a 56-year-old patient with active CD in the terminal *ileum* loop**

There is a high signal intensity (SI) in the wall of the inflamed intestinal segments, indicating a diffusion restriction within this localisation. Despite the reduced SNR, resulting in grainy images, compared to the conventional DWI sequence (white arrow), the image of the inflamed intestinal wall in the DWIBS sequence is clearer (black arrow). Images from the Author's archive.

There are two directions currently in theory in which, by improving the visualisation capabilities of DWI, the diagnostic capabilities of CD would expand:

1) **Primary diagnosis of CD.** MRE examination still requires prior preparation of a patient with an oral CA, which limits the use of this method to patients requiring general anaesthesia. There is evidence in literature that MRI without prior patient preparation in the diagnosis of intestinal wall inflammation cannot replace MRE, but the possibilities of DWI to perform MRI without patient preparation have not been fully explored so far, as the published data is based only on visual evaluation of DWI, without performing quantitative measurements.

2) **Evaluation of CD activity.** By replacing the post-contrast MRI series required to assess CD activity using the CD activity index MaRIA (Dohan et al., 2016; Ordás et al., 2019) based on relative contrast enhancement (RCE), the use of the Clermont score, or DWI-based MaRIA, is becoming relevant.

To date, there are no publications on selection of specific DWI sequences in MRI diagnostics of CD; however, given the benefits of DWIBS, this sequence may have a greater potential to characterise intestinal wall inflammation in situations where accurate diagnosis of DWI is not possible; it also allows for a more accurate reflection of the activity of the inflammatory process.

Hypothesis of the study

The DWIBS sequence has advantages, and it is superior in the diagnosis of intestinal wall inflammation when compared to conventional DWI sequences with spectrally selective fat suppression.

Aim of the study

To compare the performance of conventional DWI sequence with spectrally selective SPIR (DWI_{SPIR}) and DWIBS – the DWI sequence with the non-selective STIR – in the primary diagnosis of CD without prior peroral preparation of the patient's intestinal tract, and in the quantitative assessment of active CD in the terminal *ileum*.

Tasks of the study

1. To evaluate potential advantages of the DWIBS sequence over conventional DWI for examining patients without prior peroral preparation with osmotically active enteric CA, by studying the ADC values of conventional DWI and DWIBS prior to and post preparation of the patient's intestinal tract in patients without evidence of CD.

2. To evaluate the suitability of the DWIBS sequence used in the Clermont index for the evaluation of CD activity in comparison with the conventional DWI sequence, by evaluation of mutual correlations between the Clermont scores obtained from conventional DWI and DWIBS with the MaRIA, between the ADC values of conventional DWI and DWIBS with the MaRIA, and between the ADC values of the conventional DWI sequence and the ADC values of the DWIBS sequence in patients with radiological features of active CD, localised in the terminal *ileum*.

3. To study the repeatability of ADC measurements of the conventional DWI and DWIBS sequences, in patients with active CD in the terminal *ileum*.

Novelty of the research

This is the first research to focus on the DWIBS, in the diagnosis and the evaluation of CD activity. This is also the first research to quantify the effect of prior intestinal tract preparation on ADC values of bowel walls in diffusion-weighted images.

Publications

The present PhD thesis is based on the following three manuscripts:

I The Influence of Bowel Preparation on ADC Measurements: Comparison between Conventional DWI and DWIBS Sequences
Ilze Apine, Monta Baduna, Reinis Pitura, Juris Pokrotnieks and Gaida Krumina
Medicina 2019, 55, 394; doi:10.3390/medicina55070394

II Comparison between Diffusion-Weighted Sequences with Selective and Non-Selective Fat Suppression in the Evaluation of Crohn's Disease Activity: Are They Equally Useful?
Ilze Apine, Reinis Pitura, Ivanda Franckevica, Juris Pokrotnieks and Gaida Krumina
Diagnostics 2020, 10, 347; doi:10.3390/diagnostics10060347

III Repeatability of Magnetic Resonanse Measurements Used for Estimating Crohn's Disease Activity
Ilze Apine, Ieva Pirksta, Reinis Pitura, Juris Pokrotnieks, Ieva Pukite, and Gaida Krumina
Proceedings of the Latvian Academy of Sciences. Section B. Volume 74 (2020), No 2 (725), pp.75-82; *doi: https://doi.org/10.2478/prolas-2020-0012*

The full copies of manuscripts are enclosed in the section Supplements.

1. Literature

1.1 General characterisation of Crohn's Disease

Crohn's disease (CD) is an idiopathic chronic relapsing transmural and segmental inflammatory bowel condition, which tends to develop fistulae, abscesses and strictures (Dulai et al., 2015). The digestive tract can be affected throughout its entire length (Gajendran et al., 2018). Although CD may develop at any age, the most common age for diagnosis is between 15 and 30 years (Rajesh and Sinha, 2014; Boyapati et al., 2015). CD has high complication rates (Yoon et al., 2015), requiring surgical treatment upon progression (Cosnes et al., 2011; Sakuraba et al., 2014). Approximately half of CD patients require surgery within 10 years following diagnosis, and 35 % needs a second resection within the following ten years (Ma et al., 2017). CD results in a negative impact on patients' quality of life (Lönnfors et al., 2014).

CD most commonly affects the terminal *ileum* and *caecum* (55 %). The locations less affected are other small bowel areas (11–48 %), the colon (19–51 %), and a combination of the small and large intestine (26–48 %) (Goetsch et al., 2017). Extraintestinal symptoms of CD related to intestinal inflammatin include skin involvement (10–15 %, mainly erythema nodosum and puyoderma gangrenosum), ocular inflammation (1.6–4.6 %, mainly episcleritis and uveitis), spondylarthropathy (5–20 % – peripheral arthritis and axial arthropathy – ankylosing spondylitis and sacroileitis), osteoporosis and osteoopenia (23–59 %), oral manifestations (mainly oral aphthous stomatitis – 5–10 %), and primary sclerosing cholangitis (1.6–7.4 %). In children, CD can cause growth impairment (80 %) (Jose and Heyman, 2008). Prolonged persistence of CD may also be associated with the development of small bowel adenocarcinoma (Lichtenstein et al., 2018).

The typical presentation of CD is abdominal pain, fever, bloody or non-bloody diarrhoea, and weight loss. In children, CD may present with failure to thrive, growth restriction and delayed puberty (Laass et al., 2014).

As a chronic relapsing course of disease, CD may have periodical exacerbations and remissions throughout a patient's life. This means that patients with CD will have a greater need for repeated diagnostic tests, endoscopical and radiological examinations throughout their lives, to confirm or refuse the presence of the disease, to diagnose early relapse and assess their response to treatment. According to the *ECCO-ESGAR* consensus guidelines, the disease should be kept under control with mucosal healing (Panes J. et al., 2013). However, CD is a transmural inflammation that can persist despite healed mucosa (Castiglione et al., 2019a; Nardone et al., 2019). It is proven that, compared to mucosal healing, transmural healing is associated with

improved long-term outcomes, including sustained long-term steroid-free clinical remission, reduced less need of rescue treatment, lower rates of CD-related hospitalisations and CD-related surgical treatment (Serban, 2018). Therefore, the paradigm for the treatment of Crohn's disease has recently changed, setting the transmural healing as the new therapeutic goal of treatment CD (Peyrin-Biroulet et al., 2015), thus making it impossible for an endoscopist to answer this question.

1.2 Epidemiology

During recent decades, the prevalence and incidence of CD has grown significantly worldwide, both in adults and children (Baumgart and Sandborn, 2012; Molodecky et al., 2012; Barnes and Kappelman, 2018) at between 0.1 and 16.0 per 100,000 person-years. The highest incidence and prevalence of inflammatory bowel disease (IBD) is observed in westernised countries. Until 2012, the highest annual incidence of CD was 20.2 per 100,000 person-years in North America, 12.7 per 100,000 person-years in Europe, and 5.0 per 100,000 person-years person-years in Asia and the Middle East. The highest prevalence for CD reported in Europe is 322 per 100,000 persons and in North America – 319 per 100,000 persons (Molodecky et al., 2012). Although the actual incidence rates in children are uncertain, CD diagnosed annually in paediatric patients is 0.2–8.5 per 100,000 persons (Cuffari, 2009).

1.3 Aethiopathogenesis

Although the precise aethiopathogenesis of CD is unknown, data from studies indicates a combination of genetic, environmental and immunobiological factors (Baumgart and Sandborn, 2012; Guan, 2019). The most popular hypothesis points to an immune-mediated condition in individuals with genetic susceptibility, where disease onset is provoked by environmental factors perturbing the mucosal barrier, impairing the healthy balance of the bowel microbiome, and stimulating bowel immune responses in an abnormal way (Boyapati et al., 2015). CD may be predisposed by Western factors, such as urban environment (Baumgart and Sandborn, 2012), lack of exposure to breast milk (Barclay et al., 2009; Molodecky and Kaplan, 2010) and childhood hygiene, as well as history of appendicitis, helminths, and smoking (Molodecky and Kaplan, 2010). Smoking can also worsen the onset of CD (Guan, 2019).

1.4 Histopathology

1.4.1 Macroscopic pattern

The appearance of CD is similar within the entire gastrointestinal tract (Geboes, 2003; Riddell, 2014). The most common locations of CD are the terminal *ileum* and the proximal colon, followed by the anorectum and colon (Geboes, 2003). In CD, inflamed sites abruptly alternate with "skip areas" of intact bowel walls (i.e., skip lesions) (Magro et al., 2013; Riddell, 2014). Macroscopic lesions are present in both the mucosal and serosal surface of the bowel wall (Geboes, 2003).

The surface of the altered bowel wall may show hyperaemia (Magro et al., 2013). Serosal inflammatory exudation with or without serosal adhesions to adjacent loops may be present (Geboes, 2003). A specific sign of CD is partial or complete encroachment of the circumference of the inflamed intestine, by hypertrophic mesenterial fat named "fat wrapping" or "creeeping fat" (Riddell, 2014).

In CD, the earliest visible mucosal pattern is small aphthous ulcerations, typically appearing over lymphoid follicles. By enlarging, the aphthous ulcers converges to large deep serpinginous of linear ulcers with oedematous mucosal edges. Oedematous, non-ulcerated mucosa alternating with deep discrete ulcers, may form the classic cobblestone pattern. Inflammatory polyps and pseudopolyps may develop (Magro et al., 2013).

Fistulae are commonly found in small bowel CD; however, they are more rare in colonic CD. Strictures may result from transmural inflammation with fibrosis and fibromuscular proliferation (Magro et al., 2013; Riddell, 2014).

1.4.2 Microscopic pattern

The most common microscopic features of CD are focal chronic inflammation, focal crypt irregularity and granulomas. The chronic inflammation means an increase of cellularity within lamina propria, migration of lymphocytes and plasma cells as well as increase of the round cells (Magro et al., 2013; Zhu et al., 2015). The crypt irregularity means either crypt distortion, branching or shortening. The granuloma in CD is defined as a focal aggregation of epithelioid histiocytes (Magro et al., 2013).

Although the morphological pattern of CD is generally similar in adult and paediatric patients (Feakins, 2013), the main difference between the histopathology of paediatric and adult CD, is the more frequent appearance of epithelioid granulomas in the inflamed bowel wall of children (Geboes, 2003; Magro et al., 2013; Feakins, 2014).

1.5 Classification

CD presents itself as a complexity of phenotypes, clinical behaviour and severity. Therefore, an accurate classification is needed to assess the different signs and manifestations, to predict the course of the disease and to apply the most appropriate treatment for each case (Vermeire et al., 2012). The phenotypical Montreal classification, a revision of the former Vienna classification, is the most recognised classification widely used in both clinical practice and investigations (Table 1.1) (Gajendran et al., 2018). It includes age at the presentation of the disease, location, and the clinical behaviour. In paediatrics, an updated version, the Paris classification, is used (Table 1.1) (Laass et al., 2014). These classifications commonly are used in combination with any activity indices (Skuja, 2020).

Table 1.1

Montreal and Paris classification of Crohn's disease

(Laass et al., 2014; Gajendran et al., 2018)

Criterion	Montreal classification	Paris classification
Age at the diagnosis (years) (A)	A1: < 16 years A2: between 17 and 40 years A3: > 40 years	A1a: < 10 years A1b: from 10–16 years A2: between 17 and 40 years A3: > 40 years
Location	L1: ileal L2: colonic L3: ileocolonic L4: isolated upper disease	L1: ileal L2: colonic L3: ileocolonic L4a: upper disease proximal to ligament of Treitz L4b: upper disease distal to ligament of Treitz and proximal to 1/3 ileum
Behaviour	B1: non-stricturing, non-penetrating B2: stricturing B3: penetrating P: perianal disease modifier	B1: non-stricturing, non-penetrating B2: stricturing B3: penetrating B2B3: both penetrating and structuring disease, either at the same or different times P: perianal disease modifier G0: no growth delay G1: growth delay

CD can also be classified based on visual diagnostic findings. In this context, four distinct subtypes are distinguished: active inflammatory disease, fistulising/perforating disease, fibrostenotic disease, and reparative or regenerative disease (Maglinte et al., 2003).

1.6 Diagnosis

There is no a single gold standard for the diagnosis of CD. The diagnosis is based on a combination of clinical investigations, at least, laboratory studies, endoscopical, histological investigations, and often – radiological examinations (Maaser et al., 2019).

1.6.1 Laboratory studies

The aim of assessing laboratory studies assessed in CD is to objectively evaluate disease activity and to repeat invasive clinical tests. An ideal test should be simple, cheap, reproducible, sensitive and specific. It should support the follow-up of the disease activity and response to treatment, whilst also predicting relapse and the course of the disease (Cappello and Morreale, 2016).

To diagnose CD, patients undergo a laboratory assessment, which includes full blood count, inflammatory markers (mainly C reactive protein (CRP), electrolytes, liver enzymes, and a stool sample for microbiological analysis). The full blood count may reveal anaemia, leucocytosis and thrombocytosis caused by an inflammatory response. The presence of raised inflammatory markers may correlate with the severity of CD; however, CRP and leucocytosis are not IBD-specific. Apart from biochemical signs of malnutrition, severe hypoalbuminaemia can be an indicator of severe inflammation. The serum ferritin level can help in diagnosing iron deficiency (Maaser et al., 2019).

Faecal calprotectin (FC) is a calcium-binding protein located in the cytosol of neutrophils. In active bowel inflammation, there is a leakage of neurophils migrated from the circulation to the bowel mucosa, and FC is excreted into faeces (Walsham and Sherwood, 2016) being the most sensitive but non-specific fecal marker of inflammation in CD (Maaser et al., 2019).

While diagnosing CD, stool sample for microbiological analysis should be obtained to exclude gastrointestinal infections (Maaser et al., 2019).

Serological markers may be useful in differential diagnosis between CD and ulcerative colitis. Anti-*Saccharomyces cerevisiae* antibodies (ASCA) are antibodies against oligomannosidic epitopes of *Saccharomyces cerevisiae* present in CD patients (Abu-Freha et al., 2018). Perinuclear anti-neutrophil cytoplasmic antibodies (pANCA) are autoantibodies which fight a protein called myeloperoxidase. They are present in majority of ulcerative colitis cases (Mitsuyama et al., 2016). The combination of positive ASCA and negative pANCA tests suggest CD, whereas the inverse pattern – positive pANCA and negative ASCA test – is more

specific for ulcerative colitis (Bernstein et al., 2016). Moreover, ASCA positive CD patients face an increased risk for necessity of requirement for early surgery (Abu-Freha et al., 2018).

1.6.2 Endoscopy

For suspected diagnosis of IBD, ileocolonoscopy and biopsies from the inflamed bowel region, the terminal *ileum* or colon, are the first line procedures (Panes et al., 2013). At least two tissue specimens from the regions of altered bowel walls should be obtained, along with biopsies from unaltered regions (Maaser et al., 2019). Therefore, colonoscopy is widely used in the diagnosis of CD, assessment of its complications, validation of its severity and monitoring of response to treatment (Jesuratnam-Nielsen, 2015). However, apart from causing general patient discomfort, the ileocolonoscopy has several drawbacks as it is invasive and allows visualisation of the colon and terminal *ileum.* Its use is limited to the bowel mucosa, and only in non-stricturising disease (Van Rheenen et al., 2010; Panes et al., 2013; Buisson et al., 2017).

Wireless video capsule endoscopy (VCE) allows examination of the endoluminal mucosa within the entire length of the bowel, thus is appropriate for evaluating small bowel CD (Triester et al., 2006). There is no conclusive evidence on the suitability of VCE for colonic assessment (Sturm et al., 2018). The limitations of VCE are the chance to miss lesions and the ampulla of Vater due to lack of bowel inflation, inability to take bowel specimens and the prolonged time necessary for reading the results (Kwack and Lim, 2016). Also this endoscopy technique can be used in non-stricturising disease only.

To get a complete picture of transmural changes that cannot be evaluated by endoscopic methods, in addition to endoscopic investigations, cross-sectional imaging is used as an adjunct to assess the bowel wall within its entire thickness (Panes et al., 2013).

1.6.3 Imaging

For appropriate management of CD patients and prognosis of the disease course, assessment of the bowel wall requires objective tools for characterisation of the location, extension, severity, activity of inflammation, and identification of potential complications. For this reason, both *ECCO* and *ESGAR* scientific societies have issued evidence-based recommendations on the use of imaging methods in the diagnosis of CD (Panes et al., 2013).

Conventional radiography

The use of plain film radiographs is limited to emergency situations – for assessment of distribution and extent of faecal masses, bowel dilatation and wall thickening, bowel obstruction and perforation. Plain film radiography has no role in routine assessment of non-urgent clinical presentations (Panes et al., 2013).

Small bowel enteroclysis and small bowel follow-through have historically been considered the standard approach when evaluating suspected or established CD. In SBFT, the barium CA is ingested orally whereas in SBE it is administrated via a nasojejunal tube which is inserted under fluoroscopic guidance (Jesuratnam-Nielsen, 2015). The radiologic pattern includes irregular thickening and impairment of the circular mucosal folds, the bowel lumen narrowing,the persence of ulcerations, and the bowel adhesions and separation due to the wall thickening and inflammatory infiltration of mesentery (Panes et al., 2013). Due to insertion of the nasojejunal tube, SBE can cause patient discomfort. The disadvantage of both methods is ionising radiation exposure, as well as lack of the capability to evaluate the extent of the disease beyound the bowel mucosa (Jesuratnam-Nielsen, 2015).

Ultrasonography *(US)*

US is a cheap, quick, non-invasive and radiation-free cross-sectional imaging method. Diagnosis of CD relies on the assessment of the thickned bowel wall considered the most important US sign in CD (Panes et al., 2013). Ultrasound also shows deteriorated echogenicity, loss of normal visible bowel wall stratification, increased vascularisation via color Doppler imaging and decrease or lack of bowel peristalsis. It also reveals extra-mural findings including the thickned and hyperechoic juxtaintestinal mesenterium, enlarged lymph nodes (Casciani et al., 2014) fistula tracts and abscesses. The contrast-enhanced ultrasound (CEUS) is a new technique involving intravenous administration of ultrasound contrast media containing microbubbles. It provides information of the micro-perfusion on mural and juxtaintestinal vascularisation, which characterises the inflammatory activity (Jesuratnam-Nielsen, 2015). Ultrasonography strain elastography and shear wave elastography measures the bowel wall stiffness, and in CD patients is used in differentiating fibrotic from inflammatory strictures (De Sousa et al., 2018).

Computed tomography (CT)

CT is the choice imaging modality of IBD in the United States. It can visualise the bowel lumen, bowel wall, visceral fat, intra-abdominal lymph nodes and mesenterial vasculature around the bowels. CT is also informative in evaluation of post-surgical changes, and in diagnostis of acute complications, such as bowel obstruction and presence of abscess. However, CT cannot reveal small mucosal ulcers (Sheth and Gee, 2016).

Two ways in which CT imaging can be applied in diagnosis of IBD are using large volume enteral contrast distention of the small bowel, combined with intravenous administration of iodine CA. In CT enterography, enteric CA, water, or commercially available preparations, is ingested by the patient. CT enteroclysis, through insertion of a naso-jejunal tube under the guidance of fluoroscopy, provides a more uniform and consistent luminal filling. However, this method can cause discomfort for the patient.

The CT signs of CD are thickened bowel walls (> 3 cm), mucosal hyperenhancement, submucosal oedema, mural stratification, vasa recta adjacent to the bowel engorgement named as “comb sign”, as well as secondary signs include mesenterial fat stranding, focal effusion close to the bowel and lymphadenopathy (Sheth and Gee, 2016).

The major drawback of CT is the radiation exposure, which is an important concern for IBD patients, as the majority of them are young and often require repeated examinations for evaluation of the disease course, as well as response to treatment (Sheth and Gee, 2016). Without administration of iodine CA an adequate CT enterography cannot be performed (Baker et al., 2008). Therefore, use of CT is also limited in patients with impaired renal function.

Magnetic resonance imaging (MRI)

MRI has advantages in evaluation of CD within the entire bowel thickness and around inflamed sites, due to high soft tissue contrast resolution, lack of use ionising radiation, facility to provide both real-time and functional imaging and ability to examine locations not accessible through endoscopic techniques (Amitai et al., 2013; Jesuratnam-Nielsen et al., 2015a). MRI has been proven to be an excellent method for detecting and follow-up of perianal fistulae (Criado et al., 2012; Balcı et al., 2019). MRI can also reveal extraintestinal complications, such as sclerosing cholangitis and sacroileitis (Mollard et al., 2015). MRI for bowel imaging differs from the routine abdominal MRI since bowel distension with an enteric CA is a fundamental requirement of imaging the small intestines. Enteric CA can be administered orally (MR enterography) or injected through a naso-jejunal proble (MR enteroclysis) (Panes et al., 2013). MR enteroclysis, compared to MRE, ensures better luminal distension of both *jejunum* and

ileum within the entire length of the small bowel (Masselli and Gualdi, 2012). However, few studies comparing MR enteroclysis and MRE demonstrate equal performance of MRE (Schreyer et al., 2004; Ram et al., 2016) providing high diagnostic accuracy and reproducibility (Negaard et al., 2007). Due to insertion and positioning of the naso-jejunal probe, MR enteroclysis can be a very stressful intervention, which also involves the use of ionising radiation; therefore, MR enterography is preferred in clinical practice (Arrivé, 2013). A more detailed description on MRE in the diagnosis of CD, is provided in chapter 3.7 "Magnetic resonance enterography in the diagnosis of Crohn's Disease".

1.7 Magnetic resonance enterography in the diagnosis of Crohn's Disease

MRE is a proven tool in diagnosis of CD, including assessment of its complications, disease activity and severity as well as for follow-up during the course of CD (Ahmed et al., 2015). Established from multiple and evidence-based reports, the *ECCO-ESGAR* Guidelines for Diagnostic Assessment in IBD, issued in 2019, states that cross-sectional imaging modalities, and thus MRE, are used as an an alternative for the evaluation of disease activity (Maaser et al., 2019). Due to its high resolution, invasiveness, lack of ionising radiation and ability to obtain findings not only within but also around the bowel wall, MRE is proven to have a great potential for evaluating CD activity (Rozendorn et al., 2018).

Indications for MRE include, but are not limited to, the following:

1) diagnosis of IBD;
2) assessment of the activity and extent of IBD;
3) evaluation of IBD-related complications, such as stricture, fistulae, abscess etc.;
4) follow-up of IBD, including assessment of the disease activity and its extent;
5) differential diagnosis between CD and ulcerative colitis;
6) evaluation of suspected bowel disease in previously negative CT and/or endoscopy;
7) evaluation of small bowel masses (American College of Radiology, 2015).

Prior to the MRE examination, patients should be prepared to provide maximum distention of bowel walls. This is necessary for improvement of visibility of luminal disease, for improvement in quality of motion-sensitive MR sequences by weakening intestinal peristalsis, and for avoiding susceptibility artefacts in images acquired by gradient-echo sequences (American College of Radiology, 2015). 4–6 hours prior to the MRE examination patients may be asked to fast. 45–60 minutes prior to examination, ingestion of > 1000 ml enteric CA is necessary (Maaser and Novak, 2019). To avoid motion artefacts deteriorating image quality, intravenous antiperistaltic medications such as glucagon of buthylscopolamine

can be administered immediately prior to motion-sensitive sequences (e.g., DWI sequences and dynamic T1 post-contrast series) (Chavhan et al., 2013; American College of Radiology, 2015; Dohan et al., 2016).

Oral CA are classified into positive, negative and biphasic agents. Positive CA are not practically used. Negative CA contain superparamagnetic non-absorbable substance of iron oxide particles, yielding black intraluminal signal in both T1 and T2 sequences (Panes et al., 2013). Biphasic CA contain non-absorbable iso- or hyper-osmolar solution producing black signal in T1-weighted images and bright signal in T2 sequences (Panes et al., 2013; Yoon et al., 2015). Solutions of mannitol sorbitol and polyethylene glycol are the most popular substances used for this purpose (Panes et al., 2013; Ram et al., 2016; Schmidt et al., 2016).

The MRE protocol includes a variety of sequences:

1) coronal free-breathing ultrafast cinematic MR sequences (MR fluoroscopy), based on steady-state precession, for demonstrating bowel anatomy, motility and strictures (Mollard et al., 2015; Greer, 2016);

2) coronal and axial free-breathing T2-weighted sequences, with and without fat saturation, for visualisation of ulcers, bowel wall oedema and collections (Sinha et al., 2011a; Mollard et al., 2015);

3) coronal pre- and post-contrast gradient-echo T1-weighted fat suppression sequence, to acquire contrast-enhanced images for assessment of disease activity and for identifying penetrating disease (Rimola et al., 2009; Greer, 2016);

4) axial DWI sequences, to localise the bowel segments affected by CD, and to identify lymph nodes (Mollard et al., 2015; Greer, 2016) as well as abscesses and enteric fistulas (Dohan et al., 2016).

In addition to MRE sequences, T2 fat saturation sequences are used in the perianal region for identifying occult perianal disease, and MR cholangiopancreatography sequence – for excluding sclerosing cholangitis (Mollard et al., 2015; Sturm and White, 2019). Sequences covering sacroiliac joints (for example, STIR) to exclude sacroileitis can be added to the examination protocol (Mollard et al., 2015; Sarbu and Sarbu, 2019).

In CD, the following findings can be found in MR images:

1) bowel wall thickening,
2) bowel wall ulceration;
3) bowel wall hyperenhancement;
4) bowel wall oedema;
5) “skip” pattern of the bowel loops involved;
6) sinus tracts and fistulas;

7) luminal narrowing;
8) mesenteric hyperaemia;
9) mesenteric stranding;
10) fibrofatty proliferation;
11) lymphadenopathy;
12) abnormal fluid;
13) perineal manifestations;
14) sclerosing cholangitis;
15) sacroileitis (Sinha et al., 2011b; Mollard et al., 2015; Mantarro et al., 2017).

Since 2009, inclusion of DWI sequences in investigation protocol has made a significant improvement in MRE technology (Dohan et al., 2016).

1.8 DWI in the assessment of Crohn's disease

1.8.1 General characterisation of DWI

DWI is an MR technique sensitive to the Brownian motion of molecules. Unlike the MR basic sequences T1 and T2, the DWI sequence is based on differences of water molecules, in ability to move freely within tissues (Westbrook et al., 2011). Pathological processes alter the diffusion characteristics of water molecules. Certain pathological changes in tissues cause perfusion disorders, swelling of cells and inability of water molecules to move as far as in unchanged tissues (Graessner, 2011).

DWI is performed by supplementing a T2-weighted fat-suppressed MR sequence (Dohan et al., 2016) by two strong and symmetrical gradients on two sides of the 180° refocusing pulse. These pulses of diffusion gradients make the magnetic field variable, and the proton precession frequencies also change accordingly.

The purpose of using diffusion gradients is to suppress transverse magnetisation. The first gradient pulse disrupts the synchronous precession of proton spins in one phase (dephasing occurs), whereas the second gradient pulse having opposite direction restores this proton synchronous precession in one phase (rephasing occurs). If, during the entire pulse sequence, the spins are in a static state, i.e., the diffusion of the molecules is limited, they will all be prevented from being in one phase by the second gradient pulse. These spins will not participate in changes in tissue SI, and the tissue signal will not be suppressed. On the contrary, if the spins are highly mobile and actively participating in the diffusion process, they will move between the first and second gradient pulses. In this case, the second gradient pulse will not be able to

restore their precession in one phase, resulting in loss of proton phase coherence and tissue signal suppression (Dietrich et al., 2010).

The strength of diffusion is determined by the diffusion coefficient, or b value, reflecting the strength (amplitude), duration and temporal separation of both gradients. The b value includes several physical quantities and is calculated according to the equation:

$$b = \gamma^2 G^2 \delta^2 (\Delta - \delta/3),$$

where G is the amplitude of the gradient used, δ is the duration of the gradient used, Δ is the time between the two gradients, and γ is the gyromagnetic ratio equal to 42 MHz / T. The b value is expressed in seconds per square millimetre, sec/mm^2 (Maxfield, 2018). Increasing the diffusion coefficient will result in more rapid attenuation in areas where diffusion is not restricted, whilst in areas where diffusion processes are limited, signal attenuation will be slower (Dohan et al., 2016) (Fig. 1.1).

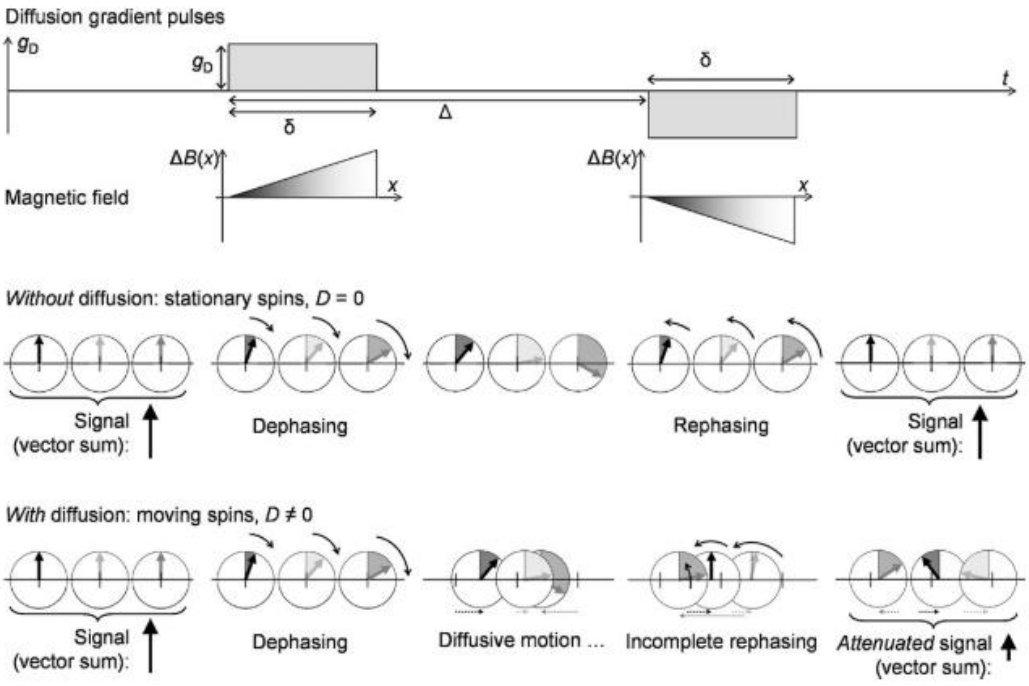

Figure 1.1. **Effect of diffusion gradients**

The diffusion gradients cause a spatially varying additional magnetic field, ΔB(x) (upper row), and thus alter precession frequencies of the spins involved. The first diffusion gradient dephases the spins. If the spins do not participate in the diffusion, the second diffusion gradient with opposite sign rephases the spins (middle row). If however, spins participate in the diffusion, rephasing is incomplete because the spins have moved between both diffusion gradients (bottom row). Thus, a diffusion-dependent signal attenuation is observed by the "vector sum" arrows (Dietrich et al., 2010).

DWI is shown to have a potential to replace the administration of gadolinium contrast media by detecting lesions earlier than they appear in conventional images (Baliyan et al., 2016). It is proven to outperform the T1 post-contrast dynamic series (Oto et al., 2011; Neubauer et al., 2013; Sirin et al., 2015; Dubron et al., 2016). DWI is proven to be useful for the detection of inflammation in CD (Oto et al., 2009; Buisson et al., 2013). The sensitivity of DWI in diagnostics of IBD can be even up to 100 % (Choi et al., 2016), and, when added to the MRE protocol, DWI yields increased sensitivity from 62 % to 83 %, compared to conventional MRE alone. By contrast, the specificity of adding DWI to the conventional MRE decresed from 94 % to 60 % (Kim et al., 2015). Also, in diagnosis of bowel inflammation, the specificity of the DWI sequence alone remains low being 39–61 % (Qi et al., 2015; Choi et al., 2016). A factor contributing to the low specificity is the false positive signal from normal bowel walls, due to the T2 *shine-through* effect from the long T2 time of the bowel wall, in the presence of bowel content (Dohan et al., 2016). This effect must be excluded from the signal of restricted diffusion. This is done by an apparent diffusion coefficient (ADC) map. The ADC map is a matematically calculed display of consolidated ADC values. It quantifies the diffusion restriction and its value for any voxel is generated by combining at least two DWI sequences with different b values. The ADC is calculated as per the following equation:

$$D = - (1/b) \ln (S/S_0).$$

The ADC values are expressed in square millimetres per second, mm^2/s (Maxfield, 2018).

On diffusion-weighted images, inflamed bowel wall presents high SI, along with low SI on the ADC maps. The ADC values are low (Sinha et al., 2013). However, despite the theory that measuring ADC values can avoid interpreting shine-through as a diffusion restriction, low ADC and an increased SI in DWI images can also be seen in disease-free bowel segments (Jesuratnam-Nielsen et al., 2015b)

The cause of restricted diffusion in bowel inflammation remains unclear; however, there are several ruling theories. Narrowing of the extracellular space is caused by increased cell density from inflammatory cells, lymphoid aggregates, dilated lymphatic vessels and granulomas. The reduced ADC values found in bowel inflammation are related to increased perfusion. Also, the presence of bowel wall fibrosis yields in restricted diffusion (Morani et al., 2015).

DWI is proven to be useful in evaluating CD activity, which allows for assessment of treatment efficacy (Dohan et al., 2016). Reports from CD activity studies suggest ADC values

of DWI is of equal importance compared to the relative contrast enhancement (RCE) used for calculation of MaRIA (Kopylov et al., 2016). A DWI-based MaRIA, or Clermont score, is designed to serve as an alternative to avoid gadolinium administration (Buisson et al., 2013). It is reported not only to have excellent correlation compared to MaRIA (Hordonneau et al., 2014), but also in the detection of ulcers (Buisson et al., 2015), mucosal healing (Buisson et al., 2017) and prediction of remission following biological therapy (Buisson et al., 2016, 2018) and reduce risk of surgery (Buisson et al., 2018). However, the Clermont score still requires validation by confirmatory studies.

The limitation of the DWI is low spatial resolution (Lin and Chen, 2015), sensitivity to motions, poor SNR caused by shorter transversal (T2) relaxation times and susceptibility artefacts (Le Bihan et al., 2006).

Due to the low sensitivity to motion-induced phase errors and advantages of short imaging times, DWI normally uses single-shot echo-planar imaging (EPI) acquisition, related to the presence of susceptibility artefacts at tissue interfaces (Drake-Pérez et al., 2018), and chemical shift-induced ghosting artefacts deflecting the fat signal several pixels away from the water signal. To avoid these artefacts, DWI protocols should include a fat saturation techniques: CHESS, SPAIR, SPIR, and STIR (Kwee et al., 2009; Luna, 2012). In relation to fat suppression, these techniques are simply classified into two categories: fat (or spectral) selective and non-selective fat saturation.

1.8.2 Fat saturation techniques used in DWI

All conventional DWI techniques use selective fat saturation, where spectrally selective pulses suppress signal from only fat protons. Chemical shift selective fat suppression (CHESS) is a common fat saturation technique where an excitation pulse with a bandwidth selective to the resonance frequency of fat is applied, followed by a dephasing gradient (Del Grande et al., 2014). A spectrally selective pulse tuned to the fat resonance, deflects the fat magnetisation to the transverse plane. The fat magnetisation is then dephased by a spoiler gradient pulse so that the net magnetisation is zero and only the water magnetisation (represented by blue arrows) is remaining. Therefore, in the subsequent excitation, only water magnetisation is available for producing MR signal (Lin et al., 2015) (Fig. 1.2).

There are also two spectrally selective hybrid sequences using an inversion recovery (IR) pulse. In spectral attenuated inversion recovery (SPAIR), the signal from fat is inverted with an adiabatic spectrally selective radiofrequency (RF) pulse. Acquisition starts from the moment of inversion time (TI) that nulls the fat signal (Del Grande et al., 2014). Another technique, a vendor-specific solution used by the company Philips, is SPIR – spectral pre-

saturation with inversion recovery. It implements a spectrally selective inversion pulse tuned to fat frequency (Del Grande et al., 2014). After the TI, a conventional 90° spin-echo pulse is applied to saturate just the fat signal (Indrati, 2017). As a result, the signal from fat protons is nulled, and only water protons are available for signal production (Fig. 1.3) (Lin et al., 2015).

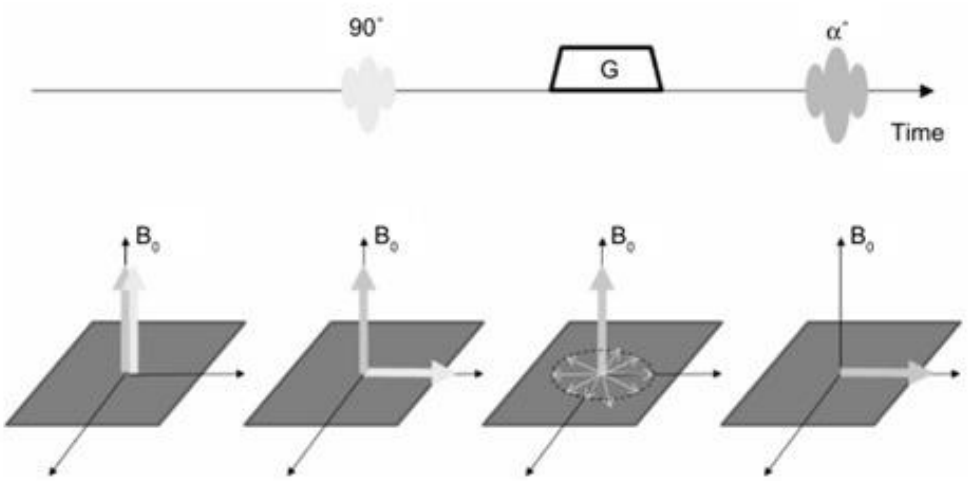

Figure 1.2. **Mechanism of CHESS fat suppression**

A spectrally selective radiofrequency pulse tuned to the resonance frequency of fat deflects the fat magnetisation vector to the transverse plane (brighter arrow). Afterwards, it is dephased by the spoiler dephasing gradient pulse (G), resulting the net magnetisation to be zero. As a result, only water protons (darker arrow) are available for signal production in the subsequent excitations (Lin et al., 2015).

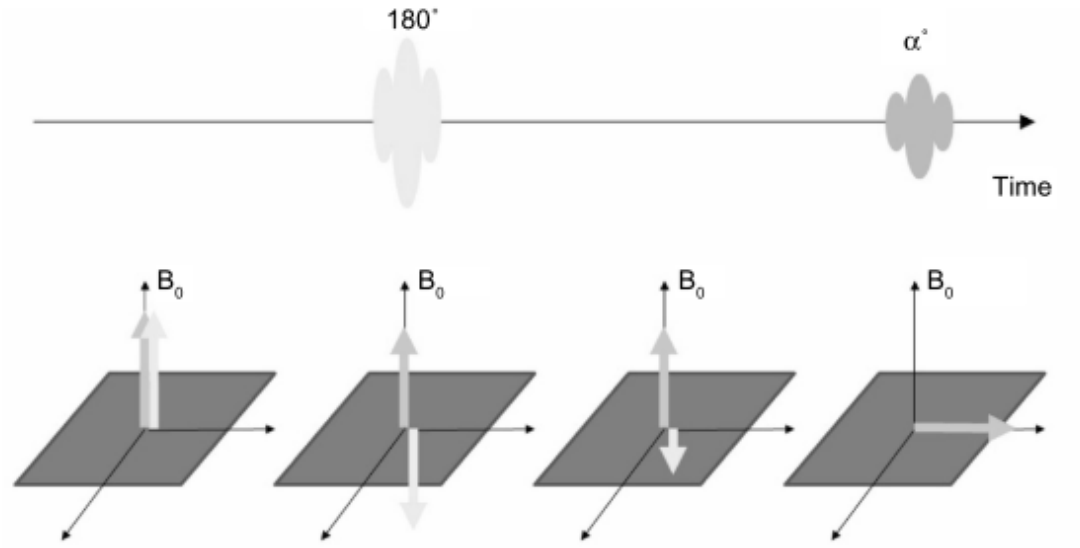

Figure 1.3. **Mechanism of SPAIR and SPIR fat suppression techniques using either adiabatic or spectrally selective FR pulse tuned to fat resonance frequency**

An adiabatic spectrally selective RF IR pulse is applied to deflect the fat protons (brighter arrow) for 180° followed by the inversion recovery process that leads to nulling of signal after a certain delay time. Meanwhile, the water magnetisation remains, and only water protons (darker arrow) are available for signal production in the subsequent excitations (Lin et al., 2015).

Alongside spectrally selective fat saturation techniques, the DWI weighted sequence with short T1 inversion recovery (STIR) fat suppression technique is also used. STIR is an IR technique that does not rely on a spectrally selective RF pulse but is based on the different relaxation behaviour between water and fat tissues. Before the excitation pulse, an inversion pulse is applied, inverting both water and fat proton spins which subsequently perform T1 relaxation. Fat has a significantly shorter T1 relaxation time compared to other tissue types. By selecting the TI such as the longitudinal magnetisation of fat at the time point zero, fat spins will not participate to the MR signal (Horger, 2007; Lin et al., 2015) (Fig. 1.4).

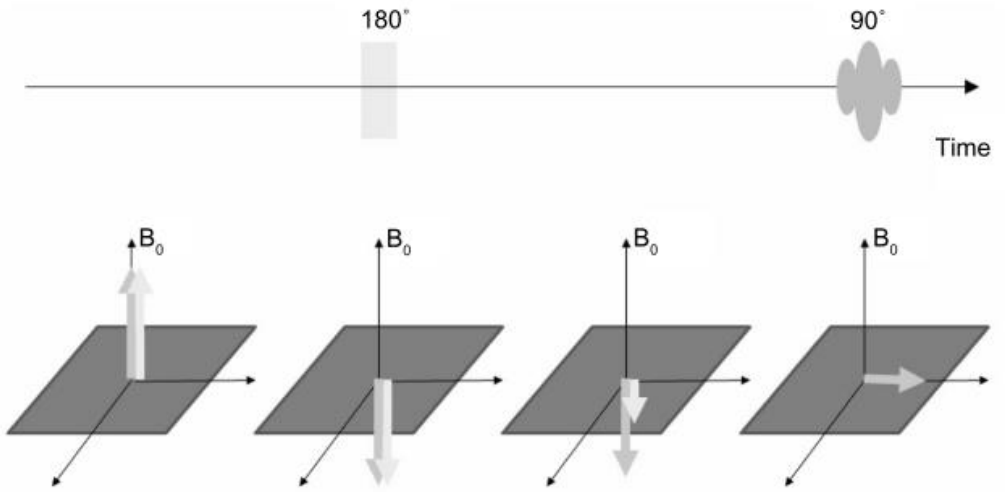

Figure 1.4. **STIR fat suppression**

In this technique, a non-selective 180° RF pulse inverts the magnetisation of both fat (brighter arrow) and water (darker arrow) protons. Due to the shorter T1 relaxation of the fat, its magnetisation recovers faster compared to water. After a definite time, the fat magnetisation is nulled (reaches zero). If the excitation pulse is given at this moment, only water protons will participate in signal production *(*Lin et al., 2015).

DWI using STIR as a fat suppression technique was developed in the early 2000s by the research group of Professor Taro Takahara from Tokai University School of Medicine, Japan, who named it Diffusion Weighted Imaging with Background Body Signal Suppression (DWIBS) (Takahara et al., 2004).

1.8.3 DWIBS sequence

The DWIBS sequence is based on free-breathing DWI acquisition, selecting STIR as the fat supression technique. This sequence allows free breathing, permitting multiple slice excitation and signal averaging over an extended period to average motion (Takahara et al., 2004). Compared to spectrally selective fat saturation techniques, the use of DWI with non-selective STIR allows robust and more homogenic fat suppression within large body regions (Takahara et al., 2004; Moore et al., 2014), including off-center localisations (Del Grande et al.,

2014). The DWIBS sequence provides an increased CNR (Kwee et al., 2009), insensitivity to magnetic field inhomogeneities and decreased image distortion (Kwee et al., 2008b), making it suitable for scanning large areas. Therefore, it is suitable for conducting high quality volumetric three-dimensional acquisitions (Takahara et al., 2004). It also suppresses the signals from bowel content (Kwee et al., 2008b).

Initially, the DWIBS sequence was developed for the whole-body imaging of patients with known neck, chest and abdominal malignancies, in order to identify results similar to the positron emission tomography (PET), used in detecting tumour relapse and metastases (Takahara et al., 2004). Nowadays, it is widely used in a number of other applications including detecting inflammation, abscesses, intravascular thrombi, visualisation of the peripheral nerves (Kwee et al., 2009) and certain kinds of arteritis (Davidovic and Tsay, 2019; Matsuoka et al., 2019; Oguro et al., 2019). Due to full suppression of the background signal, when compared to conventional DWI, DWI with STIR technique is reported to have improved image quality and less image artefacts (Ouyang et al., 2014). Regarding ADC analysis, DWI with STIR is proven to be superior in the assessment of breast lesions, compared to the conventional DWI with SPIR fat saturation technique, (Stadlbauer et al., 2009). Using DWI sequence with STIR in MRE examinations is recommended according to several publications (Kiryu et al., 2009; Park, 2016). It is also reported to be used in the assessment of CD activity (Kiryu et al., 2009; Caruso et al., 2014).

The non-selectivity of STIR can be a disadvantage wherever there is a presence of substances with short T1 time, such as methaemoglobin, mucoid tissue, proteinaceous material, and melanin (Del Grande et al., 2014). Another disadvantage of STIR is decreased SNR caused by partial loss of proton signal during the TI (Kwee et al., 2008b), resulting in noisy images. However, despite the reduced SNR, DWIBS contributes to improved detection of subtle lesions due to higher CNR (Kwee et al., 2009). This also applies to the intestinal walls affected by inflammation (Fig. 1.5).

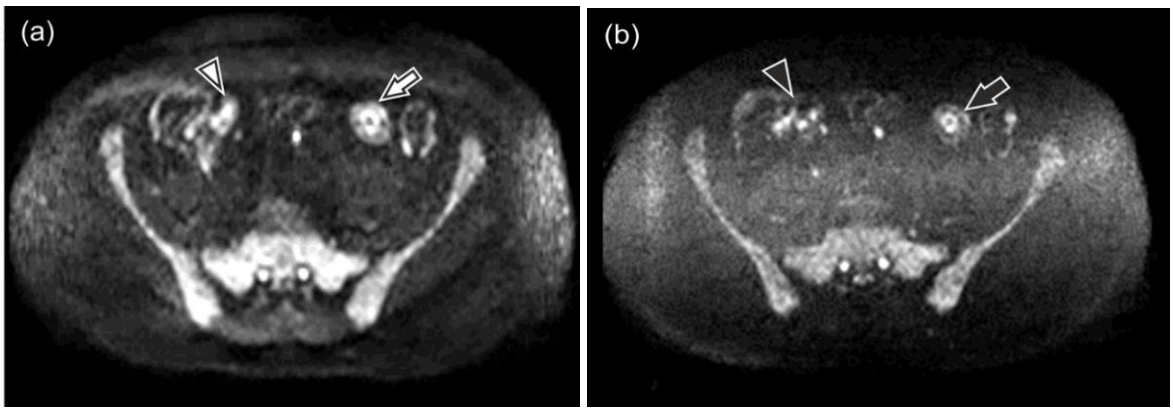

Figure 1.5. **Tracking images of DWI_{SPIR} (a) and DWIBS (b) with a b value of 800 s/mm^2 in a 35-year-old male with active CD in the terminal *ileum***
There is a high SI in the wall of the inflamed intestinal segments, indicating a diffusion restriction within this localisation. Despite the reduced SNR, resulting in grainy images compared to the DWI sequence (white arrow), the resolution of the inflamed intestinal wall in the DWIBS sequence is improved (black arrow). Small lymph nodes are also more visible in DWIBS images (black arrowhead), compared to DWI_{SPIR}. Images from the Author's archive.

Nevertheless, by allowing whole body imaging with homogenous fat suppression, DWIBS is one of the most important discoveries related to DWI (Takahara et al., 2004; Takahara, 2005). Its use improves diagnosis in oncology (tumour staging, detection of tumour relapse, monitoring response to therapy), especially in settings where PET is not available (Takahara et al., 2004; Takahara, 2005; Kwee et al., 2008a). DWI with STIR is reported to be suitable for identification and characterisation of lymph nodes in patients with uterine cervical cancer (Jeong et al., 2008). ADC values calculated from DWI images with STIR are proven to outperform ADC values derived from DWI images with spectrally selective fat suppression in differentiating between malignant and benign breast lesions (Stadlbauer et al., 2009). It is also reported to be non-dependent on motions (Stone et al., 2012), which can be crucially important in assessment of the bowel walls. However, no studies have been published on the comparison between DWI sequences with non-selective STIR and spectrally selective fat saturation techniques in the diagnosis of Crohn's disease and assessment of its activity.

1.9 Determining Crohn's disease activity

1.9.1 Clinical scoring systems

Disease activity can be grouped into mild, moderate and severe (Gajendran et al., 2018). To evaluate CD activity, various scoring systems can be used. The most commonly used scoring systems for Crohn's clinical disease activity, recommended in the *ECCO* guidelines, are the Crohn's disease activity index (CDAI) and Harvey-Bradshaw index (HBI) (Sturm et al., 2018). In paediatrics, instead of CDAI, the paediatric Crohn's disease activity index (PCDAI) is used

(Casciani et al., 2014). Measuring clinical activity is important, however as the use of clinical scoring systems is limited by subjective interpretation; it is insufficient for objective activity assessment (Sturm et al., 2018).

Crohn's disease activity index (CDAI)

The CDAI is used in adults with alrealy diagnosed CD. It allows CD activity to be quantified, comparing different patients, and monitored throughout follow-ups to evaluate the patient response to treatment (Gajendran et al., 2018). CDAI is a sum of eight clinical and laboratory parameters recorded during a period of seven days and added together after adjustment of corresponding coefficients or weighting factors. Each of the parameters evaluates a certain aspect of CD. All parameters are estimated for seven days, and each of the parameters is scored and multiplied with the corresponding weighting factor. The sum of the weighted parameters forms the total CDAI score. The parameters are as follows: number of evacuations with liquid/soft stools, patient pain score, subjective feel of well-being, number of extra-intestinal symptoms (presence of joint, eye, skin, mouth, anal manifestations or other fistula, presence of fever), necessity for anti-diarrhoeal medication, presence of abdominal mass, laboratory data (haematocrit), and body weight (Best et al., 1976; Hutchings et Alrubaiy, 2017) (Table 1.2). Despite shortcomings of the CDAI, it is currently used worldwide as a standard for evaluating CD activity in both clinical trials and daily practice. Various calculators are available for estimating CDAI in internet.

Table 1.2

Crohn's Disease Activity Index (Best et al., 1976)

	Clinical or laboratory variable	**Weighting factor**
1.	Number of very soft or liquid or stools	× 2
2.	Abdominal pain score (0 = none, 1 = mild, 2 = moderate, 3 = severe)	× 5
3.	General well-being (0 = generally well, 1 = slightly below par, 2 = poor, 3 = very poor, 4 = terrible)	× 5
4.	Presence of extraintestinal manifestations (one point for each)	× 5
1.	*Arthritis/arthralgia*	
	Iritis/uveitis	
	Erythema nodosum/ Pyoderma gangrenosum/aphthous	
	Stomatitis	
	Anal fissure, fistula, or abscess	

Table 1.2 (End)

	Other fistula	
	Fever	
5.	Taking antidiarrheal medication (1 = yes, 0 = no)	× 30
6.	Abdominal mass (0 = none, 2 = questionable, 5 = definite)	× 10
7.	Haematocrit (male: 47-critg, female 42-crit)	× 6 (add or subtract according to sign)
8.	Body weight: the maximum weight deduction of 10%	× 1

Severe CD is defined as where the total CDAI exceeds 450, whereas CD remission is considered if the total CDAI is less than 150. Response to the treatment is considered if the CDAI decreases by more than 70 points (Hutchings et Alrubaiy, 2017).

Harvey-Bradshaw index (HBI)

The HBI is a simple index including five clinical parameters based on the results regarding the previous day. Each of the parameters provides a certain number of points. These items are as follows: the patient's general well-being (0 = very well, 1 = slightly below average, 2 = poor, 3 = very poor, 4 = terrible), abdominal pain (0 = none, 1 = mild, 2 = moderate, 3 = severe), number of liquid or soft stools, abdominal mass (0 = none, 1 = dubious, 2 = definite, 3 = tender), and identically to the CDAI, complications (arthralgia, uveitis, erythema nodosum, aphrhous ulcers, pyoderma gangrenosum, anal fissure, new fistula, abscess, one score for each). Compared to CDAI, the use of HBI is simpler, and it does not require the use of laboratory results. It is based on subjective symptoms and thus refers to the well-being of patients.

Paediatric Crohn's disease activity index (PCDAI)

The PCDAI, accepted as the CD activity measure for paediatric use, is formed of 11 clinical parameters as follows: three subjective criteria of patient medical history (abdominal pain, number of liquid stools, general well-being), five physical examination parameters (abdominal examination, perirectal disease, extraintestinal manifestations, weight, height), and three laboratory tests (hematocrit, albumin, erythrocyte sedimentation rate). There are three choices for each parameter – 0, 5, or 10 points, except for hematocrit and erythrocyte sedimentation rate, which are scored as 0, 2.5, or 5 points. The PCDAI ranges from 1 to 100 points (Hyams et al., 2005). The cut-off rate for mild disease is 10–27.5 points, and for moderate disease 30–37.5 points, for severe disease 40–100 points. Remission is considered when the

PCDAI < 10 points, whereas a positive response to treatment is identified when the change of PCDAI exceeds > 12.5 points (Turner et al., 2010).

1.9.2 Endoscopical scoring systems

Several scores based on endoscopic evaluation of the bowel have also been designed for monitoring CD. The endoscopic index of severity (CDEIS) and simplified endoscopic score of CD (SES-CD) are the scoring systems most commonly used for estimation of CD activity (Sturm et al., 2018). However, as endoscopy allows visualisation of only a limited part of the small intestine, assessing solely mucosa, its use in assessment of the full extent of the disease is limited (Zorzi et al., 2014; Civitelli et al., 2016; Nardone et al., 2019).

Crohn's disease endoscopic activity index of severity (CDEIS)

The CDEIS scores CD activity in five bowel segments (terminal *ileum*, right colon, transverse, left colon and sigmoid, rectum) and assesses the presence of specific mucosal lesions (i.e., ulcers and stenosis) as well as the extent of disease. The score ranges from 0 to 44. However, this score has limitations due to the transmural nature of CD, and the fact that mucosal appearance alone cannot reflect the true extent of the condition. The assesment of CDEIS is also time consuming, its use is complicated and operator-dependent. Therefore, it has consequently not become routine in clinical practice and is used mainly in clinical trials (Sturm et al., 2018).

Simplified endoscopic score of CD (SES-CD)

The SES-CD is a simplified version of the CDEIS. It correlates highly with CDEIS. The score includes four parameters (ulcer size, extent of ulcerated surface, extent of affected surface, and stenosis), and each of them is assessed in five bowel segments. The scores range from 0 to 6. SES-CD, however, does not define the mucosal healing, thus limiting its use in clinical practice (Sturm et al., 2018).

1.9.3 Cross-sectional imaging scoring systems

According to a number of reports, cross-sectional imaging modalities have a clearly defined role for assessment of bowel alteration in patients with CD (Sturm et al., 2018). Therefore, in 2019, *ECCO-ESGAR* Guidelines for Diagnostic Assessment in IBD published a revolutionary statement, stating that cross-sectional imaging methods, US, CT and MRI, can be

used as an alternative in IBD activity assessment (Maaser et al., 2019). Due to its high contrast resolution and lack of ionising radiation, magnetic resonance imaging (MRI) is proven to be informative both in diagnosing Crohn's disease and assessing its activity along the entire length and thickness of the altered bowel. To assess CD activity, a variety of MRI scoring systems have been developed for standardising the measured outcomes (Rozendorn et al., 2018). Amongst them, the magnetic resonance index of activity (MaRIA), Clermont score and Lémann score are the most significant MRI scoring systems.

MaRIA score

Among the cross-sectional indices, the MaRIA score, developed by the scientific gropup of Jordi Rimola, is the first and the only validated MRE-based score, based on data a large population of patients as having high and significant correlation with CDEIS (Dohan et al., 2016). The MaRIA score is composed of the values of intestinal wall thickness (in mm) and relative contrast enhancement (RCE), as well as the rating of the presence of oedema (1 – present, 0 – absent) and ulcers (1 – present, 0 – absent) in the bowel wall. RCE is calculated from the wall signal intensity (WSI) series before (WSI-preGd) and after (WSI-postGd) administration of gadolinium CA (Rimola et al., 2009).

MaRIA score is to be calculated using the following formula:

$$\text{MaRIA} = 1.5 \times \text{wall thickness (mm)} + 0.02 \times \text{RCE} + 5 \times \text{oedema} + 10 \times \text{ulcers},$$

where the presence or absence of ulcers and oedema was rated as 1 or 0, accordingly. RCE was calculated as follows:

$$\text{RCE} = (\text{WSI-}\textit{post}\text{Gd} - \text{WSI-}\textit{pre}\text{Gd})/(\text{WSI-}\textit{pre}\text{Gd})) \times 100 \times (\text{SD-}\textit{pre}\text{Gd}/\text{SD-}\textit{post}\text{Gd}),$$

where the SD-*pre*Gd and SD-*post*Gd corresponded to the mean of the six SD values of SI, measured outside of the body before and after gadolinium administration, accordingly (Rimola et al., 2009).

The cut-off point for diagnosis of active CD is a MaRIA score $\geqslant 7$. The cut-off point for diagnosis of severe CD is MaRIA score $\geqslant 11$) (Rimola et al., 2011).

A global MaRIA score is calculated by adding the values from all six bowel segments (terminal ileum, ascending, transverse, descending, sigmoid colon and rectum). It produces a high and signifficant correlation with CDEIS (rho = 0.78, $p < 0.001$), the Harvey-Bradshaw index (rho = 0.56, $p < 0.001$), and C-reactive protein (rho = 0.53, $p < 0.001$) (Rozendorn et al., 2018).

The main limitation of MaRIA is that it is proven to be valid for the terminal ileum but not for the colon (Jairath et al., 2018).

A disadvantage of MaRIA is the necessity to administer gadolinium contrast media related to potentially severe adverse reactions like systemic nephrogenic fibrosis (Broome, 2008; Perez-Rodriguez et al., 2009) and accumulation of gadolinium deposits in the brain and other body tissues (Gulani et al., 2017; Quattrocchi and van der Molen, 2017). Since CD is a relapsing disease requiring multiple follow-up examinations, CD patients are exposed to the risk of gadolinium accumulation. Therefore, solutions replacing the contrast medium administration are important.

Clermont score

The Clermont score, developed by the scientific group from Clermont-Ferrand University, is an alternative MRI index of activity. It has been developed on the basis of DWI by replacing RCE with apparent diffusion coefficient (ADC), which is a quantitative measurement of diffusion restriction in bowel inflammation. It is reported to have an excellent correlation with MaRIA score (Hordonneau et al., 2014) and a moderate correlation with CDEIS (Buisson et al., 2017). The Clermont score is also proven to detect ileocolonic ulcers (Buisson et al., 2015) and mucosal healing (Buisson et al., 2017), to predict remission following biological therapy (Buisson et al., 2016, 2018) and reduce risk of surgery (Buisson et al., 2018). However, further confirmatory studies are needed to validate the Clermont score.DWI images (Hordonneau et al., 2014). Clermont score is therefore also called DWI-MaRIA. It is reported to be a reliable tool for assessment of

The Clermont score, or DWI-MaRIA, is calculated as per the following formula (Hordonneau et al., 2014):

$$\text{DWI-MaRIA} = 1.646 \times \text{wall thickness (mm)} - 1.321 \times \text{ADC} + 5.613 \times \text{oedema} + 8.306 \times \text{ulcers} + 5.039,$$

where, as in the MaRIA score, the presence or absence of ulcers and oedema was rated as 1 or 0.

A Clermont score of > 8.4 is reported to be predictive of active ileal disease, which was defined as MaRIA $\geqslant$ 7, and a score $\geqslant$12.5 is reported to be to be predictive of severe ileal disease (MaRIA $\geqslant$ 11). It is reported that the Clermont score highly correlates with the MaRIA score (rho = 0.99) in ileal CD but not in colonic CD (rho < 0.8) (Hordonneau et al., 2014).

Lémann score

The Crohn's Disease Digestive Damage Score (the Lémann score) differs from other indices since it assess bowel damage rather than activity (Pariente et al., 2011; Rimola et al., 2011; Rozendorn et al., 2018). For the assesment of the Lémann score, endoscopy, colonoscopy, or cross-sectional diagnostic imaging modalities CTE and MRE, are used to visualise the location of lesions. Each of the segments (upper gastrointestinal tract, small bowel, colon from *caecum* till *rectum*, and *anus*) is evaluated regarding to three parameters, penetrating lesions, stricturing lesions, and the history of surgical resection (Pariente et al., 2011; Rozendorn et al., 2018) (Table 1.3). The Lémann index represents the patient's disease course and assesses the response to medical treatment (Maaser et al., 2019).

Table 1.3

Estimation of Lémann index

		Upper tract	**Small bowel**	**Colon/rectum**	**Anus**
Surgical intervention	Grade 1	-	-	-	Reconstruction procedure, flap, coring out fistula track or laying open of fistula
	Grade 2	Bypass diversion or strictureplasty	Bypass diversion or strictureplasty	Stomy. Bypass diversion or strictureplasty	Major surgery leading to substantial sphincter damage Temporary diversion
	Grade 3	Resection	Resection	Resection	Resection
Stricturing lesion	Grade 1	**MRI/CT:** Wall thickening < 3 mm or segmental enhancement without pre-stenotic dilatation	**MRI/CT:** Wall thickening < 3 mm or segmental enhancement without pre-stenotic dilatation	**MRI/CT:** Wall thickening < 3 mm or segmental enhancement without pre-stenotic dilatation	**Clinical examination:** Mild stricture

	Grade 2	**Endoscopy:** Lumen narrowing, passable **MRI/CT:** Wall thickening ⩾ 3 mm/mural stratification without pre-stenotic dilatation	**MRI/CT:** Wall thickening ⩾ 3 mm/ mural stratification without pre-stenotic dilatation	**Colonoscopy:** Lumen narrowing, passable **MRI/CT:** Wall thickening ⩾ 3 mm/segmental enhancement without pre-stenotic dilatation/< 50 % of the lumen	**Clinical examination :** Frank stricture, passable
	Grade 3	**Endoscopy:** stricture, non-passable	**MRI/CT:** stricture with pre-stenotic dilatation	**Colonoscopy:** Stricture, Nonpassable **MRI/CT:** Stricture with pre-stenotic dilatation/> 50 % of the lumen	**Clinical examination :** Frank stricture, passable
Penetrating lesion	Grade 1	**Endoscopy:** Superficial ulceration	-	**Colonoscopy:** Superficial ulceration	**Clinical examination :** Anal ulceration **MRI/CT:** Simple fistula
	Grade 2	**Endoscopy:** Deep ulceration **MRI/CT:** Deep transmural ulceration	**MRI/CT:** Deep transmural ulceration	**Colonoscopy:** Deep ulceration **MRI/CT:** Trans-mural ulceration	**Clinical examination:** Multiple fistula **MRI/CT:** Branching fistula, multiple fistulae, or any type of abscess > 1 cm
	Grade 3	**Endoscopy:** Fistula **MRI/CT:** Phlegmon or any type of fistula	**MRI/CT:** Phlegmon or any type of fistula	**Colonoscopy:** Fistula **MRI/CT:** Phlegmon or any type of fistula	**Clinical examination**: Multiple fistula with extensive anal and perianal tissue destruction **MRI/CT:** Extensive anal and perianal suppuration, horseshoe abscess, or fistula(e) involving or extending above the levator plate

2. Material and methods

A prospective cross-sectional study, consisting of three parts, was carried out during the PhD thesis:

1) investigation of the effect of preparation of the patient's intestinal tract with oral hyperosmolar CA on ADC values of the conventional DWI and DWIBS sequences in intestinal and large bowel walls. This study is described in the publication by Ilze Apine, Monta Baduna, Reinis Pitura, Juris Pokrotnieks, Gaida Krumina "The Influence of Bowel Preparation on ADC Measurements: Comparison between Conventional DWI and DWIBS Sequences", published in Medicina (Kaunas, Lithuania) July 2019, 55(7): 394, pp.1–13;

2) investigation of the ADC values of conventional DWI and DWIBS sequences in patients with signs of active CD MR, and investigation of the use of these values for the calculation of the Clermont index. This study is described in the publication by Ilze Apine, Reinis Pitura, Ivanda Franckeviča, Juris Pokrotnieks, Gaida Krumina "Comparison between Diffusion-Weighted Sequences with Selective and Non-Selective Fat Suppression in the Evaluation of Crohn's Disease Activity: Are They Equally Useful?", published in Diagnostics 2020, 10, 347, pp. 1–21;

3) evaluation of the repeatability of the component measurements for the MR indices of Activity MaRIA, based on the administration of Gd CA, and the Clermont index based on the ADC-DWI and ADC-DWIBS values. The study is described in the publication by Ilze Apine, Ieva Pirksta, Reinis Pitura, Juris Pokrotnieks, Ieva Pukite, Gaida Krumina "Repeatability of magnetic resonance measurements used for estimating the Crohn's disease activity", Proceedings of the Latvian Academy of Sciences. Section B. Volume 74 (2020), No 2 (725), pp.75–82.

The dissertation was carried out in the state tertiary care institution Children's Clinical University Hospital of Riga, Latvia, from March 2016 to April 2019. The dissertation summarises data on: 1) false-positive signal hyperintensity in a DWI series of the highest b value without other radiological features of IBD and without clinical or laboratory signs of IBD in patients with dyspeptic complaints; 2) patients with active CD in the terminal *ileum.* The patients included in the study were scanned with a 1.5 T MRI scanner Philips Ingenia (Philips Medical Systems, Best, The Netherlands) using a 16-channel body coil. All patients were fasted for at least six hours prior to the MRE examination and prepared with 1.25 to 1.5 L of 2.5 % mannitol solution orally, prior to scanning. Scanning was performed in the prone position. The MRE protocol included a conventional DWI sequence with the spectrally selective fat suppression technique SPIR (DWI_{SPIR}), and DWIBS sequence. To prevent

movement artefacts in DWI_{SPIR} and DWIBS images, intestinal peristalsis was suppressed with butylscopolamine (Buscopan, Sanofi) by i/v administration with 20 ml of 0.9 % saline. In patients who required intravenous CA administration, the butylscopolamine injection was also performed before the dynamic T1 post-contrast series. Image evaluation and ADC measurements were performed using the Philips Intellispace Portal 5.0 image post-processing server (Philips Medical Systems, Best, The Netherlands). Intestinal WSI in T1-weighted images following i/v CA administration and image noise measurements were performed using the Clear Canvas DICOM Viewer, v. 13.2 (Synaptive Medical, Toronto, Canada, 2019). All images were analysed and measured by one radiologist, with experience in abdominal MRI since 2000.

In patients with active CD in the terminal ileum, MaRIA in each inflamed altered segment was calculated according to the formula:

MaRIA = 1.5 × wall thickness (mm) + 0.02 × RCE + 5 × oedema + 10 × ulcers,

where the presence or absence of ulcers and oedema was rated as 1 or 0, accordingly. RCE was calculated as per formula:

RCE = (WSI-*post*Gd – WSI-*pre*Gd) / (WSI-*pre*Gd)) × 100 × (SD-*pre*Gd / SD-*post*Gd),

where *SD-pre*Gd (standard deviation in the pre-contrast T1-weighted images) and *SD-post*Gd (standard deviation in post-contrast T1-weighted images) correspond to six mean values of standard deviation (SD), for SI measured outside the body in the pre-contrast and post-contrast T1-weighted images (Rimola et al., 2009).

The Clermont score, or DWI-MaRIA, for both DWI_{SPIR} and DWIBS sequences, was calculated per following formula (Buisson et al., 2013; Hordonneau et al., 2014):

DWI-MaRIA = 1.646 × wall thickness (mm) – 1.321 × *ADC* + 5.613 × oedema + 8.306 × ulcers + 5.039.

Since oedema was one of the inclusion criteria representing inflammation, it was present in all intestinal segments that met the study criteria; therefore, its rating was always equal to 1.

The study was performed in accordance with the Declaration of Helsinki and approved by the statement on compliance with bioethical norms 6/10.09.2015 issued at the meeting of the Ethics committee of Rīga Stradiņš University on September 10, 2015. All patients included in the study or their legal representatives (parents of children), signed a written informed consent form to participate in the study.

2.1 First study. Effect of previous preparation of the patient's intestinal tract with enteric hyperosmolar CA on the ADC-DWI$_{SPIR}$ and ADC-DWIBS values of the intestinal and large bowel walls

The study is described in the publication by Apine, I., Baduna, M., Pitura, R., Pokrotnieks, J., Krumina, G. 2019. "The Influence of Bowel Preparation on ADC Measurements: Comparison between Conventional DWI and DWIBS Sequences", *Medicina* (Kaunas, Lithuania), 55(7): 394, pp. 1–13.

2.1.1 Patient population

This prospective study included 106 primary care patients (18–76 y.o.). The patients were referred to MRE from March 2015 till March 2018, due to dyspeptic complaints but with no clinical, laboratory and radiological evidence of IBD. The inclusion criteria were: absence of typical IBD symptoms – diarrhoea, bloody and/or mucous stool, severe and/or crampy abdominal pain and rectal involvement (Tontini et al., 2015; Mazza M, Cilluffo MG, 2016) as well as absence of any radiological or laboratory evidence of IBD.

The exclusion criteria were: age < 18 years, FC level > 200 μg/g, acute bowel infection, proven or previously diagnosed IBD, endoscopically proven enteropathy (e.g., coeliac disease, collagenous colitis etc.), radiological signs of IBD, present bowel tumour and systemic diseases such as cystic fibrosis.

2.1.2 The study

In this prospective observational cross-sectional study, ADC of DWI$_{SPIR}$ (ADC-DWI$_{SPIR}$) and DWIBS (ADC-DWIBS) were assessed in bowel walls before and after preparation with hyperosmolar enteric CA. The DWI$_{SPIR}$ and DWIBS scanning sequences were solely performed in patients prior to bowel preparation. Afterwards, patients were given the enteric CA, and scanned as per complete MRE protocol with DWI$_{SPIR}$ and DWIBS sequences included.

The study included two cohorts: 1) assessment of ADC-DWI$_{SPIR}$ and ADC-DWIBS in intestinal walls before and after patient preparation, and 2) assessment of ADC-DWI$_{SPIR}$ and ADC-DWIBS in colonic walls before and after preparation. The ADC measurements were only performed on bowel segments where high SI was present at b = 800 mm^2/s image mimicking bowel inflammation. In order to compare ADC before and after bowel preparation, only patients with measurements both before and after preparation were included in the further data analysis. Similarly, for comparison between ADC-DWI$_{SPIR}$ and ADC-DWIBS, only patients with

measurements performed in both DWI_{SPIR} and DWIBS sequences were included in the further analysis. In both cohorts, data was grouped by the preparation state of the patient (non-prepared versus prepared bowels) and mutually compared.

2.1.3 1st cohort

The first cohort was formed of patients in whom high SI bowel walls at b = 800 s/mm^2 showing false-positive bowel wall hyperintensity in DWI sequences, mimicking bowel inflammation were identified in at least one intestinal site. High SI regions in at least one intestinal region were identified in all 106 patients. Prior to bowel preparation, one collapsed jejunal segment in DWI_{SPIR} and DWIBS image series was identified for each patient. After bowel preparation, one distended jejunal segment in DWI_{SPIR} and DWIBS image series was identified in for each patient. ADC values were measured in three sites per segment using 10–20 mm^2 region of interest (ROI), both before and after preparation (Fig.2.1).

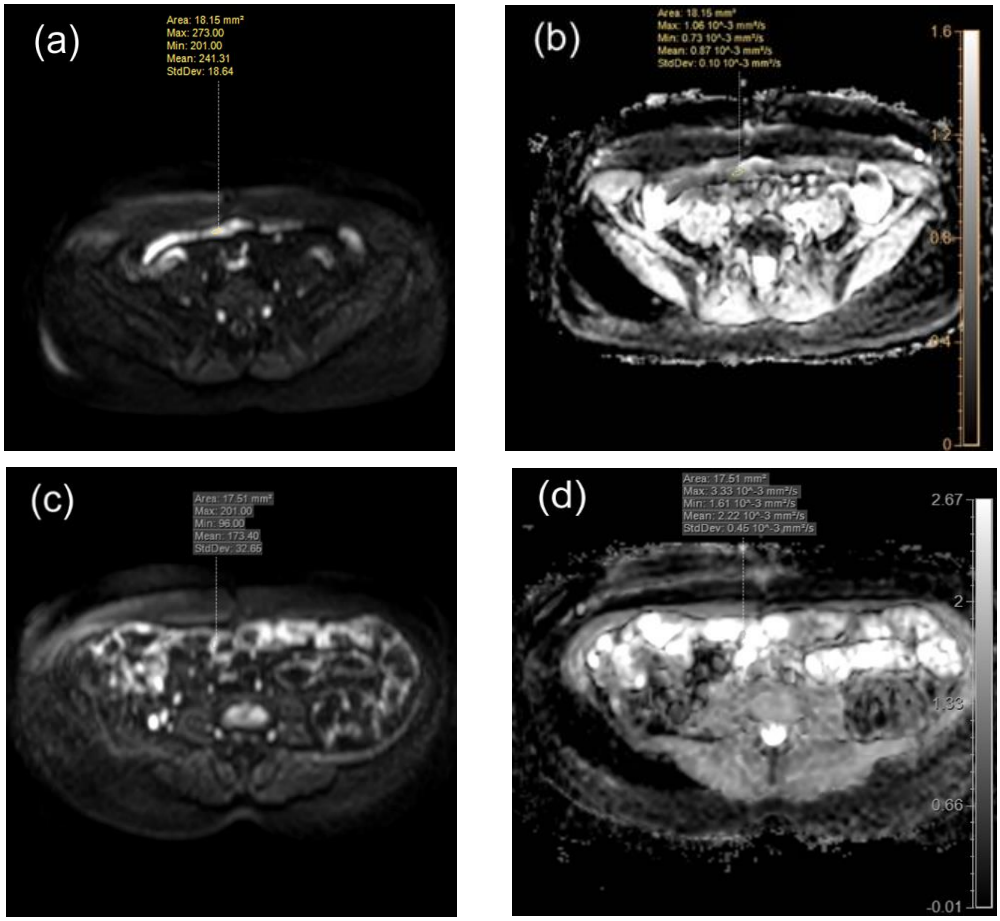

Figure 2.1. **Selecting ROIs for apparent diffusion coefficient (ADC) measurements, in localisations of false-positive hyperintensity mimicking inflammation on DWI_{SPIR} tracking images of b = 800 s/mm^2 of collapsed (a) and distended (c) *jejunum***

ADC values appear on the ADC map (b, for collapsed *jejunum*, d, for distended *jejunum*). MRE examination of a 53 y.o. female patient with dyspeptic complaints, with no morphologically proven CD, Images from the Author's archive.

2.1.4 2nd cohort

The second cohort was formed of patients in whom high SI bowel walls at b = 800 showing false-positive bowel wall hyperintensity in DWI sequences mimicking bowel inflammation were identified in at least one colonic site. 78 of the 106 patients were identified to have high SI regions in at least one colonic region. Before bowel preparation in the DWI_{SPIR} and DWIBS image series, one *caecum* or ascending colon segment with presence of intraluminal faeces was identified in each patient. After bowel preparation in the DWI_{SPIR} and DWIBS image series, one *caecum* or ascending colon segment with presence of intraluminal mannitol was identified in each patient. ADC values were measured in three sites per segment using 10–20 mm^2 ROI both before and after preparation (Fig. 2.2).

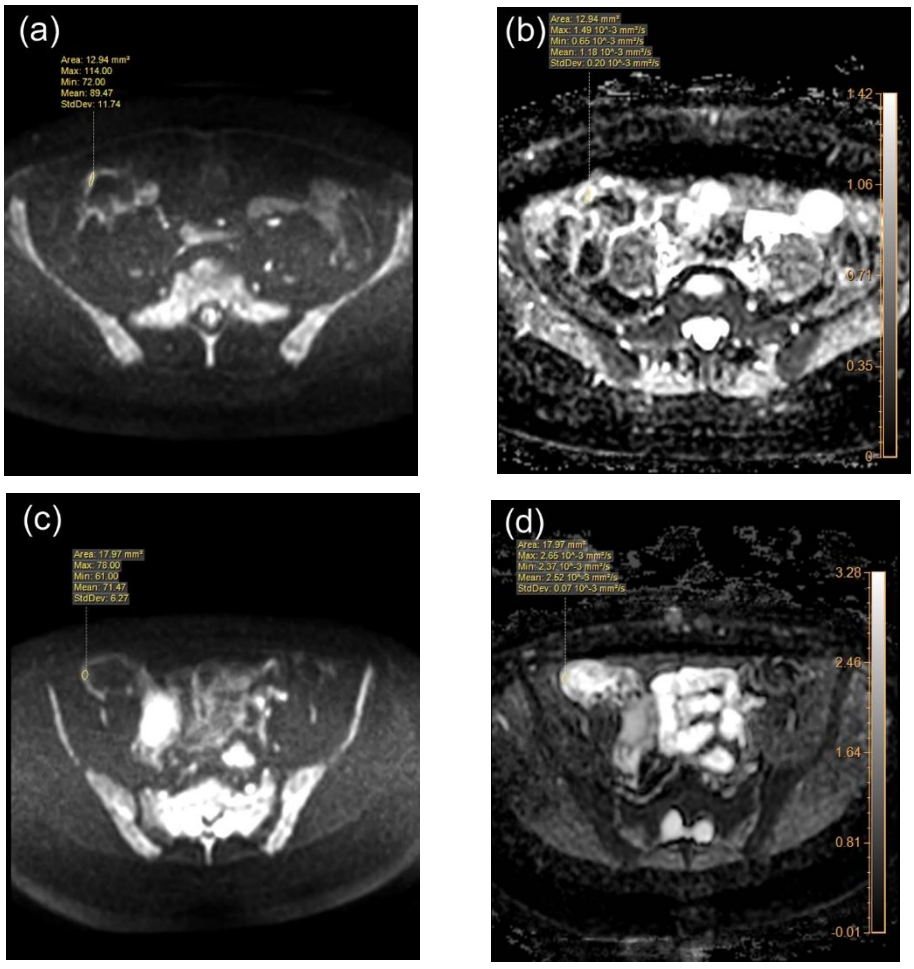

Figure 2.2. **Selecting ROIs for ADC measurements in localisations of false-positive hyperintensity, mimicking inflammation on DWIBS tracking images of b = 800 s/mm^2 of the walls of ascending colon before preparation of patient with mannitol, at presence of intraluminal faeces (a) and after preparation, at presence of enteric contrast agent (b)**
Note the higher SI of colonic wall in presence of mannitol, when compared to the presence of faeces in the colonic lumen. ADC values appear on the ADC map (b, for non-prepared colon, d, for prepared colon). MRE examination of a 45-year-old male patient with dyspeptic complaints, with no morphologically verified inflammatory bowel disease (IBD). Images from the Author's archive.

2.1.5 MRI examination

All patients fasted for at least 6 hours prior to MRE. After the initial scanning of DWI_{SPIR} and DWIBS in the prone position, patients were instructed to intake 1.250–1.500 l of 2.5 % mannitol solution within 45–60 minutes, followed by a full MRE exam in the prone position. During the MRE exam and prior to DWI_{SPIR} and DWIBS sequences, 20 mg dose of butylscopolamin was intravenously administered to reduce bowel peristalsis.

Patients were scanned with 1.5 T MRI system (Ingenia, Philips Medical Systems, Best, the Netherlands) using a 16-channel body coil. The applied DWI_{SPIR} and DWIBS protocols were obtained from the Philips standard abdominal protocol, and included in the protocol repository of the MRI system. To enable DWIBS-ADC measurements, the standard DWIBS protocol was amended by replacing a single b factor b = 1000 by three b factors 0, 600 and 800 s/mm^2, consistent to b values in DWI_{SPIR} protocol.

The scanning parameters for DWI_{SPIR} and DWIBS protocols are given in table 2.1.

Table 2.1

Scanning parameters of DWI_{SPIR} and DWIBS techniques included in the MRE protocol

Scanning Protocol	**DWI_{SPIR}[1]**	**DWIBS[2]**
Sequence	SE-EPI[3]	STIR-EPI[4]
Mode	Single shot	Single shot
Coil	SENSE[5] body	SENSE body
Slice orientation	Axial	Axial
FOV[6]	RL[7] 400 mm, AP[8] 350 mm, FH[9] 303 mm	RL 400 mm, AP 350 mm, FH 303 mm
ACQ[10] voxel size	RL 3.03 mm × AP 3.57 mm × slice thickness 6 mm	RL 2.50 mm × AP 2.98 mm × slice thickness 6 mm
Reconstruction voxel size	RL 1.79 mm × AP 1.79 mm × slice thickness 6 mm	RL 1.39 mm × AP 1.39 mm × slice thickness 6 mm
Fold-over suppression	No	No
Reconstruction matrix	224	288
SENSE	Yes	Yes
P reduction (AP)	2	2.5
Number of stacks	1	1
Type	Parallel	Parallel
Slices	46	46
Slice gap (mm)	0.6	0.6
Slice orientation	Transverse	Transverse
Fold-over direction	AP	AP
Fat shift direction	A	P
TE[11]	66 ms	78 ms
TR[12]	1426 ms	7055 ms

Table 2.1 (End)

Scanning Protocol	DWI_{SPIR}[1]	DWIBS [2]
TI[13]	-	180 ms
Fast imaging mode	EPI[14]	EPI
Flip angle	90°	
Fat suppression	SPIR	STIR
b factors	0, 600, 800 s/mm^2	0, 600, 800 s/mm^2
Respiratory compensation	Trigger	No
Number of signal averages	3	5
Total scan time	4 min. 12 s	5 min. 56 s

[1] DWI_{SPIR} – Diffusion-weighted imaging with spectral pre-saturation with inversion recovery technique. [2] DWIBS – diffusion-weighted imaging with background body signal suppression. [3] SE-EPI – spin echo-echo planar imaging. [4] STIR-EPI – short T1 inversion recovery-echo planar imaging. [5] SENSE – sensivity encoding. [6] FOV – field of view. [7] RL – right-left direction. [8] AP – anterior-posterior direction.[9] FH – foot-head direction.[10] ACQ – acquisition. [11] TE – echo time. [12] TR – repetition time. [13] TI – inversion time. [14] EPI – echo planar imaging.

2.1.6 Image analysis

The ADC values were measured by one radiologist with 17 years of MR experience in abdominal radiology, using standard diffusion calculation software provided by the image post-processing server Intellispace Portal v.5 (Philips Medical Systems, Best, the Netherlands).

2.1.7 Statistical analysis

Statistical analysis was performed using software Stata/IC, mean ADC values were compared with unpaired t-test, and 99 % CI were calculated for differences. The statistical significance of differences between mean values within groups was determined using a one-way ANOVA with Bonferroni correction. P values of < 0.05 were considered to be statistically significant.

2.2 Second study. Investigation of ADC-DWI_{SPIR} and ADC-DWIBS values in patients with MRI signs of active CD and use of ADC-DWI_{SPIR} and ADC-DWIBS values in calculating of Clermont index

The study is described in the publication by Apine, I., Pitura, R., Franckevica, I., Pokrotnieks, J., Krumina, G. 2020. “Comparison between Diffusion-Weighted Sequences with Selective and Non-Selective Fat Suppression in the Evaluation of Crohn’s Disease Activity: Are They Equally Useful?”, *Diagnostics*, 10, 347, pp. 1–21.

2.2.1 Patient population

In this prospective observational cross-sectional study, the patients underwent MRE examinations between April 2016 and April 2019. All patients involved in the research had either symptomatic CD, or they underwent MRE examinations for monitoring the disease course under treatment. The faecal calprotectin levels in all study subjects exceeded 1000 μg/g. The inclusion criteria were: proven active non-stricturing non-penetrating CD in the terminal *ileum,* presenting with thickened bowel wall (thickness > 3 mm), presence of mural oedema (hyperintensity of the bowel wall in T2-weighted images compared to the psoas muscle) (Rimola et al., 2009), signs of restricted diffusion in both DWI_{SPIR} and DWIBS sequences, presenting with high SI in DWI tracking images of b = 800 s/mm^2 along with low SI in the ADC map and early mucosal hyperenhancement in the postGd series (Moy et al., 2016). The exclusion criteria were: locations of CD other than the terminal *ileum*, bowel thickness less than 3 mm, dynamic blurring in either of the DWI or T1 *post*Gd images, inability to locate active bowel wall inflammation in both DWI_{SPIR} and DWIBS sequences, and *post*Gd T1 within one and the same segments.

2.2.2 MRI examination

All patients fasted for 6 hours prior the MRE examination, being allowed to intake only water. No bowel cleansing was carried out. The bowel distension was maintained with 1.000–1.500 mL of 2.5 % mannitol solution, consumed slowly before the MRE procedure for 45 minutes. After that, patients were asked to lie in the right decubitus position, and they received another 250 mL of 2.5 % mannitol solution to intake slowly for another 20 minutes. The MRE examinations were performed with a 1.5T scanner (Ingenia, Philips Medical Systems, Best, The Netherlands) covering the region from the diaphragm to the pelvis with a 16-element phased array body coil. The patients were scanned in the prone position. The MRE protocol included:

1) coronal bTFE (Balanced Turbo Field Echo) cine sequence for real-time assessment of the bowel peristalsis;

2) axial DWI_{SPIR} sequence, using diffusion factors b fixed at 0, 600 and 800 s/mm^2, with corresponding ADC maps;

3) axial DWIBS sequence, using diffusion factors b fixed at 0, 600 and 800 s/mm^2, with corresponding ADC maps;

4) axial and coronal T2-weighted sequences without fat suppression (T2 TSE);

5) axial and coronal T2-weighted sequences with fat suppression (T2 SPAIR);

6) coronal T2 fat suppression magnetic resonance cholangiopancreatography (MRCP) sequence with radial 3D reconstructions;

7) coronal T1-weighted dynamic postcontrast images e-THRIVE (T1 high-resolution isotropic volume excitation), followed by delayed post-contrast axial e-THRIVE images.

The scanning parameters of the DWI_{SPIR} and DWIBS protocols are given in Table 2.1. To reduce bowel peristalsis, hyoscine butylbromide (Buscopan, Sanofi, Athens, Greece) was intravenously administered, prior to the DWI_{SPIR} and DWIBS sequences and the coronal dynamic contrast sequences. The dosage was 10 mg in patients under 50 kg and 20 mg in patients 50 kg or above, diluted in 20 mL of saline solution.

2.2.3 MR image analysis

All measurements used in MR image analysis were standardised across the patient groups. The altered locations of the terminal ileum were identified and divided into approximately 3 cm long segments. The total number of segments was 78, 32 in adults and 46 in paediatric patients. In each segment, wall thickness was measured in mm, the presence of ulcers (present or absent) was estimated, and six measurements of ADC-DWI_{SPIR} and ADC-DWIBS in the corresponding DWI_{SPIR} and DWIBS tracking images of b = 800 s/mm^2 were performed in each segment, in the zone of the highest SI within the bowel wall. Six measurements of the WSI were taken in the same location both before (WSI-*pre*Gd) and after (WSI-*post*Gd) administration of gadolinium contrast medium, in the site with the highest SI in the postcontrast images. Six measurements of SD representing the image noise were performed outside the body before (SD-*pre*Gd) and after (SD-*post*Gd) administration of gadolinium contrast medium (Rimola et al., 2009). The mean value of all measurements was used for calculations. In each altered bowel segment MaRIA was calculated using the following formula:

$$\text{MaRIA} = 1.5 \times \text{wall thickness (mm)} + 0.02 \times \text{RCE} + 5 \times \text{oedema} + 10 \times \text{ulcers},$$

where the presence or absence of ulcers and oedema was rated as 1 or 0, accordingly. RCE was calculated as follows:

$$\text{RCE} = (\text{WSI-}post\text{Gd} - \text{WSI-}pre\text{Gd})/(\text{WSI-}pre\text{Gd})) \times 100 \times (\text{SD-}pre\text{Gd}/\text{SD-}post\text{Gd})$$

where the SD-*pre*Gd and SD-*post*Gd corresponded to the mean of the six SD values of SI, measured outside of the body before and after gadolinium administration, accordingly (Rimola et al., 2009). Since oedema was one of the inclusion criteria representing inflammation, it was always present, and its rating was always equal to 1. The Clermont score or DWI-MaRIA for both DWI_{SPIR} and DWIBS sequences was calculated per formula (Hordonneau et al., 2014):

$$\text{DWI-MaRIA} = 1.646 \times \text{bowel thickness} - 1.321 \times \text{ADC} + 5.613 \times \text{oedema} + 8.306 \times \text{ulceration} + 5.039$$

The i/v gadolinium CA used before October 2018 for all adult patients and all but two children was gadodiamide (Omniscan 0.05 mmol/mL, GE Healthcare, Cork, Ireland, dosage 0.2 mL/kg, or 0.1 mmol/kg). Gadobutrol (Gadovist 1 mmol/mL, Bayer, Berlin, Germany, dosage 0.1 mL/kg, or 0.1 mmol/kg) was used for the two paediatric patients examined after October 2018.

The ADC, WSI and SD measurements were performed using 4–9 mm^2 oval ROI. The image analysis and the measurements were performed by one radiologist with 19 years' experience in abdominal MRI imaging. The review of images and ADC measurements were performed using a dedicated Philips Intellispace Portal postprocessing server, v. 5.0 (Philips Medical Systems, Best, the Netherlands, 2014). The WSI and image noise measurements were performed using Clear Canvas DICOM Viewer, v. 13.2 (Synaptive Medical, Toronto, ON, Canada, 2019).

2.2.4 Statistical analysis

The statistical analysis was performed using software SPSS 20.0 (IBM Corporation, Armonk, NY, USA, 2011). The median values with SD for ADC-DWI_{SPIR} and ADC-DWIBS, MaRIA, DWI_{SPIR}-Clermont, and DWIBS-Clermont scores were calculated. 95 % CI was calculated for median differences. The statistical significance of differences between the groups was determined using the Wilcoxon signed rank test. Spearman's correlation coefficient was used to assess the correlations between quantitative parameters. P values of < 0.05 (two-tailed) were chosen as a level of statistical significance. The Bonferroni correction was used to control Type 1 error in multiple comparisons.

2.3 Third study. Evaluation of repeatability of magnetic resonance measurements used to determine CD activity

The study is described in the publication by Apine, I., Pirksta, I., Pitura, R., Pokrotnieks, J., Pukite, I., Krumina, G. 2020. "Repeatability of magnetic resonance measurements used for estimating the Crohn's disease activity", *Proceedings of the Latvian Academy of Sciences*. Section B. Volume 74, No 2 (725), pp.75–82.

2.3.1 Patient population

The study involved 17 patients (5 adults, 23–57 y.o., and 12 children, 10–17 y.o.; see Table 2.2 for details) with faecal calprotectin levels over 1000 μg/mg and histologically proven active Crohn's non-stricturising and non-penetrating disease in the terminal *ileum*, and signs of active Crohn's disease in MRE examination: these signs included small bowel wall thickness > 3 mm, presence of mural oedema (hyperintensity of the bowel wall in T2-weighted images comparing to the psoas muscle) (Rimola et al., 2009), signs of active inflammation in DWI_{SPIR} sequence (high SI in DWI tracking images of b=800 s/mm^2, along with low SI in the ADC map) and early mucosal hyperenhancement in the series following administration of gadolinium CA (postGd) (Moy et al., 2016). CD located outside the terminal *ileum*, areas of bowel thickness of less than 3 mm, lack of signs of active bowel wall inflammation in DWI_{SPIR}, DWIBS and *post*Gd T1 series within one and the same segments, and dynamic blurring in either of the DWI or T1 *post*Gd images were not accepted for performing measurements.

Table 2.2

Demographic data of patients included in the study

Data	Adult group	Paediatric group
Gender	Males; n = 4, females; n = 1	Males; n = 9, females; n = 3
Age	23 y.o.; n = 1, 25 y.o.; n = 1, 36 y.o.; n = 1, 40 y.o.; n = 1, 57 y.o.; n = 1	11 y.o.; n = 2, 12 y.o.; n = 3, 13 y.o.; n = 1, 14 y.o.; n = 4, 17 y.o.; n = 2

According to the Montreal and Paris classification of CD (Moon, 2019), the phenotype of 10 patients was A1 L1 B1, the phenotype of the remaining seven patients was A2 L1 B1.

2.3.2 MRI examination

All patients were examined without prior bowel cleansing. Fasting was required 6 hours prior to MRE procedures. Patients were asked to slowly intake 1.000–1.500 ml of 2.5 % peroral mannitol solution 45 minutes prior to the MRI procedure, and then to lie in the right decubitus position, drinking extra 250 ml of 2.5 % mannitol solution for another 20 minutes. The MRE examinations were performed with 1.5T MRI scanner (Ingenia, Philips Medical Systems, Best, the Netherlands), covering the region from the diaphragm to the pelvis with a 16-channel body coil. All patients were scanned in the prone position.

The MRE protocol included:

1) coronal breath-hold balanced turbo field echo (bTFE) cine *sequence* for real-time assessment of the *bowel* peristalsis;

2) axial and coronal breath-hold turbo spin echo, T2-weighted sequences without fat suppression (T2 TSE);

3) axial and coronal breath-hold spectral attenuated enversion recovery T2-weighted sequences with fat suppression (T2 SPAIR);

4) axial respiratory triggered conventional DWI sequence – DWI with spectral pre-saturation inversion recovery (SPIR) fat saturation technique, using diffusion factors b fixed at 0, 600 and 800 s/mm2, with the corresponding ADC map;

5) axial free-breathing DWIBS sequence – DWI with Short T1 Inversion Recovery (STIR) fat saturation technique, using diffusion factors b fixed at 0, 600 and 800 s/mm^2, with the corresponding ADC map,

6) coronal respiratory triggered T2 fat suppression magnetic resonance cholangiopancreatography (MRCP) sequence with radial 3D reconstructions;

7) coronal breath-hold dynamic T1-weighted high-resolution isotropic volume (THRIVE), where scanning was started simultaneously with intravenous administration of gadolinium contrast media. Gadodiamide (Omniscan) 0.05 mmol/ml, GE Healthcare, dosage 0.2 ml/kg, or 0.1 mmol/kg was used in patients before October 2018, except in 2 children examined after October 2018, who received gadobutrol (Gadovist) 1 mmol/ml, Bayer, dosage 0.1 ml/kg, or 0.1 mmol/kg.

To stop intestinal peristalsis, hyoscine butylbromide (Buscopan, Sanofi) was administered in slow intravenous injection prior to DWI_{SPIR} and DWIBS sequences as well as the dynamic contrast sequences. A dosage of 10 mg was used in patients under 50 kg, increased to 20 mg in patients of 50 kg or above, and the dose was diluted in 20 ml of saline solution.

2.3.3 Image analysis

The measurements were performed by one radiologist with 19 years' experience in gastrointestinal MRI imaging, and repeated by the same radiologist after two months.

The measurement approach was standardised. Prior to measurements, the whole parts of the inflamed terminal *ileum* were divided into approximately 3 cm long segments (n = 32 in adult patients, n = 46 in children), and the below process was performed when taking measurements in each of the segments: 1) one measurement of bowel wall thickness was performed in the location of the largest thickness, 2) presence or absence of ulcers was defined (1 – yes, 0 – no), 3) three measurements of ADC of the DWI_{SPIR} (Fig. 2.4.a), and ADC of the DWIBS (Fig. 2.5.a) were performed at the site of the maximum SI within the inflamed bowel wall. The ADC value along with the ROI was automatically propagated on the corresponding ADC map (Fig. 2.4.b for DWI_{SPIR} and 4.5.b for DWIBS), 4) three measurements of WSI were

taken before (WSI-*pre*GD) and after (WSI-*post*Gd) administration of gadolinium contrast medium in exactly the same locations of the highest SI in the bowel wall in both DWI sequences, and 5) three measurements of the image noise – SD were performed outside the patient's body before (SD-*pre*Gd) and after (SD-*post*Gd) administration of the contrast medium (Rimola et al., 2009). The ADC, WSI and SD measurements were performed using 4–9 mm^2 oval ROI. The average values of the three measurements of ADC, WSI and SD were used for further calculations.

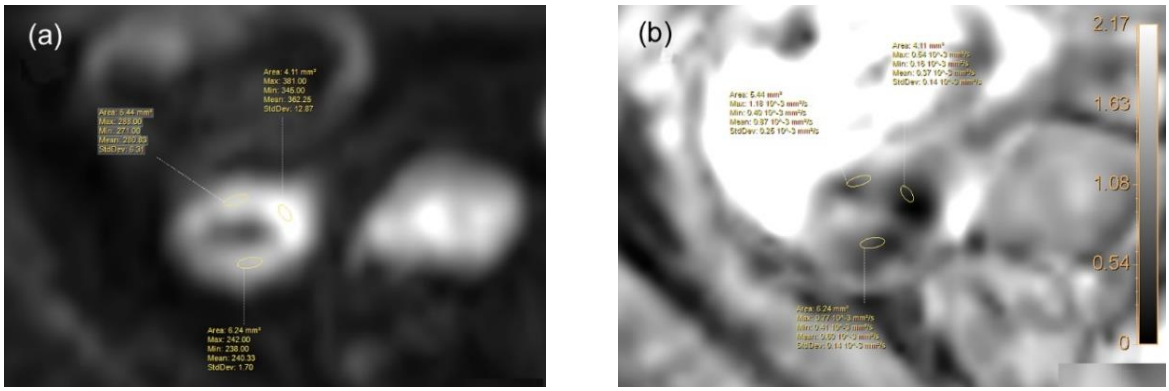

Figure 2.4. **Selecting the ROI for ADC measurements in DWI$_{SPIR}$ images of b = 800 s/mm^2 (a)**.
On the corresponding ADC map (b), the chosen ROI appears automatically. MRE of a 56-year old male patient with proven CD in the terminal ileal loop. Images from the Author's archive.

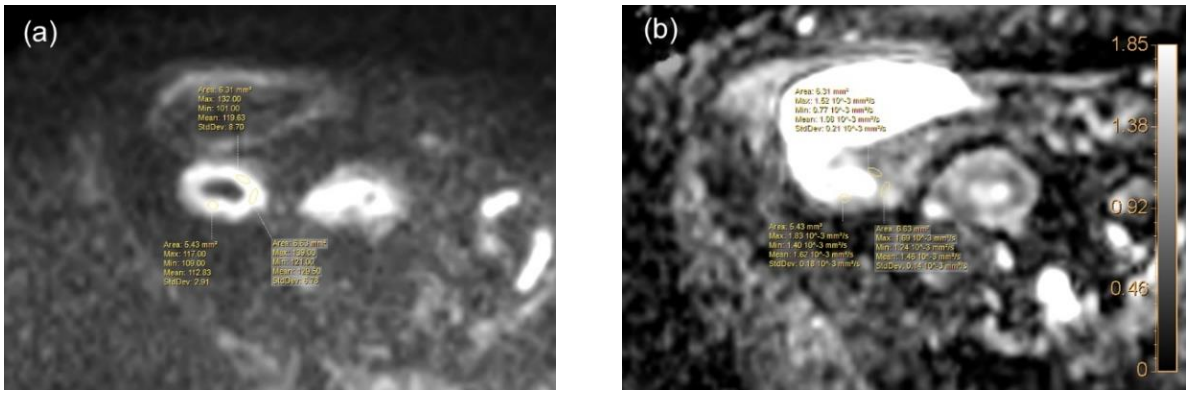

Figure 2.5. **Selecting the ROI for ADC measurements in DWIBS images of b = 800 s/mm^2 (a)**.
On the corresponding ADC map (b), the chosen ROI appears automatically. MRE of a 56-year old male patient with proven CD in the terminal ileal loop. Images from the Author's archive.

In each inflamed segment, segmental MaRIA score was calculated per formula:

1.5 × bowel thickness (mm) + 0.02 × RCE + 5 × oedema + 10 × ulceration.

The presence of ulcers was rated as 1 and absence of ulcers – as 0, RCE was calculated per: RCE = (WSI-*post*Gd – WSI-*pre*Gd)/(WSI-*pre*Gd) × 100 × (SD-*pre*Gd/SD-*post*Gd), where the SD-*pre*Gd and SD-*post*Gd corresponded to the mean of the three SD values of the SI. This

was measured outside of the body before and after administration of gadolinium contrast medium, accordingly (Rimola et al., 2009). Since oedema was a criterion of inclusion in the study, it was present in all patients and was always equal to 1.

The Clermont score, or DWI-MaRIA, for both DWI_{SPIR} and DWIBS sequences, was calculated per formula:

DWI-MaRIA = 1.646 × bowel thickness - 1.321 × ADC + 5.613 ×

oedema + 8.306 × ulceration + 5.039 (Hordonneau et al., 2014).

Similar to calculating MaRIA score, presence of ulcers was rated as 1, absence of ulcers – as 0, and presence of oedema was rated as 1.

The assessment of images and measurements of ADC values was performed using a dedicated post-processing server Philips Intellispace Portal 5.0 (Philips Medical Systems, Best, the Netherlands). WSI and image noise measurements were performed using Clear Canvas DICOM Viewer, v. 13.2 (Synaptive Medical, Toronto, Canada, 2019).

2.3.4 Statistical analysis

Statistical analysis was performed using software Stata/IC (StataCorp LLC, Texas, USA). The mean values and SD were calculated for DWI_{SPIR} and DWIBS-based ADC, as well as RCE, MaRIA and Clermont scores. The mean values of the first and second measurement were compared, and statistical significance of the differences was tested using a paired t-test; 95 % confidence intervals (CI) were calculated for differences. The statistical significance of difference was determined using one-way ANOVA with Bonferroni correction. P value of < 0.05 was considered as statistically significant. The presence or absence of ulcers was evaluated with Pearson χ^2 test.

3. Results

3.1 First study. Effect of prior preparation of the patient's intestinal tract with enteric hyperosmolar CA, on the ADC-DWI$_{SPIR}$ and ADC-DWIBS values of the intestinal and large bowel walls

3.1.1 First cohort: Comparison of ADC-DWI$_{SPIR}$ and ADC-DWIBS measurements in unprepared and prepared walls of small intestines

To perform the ADC measurements amongst the 106 patients, ADC-DWI$_{SPIR}$ was measured in 91 collapsed and 106 distended jejunal segments. ADC-DWIBS was measured in 86 collapsed and in 95 distended jejunal segments. Comparisons were drawn by analysis of segment pairs before and after preparation as follows; 88 segment pairs for comparison between ADC-DWI$_{SPIR}$ and 83 pairs for ADC-DWIBS. For comparison, between ADC-DWI$_{SPIR}$ and ADC-DWIBS before preparation, 85 segment pairs were analysed, and 95 pairs were analysed to compare ADC-DWI$_{SPIR}$ and ADC-DWIBS after preparation. The ADC-DWI$_{SPIR}$ and ADC-DWIBS values of the walls of non-prepared and prepared small intestines are given in Table 3.1.

Table 3.1

The ADC-DWI$_{SPIR}$ and ADC-DWIBS values of the walls of non-prepared and prepared small intestines (*jejunum*)

	Minimum value	Maximum value	Mean value	Median value	SD
Non-Prepared (collapsed) *jejunum*, ADC-DWI$_{SPIR}$ value $\times 10^{-3}$ mm^2/s	0.30	2.5	1.09	1.07	0.37
Prepared (filled) *jejunum*, ADC-DWI$_{SPIR}$ value $\times 10^{-3}$ mm^2/s	0.59	2.71	1.76	1.72	0.41
Non-prepared (collapsed) *jejunum*, ADC-DWIBS value $\times 10^{-3}$ mm^2/s	0.07	2.49	0.91	0.90	0.47
Prepared (filled) *jejunum*, ADC-DWIBS value $\times 10^{-3}$ mm^2/s	0.53	2.97	1.75	1.82	0.51

In both DWI$_{SPIR}$ and DWIBS sequences, the study found marked significant difference between ADC of non-prepared and prepared bowels. In both DWI$_{SPIR}$ and DWIBS ADC, the

values of non-prepared *jejunum* were lower than in prepared *jejunum*. The difference between mean values of non-prepared and prepared bowel was 38.1 % in DWI_{SPIR} and 48 % – in DWIBS (Table 3.2).

Table 3.2

Comparison of ADC values between DWI_{SPIR} and DWIBS in walls of non-prepared and prepared *jejunum*

Bowel preparation status	**Non-prepared (collapsed) *jejunum***	**Prepared (filled) *jejunum***	**p value**	**Difference between mean ADC values of filled vs. collapsed jejunal loops**
Mean ADC-DWI_{SPIR} value $\times 10^{-3}$ mm^2/s	1.09 (SD = 0.37)	1.76 (SD = 0.41)	< 0.0001	0.67 (38.1 %)
Mean ADC-DWIBS value $\times 10^{-3}$ mm^2/s	0.91 (SD = 0.47)	1.75 (SD = 0.51)	< 0.0001	0.84 (48 %)

Within the walls of non-prepared *jejunum,* our data showed a statistically significant ADC difference ($p < 0.0001$) of 16.5 % between DWI_{SPIR} and DWIBS, being lower in DWIBS. No significant ADC difference ($p = 0.84$) between DWI_{SPIR} and DWIBS was observed within walls of prepared *jejunum.*

3.1.2 Second cohort: Comparison of ADC-DWI_{SPIR} and ADC-DWIBS measurements in walls of non-prepared and prepared large intestines

To perform the ADC measurements amongst the 106 patients, ADC-DWI_{SPIR} was measured in 41 non-prepared and in 42 prepared *caecum* or ascending colon segments. ADC-DWIBS was measured in 25 non-prepared *caecum* or ascending colon segments, and in 18 prepared *caecum* or ascending colon segments. 41 segment pairs were analysed for comparison between ADC-DWI_{SPIR} before and after preparation, and 18 segment pairs were analysed to compare ADC-DWIBS before and after preparation. For comparison between ADC-DWI_{SPIR} and ADC-DWIBS before preparation 25 segment pairs were analysed, and 18 pairs were analysed to compare ADC-DWI_{SPIR} and ADC-DWIBS after preparation. The ADC-DWI_{SPIR} and ADC-DWIBS values of the walls of non-prepared and prepared large intestines (*caecum/colon ascendens*) are presented in Table 3.3.

Table 3.3

The ADC-DWI$_{SPIR}$ and ADC-DWIBS values of the walls of non-prepared and prepared large intestines (*caecum/colon ascendens*).

	Minimum value	**Maximum value**	**Mean value**	**Median value**	**SD**
Non-Prepared (with intraluminal faecal content) *caecum/colon ascendens*, ADC-DWI$_{SPIR}$ value $\times 10^{-3}$ mm^2/s	0.78	2.68	1.41	1.43	0.31
Prepared (with intraluminal mannitol substrate) *caecum/colon ascendens*, ADC-DWI$_{SPIR}$ value $\times 10^{-3}$ mm^2/s	1.19	2.89	2.13	2.16	0.41
Non-Prepared (with intraluminal faecal content) *caecum/colon ascendens*, ADC-DWIBS value $\times 10^{-3}$ mm^2/s	0.18	2.49	1.01	1.04	0.41
Prepared (with intraluminal mannitol substrate*) caecum/colon ascendens*, ADC-DWIBS value $\times 10^{-3}$ mm^2/s	1.07	3.25	2.04	1.98	0.58

In both DWI$_{SPIR}$ and DWIBS sequences, the study found marked significant difference between ADC in non-prepared and prepared bowels. In both DWI$_{SPIR}$ and DWIBS ADC, values of the non-prepared colon were lower than in the prepared colon. The ADC differences between non-prepared and prepared bowel was 33.8 % in DWI$_{SPIR}$ and 50.5 % – in DWIBS. The ADC values are presented in Table 3.4.

Table 3.4

Comparison of ADC values between DWI_{SPIR} and DWIBS in walls of non-prepared and prepared *colon*

Bowel preparation State	**Non-prepared (with intraluminal faecal content) *caecum/colon ascendens***	**Prepared (with intraluminal mannitol substrate) *caecum/colon ascendens***	**p value**	**Difference between mean ADC values of prepared vs. non prepared colonic walls**
Mean ADC-DWI_{SPIR} value $\times 10^{-3}$ mm^2/s	1.41 (SD = 0. 31)	2.13 (SD = 0.41)	< 0.0001	0.72 (33.8 %)
Mean ADC-DWIBS value $\times 10^{-3}$ mm^2/s	1.01 (SD = 0.40)	2.04 (SD = 0.58)	< 0.0001	1.03 (50.5 %)

By mutually comparing ADC-DWI_{SPIR} and ADC-DWIBS values within walls of both non-prepared and prepared colon, the data showed statistically significant ADC differences ($p < 0.0001$) of 28.4 % between DWI_{SPIR} and DWIBS, being lower in DWIBS. No significant ADC difference ($p = 0.58$) between DWI_{SPIR} and DWIBS values was found.

3.2 Second study. Investigation of ADC-DWI_{SPIR} and ADC-DWIBS values in patients with MRI signs of active CD, and the use of ADC-DWI_{SPIR} and ADC-DWIBS values in calculating of Clermont index

During the study, 57 patients – 20 adults and 37 children – with active Crohn's disease underwent MRE examination. Amongst them, 17 patients – five adults (23, 25, 36, 40 and 57 years old) and 12 children (11 years old; n = 2, 12 years old; n = 3, 13 years old; n = 1, 14 years old; n = 4, 17 years old; n = 2) were enrolled in the study as meeting the study criteria. 15 adults and 25 children did not meet the study criteria: in 14 patients (6 adults and 8 children) CD was localised in the colon, and in 3 paediatric patients it was localised in the *jejunum*. 9 patients (1 adult and 8 children) with ileal CD had history of resection of the terminal *ileum*. 7 patients (2 adults and 5 children) had MR appearance of CD, but the diagnosis was not endoscopically proven. 5 adult patients with the history of known proven CD had no conclusive visual signs of CD. Images of one adult patient showed blurring in T1 postcontrast images, and images of one paediatric patient showed both blurring in conventional DWI and T1 post-contrast images.

Amongst the enrolled 17 patients, in one adult patient the duration of medical history prior to the MRE examination was more than two years, in three adult patients – from 6 till 12 months, but in one adult patient CD was asymptomatic, of unknown length, and was detected upon performing a set of infertility tests. In one paediatric patient, the duration of CD was slightly less than two years, but in the remaining 11 patients the duration of medical history was less than 6 months.

The overview of measured ADC-DWI_{SPIR} and ADC-DWIBS values, as well as calculated values of MaRIA, DWI_{SPIR}-based Clermont score and DWIBS-based Clermont score, is presented in Table 3.5.

Table 3.5

Values of ADC-DWI_{SPIR}, ADC-DWIBS, MaRIA as well as ADC-DWI_{SPIR} and ADC-DWIBS-based Clermont scores in the groups of adult and paediatric patients

Measurement	N	Minimum value	Maximum value	Median value	SD
ADC-DWI_{SPIR} (mm^2/s), adults	32	0.66×10^{-3}	2.16×10^{-3}	1.26×10^{-3}	0.29
ADC- DWI_{SPIR} (mm^2/s), children	46	0.18×10^{-3}	2.23×10^{-3}	1.13×10^{-3}	0.31
ADC-DWIBS (mm^2/s), adults	32	0.01×10^{-3}	2.37×10^{-3}	1.15×10^{-3}	0.49
ADC-DWIBS (mm^2/s), children	46	0.20×10^{-3}	2.74×10^{-3}	1.16×10^{-3}	0.44
MaRIA, adults	32	10.65	36.65	24.43	5.31
MaRIA, children	46	9.96	37.67	22.08	6.67
ADC-DWI_{SPIR}-based Clermont score, adults	32	12.85	39.23	26.23	4.76
DWI_{SPIR}-based Clermont score, children	46	13.59	40.74	23.53	5.42
DWIBS-based Clermont score, adults	32	5.92	38.78	24.28	4.65
DWIBS-based Clermont score, children	46	8.25	39.52	24.39	5.77

There was a statistically significant difference of 10.32 % ($p = 0.02$) between the median values of ADC-DWI_{SPIR} in adults and children, appearing lower in children than in adults; no statistically significant difference ($p = 0.38$) between ADC-DWIBS in adults and children was detected. There was a statistically significant difference of 8 % ($p = 0.03$) between ADC-DWI_{SPIR} and ADC-DWIBS values in adults, appearing lower in DWIBS, but no statistically significant difference ($p = 0.97$) between ADC-DWI_{SPIR} and ADC-DWIBS values in children.

The graphical comparative distribution of the ADC-DWI$_{SPIR}$ and ADC-DWIBS values between both patient groups is shown in Fig. 3.1 a and b. The graphical comparative distribution of the ADC-DWI$_{SPIR}$ and ADC-DWIBS values within each of the patient groups is shown in Fig. 3.2, a and b.

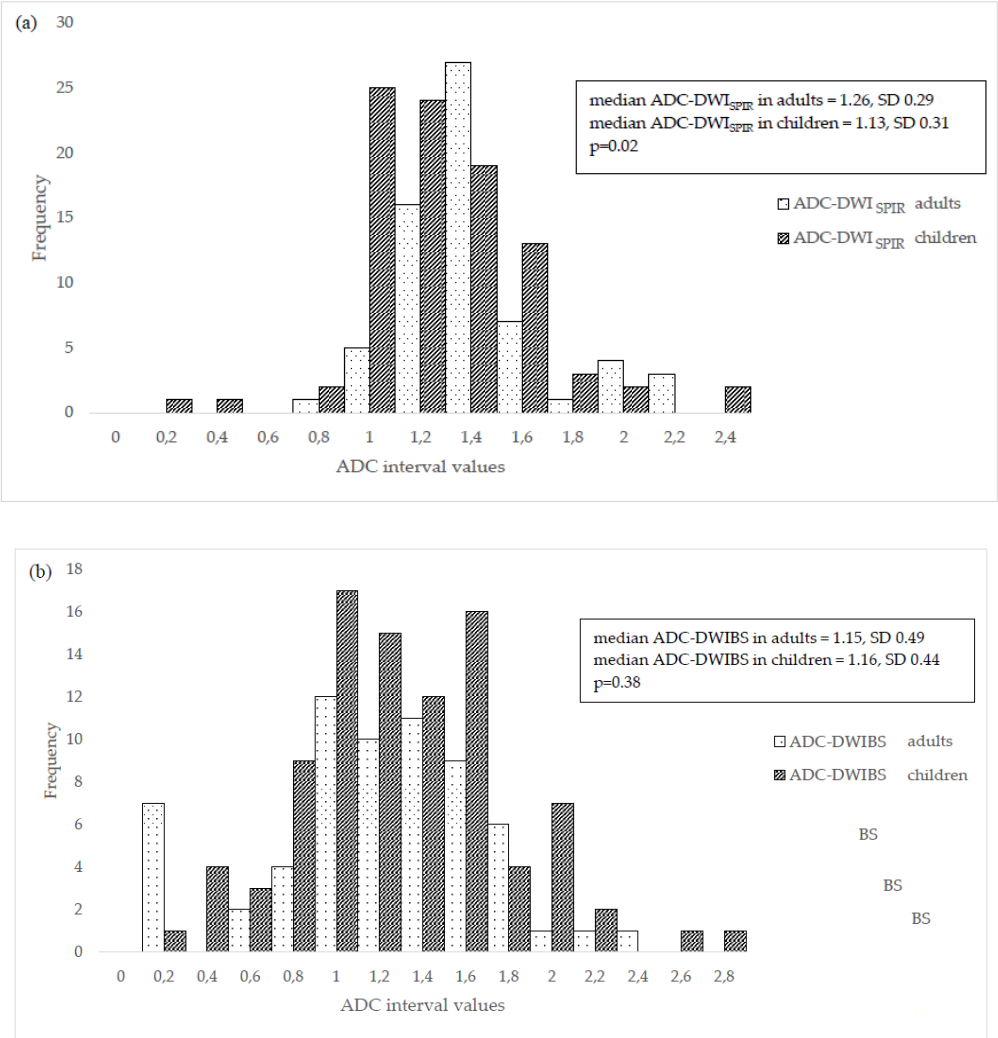

Figure 3.1 **Comparison of ADC-DWI$_{SPIR}$ values (a), and ADC-DWIBS values (b) between adults and children**

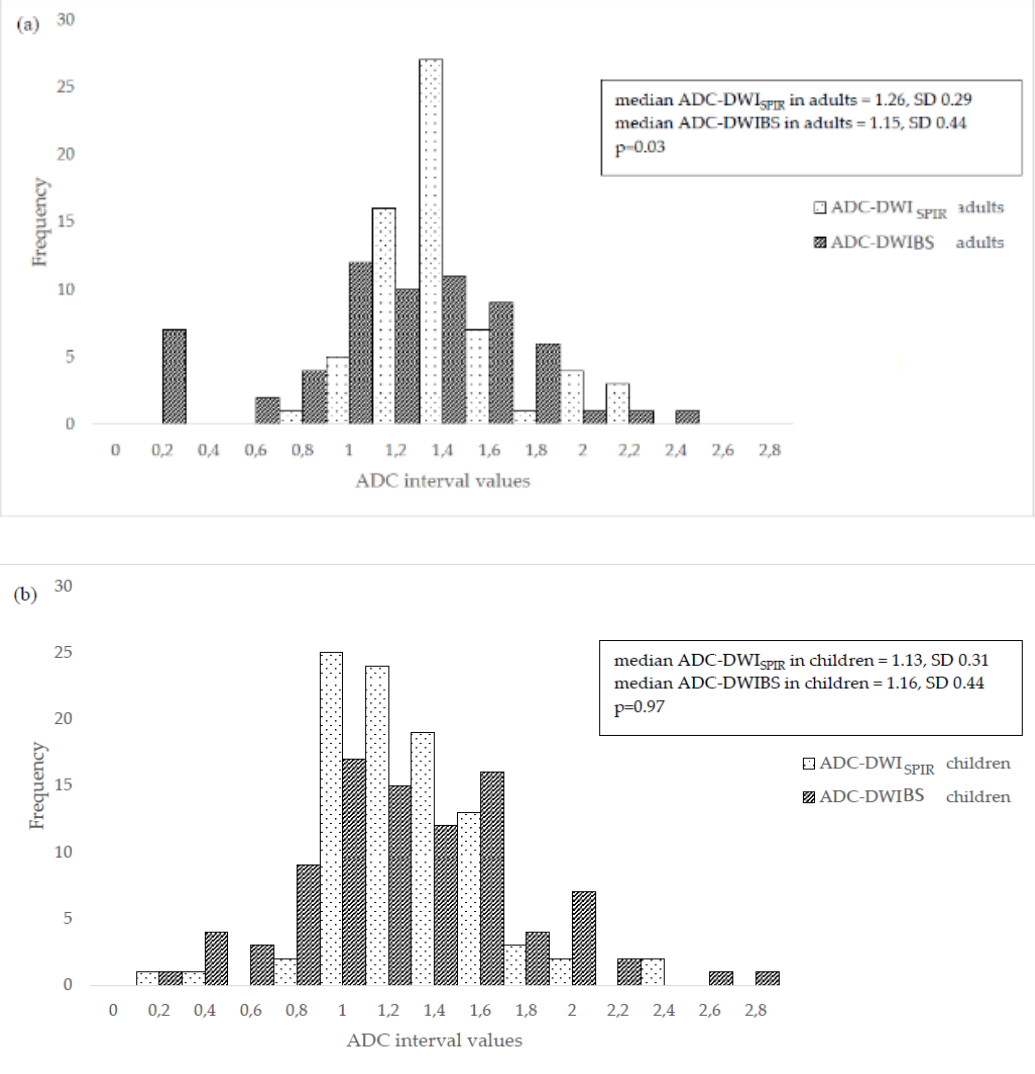

Figure 3.2. **Comparison between ADC-DWI$_{SPIR}$ and ADC-DWIBS values in adults (a) and in children (b)**

In all patients of both groups the MaRIA value corresponded to active disease (i.e., ≥ 7) (Rozendorn et al., 2018). Excluding one patient with the score value of 10.65, MaRIA score values in all adult patients also corresponded to severe disease (i.e., ≥ 11). In the paediatric group, in all but three patients, with the values of 9.95, 10.25 and 10.66, MaRIA values exceeded 11 thus corresponding to severe disease (Rozendorn et al., 2018).

In all patients of both groups, the DWI$_{SPIR}$-based Clermont score value corresponded not only to active disease (i.e., > 8.4) but severe disease (i.e., ≥ 12.5). In two adult patients, the DWIBS-based Clermont score values (i.e., 5.92 and 8.20) were below the threshold of 8.4 for active disease, however the values of all other patients corresponded both to active and to severe disease. In one paediatric patient, the DWIBS-based Clermont score value (i.e., 8.24) was slightly below the threshold of 8.4 for active disease; two patients with values of 11.26 and 12.38 corresponded to active disease, and all other patients corresponded to severe disease (Rozendorn et al., 2018).

The correlation between ADC-DWI$_{SPIR}$ and ADC-DWIBS was weak and statistically unreliable in both adults (rho = 0.27; p = 0.13) (Fig. 3.3a) and children (rho = 0.22; p = 0.15) (Fig. 3.3b).

There was a strong and statistically significant correlation between MaRIA and ADC-DWI$_{SPIR}$-based Clermont score in both adults (rho = 0.93; p < 0.0001) (Fig. 3.4a) and in children (rho = 0.98; p < 0.0001) (Fig. 3.4b). There was also a strong and statistically significant correlation between MaRIA and ADC-DWIBS-based Clermont score in adults (rho = 0.89; p < 0.0001) (Fig. 3.5a) and in children (rho = 0.95; p < 0.0001) (Fig. 5.5b). The correlation between ADC-DWI$_{SPIR}$ and MaRIA was a moderate negative and statistically reliable in both adults (rho = -0.50, p = 0.004) (Fig. 3.6a) and children (rho = -0.54, p < 0.0001) (Fig. 3.6b). There was no correlation between ADC-DWIBS and MaRIA (rho = -0.001, p = 0.99) in adults (Fig. 3.7a), and a low negative statistically reliable correlation (rho = -0.374, p = 0.01) in children (Figure 3.7b).

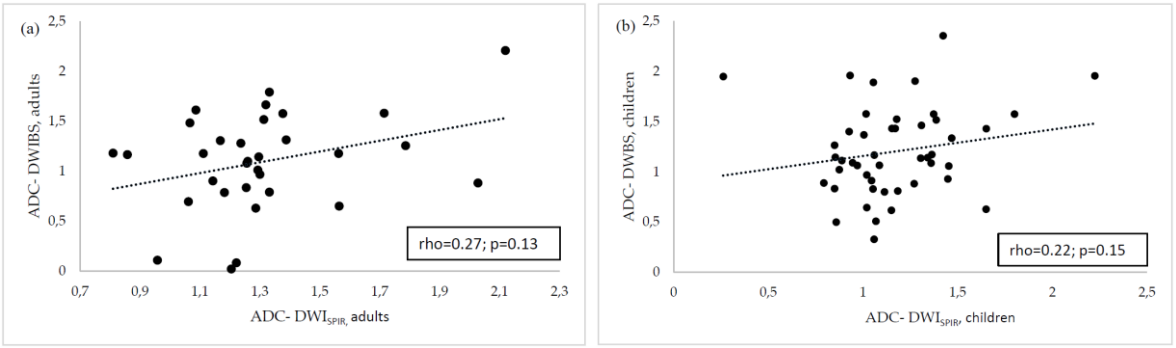

Figure 3.3. **Correlation curve between ADC-DWI$_{SPIR}$ and ADC-DWIBS in adults (a) and children (b) showing no correlation**

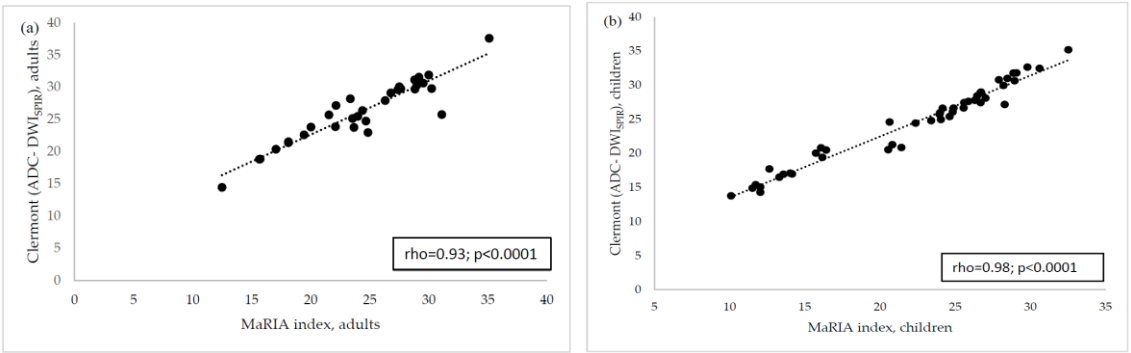

Figure 3.4 **Correlation curve between MaRIA and ADC-DWI$_{SPIR}$-based Clermont score in adults (a) and children (b) showing high correlation**

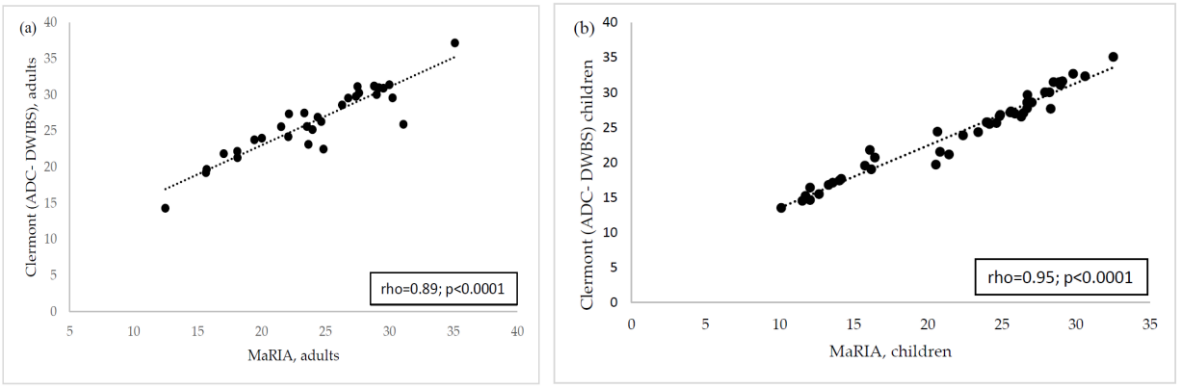

Figure 3.5. **Correlation curve between MaRIA and ADC-DWIBS-based Clermont score in adults (a) and children (b) showing high correlation**

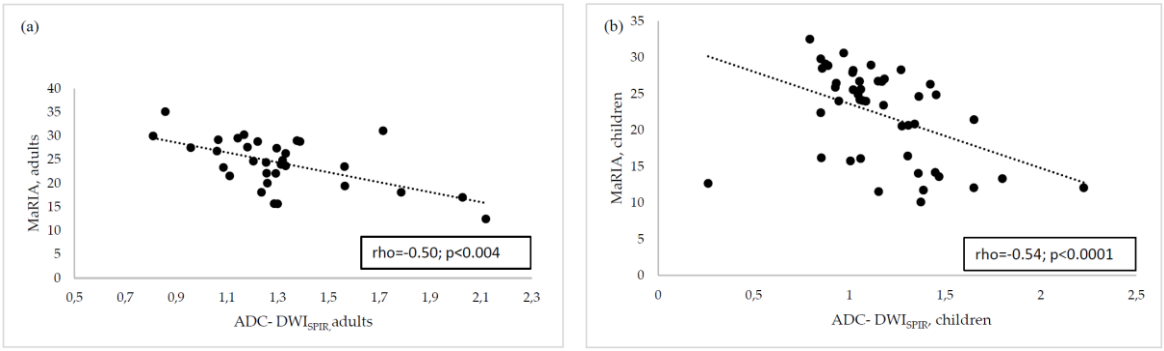

Figure 3.6. **Correlation curve between ADC-DWI$_{SPIR}$ and MaRIA in adults (a) and children (b) showing moderate negative correlation**

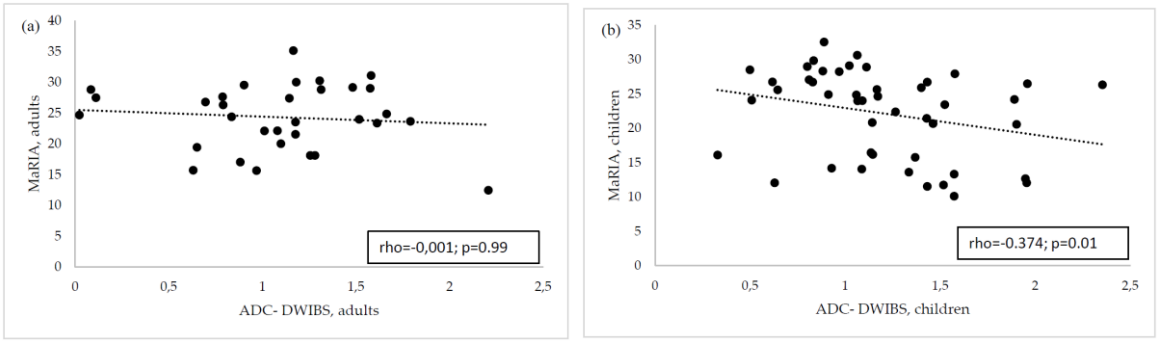

Figure 3.7. **Correlation curve between ADC-DWIBS and MaRIA in adults (a) showing no correlation and in children (b) showing low negative correlation**

3.3 Third study. Evaluation of repeatability of magnetic resonance measurements used to determine CD activity

No statistically significant difference was observed between the two measurements performed by a single observer, either in the measurement of the bowel wall thickness ($p = 0.42$), or in the assessment of ADC-DWI$_{SPIR}$ values ($p = 0.65$) and ADC-DWIBS values ($p = 0.23$). There was also no statistically significant difference between the two measurements performed by a single observer in the assessment of WSI-*pre*Gd ($p = 0.06$) or WSI *post*Gd

(p = 0.57). The highest absolute difference between two measurements was observed for WSI-*pre*Gd measurements being 8 %, and the lowest absolute difference – for ADC-DWI_{SPIR} measurements being 1 %. The results of measurements, along with absolute differences between the two measurements, are presented in Table 3.6.

Table 3.6

Numerical values of the first and the second measurements of the bowel wall thickness, ADC-DWI_{SPIR} and ADC-DWIBS, WSI-*pre*Gd and WSI-*post*Gd

Measurement	First assessment (mean)	Second assessment (mean)	Difference	
			Difference (%)	p value
Wall thickness (mm)	6.4	6.6	0.2 (5 %)	0.42
ADC-DWI_{SPIR} (mm^2/s)	1.219 (SD 0.320)	1.227 (SD 0.321)	0.008 (1 %)	0.65
ADC-DWIBS (mm^2/s)	1.180 (SD 0.505)	1.132 (SD 0.478)	0.048 (4 %)	0.23
WSI-*pre*Gd	162.925 (SD 127,57)	150.305 (SD 99.68)	12.61 (8 %)	0.06
WSI-*post*Gd	336.39 (SD 235,35)	316.11 (SD 212,90)	20.33 (6 %)	0.57

For the assessment of presence of bowel ulcers between the 1st and the 2nd assessment, the Pearson χ^2 was 13.70 ($p < 0.0005$), indicating a systemic difference between the two assessments of absence or presence of ulcers. The results of the assessment of presence or absence of ulcers are presented in Table 3.7.

Table 3.7

Evaluation of first and the second measurements of the presence/absence of ulcers

Evaluation	Ulcers	Number of segments	%	Pearson χ^2	p Value
First	Absence	43	55.13	13.70	< 0.0005
	Presence	35	44.87		
Second	Absence	26	33.33		
	Presence	52	66.67		

4. Discussion

4.1 Use of the DWIBS sequence in primary diagnostics of CD (first study)

The use of DWI has been shown to improve the accuracy of CD diagnosis, to assess the disease activity, and to assist in the dynamic follow-up by evaluation of the effectiveness of treatment. It also is able to replace the i/v CA administration (Dohan et al., 2016). However, despite sensitivity of the method up to 100 %, its disadvantage is the low specificity of 39–61 %. The reason for the low specificity of DWI, is the high intensity signal in DWI tracking images with high b values in the intestinal wall. This phenomenon is usually explained by the T2 "shine-through" effect, which is related to the long T2 relaxation time of tissues. Although in this case ADC values in intact bowel walls should be high (Koh et al*.,* 2012), and in the case of inflammatory changes – low, high SI in the DWI tracking images in combination with low ADC values, is observed not only in inflamed, but also in intact intestinal walls. (Jesuratnam-Nielsen et al*.*, 2015b).

According to a number of studies, the performance of DWI varies among authors. The range of ADC values in the normal bowel wall was 1.18–3.69 mm^2/s, whereas in inflamed bowel segments – 1.24–1.988 mm^2/s, being significantly lower by 0.8–2.4 $\times 10^{-3}$ mm^2/s than in intact bowels. Several authors have also provided their cut-off ADC values for discriminating between inflamed and intact bowel walls. These values are mutually different and lie between the ADC ranges of inflamed and intact bowel walls, except in one study where the cut-off value lies within the range of the inflamed bowel. According to the data from all researchers, ADC ranges of IBD and intact bowels do not mutually overlap (Dohan et al., 2016). Therefore, assuming that the ranges of DWI ADC values do not overlap in the wall of unprepared intestines, the theory has been proposed that DWI could have a possible advantage in performing MRE examinations without prior preparation of the intestinal tract of patients with hyperosmolar oral CA. This would allow the examination of patients under general anaesthesia, for whom oral preparation is contraindicated. Therefore, it is important to understand whether the ADC values of the intestinal wall before and after prior preparation with osmotically active oral CA differ, how large these differences are, and whether the ADC range of the intestinal wall does not partially overlap with the ADC range of the inflamed intestinal wall.

Most intestinal wall DWI studies have been performed by preparing patients with large volumes (1000–2000 ml) of hyperosmolar oral CV prior to the MRE examination. To the best of our knowledge, the team of Kiryu et al*.* is the only research group reporting ADC values in Crohn's disease patients without prior patient preparation using free-breathing DWI with STIR

as the fat suppression technique. The reported ADC values show a similar trend, with that in prepared bowels being lower in disease-active segments and higher in disease-inactive areas ($1.61 \pm 0.44 \times 10^{-3}$ mm^2/s versus $2.56 \pm 0.51 \times 10^{-3}$ mm^2/s in intestines, respectively) (Kiryu et al., 2009). This difference is large enough to allow the diagnosis of CD on the basis of ADC measurements, without prior preparation of the patients' intestinal tract. If the differing ADC values in inflamed and unaltered intestinal walls also apply to unprepared intestinal walls, this would allow ADC values to be properly assessed without preparing patients prior to the examination. Therefore, one of the study tasks was to compare the ADC values of unprepared and prepared intestinal walls.

Upon reporting multiple MRE exams, several observations were performed regarding the high SI bowel wall in the DWI tracking images of b = 800 s/mm^2. Firstly, it was noticed that intestinal SI was markedly higher in the bowel wall before preparation, i.e., in a totally collapsed bowel, compared to the intestinal wall after preparation, i.e., in a fully distended bowel. In contrast, in the colon, SI was markedly higher in the bowel wall after preparation, i.e., in the presence of enteric CA, compared to the colonic wall before preparation, i.e., in the presence of faeces. In both situations, high SI bowel walls in the ADC map frequently presented low SI. These observations raised a question regarding ADC differences between the bowel wall before and after patient preparation, in both the intestines and colon.

Results from the first cohort comparing ADC values of DWI_{SPIR} and DWIBS between non-prepared (collapsed) and prepared (filled) intestines showed that ADC values in both DWI_{SPIR} and DWIBS in the collapsed bowel sample were markedly lower than in distended bowel samples. As the bowel collapses, the number of cells per volume unit increases; however, the cells are not altered. The measurement results therefore could be explained by the partial volume effect (Scherrer et al., 2011). In the prepared (filled) jejunal wall, the signal of the very thin bowel wall was contaminated by the high intensity signal from the massive volume of enteric CA, therefore the ADC value is high. However, in the non-prepared (collapsed) intestinal samples, the amount of high SI intraluminal content is less, therefore, the contamination of the intestinal wall signal is also less. A similar explanation applies to the second cohort comparing ADC values of DWI_{SPIR} and DWIBS between the non-prepared (presence of low SI intraluminal faeces) and prepared (presence of mannitol) colon. The results showed that ADC values in both DWI_{SPIR} and DWIBS were dependent on colonic intraluminal content, and in the presence of low SI faeces, were nearly two times lower than in the presence of high SI mannitol.

By mutually comparing ADC-DWI_{SPIR} and ADC-DWIBS values, no statistically significant difference was observed in the wall of prepared bowels, both regarding the intestines

and the colon. On the contrary, ADC-DWIBS values of both the non-prepared small intestine and colon are significantly lower compared to the ADC-DWI_{SPIR} values. This is explained by the large amount of liquid oral CA in the intestinal lumen, which generates the high signal in both the small and large intestinal wall to the same extent, and equally affects the ADC values of the bowel walls. On the contrary, in the non-prepared bowel, there is a presence of high-viscosity intraluminal content – chyme, in the intestines and faeces, in the colon. The T1 relaxation time of high viscosity content is short, like that of fat. Therefore, STIR, being a non-selective fat suppression technique for the DWIBS sequence, suppresses not only the fat signal but also the signal from another type of substrate with a short T1 relaxation time (Krinsky G, Rofsky and Weinreb, 1996; Del Grande et al., 2014). Therefore, the lower ADC-DWIBS values, in the presence of the bowel content, are more likely to overlap the ADC range of the inflamed bowel compared to ADC-DWI_{SPIR}. When comparing the ADC values of the intact intestinal wall in adult patients obtained in the first study, with the ADC values in adult patients with active CD in the terminal *ileum*, obtained in the second study, there was a clear difference in ADC values. In adult patients, the median ADC DWI_{SPIR} value for the previously prepared unaltered small intestinal wall is 1.72×10^{-3} mm^2/s, for the non-prepared unaffected small intestinal wall – 1.07×10^{-3} mm^2/s, while the median ADC value for the terminal loop affected by CD, is 1.26×10^{-3} mm^2/s. The median ADC-DWIBS value for the prepared unaltered small intestinal wall is 1.82×10^{-3} mm^2/s, for the previously unprepared unaltered small intestinal wall – 0.90×10^{-3} mm^2/s, while the median ADC-DWIBS value for the terminal *ileum* affected by CD is 1.15×10^{-3} mm^2/s. Thus, in both DWI_{SPIR} and DWIBS sequences, the ADC values of the bowel wall affected by CD is higher than the ADC values of the unprepared intestinal wall. Thus, the ADC measurements in both DWI_{SPIR} and DWIBS sequences are unlikely to be suitable for scanning patients without prior intestinal preparation.

The study, however, had several limitations. Measurements were performed by one radiologist, not assessing inter-observer agreement, and in such a small volume ADC values reported are hardly reproducible (Dohan et al., 2016; Watson et al., 2018), as they rest on subjectivity. Nevertheless, the data from ADC measurements in liver imaging suggested better reproducibility of free-breathing DWIBS over respiratory-triggered DWI (Kwee et al., 2008a), which could be also proven better for bowel walls, but requires further investigation. In intestines, the most uniform luminal distension was present in the *jejunum,* which was therefore chosen for intestinal measurements; however, the *ileum* is the main location of CD. The terminal *ileum* also has different morphological patterns, such as abundance of lymphoid tissues (Gullberg and Söderholm, 2006), which also could influence ADC measurements. In the colon,

measurements were performed only in the walls of the *caecum* and the ascending colon, since presence or mannitol was mainly observed in these locations. Location of the sites with high SI signal in DWI tracking images of b = 800 s/mm^2 was not consistent among the series; therefore, measurements could not be performed precisely at the same locations. No special attention was paid to the T2 "shine through" effect of bowel walls, and measured ADC values in the DWI tracking images of b = 800 s/mm^2 regardless of SI appearance in ADC map. The goal was to observe properties of ADC-DWI$_{SPIR}$ and ADC-DWIBS in the sites of bowel walls showing high SI at tracking images of b = 800 s/mm^2 resembling bowel inflammation, whereas no other signs of bowel inflammation were considered such as oedema, increased bowel wall thickness, contrast enhancement, which were absent in patients with no presence of IBD as required by the study.

4.2 Use of the DWIBS sequence to evaluate CD activity (second and third study)

The primary goal of treatment for CD is to achieve remission. Therefore, the assessment of disease activity is crucial to guide patients' therapeutic decisions regarding the treatment of CD. Although the primary endpoint of treatment has long been endoscopic remission, i.e., mucosal healing (Rimola et al., 2009; Moy et al., 2016; Maaser et al., 2019), CD is a transmural inflammation that can persist in patients with long-term mucosal healing (Zorzi et al., 2014; Civitelli et al., 2016; Nardone et al., 2019). It is proven that compared to mucosal healing, transmural healing is related to improved long-term outcomes, including sustained long-term steroid-free clinical remission, less need for rescue therapy, less CD-related hospitalisations and CD-related surgery (Serban, 2018). Therefore, transmural healing has recently been proposed as a new target for CD treatment (Castiglione et al., 2019b). To assess transmural changes, imaging techniques are required allowing evaluation of the altered intestinal wall along its entire length and thickness. It has been shown that MRE can replace endoscopy in the assessment of CD activity (Rimola et al., 2009).

The MaRIA score is the only validated index for measuring inflammatory activity in the *ileum,* tested in large patient populations and multi-centre research (Dohan et al., 2016; Ordás et al., 2019). It requires i/v administration of Gd CA. The Clermont score is based on DWI (therefore called DWI-MaRIA), and it was derived as an alternative for MaRIA, replacing RCE with ADC, thus avoiding the administration of gadolinium contrast media. The authors of the Clermont score state it is not only useful in estimation of ileal CD activity, with excellent correlation with RCE-based MaRIA (Buisson et al., 2013; Hordonneau et al., 2014), but also, in the detection of ulcers (Buisson et al., 2015) and prediction of remission after biological therapy (Buisson et al., 2018). The authors of the Clermont score state it is not only useful in

the estimation of ileal CD activity, but also in the detection of ulcers (Buisson et al., 2015) and the prediction of remission following biological treatment (Buisson et al., 2018). In their reports, the authors cite an outstanding correlation of the Clermont index with MaRIA (Buisson et al., 2013; Hordonneau et al., 2014).

In this study, the correlation between ADC-DWI_{SPIR} and ADC-DWIBS values was calculated. Although ADC-DWI_{SPIR} and ADC-DWIBS values appeared to be comparable visually, virtually no correlation was observed between ADC-DWI_{SPIR} and ADC-DWIBS values in both adults (rho = 0.27; p = 0.13) and children (rho = 0.22; p = 0.15). Although the DWIBS sequence is performed under free breathing, and availability of both repeated stimulations and acquisitions contributes to improved SNR and both spatial and temporal resolution (Kwee et al., 2008b), the possibility of respiratory motion in DWIBS, means that slice levels of images obtained with different b-values may not be identical. Since DWIBS employs multiple slice excitations, slice levels of images obtained with the same b-value may be different (Ouyang et al., 2014). The weak correlation between ADC-DWI_{SPIR} and ADC-DWIBS values, may also be impacted by the conceptually different fat suppression mechanisms of SPIR and STIR on ADC values of the intestinal wall, in relation to histopathological characteristics of bowel inflammation, due to differences in gut wall histopathology in adults and children.

Within the study, the ADC-DWI_{SPIR} and ADC-DWIBS values were analysed in two dimensions:

1) ADC values of both adults and children were compared within a single fat suppression technique, and a statistically significant ADC-DWI_{SPIR} difference was observed between adults and children, being lower in children, compared to adults. In contrast, no statistically significant difference was found between the ADC-DWIBS values in adults and children;

2) ADC values obtained with each of the DWI sequences were compared within one patient group, both in adults and children. The analysis showed differences between ADC-DWI_{SPIR} and ADC-DWIBS values in adults, being lower in DWIBS, but did not show a difference between ADC-DWI_{SPIR} and ADC-DWIBS values in the children's group.

To interpret the results, it is necessary to consider the differences in the histopathological picture of adult and paediatric CD, the different physical basis of both DWI_{SPIR} and DWIBS sequences as well as the duration of CD history.

There are three ruling theories considering the exact cause of the restricted diffusion in CD as follows: 1) narrowing of extracellular space caused by presence of oedema and increased cell density, dilated lymphatic vessels as well as formation of lymphoid aggregates, epithelioid

granulomas and micro-abscesses (Geboes, 2003; Feakins, 2013; Morani et al., 2015; Zhu et al., 2015); 2) increased perfusion, and 3) mural fibrosis (Morani et al., 2015; Zhu et al., 2015). Although the morphological pattern of CD is generally similar in adult and paediatric patients (Magro et al., 2013), the main difference between the histopathology of paediatric and adult CD, is the more frequent appearance of epithelioid granulomas in the inflamed bowel wall of children (Feakins, 2013; Riddell, 2014; Feakins, 2014).

When analysing the performance of ADC-DWIBS, the non-selectivity of STIR fat suppression must be considered. Unlike the SPIR technique, which uses a spectrally selective RF pulse, suppressing solely the fat signal, STIR technique uses an inversion recovery technique based on the T1 relaxation time of the tissues examined. Apart from fat having a short T1 time, STIR technique suppresses other substances of short T1 time, thus adding to the decrease of ADC value by suppression of signal from methaemoglobin, melanin, mucoid tissue, and proteinaceous fluid (Del Grande et al., 2014). Although early mucosal lesions in CD can be associated with the damage of small capillaries (Geboes, 2003), there is no literary data on haemorrhagic changes in the intestinal wall, which could lead to the formation of methaemoglobin in the intestinal wall (Riddell, 2014). There is also no evidence that any patient has chronic bowel melanosis associated with the development of melanin deposits, rarely associated with CD. (Lambert, Luk, 1980; Li et al., 2015). The inflammatory bowel wall tends to contain crypt abscesses, the contents of which could be considered as both mucoid and protein-rich tissues. However, they are occasional and are only observed in 19% of patients (Riddell, 2014).

A very important consideration influencing the SI of fine and thin structures, such as the bowel wall, is the partial volume effect (González Ballester et al., 2002). Typically, an achievable DWI resolution is in the order of 2 mm × 2 mm × 2 mm (Scherrer et al., 2011). In our DWIBS protocol, the acquisition voxel size is 2.50 mm (RL) × 2.98 AP (AP) × 6 mm (slice thickness), therefore within the single voxel, there will be signal contamination from the adjacent media. The bowel lumen contains the viscous and proteinaceous chyme, and occasionally faecal admixture, so the ADC-DWIBS values will be influenced not only by suppression of the mesenterial fat tissue, but also by saturation of signal from the bowel content with short T1 relaxation time. Therefore, when measured at a short distance from the intestinal lumen as carried out in the group of adults, ADC-DWIBS values are artificially lower, compared to ADC values of conventional DWI, i.e., DWI_{SPIR}.

The lower ADC-DWI_{SPIR} values in children, compared to adults are explained by differences in medical history. Although all adult patients had active CD, their medical history prior to the MRE examination was at least six months long (except for one patient whose

duration of illness was unknown), whereas all children (except one with an almost 2-year history of CD) were examined no longer than six months after the onset of symptoms. Therefore, the oedema component in the paediatric bowel wall was more pronounced, resulting in a greater diffusion restriction when compared to the adult patients. The presence of epithelioid granulomas may further limit diffusion in the inflamed wall.

In turn, lack of difference in ADC-DWIBS values for adults and children can be explained as follows. The medical history of children included in the study was shorter and therefore intestinal wall oedema was more severe. The ROIs for performing ADC measurements were positioned at the sites with the highest SI (within the submucosal layer of the bowel wall), therefore the distance to the intestinal lumen was sufficient to prevent the signal contamination caused by the partial volume effect. In turn, since the history of CD was longer in the group of adult patients, apart from oedema, fibrosis was also present. In these locations, the bowel wall was thinner, and ADC-DWIBS values were influenced by the partial volume effect from the bowel content with short T1 time, artificially lowering the ADC values.

The absence of difference between ADC-DWI_{SPIR} and ADC-DWIBS values in the children's group could also be explained with the predominance of the oedematous component, which, by increasing the thickness of the intestinal wall, does not allow the partial volume effect to affect the ADC-DWIBS values measured in the middle of the submucosal layer of the intestinal wall.

In the study, a moderate negative correlation was found between ADC-DWI_{SPIR} and MaRIA in both adults (rho = 0.50, $p = 0.004$) and children (rho = -0.54, $p < 0.0005$) being weaker than reported by the study group of the Clermont-Ferrand university showing excellent correlation (Buisson et al., 2013; Hordonneau et al., 2014). However, in the systematic review and meta-analysis on using diffusion-weighted MRE for evaluating bowel inflammation in CD, Choi et al. states that ADC demonstrates a moderate strength of correlation at best, and the Clermont score performs better (Choi et al., 2016). This is also consistent with the obtained results, since like the studies by the research group from Clermont-Ferrand University, in the current study there was also observed excellent correlation between MaRIA and both DWI_{SPIR}- and DWIBS-based Clermont scores. However, there may be a methodological error in using correlation between MaRIA and Clermont score, as the data to be correlated should be mutually independent, and should not be used if it includes more than one observation on any individual (Aggarwal and Ranganathan, 2016). Apart from RCE used in MaRIA and ADC used in the Clermont score, all other three variables (wall thickness, presence of oedema and presence of ulcerations), are used in both equations. The use of correlation analysis opposes the conditions in which correlation can be applied, and in the instances of highest probability, could lead to an

overestimation of the similarity between MaRIA and the Clermont score. The accuracy of this statement is supported by the contradiction between correlation of ADC-DWIBS and the ADC-DWIBS-based Clermont score with MaRIA, as despite no apparent correlation between ADC-DWIBS and MaRIA (rho = -0.001, p = 0.99) in the adult group, and low negative correlation between ADC-DWIBS and MaRIA in the paediatric group (rho = -0.37, p = 0.01), the correlation between DWIBS-based Clermont score and MaRIA remained strong in both adults (rho = 0.89; p < 0.0005) and children (rho = 0.95; p < 0.0005).

In the study, endoscopy was not used as the reference standard but the study groups were selected exclusively by visual MRE findings of CD. Lack of an endoscopic picture for comparison can be considered as a limitation of the study, but the possible incomplete correlation of the MR picture with the endoscopic picture should also be taken into account. The endoscopic visual image and the histopathological pattern of the endoscopically obtained tissue samples reflect changes in the intestinal mucosa, whereas the components that form the MR activity indices characterise changes not only in the intestinal mucosa, but also within the entire thickness of the intestinal wall. Both the literary data and the experience of the Children's Clinical University Hospital suggest situations in which intact intestinal mucosa is observed endoscopically in the case of active CD, while MRI examination reveals marked transmural inflammatory changes. However, literature provides a broad picture of the correlation not only between MRE and endoscopic findings, but also between MRE and surgery specimens of resected intestinal segments with certain defined criteria, along with the conclusion that MRI is an informative and sufficiently accurate method to assess altered bowel walls in CD. Based on these observations, for several years now, when referring patients for MRE examinations, clinicians do not duplicate their results with the invasive endoscopy that is also cumbersome for patients. Consequently, in 2019, for the first time, the ECCO-ESGAR guidelines were introduced with a revolutionary statement that radiological cross-sectional imaging methods (and, therefore, MR) can be used as an alternative to endoscopy to assess CD activity (Maaser et al., 2019). Therefore, although CD had been endoscopically confirmed in all patients included in the study, the results of the MRE examination were not duplicated by the endoscopic and histopathological findings in any of cases. The correlation between histopathological and radiological scenes could best be reflected if a representative number of surgically resected intestinal segments were available. However, surgical resection with subsequent histopathological analysis of the specimen, which would provide the most complete picture of intestinal wall changes, was performed in only one patient.

Obtaining high quality and precisely interpretable DWI images requires a uniform magnetic field, very strong gradients and fast image capture, which is not possible with

currently available MR equipment. The quality of DWI images is therefore inferior than that of conventional MR images, due to low resolution, noise, distortions, and limited morphological interpretability (Chilla et al., 2015). Opinions on reproducibility of ADC-DWI measurements used in the Clermont score varies among authors, and despite good to excellent repeatability reported from certain authors (Hao Yu, Ya-Qi Shen, Fang-Qin Tan, Zi-Ling Zhou, Zhen Li, Dao-Yu Hu, 2019), contrary concerns on low reproducibility based on research data also exist (Watson et al., 2018). Due to equivocal data on the repeatability of measurements that form the MaRIA and Clermont scores, our interest was to assess the repeatability of measurements contributing to both of these indices, i.e., WSI-*pre*Gd and WSI-*post*GD forming RCE in MaRIA, ADC-DWI used in the Clermont score, as well as bowel thickness and estimation of presence of bowel ulcers, which are common to both MaRIA and Clermont scores.

In the study, the repeatability of both ADC-DWI_{SPIR} and ADC-DWIBS measurements performed by one observer at two-month intervals was good, as no statistically significant differences were found between the mean ADC-DWI_{SPIR} ($p = 0.65$) and *ADC*-DWIBS values ($p = 0.23$). In the case of ADC-DWI_{SPIR}, the differences between the mean values was only 1 %, while in the case of ADC-DWIBS – 4 %.

Several authors found poor repeatability of RCE measurements (Sharman, Zealley et al., 2009; Tielbeek et al., 2013). No statistically significant difference was found in WSI-*pre*Gd ($p = 0.06$) or in WSI *post*Gd ($p = 0.57$) values used in calculating RCE. It is believed that a strict definition of ROI size and accurate site-by-site WSI-*pre*Gd and *post*Gd measurement in the same bowel segment would result in good inter-observer agreement. It should, however, be noted that the results show high SD in both WSI-*pre*GD (*SD* = 127.57 for the first assessment and *SD* = 99.68 for the first assessment), and WSI *post*Gd measurements (*SD* = 235.35 for the first assessment and *SD* 212.9 for the second assessment), covering 66–78 % of the WSI values. The observations suggest that if WSI-*pre*Gd values were in the tens, the WSI-post Gd values would also be in the tens; if WSI-*pre*Gd values were in the hundreds, this would also be replicated in the WSI-post Gd values. This observation can be explained through individual tissue characteristics of patients, magnetic field inhomogeneity and linearity of gradients yielding wide distribution of WSI values. Detailed analysis of this finding, is however beyond the scope of our current research.

Tielbeek et al. reported moderate repeatability of bowel thickness measurements and excellent repeatability when the thickness measurements were performed by an experienced radiologist (Tielbeek et al., 2013). In the study, no statistically significant difference was found between the first and the second measurements. It should, however, be noted that wall thickness differed within the same bowel segment, and the maximum thickness was always chosen for

the calculations. However, identifying the same exact location of the maximum thickness often was not possible in DWI images due to their low spatial resolution. Similarly, in the pre- and post-contrast series, bowel thickness was always measured in the axial images, but pre- and post-T1 images were acquired in the coronal plane. Therefore, the ROI in these images was not always placed exactly at the site the intestinal wall thickness measurement was performed.

In the study there was a systematic difference in the assessment of ulcers. The inconsistency of ulcer detection in the study could be associated with lack of strict consensus regarding a standardised MR definition of an ulcer. Developers of the MaRIA index defined ulcers as deep depressions in the mucosal surface (Rimola et al., 2009). However, MRI reveals a wide range of ulcers. Even small aphthous ulcers can be seen in MRI images (Ram et al., 2016), and there is no clear definition of the size and appearance of ulcers that should be included in calculation of disease activity indices, or excluded from it. The rating of ulcers could be improved with a 3 T MR scanner, as this provides better spatial and temporal resolution. Literary data indicates that the resolution of 3 T MR scanner in the diagnosis of ulceration is superior compared to that of the 1.5 T device (Fiorino et al., 2013).

It is considered that the strengths of both studies on assessment of the ADC-DWI_{SPIR} and ADC-DWIBS values in patients with active CD were: 1) the prospective study design, 2) exact site-by-site comparison in the same bowel segment, and 3) exact ROI size that was not defined in other studies on MaRIA and Clermont scores, except the study conducted by Caruso's team (Caruso et al., 2014) performing measurements with ROI size between 12–20 mm^2. However, both studies also faced several limitations: 1) the relatively low number of participants in study groups; 2) patients included in the study were selected according to the visual diagnostic criteria described in the ECCO-ESGAR guidelines "Imaging techniques for the assessment of inflammatory bowel disease: Joint ECCO and ESGAR evidence-based consensus guidelines" (Panes et al., 2013) namely intestinal wall thickening, wall oedema and hyperenhancement following i/v administration of CA, but due to the limited availability of laboratory parameters in the group of adult patients, no correlation of visual finding with laboratory characteristics of disease activity was performed; 3) there was a possible sampling error in the study population, as both adult and paediatric groups were not homogeneous in terms of disease duration. This, however, did not affect the repeatability assessment, as all measurements (intestinal wall thickness, WSI-*pre*Gd, WSI-p*ost*Gd, ADC- DWI_{SPIR} and ADC-DWIBS) and ulcer assessment were identical in both adults and children; 4) in both *post*Gd and DWI images, the ROIs were placed on the site of the maximum SI. After administration of gadolinium contrast media, in some cases the most intense contrast enhancement was predominantly observed in ileal mucosa; however, in other cases the enhancement was evenly

distributed throughout the intestinal wall. In contrast, in both DWI techniques, bowel wall layers were indistinguishable as the diffusion restriction throughout the intestinal walls was equally intense, which could result in differences of positioning ROI between the T1 post-contrast and DWI sequences; 5) the MaRIA studies are based on a comparison of the visual image with the Crohn's disease endoscopic index of severity (CDEIS), the CD endoscopic activity index in adult patients. Unlike in adults, the estimation of inflammatory activity in children does not rely on endoscopy findings due to its invasiveness, but rather on the paediatric Crohn's disease activity index (PCDAI), and the correlation with MaRIA is weak to moderate (rho = 0.42, p = 0.016) (Rozendorn et al., 2018). Its correlation with the Clermont index has not yet been assessed, so the usefulness of the Clermont index for children remains unclear.

Conclusions

1. Compared to conventional DWI sequence, the DWIBS sequence has no advantages and it is inferior for quantitative assessment of bowel walls walls in patients without prior peroral preparation with osmotically active enteric CA. The use of ADC measurements in patients without prior bowel preparation is not appropriate for either DWI or DWIBS sequences.
2. Compared to conventional DWI sequence, DWIBS sequence has no advantages and it is inferior for quantitative assessment of CD activity in patients with already diagnosed disease in the terminal *ileum.* The use of ADC-DWIBS measurements for quantitative assessment of CD activity is not appropriate.
3. By defining a strict measurement standard ADC values of both conventional DWI and DWIBS values are well repeatable, which means capability of providing reproducible and equally accurate measurement results in both of the investigated sequences.

Recommendations

1. Neither the conventional DWI, nor DWIBS sequence, has the potential for quantitative diagnostics of primary CD in patients without prior peroral intestinal tract preparation. Therefore, in the diagnosis of CD, measurements of ADC values do not give grounds to abandon the preparation of the intestinal tract with hyperosmolar oral contrast agent, regardless of the fat suppression technique used.
2. According to the results of the study, compared to the DWI sequence with spectrally selective fat signal suppression, the DWIBS sequence is less accurate and is not suitable for use in the Clermont index for quantitative evaluation of CD activity in either adults or children. The DWIBS sequence can only be used for qualitative visual identification of CD changes in the intestinal wall. The conventional DWI sequence remains the choice DWI sequence to be used in the Clermont score to evaluate the activity of CD localised in the terminal *ileum*.

Publications and Thesis of the Author

Publications in cited and peer-reviewed journals

1. **1. Apine, I.,** Baduna, M., Pitura, R., Pokrotnieks, J., Krumina, G. 2019. The Influence of Bowel Preparation on ADC Measurements: Comparison between Conventional DWI and DWIBS Sequences. *Medicina,* 55, 394; doi: 10.3390/medicina55070394, PubMed, Scopus (**Publication I**).
2. **Apine, I.,** Pitura, R., Franckevica, I., Pokrotnieks, J., Krumina, G. 2020. Comparison between Diffusion-Weighted Sequences with Selective and Non-Selective Fat Suppression in the Evaluation of Crohn's Disease Activity: Are They Equally Useful? *Diagnostics*, 10, 347; doi:10.3390/diagnostics10060347, PubMed, Scopus **(Publication II**).
3. **Apine, I.,** Pirksta, I., Pitura, R., Pokrotnieks, J., Pukite, I., Krumina, G. 2020. Repeatability of Magnetic Resonanse Measurements Used for Estimating Crohn's Disease Activity. *Proceedings of the Latvian Academy of Sciences.* Section B, Volume 74, No 2 (725), pp.75–82, PubMed, Scopus (**Publication III**).

Other publications

1. **Apine, I.**, Pokrotnieks, J., Leja, M., Atteka, S., Krumina, G. 2016. Apparent Diffusion Coefficient Values in Collapsed and Distended Small Bowel Loops and Their Potential Importance for Excluding Inflammatory Bowel Disease: a Study in Healthy Subjects, *Acta Chirurgica Latviensis* (16/1), pp. 23–30.

Thesis and presentations in international conferences

1. **Apine, I.** 2015. Magnetic resonance enterography with diffusion-weighted imaging (DWI) sequence helps to reveal early inflammatory changes in patients with suspect bowel disease. *VII Latvian Gastroenterology Congress with International Participation,* Riga, December 5, 2015, oral presentation.
2. **Apine, I.**, Atteka, S., Krumina, G. 2016. Measuring apparent diffusion coefficient values in collapsed and distended small bowel loops has a potential in excluding inflammatory bowel disease in patients without bowel preparation: a study in healthy subjects. *United European Week of Gastroenterology (UEG Week* 2016*)*, Vienna, Austria, October 15–19, 2016, poster presentation.
3. **Apine, I.**, Atteka, S., Pokrotnieks, J., Leja, M., Krūmiņa, G. 2017. Bowel distention degree does influence DWI ADC values throughout the whole bowel length: results from two

consecutive studies in healthy subjects. *European Congress of Radiology (ECR 2017)*, Vienna, Austria, February 27 – March 3, 2017, oral presentation.

4. **Apine, I.**, Atteka S., Pokrotnieks J., Leja M., Krūmiņa G. 2017. Bowel distention degree does influence DWI ADC values throughout the whole bowel length: results from two consecutive studies in healthy subjects. *European Congress of Radiology (ECR 2017)*, Vienna, Austria, February 27 – March 3, 2017, poster presentation.
5. **Apine, I**. 2017. MRI enterography vs. capsule endoscopy. *VIII Latvian Gastroenterology Congress with International Participation*, Riga, Latvia, December 9, 2017, oral presentation.
6. **Apine, I**, Angerer, M. P. M., Baduna, M., Krumina, G. 2018. DWI ADC values are influenced not only by bowel distention degree but also the presence of osmotically active agent: results from research in healthy subjects. *European Congress of Radiology (ECR 2018)*, Vienna, Austria, February 28 – March 4, 2018, oral presentation.
7. **Apine I.**, Baduna, M., Pitura, R., Krumina. G. 2019. ADC values of DWI and DWIBS in bowel imaging: when they are consistent and when not? *European Congress of Radiology (ECR 2019)*, Vienna, Austria, February 27 – March 3, 2019**,** oral presentation.
8. **Apine, I.,** Pukite, I., Samma, M. 2019. Imaging of IBD beyond the reach of endoscope: case report series. 55th Annual Meeting & 41st Post-Graduate Course of the European Society of Paediatric Radiology, Helsinki, Finland, May 16–18, 2019, poster presentation.
9. **Apin**e, **I.**, Pitura R. 2019. Which diffusion-weighted imaging – Short-TI Inversion Recovery or Spectral Presaturation with Inversion Recovery-based – is better for the assessment of quantification of Crohn's disease inflammation? *European Society of Gastrointestinal and Abdominal Radiology (ESGAR 2019)*, Rome, Italy, June 1-5, 2019, oral presentation
10. **Apine, I**. 2019. MRI beyond the reach of endoscope. *IX Latvian Gastroenterology Congress with International Participation,* Riga, December 9, 2019, oral presentation.
11. **Apine, I**, Pitura, R., Pukite, I., Krumina, G. 2020. Utility of DWIBS-ADC in evaluation of inflammatory activity in adults and children with active Crohn's disease. *European Congress of Radiology (ECR),* July 15–19**,** 2020, poster presentation.

Thesis and presentations in local conferences

1. **Apine, I.**, Pokrotnieks, J., Leja, M., Pukite, I., Supe, A., Krūmiņa, G. 2016. Magnetic resonance enterography with diffusion weighted imaging (DWI) sequence helps to reveal

early inflammatory changes in patients with suspect bowel disease. *74th Conference of University of Latvia, Medicine section*, Riga, Latvia February 15, 2016, oral presentation.

2. **Apine I.**, Atteka, S., Pokrotnieks, J., Leja, M., Krūmiņa, G. 2017. Zarnu šķietamais difūzijas koeficients MR DWI uzsvērtajos attēlos ir atkarīgs no zarnu sieniņas iestiepuma pakāpes (The apparent diffusion coefficient in DWI images depends on the degree of intestinal wall distention). *The Scientific Conference of RSU*, April 6–7, 2017, oral presentation.

3. **Apine, I.**, Pitura, R., Bērziņa, D. Consistency of ADC-DWI and ADC-DWIBS in Bowel Walls Depending on Measurement area in Active Chron's disease. *RSU Research Week*, April 1–3, 2019**,** oral presentation.

4. Bērziņa, D., **Apine, I**. Is MRE ADC-DWIBS an Appropriate Diagnostic Method for a Disease? *RSU Research Week*, April 1–3, 2019, poster presentation.

References

1. Abu-Freha, N., Badarna, W., Sigal-Batikoff, I., Abu Tailakh, M., Etzion, O., Elkrinawi, J., et al. 2018. ASCA and ANCA among Bedouin Arabs with inflammatory bowel disease, the frequency and phenotype correlation. *BMC Gastroenterology* 18: 1–5.

2. Aggarwal, R., Ranganathan, P. 2016. Common pitfalls in statistical analysis: The use of correlation techniques. *Perspectives in Clinical Research* 7: 187–190.

3. Ahmed, O., Rodrigues, D. M., Nguyen, G C. 2015. Magnetic resonance imaging of the small bowel in Crohn disease: A systematic review and meta-analysis. *Canadian Journal of Gastroenterology & hepatology* 2016: 1–10.

4. American College of Radiology. 2015. ACR – SAR – SPR Practice Parameter for the Performance of Magnetic Resonance (MR) Enterography. *ACR – SAR – SPR Practice Parameter for the Performance of Magnetic Resonance (MR) Enterography by American College of Radiology*: 1–10.

5. Amitai, M. M., Ben-Horin, S., Eliakim, R., Kopylov, U. 2013. Magnetic resonance enterography in Crohn's disease: A guide to common imaging manifestations for the IBD physician. *Journal of Crohn's and Colitis* 7: 603–615.

6. Anupindi, S. A., Terreblanche, O., Courtier, J. 2013. Magnetic resonance enterography: Inflammatory bowel disease and beyond. *Magnetic Resonance Imaging Clinics of North America* 21: 731–750.

7. Baker, M. E., Einstein, D. M., Veniero, J. C. 2008. Computed tomography enterography and magnetic resonance enterography: The future of small bowel imaging. *Clinics in Colon and Rectal Surgery* 21: 193–212.

8. Balcı, S., Onur, M. R., Karaosmanoğlu, A. D., Karçaaltıncaba, M., Akata, D., Konan, A., Özmen, M. N. 2019. Mrievaluation of anal and perianal diseases. *Diagnostic and Interventional Radiology* 25: 21–27.

9. Baliyan, V., Das, C. J., Sharma, R., Gupta, A. K. 2016. Diffusion weighted imaging: Technique and applications. *World Journal of Radiology* 8: 785–798.

10. Barclay, A. R., Russell, R. K., Wilson, M. L., Gilmour, W. H., Satsangi, J., Wilson, D. C. 2009. Systematic Review: The Role of Breastfeeding in the Development of Pediatric Inflammatory Bowel Disease. *Journal of Pediatrics* 155: 421–426.

11. Barnes, E. L., Kappelman, M. D. 2018. Increasing incidence of pediatric inflammatory bowel disease in France: Implications for etiology, diagnosis, prognosis, and treatment. *American Journal of Gastroenterology* 113: 273–275.

12. Baumgart, D. C., Sandborn, W. J. 2012. Crohn's disease. *The Lancet* 380: 1590–1605.

13. Bernstein, C. N., Eliakim, A., Fedail, S., Fried, M., Gearry, R., Goh, K. L., Hamid, S., Khan, A. G., Khalif, I., Ng, S. C., et al. 2016. World gastroenterology organisation global guidelines inflammatory bowel disease. *Journal of Clinical Gastroenterology* 50: 813–818.

14. Best, W. R., Becktel, J. M., Singleton, J. W., Kern, F. 1976. Development of a Crohn's Disease Activity Index: National Cooperative Crohn's Disease Study. *Gastroenterology* 70: 439–444.

15. Le Bihan, D., Poupon, C., Amadon, A., Lethimonnier, F. 2006. Artifacts and pitfalls in diffusion MRI. *J Magn Reson Im* 24: 478–488.

16. Boyapati, R., Satsangi, J., Ho, G. T. 2015. Pathogenesis of Crohn's disease. *F1000Prime Reports* 7.

17. Broome, D. R. 2008. Nephrogenic systemic fibrosis associated with gadolinium based contrast agents : A summary of the medical literature reporting. *European Journal of Radiology* 66: 230–234.

18. Buisson, A., Joubert, A., Montoriol, P. F., Ines, D. D., Hordonneau, C., Pereira, B., Garcier, J. M., Bommelaer, G., Petitcolin, V. 2013. Diffusion-weighted magnetic resonance imaging for detecting and assessing ileal inflammation in Crohn's disease. *Alimentary Pharmacology and Therapeutics* 37: 537–545.

19. Buisson, A., Hordonneau, C., Goutte, M., Boyer, L., Pereira, B., Bommelaer, G. 2015. Diffusion-weighted magnetic resonance imaging is effective to detect ileocolonic ulcerations in Crohn's disease. *Alimentary Pharmacology and Therapeutics* 42: 452–460.

20. Buisson, A., Hordonneau, C., Goutte, M., Scanzi, J., Goutorbe, F., Klotz, T., Boyer, L., Pereira, B., Bommelaer, G. 2016. Diffusion-weighted magnetic resonance enterocolonography in predicting remission after anti-TNF induction therapy in Crohn's disease. *Digestive and Liver Disease* 48: 260–266.

21. Buisson, A., Pereira, B., Goutte, M., Reymond, M., Allimant, C., Obritin-Guilhen, H., Bommelaer, G., Hordonneau, C. 2017. Magnetic resonance index of activity (MaRIA) and Clermont score are highly and equally effective MRI indices in detecting mucosal healing in Crohn's disease. *Digestive and Liver Disease* 49: 1211–1217.

22. Buisson, A., Hordonneau, C., Goutorbe, F., Allimant, C., Goutte, M., Reymond, M., Pereira, B., Bommelaer, G. 2018. Bowel wall healing assessed using magnetic resonance imaging predicts sustained clinical remission and decreased risk of surgery in Crohn's disease. *Journal of Gastroenterology* 54: 312–320.

23. Cappello, M., Morreale, G. C. 2016. The role of laboratory tests in Crohn's disease. *Clinical Medicine Insights: Gastroenterology* 9: 51–62.

24. Caruso, A., D'Incà, R., Scarpa, M., Manfrin, P., Rudatis, M., Pozza, A., Angriman, I, Buda, A, Sturniolo, G. C., Lacognata, C. 2014. Diffusion-weighted magnetic resonance for assessing ileal Crohn's disease activity. *Inflammatory Bowel Diseases* 20: 1575–1583.

25. Casciani, E., De Vincentiis, C., Polettini, E., Masselli, G., Di Nardo, G., Civitelli, F., Cucchiara, S., Gualdi, G. F. 2014. Imaging of the small bowel: Crohn's disease in paediatric patients. *World Journal of Radiology* 6: 313–28.

26. Castiglione, F., Imperatore, N., Testa,A., De Palma, G. D., Nardone, O. M., Pellegrini, L., Caporaso, N., Rispo, A. 2019. One-year clinical outcomes with biologics in Crohn's disease: transmural healing compared with mucosal or no healing. *Alimentary Pharmacology and Therapeutics* 49: 1–14.

27. Chavhan,. G., Babyn, P., Walters, T. 2013. MR enterography in children: Principles, technique, and clinical applications. *Indian Journal of Radiology and Imaging* 23: 173.

28. Chilla, G. S., Tan, C. H., Xu, C., Poh, C. L. 2015. Diffusion weighted magnetic resonance imaging and its recent trend-a survey. *Quantitative imaging in medicine and surgery* 5: 407–422.

29. Choi, S. H., Kim, K. W., Lee, J. Y., Kim, K. J., Park S. H. 2016. Diffusion-weighted Magnetic Resonance Enterography for Evaluating Bowel Inflammation in Crohn's Disease: A Systematic Review and Meta-analysis. *Inflammatory Bowel Diseases* 22: 669–679.

30. Civitelli, F., Nuti, F., Oliva, S., Messina, L., La Torre, G., Viola, F., Cucchiara, S., Aloi, M. 2016. Looking beyond Mucosal Healing: Effect of Biologic Therapy on Transmural Healing in Pediatric Crohn's Disease. *Inflammatory Bowel Diseases* 22: 2418–2424.

31. Cosnes, J., Gowerrousseau, C., Seksik, P., Cortot, A. 2011. Epidemiology and natural history of inflammatory bowel diseases. *Gastroenterology* 140: 1785–1794.

32. Criado, J. de M., del Salto, L. G., Rivas, P. F., del Hoyo, L. F. A, Velasco, L. G., Díez Pérez de las Vacas, M. I., Marco Sanz, A. G., Paradela, M. M., Moreno, E. F. 2012. MR imaging evaluation of perianal fistulas: Spectrum of imaging features. *Radiographics* 32: 175–194.

33. Cuffari, C. 2009. Diagnostic considerations in pediatric inflammatory bowel disease management. *Gastroenterology and Hepatology* 5: 775–783.

34. Daram, S.,Cortese, C. C., Bastani, B. 2005. Nephrogenic fibrosing dermopathy/nephrogenic systemic fibrosis: Report of a new case with literature review. *American Journal of Kidney Diseases* 46: 754–759.

35. Davidovic, L., Tsay, V. 2019. Potential Application of Diffusion-Weighted Whole-Body Imaging with Background Body Signal Suppression for Disease Activity Assessment in Takayasu Arteritis—In Search of the "Golden Mean": Case Report. *Annals of Vascular Surgery* 61: 468.e9-468.e12.

36. Dietrich, O., Biffar, A., Baur-Melnyk, A., Reiser, M. F. 2010. Technical aspects of MR diffusion imaging of the body. *European Journal of Radiology* 76: 314–322.

37. Dohan, A., Taylor, S., Hoeffel, C., Barret, M., Allez, M., Dautry, R., Zappa, M., Savoye-Collet, C., Dray, X., Boudiaf, M., et al. 2016. Diffusion-Weighted MRI in Crohn's Disease: Current Status and Recommendations. *Journal of Magnetic Resonance Imaging* 44: 1381–1396.

38. Drake-Pérez, M., Boto, J., Fitsiori, A., Lovblad, K., Vargas, M. I. 2018. Clinical applications of diffusion weighted imaging in neuroradiology. *Insights into Imaging* 9: 535–547.

39. Dubron, C., Avni, F., Boutry, N., Turck, D., Duhamel, A., Amzallag-Bellenger, E,. 2016. Prospective evaluation of free-breathing diffusion weighted imaging for the detection of inflammatory bowel disease with MR enterography in childhood population. *British Journal of Radiology* 89: 2–10.

40. Dulai, P. S., Siddharth, S., Monica, C., Bouguen, G., Nelson, S., Peyrin-Biroulet, L., Feagan, B. G., Ordas, I., Sandborn, W. J., Santillan, C., et al. 2015. Cochrane Database of Systematic Reviews MRI scoring indices for evaluation of disease activity and severity in Crohn ' s disease (Methodology Protocol). *Cochrane Database of Systematic Reviews*: 1–8.

41. Feakins, R. M. 2013. Inflammatory bowel disease biopsies: Updated British Society of Gastroenterology reporting guidelines. *Journal of Clinical Pathology* 66: 1005–1026.

42. Fiorino, G., Bonifacio, C., Padrenostro, M., Sposta, F. M., Spinelli, A., Malesci, A., Balzarini, L., Peyrin-Biroulet, L., Danese, S. 2013. Comparison between 1.5 and 3.0 tesla magnetic resonance enterography for the assessment of disease activity and complications in ileo-colonic crohn's disease. *Digestive Diseases and Sciences* 58: 3246–3255.

43. Gajendran, M., Loganathan, P., Catinella, A. P., Hashash J. G. 2018. A comprehensive review and update on Crohn's disease. *Disease-a-Month* 64: 20–57.

44. Geboes, K. 2003. "Histopathology of Crohn's Disease and Ulcerative Colitis". In: Satsangi J., Sutherland L. R. *Inflammatory Bowel Diseases* Vol. 18 Edinburgh, London, Melbourne: Churchill-Livingstone Elsevier. Pp. 255–276

45. Gibby, W., Gibby, K. and Gibby, A. 2004. “Comparison of Gd DTPA-BMA (Omniscan) versus Gd HP-DO3A (ProHance) Retention in Human Bone Tissue by Inductively Coupled Plasma Atomic Emission Spectroscopy.” *Investigative Radiology* 39(3):138–142.

46. Goetsch, A. L., Kimelman, D., Woodruff, T. K. 2017. *Fertility Preservation and Restoration for Patients with Complex Medical Conditions*.

47. González Ballester, M. Á., Zisserman, A. P., Brady M. 2002. Estimation of the partial volume effect in MRI. *Medical Image Analysis* 6: 389–405.

48. Graessner, J. 2011. Frequently Asked Questions: Diffusion-Weighted Imaging (DWI). *MAGNETOM Flash* 1: 84–87.

49. Del Grande, F., Santini, F., Aro, M. R., Gold, G. E., Carrino, J. A. 2014. Fat-Suppression Techniques for 3-T MR Imaging of the Musculosceletal system. 34: 217–233.

50. Greer, M. L. C. 2016. How we do it: MR enterography. *Pediatric Radiology* 46: 818–828.

51. Guan, Q. 2019. A Comprehensive Review and Update on the Pathogenesis of Inflammatory Bowel Disease. *Journal of Immunology Research* 2019.

52. Gulani, V., Calamante, F., Shellock, F. G., Kanal, E., Reeder, S. B. 2017. Gadolinium deposition in the brain: summary of evidence and recommendations. *The Lancet Neurology* 16: 564–570.

53. Gullberg, E., Söderholm, J. D. 2006. Peyer’s patches and M cells as potential sites of the inflammatory onset in Crohn’s disease. *Annals of the New York Academy of Sciences* 1072: 218–232.

54. Hao, Y., Ya-Qi, S., Fang-Qin, T., Zi-Ling, Zhen, L. Dao-Yu, H., Morelli, J. N. . 2019. Quantitative diffusion-weighted magnetic resonance enterography in ileal Crohn’s disease: A systematic analysis of intra and interobserver reproducibility. 25: 3619–3633.

55. Hordonneau, C., Buisson, A., Scanzi, J., Goutorbe, F., Pereira, B., Borderon, C., Ines, D. D., Montoriol, P. F., Garcier, J. M., Boyer, .L, et al. 2014. Diffusion-weighted magnetic resonance imaging in ileocolonic Crohn’s disease: validation of quantitative index of activity. *The American journal of gastroenterology* 109: 89–98.

56. Horger, W. 2007. Fat Suppression in the Abdomen (Siemens). *MAGNETOM Flash* 3: 114–119.

57. Hyams, J., Markowitz, J., Otley, A., Rosh, J., Mack, D., Bousvaros, A., Kugathasan, S., Pfefferkorn, M., Tolia, V., Evans J., et al. 2005. Evaluation of the pediatric Crohn disease activity index: A prospective multicenter experience. *Journal of Pediatric Gastroenterology and Nutrition* 41: 416–421.

58. Indrati, R. 2017. Comparing SPIR and SPAIR Fat Suppression Techniques in Magnetic Resonance Imaging (MRI) of Wrist Joint. *Journal of Medical Science And clinical Research* 05: 23180–23185.

59. Jairath, V., Ordas, I., Zou, G., Panes, J., Stoker, J., Taylor, S. A., Santillan, C., Horsthuis, K., Samaan, M. A., Shackelton, L. M., et al. 2018. Reliability of Measuring Ileo-Colonic Disease Activity in Crohn’s Disease by Magnetic Resonance Enterography. *Inflammatory Bowel Diseases* 24: 440–449.

60. Jeong, K. K., Kyoung, A. K., Park, B. W., Kim, N., Cho, K. S. 2008. Feasibility of diffusion-weighted imaging in the differentiation of metastatic from nonmetastatic lymph nodes: Early experience. *Journal of Magnetic Resonance Imaging* 28: 714–719.

61. Jesuratnam-Nielsen, K. 2015. Inflammatory bowel disease and magnetic resonance imaging: Doctoral Thesis. Copenhagen.

62. Jesuratnam-Nielsen, K., Løgager, V. B., Munkholm, P., Thomsen, H. S. 2015a. Diagnostic accuracy of three different MRI protocols in patients with inflammatory bowel disease. *Acta radiologica open* 4: 1–7.

63. Jesuratnam-Nielsen, K., Løgager V. B., Rezanavaz-Gheshlagh ,B., Munkholm, P., Thomsen, H. S. 2015b. Plain magnetic resonance imaging as an alternative in evaluating inflammation and bowel damage in inflammatory bowel disease – a prospective comparison with conventional magnetic resonance follow-through. *Scandinavian Journal of Gastroenterology* 50: 519–527.

64. Jose, F. A, Heyman, M. B. 2008. Extraintestinal manifestations of inflammatory bowel disease. *Journal of Pediatric Gastroenterology and Nutrition* 46: 124–133.

65. Kim, K. J., Lee, Y., Park, S. H., Kang, B-K., Seo, N., Yang, S-K., Ye, B. D., Park, S. H., Kim, S. Y., Baek, S., et al. 2015. Diffusion-weighted MR Enterography for Evaluating Crohn's Disease: How Does It Add Diagnostically to Conventional MR Enterography? *Inflammatory bowel diseases* 21: 101–109.

66. Kiryu, S., Dodanuki, K., Takao, H., Watanabe, M., Inoue, Y., Takazoe, M., Sahara, R., Unuma, K., Ohtomo, K.. 2009. Free-breathing diffusion-weighted imaging for the assessment of inflammatory activity in Crohn's disease. *J Magn Reson Imaging* 29: 880–886.

67. Koh, D. M., Blackledge, M., Padhani, A. R., Takahara, T., Kwee, T. C., Leach, M. O., Collins, D. J. 2012. Whole-body diffusion-weighted mri: Tips, tricks, and pitfalls. *American Journal of Roentgenology* 199: 252–262.

68. Kopylov, U., Klang, E., Yablecovitch, D., Lahat, A., Avidan, B., Neuman, S., Levhar, N., Greener, T., Rozendorn, N., Beytelman, A., et al. 2016. Magnetic resonance enterography versus capsule endoscopy activity indices for quantification of small bowel inflammation in Crohn's disease. *Therapeutic Advances in Gastroenterology* 9: 655–663.

69. Koreishi, A., Nazarian, R., Saenz, A., Klepeis, V., McDonald, A., Farris, A., Colvin, R., Duncan, L., Mandal, R. K. J. 2009. Nephrogenic Systemic Fibrosis - A Pathologic Study of Autopsy Cases. *Archives of Pathology and Laboratory Medicine* 133: 1943–1948.

70. Krinsky, G., Rofsky, M., Weinreb, C.. 1996. Nonspecificity of Short Inversion Time Inversion Recovery (STIR) as a Technique of Fat Suppression: Pitfalls in Image Interpretation. *AJR* 166: 523–526.

71. Kwack, W. G., Lim, Y. J. 2016. Current status and research into overcoming limitations of capsule endoscopy. *Clinical Endoscopy* 49: 8–15.

72. Kwee, T. C., Takahara, T., Koh, D. M, Nievelstein, R. A. J, Luijten, P. R. 2008a. Comparison and reproducibility of ADC measurements in breathhold, respiratory triggered, and free-breathing diffusion-weighted MR imaging of the liver. *Journal of Magnetic Resonance Imaging* 28: 1141–1148.

73. Kwee, T. C., Takahara T., Ochiai, R., Nievelstein, R. A. J., Luijten, P. R. 2008b. Diffusion-weighted whole-body imaging with background body signal suppression (DWIBS): Features and potential applications in oncology. *European Radiology* 18: 1937–1952.

74. Kwee, T. C., Takahara, T., Ochiai, R., Katahira, K., Van Cauteren, M., Imai, Y., Nievelstein R. A. J., Luijten, P. R. 2009. Whole-body diffusion-weighted magnetic resonance imaging. *European Journal of Radiology* 70: 409–417.

75. Laass, M. W., Roggenbuck, D., Conrad K. 2014. Diagnosis and classification of Crohn's disease. *Autoimmunity Reviews* 13: 467–471.

76. Lambert, J. R., Luk, S..C. PKPH. 1980. Brown bowel syndrome in Crohn' disease. *Archives of pathology & laboratory medicine* 104: 201–205.

77. Li, X. A., Zhou ,Y., Zhou, S. X., Liu, H. R., Xu, J. M., Gao, L., Yu, X. J., Li, X. H. 2015. Histopathology of melanosis coli and determination of its associated genes by comparative analysis of expression microarrays. *Molecular Medicine Reports* 12: 5807–5815.

78. Lichtenstein, G. R., Loftus, E. V., Isaacs, K. L., Regueiro, M. D., Gerson, L. B., Sands, B. E. 2018. ACG Clinical Guideline: Management of Crohn's Disease in Adults. *American Journal of Gastroenterology* 113: 481–517.

79. Lin, C., Rogers, C. D., Majidi, S. 2015. Fat suppression techniques in breast magnetic resonance imaging: A critical comparison and state of the art. *Reports in Medical Imaging* 8: 37–49.

80. Lin, W., Chen, J. 2015. Pitfalls and Limitations of Diffusion-Weighted Magnetic Resonance Imaging in the Diagnosis of Urinary Bladder Cancer. *Translational Oncology* 8: 217–230.

81. Lionel Arrivé, S. E. M. 2013. MR Enterography versus MR Enteroclysis. *Radiology* 266: 688.

82. Lönnfors, S., Vermeire, S., Greco, M., Hommes, D., Bell, C., Avedano, L. 2014. IBD and health-related quality of life - Discovering the true impact. *Journal of Crohn's and Colitis* 8: 1281–1286.

83. Ma, C., Moran, G. W., Benchimol, E. I., Targownik, L. E. , Heitman, S. J., Hubbard, J. N., Seow, C. H., Novak, K. L., Ghosh, S., Panaccione, R., et al. 2017. Surgical Rates for Crohn's Disease are Decreasing: A Population-Based Time Trend Analysis and Validation Study. *American Journal of Gastroenterology* 112: 1840–1848.

84. Maaser, C., Novak, K. 2019. Radiology. In: Sturm A., White L., ed. *Inflammatory Bowel Disease Nursing Manual*. Cham: Springer. 51-60.

85. Maaser, C., Sturm, A., Vavricka, S. R., Kucharzik, T., Fiorino, G., Annese, V., Calabrese, E., Baumgart, D. C., Bettenworth, D., Borralho, Nunes P., et al. 2019. ECCO-ESGAR Guideline for Diagnostic Assessment in IBD Part 1: Initial diagnosis, monitoring of known IBD, detection of complications. *Journal of Crohn's and Colitis*: 144-164J.

86. Maglinte, D. D. T., Gourtsoyiannis, N., Rex, D., Howard, T.J., Kelvin, F. M. 2003. Classification of small bowel Crohn's subtypes based on multimodality imaging. *Radiologic Clinics of North America* 41: 285–303.

87. Magro, F., Langner, C., Driessen, A., Ensari, A., Geboes, K., Mantzaris, G. J., Villanacci, V., Becheanu, G., Nunes, P. B., Cathomas, G., et al. 2013. European consensus on the histopathology of inflammatory bowel disease. *Journal of Crohn's and Colitis* 7: 827–851.

88. Mantarro, A., Scalise, P., Guidi, E., Neri, E. 2017. Magnetic resonance enterography in Crohn's disease: How we do it and common imaging findings. *World Journal of Radiology* 9: 46.

89. Martin, D. R., Kalb, B., Sauer, C. G., Alazraki, A., Goldschmid, S. 2012. Magnetic resonance enterography in Crohn's disease: Techniques, interpretation, and utilization for clinical management. *Diagnostic and Interventional Radiology* 18: 374–386.

90. Masselli, G., Gualdi, G.. 2012. MR Imaging of the Small Bowel. *RadioGraphics* 264: 333–348.

91. Matsuoka, H,. Yoshida, Y., Oguro, E., Murata, A., Kuzuya, K., Okita, Y., Teshigawara, S., Yoshimura, M., Isoda, K., Harada, Y., et al. 2019. Diffusion weighted whole body imaging with

background body signal suppression (DWIBS) was useful for the diagnosis and follow-up of giant cell arteritis. *Internal Medicine* 58: 2095–2099.

92. Maxfield, C. M. 2019. Diffusion Magnetic Resonance Imaging. In: Mangrum, T., Amrhein, T., Duncan, S., Hoang, P. B., Maxfield, C., Song, A., Merkle, E. *Duke Review of MRI Physics*. Philadelphia: Elsevier. 73.

93. Mazza, M., Cilluffo, M. G., and Capello, M. 2016. "Crohn's Disease." Pp. 7–8 in *Crohn's Disease*. Switzerland: Springer.

94. Hutchings, H., Alrubaiy, L. 2017. Crohn's Disease Activity Index. In: Michalos A. C. Ed. *The encyclopedia of quality of life and well-being research*. Dordrecht, New York, London: Elsevier. 1354–1357.

95. Mitsuyama, K., Niwa, M., Takedatsu, H., Yamasaki, H., Kuwaki, K., Yoshioka, S., Yamauchi, R., Fukunaga, S., Torimura, T. 2016. Antibody markers in the diagnosis of inflammatory bowel disease. *World Journal of Gastroenterology* 22: 1304–1310.

96. Mollard, B. J, Smith, E. A, Dillman J. R. 2015. Pediatric MR enterography: Technique and approach to interpretation-how we do it. *Radiology* 274: 29–43.

97. Molodecky, N. A., Kaplan, G. G. 2010. Environmental risk factors for inflammatory bowel disease. *Gastroenterology and Hepatology* 6: 339–346.

98. Molodecky, N. A, Soon, I. S., Rabi, D. M., Ghali, W. A., Ferris, M., Chernoff, G., Benchimol, E. I., Panaccione, R., Ghosh S.,, Barkema, H. W., et al. 2012. Increasing incidence and prevalence of the inflammatory bowel diseases with time, based on systematic review. *Gastroenterology* 142: 46–54.

99. Moon, J. S. 2019. Clinical aspects and treatments for pediatric inflammatory bowel disease. *Intestinal Research* 17: 17–23.

100. Moore, W. A., Khatri, G., Madhuranthakam, A. J., Sims, R. D., Pedrosa, I. 2014. Added value of diffusion-weighted acquisitions in MRI of the abdomen and pelvis. *American Journal of Roentgenology* 202: 995–1006.

101. Morani, A. C, Smith, E. A., Ganeshan, D., Dillman, J. R. 2015. Diffusion-Weighted MRI in Pediatric Inflammatory Bowel Disease. *American Journal of Roentgenology* 204: 1269–1277.

102. Moy, M. P, Sauk, J., Gee, M. S. 2016. The role of MR enterography in assessing Crohn's disease activity and treatment response. *Gastroenterology Research and Practice* 2016: 1–13.

103. Nardone O. M, Iacucci M., Cannatelli R., Zardo D., Ghosh S. 2019. Can advanced endoscopic techniques for assessment of mucosal inflammation and healing approximate histology in inflammatory bowel disease ? 12: 1–17.

104. Negaard A., Paulsen V., Sandvik L., Berstad A. E., Borthne A., Try K., Lygren I., Storaas T., Klow N. E. 2007. A prospective randomized comparison between two MRI studies of the small bowel in Crohn's disease, the oral contrast method and MR enteroclysis. *European Radiology* 17: 2294–2301.

105. Neubauer, H., Pabst, T., Dick, A., MacHann, W., Evangelista, L., Wirth, C., Köstler, H., Hahn, D., Beer, M. 2013. Small-bowel MRI in children and young adults with Crohn disease: Retrospective head-to-head comparison of contrast-enhanced and diffusion-weighted MRI. *Pediatric Radiology* 43: 103–114.

106. Oguro, E., Ohshima, S., Kikuchi-Taura, A., Murata, A., Kuzuya, K., Okita, Y., Matsuoka, H.,

Teshigawara, S., Yoshimura, M., Yoshid,a Y., et al. 2019. Diffusion-weighted whole-body imaging with background body signal suppression (DWIBS) as a novel imaging modality for disease activity assessment in takayasu's arteritis. *Internal Medicine* 58: 1355–1360.

107. Okamoto, R. 2011. Epithelial regeneration in inflammatory bowel diseases. *Inflammation and Regeneration* 31: 275–281.

108. Ordás, I., Rimola, J., Alfaro, I., Rodríguez, S., Castro-Poceiro, J., Ramírez-Morros, A., Gallego, M., Giner, À., Barastegui, R., Fernández-Clotet, A., et al. 2019. Development and Validation of a Simplified Magnetic Resonance Index of Activity for Crohn's Disease. *Gastroenterology* 157: 432–439.

109. Oto A., Zhu F., Kulkarni K., Karczmar G. S., Turner J. R., Rubin D. 2009. Evaluation of diffusion-weighted MR imaging for detection of bowel inflammation in patients with Crohn's disease. *Academic radiology* 16: 597–603.

110. Oto, A., Kayhan, A., Williams, J. T. B., Fan, X., Yun L., Arkani, S., Rubin D. T.. 2011. Active Crohn's disease in the small bowel: evaluation by diffusion weighted imaging and quantitative dynamic contrast enhanced MR imaging. *Journal of magnetic resonance imaging : JMRI*.

111. Ouyang, Z., Ouyang, Y., Zhu, M., Lu, Y., Zhang, Z., Shi, J., Li, X., Ren, G. 2014. Diffusion-weighted imaging with fat suppression using short-tau inversion recovery: Clinical utility for diagnosis of breast lesions. *Clinical Radiology* 69: e337–e344.

112. Panes, J., Bouhnik, Y., Reinisch, W., Stoker, J., Taylor, S. A., Baumgart, D. C., Danese, S., Halligan, S., Matos, C., Peyrin-Biroulet, L., et al. 2013. Imaging techniques for assessment of inflammatory bowel disease: Joint ECCO and ESGAR evidence-based consensus guidelines. *Journal of Crohn's and Colitis* 7: 556–585.

113. Pariente, B., Cosnes, J., Danese, S., Sandborn, W. J., Lewin, M., Fletcher, J. G., Chowers, Y., D'Haens, G., Feagan, B. G., Hibi, T., et al. 2011. Development of the Crohn's disease digestive damage score, the Lémann score. *Inflammatory Bowel Diseases* 17: 1415–1422.

114. Park, S. H. 2016. DWI at MR Enterography for Evaluating Bowel Inflammation in Crohn Disease. *American Journal of Roentgenology* 207: 40–48.

115. Perez-Rodriguez, J., Lai, S., Ehst, B. D., Fine, D. M., Bluemke, D. A. 2009. Nephrogenic Systemic Fibrosis: Incidence, Associations, and Effect of Risk Factor Assessment—Report of 33 Cases. *Radiology* 250: 371–377.

116. Peyrin-Biroulet, L., Sandborn, W., Sands, B. E, Reinisch, W., Bemelman, W., Bryant, R. V., D'Haens, G,. Dotan, I., Dubinsky, M., Feagan, B., et al. 2015. Selecting Therapeutic Targets in Inflammatory Bowel Disease (STRIDE): Determining Therapeutic Goals for Treat-to-Target. *American Journal of Gastroenterology* 110: 1324–1338.

117. Qi, F., Jun, S., Qi, Q. Y., Chen, P. J., Chuan, G. X., Jiong, Z., Rong, X. J. 2015. Utility of the diffusion-weighted imaging for activity evaluation in Crohn's disease patients underwent magnetic resonance enterography. *BMC gastroenterology* 15: 12.

118. Quattrocchi, C. C., van der Molen, A. J. 2017. Gadolinium Retention in the Body and Brain: Is It Time for an International Joint Research Effort? *Radiology* 282: 12–16.

119. Sheth, R.A. and Gee, M. S. 2016. The Imaging of Inflammatory Bowel Disease: Current Concepts and Future Directions. In *Intech* 1–21.

120. Rajesh, A., Sinha, R. 2014. *Crohn ' s Disease: Current concepts* (Arumugam Rajesh and Rakesh Sinha, Ed). Springer.

121. Ram, R., Sarver, D., Pandey, T., Guidry, C. L., Jambhekar, K. R. 2016. Magnetic resonance enterography: A stepwise interpretation approach and role of imaging in management of adult Crohn's disease. *Indian Journal of Radiology and Imaging* 26: 173–184.

122. Van Rheenen, P. F., Van de Vijver, E., Fidler, V. 2010. Faecal calprotectin for screening of patients with suspected inflammatory bowel disease: diagnostic meta-analysis. *BMJ (Clinical Research Ed.)* 341: c3369.

123. Rimola, J., Rodriguez, S., García-Bosch, O., Ordás, I., Ayala, E., Aceituno, M., Pellisé, M., Ayuso, C., Ricart, E., Donoso, L., et al. 2009. Magnetic resonance for assessment of disease activity and severity in ileocolonic Crohn's disease. *Gut* 58: 1113–1120.

124. Rimola, J., Ordás, I., Rodriguez, S., García-Bosch, O., Aceituno M., Llach J,., Ayuso C., Ricart, E., Panés, J. 2011. Magnetic resonance imaging for evaluation of Crohn's disease: Validation of parameters of severity and quantitative index of activity. *Inflammatory Bowel Diseases* 17: 1759–1768.

125. Riddell, R. D. J. 2014. Inflammatory Bowel Diseases. In: in *Gastrointestinal Pathology and Its Clinical Implications*. Vol. II. 2nd ed. edited by Lippincott Williams & Wilkins. Philadelphia: Wolters Kluwer. Pp. 983-1208

126. Rozendorn, N., Amitai, M. M., Eliakim, R. A., Kopylov, U , Klang, E. 2018. A review of magnetic resonance enterography-based indices for quantification of Crohn's disease inflammation. *Therapeutic advances in gastroenterology* 11: 1–21.

127. Sakuraba, H., Ishiguro, Y., Hasui, K., Hiraga, H., Fukuda, S., Shibutani, K., Takai, Y. 2014. Prediction of maintained mucosal healing in patients with Crohn's disease under treatment with infliximab using diffusion-weighted magnetic resonance imaging. *Digestion* 89: 49–54.

128. Sánchez-González, J., Lafuente-Martínez, J. 2012. "Diffusion-Weighted Imaging: Acquisition and Biophysical Basis." Pp. 1–15 in *Diffusion MRI Outside the Brain*: A Case-Based Review and Clinical Applications. Berlin Heidelberg: Springer-Verlag.

129. Sankey, E. A., Dhillon, A. P, Anthony, A, Wakefield, A. J, Sim, R, More, L, Hudson, M, Sawyerr, A. M., Pounder, R.E. 1993. Early mucosal changes in Crohn's disease. *Gut* 34: 375–381.

130. Sarbu, M. I., Sarbu, N. 2019. Musculoskeletal clinical and imaging manifestations in inflammatory bowel diseases. *Open Medicine (Poland)* 14: 75–84.

131. Scherrer, B., Gholipour, A., Warfield S. K. 2011. Super-Resolution in Diffusion-Weighted Imaging Benoit. *Med Image Comput Comput Assist Interv.* 14: 124–132.

132. Schlaudecker, J. D., Bernheisel, C. R. 2009. Gadolinium-associated nephrogenic systemic fibrosis. *American Family Physician* 80: 711–714.

133. Schmidt, S. A., Baumann, J. A., Stanescu-Siegmund, N., Froehlich, E., Brambs, H. J., Juchems, M. S. 2016. Oral distension methods for small bowel MRI: Comparison of different agents to optimize bowel distension. *Acta Radiologica* 57: 1460–1467.

134. Schreyer, A. G., Geissler, A., Albrich, H., Schölmerich, J., Feuerbach, S., Rogler, G., Völk, M., Herfarth, H. 2004. Abdominal MRI After Enteroclysis or With Oral Contrast in Patients With Suspected or Proven Crohn's Disease. *Clinical Gastroenterology and Hepatology* 2: 491–497.

135. Serban, E. D. 2018. Treat-to-target in Crohn's disease: Will transmural healing become a therapeutic endpoint? *World Journal of Clinical Cases* 6: 501–513.

136. Sharman, A., Zealley, I. A., Bassett, P., Greenhalg, R., Taylor, S. A. 2009. MRI of small bowel

Crohn's disease : determining the reproducibility of bowel wall gadolinium enhancement measurements. European Radiology 19: 1960–1967.

137. Shimizu, H., Suzuki, K., Watanabe, M., Okamoto, R.. 2019. Stem cell-based therapy for inflammatory bowel disease. *Intestinal Research* 17: 311–316.

138. Sinha, R., Verma, R., Verma, S., Rajesh, A. 2011a. MR enterography of Crohn disease: Part 1, rationale, technique, and pitfalls. *American Journal of Roentgenology* 197: 76–79.

139. Sinha, R., Verma, R., Verma, S., Rajesh, A. 2011b. MR enterography of Crohn disease: Part 2, imaging and pathologic findings. *American Journal of Roentgenology* 197: 80–85.

140. Sinha, R., Rajiah, P., Ramachandran, I., Sanders, S., Murphy, P. D. 2013. Diffusion-weighted MR imaging of the gastrointestinal tract: technique, indications, and imaging findings. *Radiographics* 33: 655–676.

141. Sirin, S., Kathemann, S., Schweiger, B., Hahnemann, M. L., Forsting, M., Lauenstein, T. C., Kinner, S. 2015. Magnetic resonance colonography including diffusion-weighted imaging in children and adolescents with inflammatory bowel disease: Do we really need intravenous contrast? *Investigative Radiology* 50: 32–39.

142. Skuja, V. 2020. Iekaisīgo zarnu slimību aktivitāte iepriekš hospitalizētiem pacientiem ar paplašināta spektra beta-laktamāzes producējošām Enterobacteriaceae dzimtas baktērijām zarnu traktā: Promocijas darbs: specialitāte – klīniskā medicīna. Riga.

143. Smith, E. A., Dillman, J. R., Adler, J., Dematos-Maillard, V. L., Strouse, P. J. 2012. MR enterography of extraluminal manifestations of inflammatory bowel disease in children and adolescents: Moving beyond the bowel wall. *American Journal of Roentgenology* 198: 38–45.

144. De Sousa, H. T, Brito, J., Magro, F. 2018. New cross-sectional imaging in IBD. *Current Opinion in Gastroenterology* 34: 194–207.

145. Stadlbauer, A., Salomonowitz, E., Bernt, R., Haller, J., Gruber, S., Bogner, W., Pinker, K., van der Riet, W. 2009. Diffusion-weighted MR imaging with background body signal suppression (DWIBS) for the diagnosis of malignant and benign breast lesions. *European Radiology* 19: 2349–2356.

146. Stanescu-Siegmund, N., Nimsch, Y., Wunderlich, A. P., Wagner, M., Meier, R., Juchems, M. S., Beer, M., Schmidt, S. A. 2017. Quantification of inflammatory activity in patients with Crohn's disease using diffusion weighted imaging (DWI) in MR enteroclysis and MR enterography. *Acta Radiologica* 58: 264–271.

147. Stone, A. J., Browne, J. E., Lennon, B., Meaney, J. F., Fagan, A. J. 2012. Effect of motion on the ADC quantification accuracy of whole-body DWIBS. *Magnetic Resonance Materials in Physics, Biology and Medicine* 25: 263–266.

148. Sturm, A., Maaser, C., Calabrese, E., Annese, V., Fiorino, G., Kucharzik, T., Vavricka, S. R., Verstockt, B., Van Rheenen, P., Tolan, D., et al. 2018. ECCO-ESGAR Guideline for Diagnostic Assessment in IBD Part 2: IBD scores and general principles and technical aspects. *Journal of Crohn's and Colitis* 13: 273-284E.

149. Surawicz, C. M., Haggitt, R. C., Husseman, M., McFarland, L. V. 1994. Mucosal biopsy diagnosis of colitis: Acute self-limited colitis and idiopathic inflammatory bowel disease. *Gastroenterology* 107: 755–763.

150. Takahara, T. 2005. DWIBS: Diffusion-weighted whole-body imaging with background body signal suppression. *MEDICAMUNDI* 49: 38–41.

151. Takahara, T., Imai, Y., Yamashita, T., Yasuda, S., Nasu, S., Van Cauteren, M. 2004. Diffusion weighted whole body imaging with background body signal suppression (DWIBS): technical improvement using free breathing, STIR and high resolution 3D display. *Radiation medicine* 22: 275–282.

152. Tielbeek, J. A. W., Makanyanga, J. C., Bipat, S., Pendse, D. A., Nio, C. Y., Vos, F. M., Taylor, S. A., Stoker, J. 2013. Grading Crohn Disease Activity With MRI: Interobserver Variability of MRI Features, MRI Scoring of Severity, and Correlation With Crohn Disease Endoscopic Index of Severity. *American Journal of Roentgenology* 201: 1220–1228.

153. Tontini, G. E., Vecchi, M., Pastorelli, L., Neurath, M. F., Neumann, H. 2015. Differential diagnosis in inflammatory bowel disease colitis: State of the art and future perspectives. *World Journal of Gastroenterology* 21: 21–46.

154. Torres, J., Bonovas, S., Doherty, G., Kucharzik, T., Gisbert, J. P., Raine, T., Adamina, M., Armuzzi, A., Bachmann, O., Bager, P., et al. 2020. ECCO guidelines on therapeutics in Crohn's disease: Medical treatment. *Journal of Crohn's and Colitis* 14: 4–22.

155. Triester, S. L., Leighton, J. A., Leontiadis, G. I., Gurudu, S. R., Fleischer, D. E., Hara, A. K., Heigh, R. I., Shiff, A. D., Sharma, V., K. 2006. A Meta-Analysis of the Yield of Capsule Endoscopy Compared to Other Diagnostic Modalities in Patients with Non-Stricturing Small Bowel Crohn's Disease. *American Journal of Gastroenterology* 101: 954–964.

156. Turner, D., Griffiths, A. M., Walters, T. D., Seah, T., Markowitz, J., Pfefferkorn, M., Keljo, D., Otley, A., LeLeiko, N. S., Mack, D., et al. 2010. Appraisal of the Pediatric Crohn's Disease Activity Index on Four Prospectively Collected Datasets: Recommended Cutoff Values and Clinimetric Properties. *American Journal of Gastroenterology* 105: 2085–2092.

157. Vermeire, S., Van Assche, G., Rutgeerts, P. 2012. Classification of inflammatory bowel disease: The old and the new. *Current Opinion in Gastroenterology* 28: 321–326.

158. Walsham, N. E., Sherwood, R. A. 2016. Faecal calprotectin in inflammatory bowel disease. *Clinical and experimental gastroenterology* 9: 21–29.

159. Wang, A., Banerjee, S., Barth, B. A., Bhat, Y. M., Chauhan, S., Gottlieb, K. T., Konda, V., Maple, J. T., Murad, F., Pfau, P. R., et al. 2013. Technology status evaluation report: Wireless capsule endoscopy. *Gastrointestinal Endoscopy* 78: 805–815.

160. Watson, T., Calder, A., Barber, J. L. 2018. Quantitative bowel apparent diffusion coefficient measurements in children with inflammatory bowel disease are not reproducible. *Clinical Radiology* 73: 574–579.

161. Westbrook, C., Roth, C. K, Talbot, J. 2011. *MRI in Practice, 4th edition*. Wiley-Blackwell. 396-400.

162. Yoon, K., Chang, K., Lee, H. J. 2015. MRI for Crohn ' s Disease: Present and Future. *BioMed Research International* 2015: 1–9.

163. Zhu, J., Zhang, F., Liu, F., He, W., Tian, J., Han, H., Cao, P. 2015. Identifying the inflammatory and fibrotic bowel stricture: MRI diffusion-weighted imaging in Crohn's disease. *Radiology of Infectious Diseases* 2: 128–133.

164. Zorzi, F., Stasi, E., Bevivino, G., Scarozza, P., Biancone, L., Zuzzi, S., Rossi, C., Pallone, F., Calabres,e E. 2014. A Sonographic Lesion Index for Crohn's Disease Helps Monitor Changes in Transmural Bowel Damage During Therapy. *Clinical Gastroenterology and Hepatology* **12**: 2071–2077.

Acknowledgements

I would like to sincerely thank my supervisor, Professor Gaida Krūmiņa, for her support and patience throughout the dissertation process. Thanks to Professor Juris Pokrotnieks, the scientific advisor of my work, for his valuable advice and encouragement.

Thank you to my *Alma mater* – Rīga Stradiņš University for the valuable doctoral studies and financial support in publishing the dissertation research.

I am very grateful to Assistant Professor Irena Rogovska for her help in selecting the statistical methods for the research and data processing. Her responsiveness and practical support at the right time allowed me to persevere and get the job done. Special thanks to Professor Ilze Konrāde for her encouragement and support in times of doubt.

I would like to thank Dr. Ieva Puķīte for her enthusiasm and motivation to develop MR enterography examinations in the Children's Clinical University Hospital. Thanks to my staff of the Diagnostic Radiology Department of Children's Clinical University Hospital for their patience and understanding. Special heartful thanks to the radiographers Jeļena Kasatkina, Rimma Siliņeviča, Reinis Kārklevalks and Roberts Purmalis, who performed all the MR enterography examinations included in the dissertation analysis in technical and high quality.

I am immensely grateful to my students Santa Pūre, Monta Baduna, Reinis Pitura and Ieva Pirksta for practical help in data collection and compilation, preparation of publications, and for being my greatest teachers in my growth as a researcher.

Any great achievement is based on early experiences and our first teachers; I sincerely regret misunderstanding the meaning of physics during secondary school, and thank Mazsalaca Secondary School physics teacher Guntars Bērziņš for providing me with the knowledge required to select my specialty. Heartfelt thanks to the late Assistant Professor Ēriks Reinholds for his support and encouragement to study abroad, Dr. Arnolds Atis Veinbergs, the head of the Institute of Diagnostic Radiology at P. Stradiņš Clinical University Hospital, for giving me freedom and independence at the start of my professional career. Thanks for the kindness and teaching of abdominal radiology to Assistant Professor Pēteris Priedītis and Dr. Andris Laganovskis. I would also like to thank Dr. Karl Olof Gunnar Åström, a radiologist at Uppsala University Hospital, for the time dedicated to me, knowledge of the basics of MRI, a welcome seat in his office and his heartfelt jokes.

My heartfelt thanks to Professor Taro Takahara from Tokai University, the "father" of the DWIBS sequence, for his valuable advice and practical help during the preparation of this dissertation. Thanks to Dr. Jordi Rimola from the University of Barcelona, the author of the MaRIA, for his wonderful ideas and inspiration at a time when the research process seemed to

be at a standstill. Thanks also to Jochen Herrmann, Head of the Department of Paediatric Radiology, University Hospital Eppendorf, Hamburg, for introducing the "German concept of precision" to my research process. I would like to thank medical physicists Bert Principaal and Rogeriolopes Pintolopes for their valuable explanation of physics throughout the work process.

Thanks to the Latvian Association of Physicians and Dentists for the funding allocated to me to complete a part of my doctoral research at Ependorf University Hospital in Hamburg.

Many thanks to my colleagues and friends, especially Zane Dāvidsone, Arta Bārzdiņa and Madara Kreile, for their moral support throughout the research work and whilst writing the publications. My heartfelt thanks to Laura Dennler for her knowledge of how to climb a mountain with two steps forward and three steps back. Special thanks to Anita Straujuma, Sigita Kazūne and Lāsma Līdaka for sharing their own experiences in the fight against procrastination, the integral part of writing the Doctoral Thesis. Thanks to my friends, artists and musicians, especially violinists Professor Gunārs Larsens, Skaidrīte Rakovska and Velga Polinska, for their influence on my personal and professional development, providing a fresh perspective on my life and work.

Thanks to Rūta Lapsa, Guna Zvirbule and Katrina Marija Nielsen for text corrections, as well as Rihards Rūmnieks and Maija Lavrinoviča for their help with the image processing.

Finally, I would like to thank my parents, medical doctors Pārsla Radziņa and Māris Radziņš, for their cosy shelter, delicious cottage cheese dumplings and skiing in the snowy forests of Mazsalaca, pampering me in the most difficult stages of writing. My sincere thanks to my husband Jānis, daughters Alma and Maria for their patience, understanding, support and love throughout the work.

Supplements

Publication I

medicina

MDPI

Article

The Influence of Bowel Preparation on ADC Measurements: Comparison between Conventional DWI and DWIBS Sequences

Ilze Apine [1,2,*], Monta Baduna [2], Reinis Pitura [3], Juris Pokrotnieks [4] and Gaida Krumina [2]

1 Children Clinical University Hospital, LV-1004 Riga, Latvia
2 Department of Diagnostic Radiology, Riga Stradin's University, LV-1038 Riga, Latvia
3 Faculty of Medicine, Riga Stradin's University, LV-1007 Riga, Latvia
4 Department of Internal Diseases, Riga Stradin's University, LV-1038 Riga, Latvia
* Correspondence: dr.ilze.apine@gmail.com; Tel.: +371-294-616-16

Received: 5 June 2019; Accepted: 18 July 2019; Published: 21 July 2019

Abstract: *Background and objectives:* The aim of the study was to assess whether there were differences between apparent diffusion coefficient (ADC) values of diffusion-weighted imaging (DWI) and diffusion-weighted imaging with background body signal suppression (DWIBS) sequences in non-prepared and prepared bowels before and after preparation with an enteric hyperosmolar agent, to assess whether ADC measurements have the potential to avoid bowel preparation and whether ADC-DWIBS has advantages over ADC-DWI. *Materials and Methods:* 106 adult patients without evidence of inflammatory bowel disease (IBD) underwent magnetic resonance (MR) enterography before and after bowel preparation. ADC-DWI and ADC-DWIBS values were measured in the intestinal and colonic walls demonstrating high signal intensity (SI) at DWI tracking images of b = 800 s/mm^2 before and after preparation. *Results:* There were significant difference ($p < 0.0001$) in both ADC-DWI and ADC-DWIBS results between non-prepared and prepared jejunum for DWI being 1.09×10^{-3} mm^2/s and 1.76×10^{-3} mm^2/s, respectively, and for DWIBS being 0.91×10^{-3} mm^2/s and 1.75×10^{-3} mm^2/s, respectively. Both ADC-DWI and DWIBS also showed significant difference between non-prepared and prepared colon ($p < 0.0001$), with DWI values 1.41×10^{-3} mm^2/s and 2.13×10^{-3} mm^2/s, and DWIBS—1.01×10^{-3} mm^2/s and 2.04×10^{-3} mm^2/s, respectively. No significant difference between ADC-DWI and ADC-DWIBS was found in prepared jejunum ($p = 0.84$) and prepared colon ($p = 0.58$), whereas a significant difference was found in non-prepared jejunum and non-prepared colon ($p = 0.0001$ in both samples). *Conclusions:* ADC between DWI and DWIBS does not differ in prepared bowel walls but demonstrates a difference in non-prepared bowel. ADC in non-prepared bowel is lower than in prepared bowel and possible overlap with the ADC range of IBD is possible in non-prepared bowel. ADC-DWIBS has no advantage over ADC-DWI in regard to IBD assessment.

Keywords: MR enterography; MRE; diffusion-weighted imaging; DWI; DWIBS; ADC

1. Introduction

Crohn's disease (CD) is a chronic inflammatory bowel disease (IBD) of rising incidence and prevalence [1]. It has high complication rates [2], requiring surgical treatment upon progression [3] and resulting in a negative impact on patients' quality of life [4]. It can however be treated more successfully if the disease is detected early.

Superior soft tissue contrast resolution enables magnetic resonance imaging (MRI) to track bowel inflammation beyond the reach of the endoscope. However, magnetic resonance enterography (MRE)

requires bowel distension by an oral hyperosmolar enteric contrast agent [5], causing adverse effects sometimes leading to poor tolerance by patients [6,7]. MRE is contraindicated in patients requiring general anesthesia. MRE in IBD requires the use of intravenous gadolinium contrast agents [5], potentially causing systemic nephrogenic fibrosis [8] and formation of gadolinium deposits in the brain and body tissues [9–11]. This demonstrates that solutions allowing avoiding gadolinium administration are important.

Diffusion-weighted imaging (DWI) has shown a potential to replace contrast medium administration and to detect lesions before they come visible in conventional images [12]. DWI images use diffusion gradient applied in three perpendicular axes, with several b values (for example, 0, 50, 800 s/mm^2) [13]. Inflamed segments as high signal intensity (SI) zones are best identified in the DWI tracking images of high b value, most commonly, b = 800 s/mm^2 [14]. Diffusion is measured quantitatively by the apparent diffusion coefficient (ADC). Nevertheless, in spite of the high sensitivity and specificity of adding DWI to the MR imaging protocol, the specificity of DWI alone in assessment of IBD is still low, being 39–61% [15,16], since intact bowel walls also often present high SI in DWI tracking images of high b values (Figure 1).

A derivation of DWI, diffusion-weighted imaging with background body signal suppression (DWIBS), was introduced for whole body imaging of patients in order to detect metastases and tumour relapse. DWIBS provides more uniform fat suppression through the use of short T1 inversion recovery (STIR) based approach. This is a free breathing technique permitting multiple number of signal acquisitions to average motion [17]. Therefore, DWIBS provides a higher contrast-to-noise ratio, reduced image distortion, and better detection of subtle lesions [18]. A disadvantage of DWIBS is poorer signal-to noise ratio (SNR) [19], resulting in grainy image appearance. Despite the extensive use of DWIBS, there are very few studies regarding its use in assessment of the digestive tract. Tomizawa et al. performed studies on DWIBS in regards to assessing gall bladder walls and gastrointestinal tract [20–23]. Several researchers included a free breathing DWI sequence in their MRE protocol for the assessment of inflammatory bowel disease [13,24,25], however, no research data exist on comparison between DWI and DWIBS in bowel imaging. Whilst similar to other body tissue, the bowel wall presents a better resolution in DWIBS, compared to DWI sequence in both intact (Figure 1) and inflamed (Figure 2) bowel walls. Besides, DWIBS is more reproducible than DWI [26], and ADC-DWIBS values are also unaltered by motion [27]. Therefore, DWIBS could be beneficial over routinely used DWI in assessment of bowel inflammation.

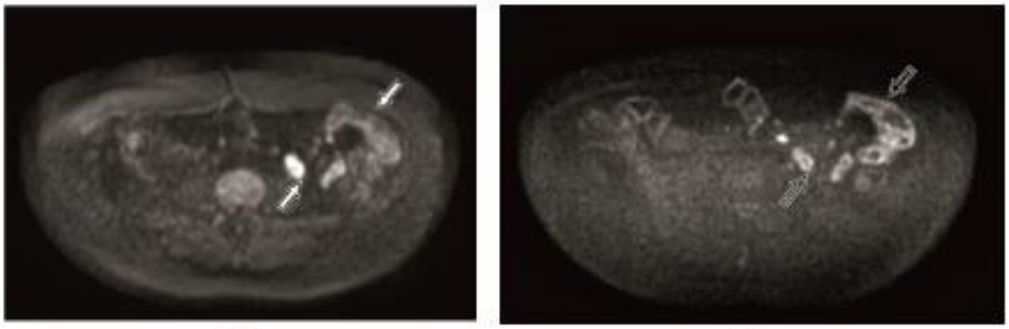

(**a**) (**b**)

Figure 1. Diffusion-weighted imaging (DWI) (**a**) and diffusion-weighted imaging with background body signal suppression (DWIBS) (**b**) tracking images of b = 800 s/mm^2 within the magnetic resonance enterography (MRE) of 41-year-old female patient with intact bowels. The unaltered bowel wall shows high signal intensity (SI). Better resolution of the bowel loop in the DWIBS image (**b**, black arrow) is seen comparing to the DWI image (**a**, white arrow).

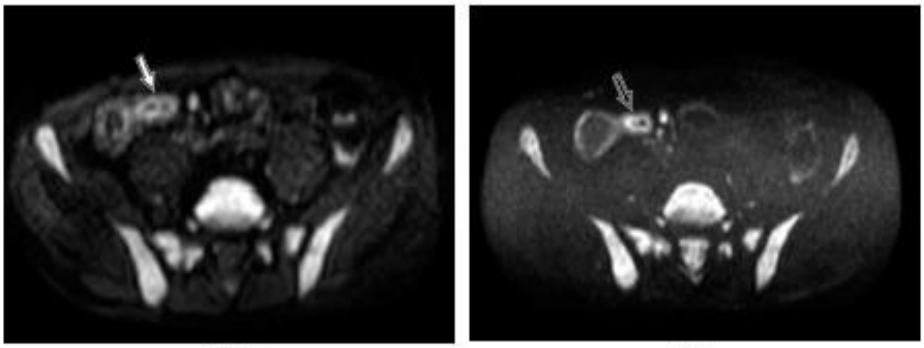

(**a**) (**b**)

Figure 2. DWI (**a**) and DWIBS (**b**) tracking images of b = 800 s/mm^2 within the MRE of 40-year-old male patient with histologically proven Crohn's disease. Altered bowel loop shows high SI. Better resolution and delineation of the inflamed bowel mucosa in the DWIBS image (**b**, black arrow) is seen as compared to the DWI image (**a**, white arrow).

The purpose of our study was to estimate the potential significance of using ADC measurements in DWI and DWIBS in patients, without preparing bowels with a hyperosmolar enteric contrast agent by setting the following tasks:

1. assessing ADC-DWI and ADC-DWIBS values in intestines without preparation (collapsed bowel) and after preparation with hyperosmolar enteric contrast agent (filled bowel);
2. assessing ADC-DWI and ADC-DWIBS values in the colon without preparation (in presence of intraluminal faeces) and after ingestion of enteric contrast agent (presence of it in the bowel lumen);
3. comparing the consistency between ADC values of DWI and DWIBS, in conditions with and without bowel preparation in both intestines and the colon, and analyzing the utilization of DWIBS in MR of bowel imaging.

2. Materials and Methods

2.1. Patient Population

This prospective study included 106 primary care patients (18–76 years old), referred to MRE from March 2015 until March 2018, due to dyspeptic complaints but with no clinical and/or morphological evidence of IBD. The inclusion criteria were: absence of typical IBD symptoms—diarrhea, bloody and/or mucous stool, severe and/or crampy abdominal pain and rectal involvement [28,29].

The exclusion criteria were: age <18 years, fecal calprotectin (FC) level >200 µg/g, acute bowel infection, proven or previously diagnosed IBD, endoscopically proven enteropathy (e.g., coeliac disease, collagenous colitis etc.), present bowel tumor, and systemic diseases such as cystic fibrosis.

2.2. The Study

In this prospective observational cross-sectional study, ADC of DWI and DWIBS were assessed in bowel walls before and after preparation with hyperosmolar enteric contrast agent. Prior to bowel preparation, DWI and DWIBS scanning sequences were performed in all patients. Afterwards, patients were given enteric contrast agent, and scanned as per complete MRE protocol with DWI and DWIBS sequences included.

The study included two cohorts: (1) assessment of ADC-DWI and ADC-DWIBS intestinal walls before and after patient preparation, and (2) assessment of ADC-DWI and ADC-DWIBS in colonic walls before and after preparation. ADC measurements were only performed on bowel segments where high SI was present in DWI tracking images of b = 800 s/mm^2. In order to compare ADC before and after

bowel preparation, only patients with measurements both before and after preparation were included in the further data analysis. Similarly, for comparison between ADC-DWI and ADC-DWIBS, only patients with measurements performed in both DWI and DWIBS sequences were included in the further analysis. In both cohorts, data were grouped by the preparation state of the patient—non-prepared versus prepared bowels—and mutually compared.

All patients fasted for at least 6 h prior to MRE. After the initial scanning of DWI and DWIBS in prone position, patients were instructed to intake 1.250–1.500 l of 2.5% mannitol solution within 45–60 min, followed by full MRE exam in prone position. During the MRE exam and prior to DWI and DWIBS sequences, 20 mg dose of butylscopolamin was intravenously administered to reduce bowel peristalsis.

Patients were scanned with 1.5 T MRI system (Ingenia, Philips Medical Systems, Best, The Netherlands) using a 16-channel body coil. The applied DWI and DWIBS protocols were obtained from the Philips standard abdominal protocol and included in the protocol repository of the MRI system. To enable DWIBS-ADC measurements, the standard DWIBS protocol was amended by replacing a single b factor b = 1000 s/mm^2 by three b factors 0 s/mm^2, 600 s/mm^2 and 800 s/mm^2, consistent to DWI protocol.

The scanning parameters for DWI and DWIBS protocols are given in the Table 1.

Table 1. Scanning parameters for DWI and DWIBS protocols.

Scanning Protocol	DWI [1]	DWIBS [2]
Sequence	SE-EPI [3]	STIR-EPI [4]
Mode	Single shot	Single shot
Coil	SENSE [5] body	SENSE body
Slice orientation	Axial	Axial
FOV [6]	RL [7] 400 mm, AP [8] 350 mm, FH [9] 303 mm	RL 400 mm, AP 350 mm, FH 303 mm
ACQ [10] voxel size	RL 3.03 mm x AP 3.57 mm x slice thickness 6 mm	RL 2.50 mm x AP 2.98 mm x slice thickness 6 mm
Reconstruction voxel size	RL 1.79 mm x AP 1.79 mm x slice thickness 6 mm	RL 1.39 mm x AP 1.39 mm x slice thickness 6 mm
Fold-over suppression	No	No
Reconstruction matrix	224	288
SENSE	Yes	Yes
P reduction (AP)	2	2.5
Number of stacks	1	1
Type	Parallel	Parallel
Slices	46	46
Slice gap (mm)	0.6	0.6
Slice orientation	Transverse	Transverse
Fold-over direction	AP	AP
Fat shift direction	A	P
TE [11]	66 ms	78 ms
TR [12]	1426 ms	7055 ms
TI [13]	-	180 ms

Table 1. *Cont.*

Scanning Protocol	DWI [1]	DWIBS [2]
Fast imaging mode	EPI [14]	EPI
Flip angle	90°	
Fat suppression	SPIR [15]	STIR [16]
b factors	0, 600, 800	0, 600, 800
Respiratory compensation	Trigger	No
Number of signal averages	3	5
Acquisition time	4 min 12 s	5 min 56 s

[1] DWI, diffusion-weighted imaging; [2] DWIBS, diffusion-weighted imaging with background body signal suppression; [3] SE-EPI, Spin-Echo – Echo Planar Imaging; [4] STIR-EPI, Short TI Inversion Recovery-Echo Planar Imaging; [5] SENSE, SENSitivity Encoding; [6] FOV, Field of View; [7] RL, Right-Left direction; [8] AP, Anterior-Posterior direction; [9] FH, Foot-Head direction; [10] ACQ, Acquisition; [11] TE; [12] TR, Repetition Time; [13] TI, Inversion Time; [14] EPI, Echo Planar Imaging; [15] SPIR, Spectral Presaturation with Inversion Recovery; [16] STIR, short T1 inversion recovery.

The study was approved by the Ethics committee of Riga Stradin's University, and written informed consent was obtained from all patients. The permission number by the Ethics committee of Riga Stradin's University is 6/10.09.2015.

2.3. 1st Cohort

The first cohort was formed of patients in whom high SI bowel walls in DWI tracking images of b = 800 s/mm^2 were identified in at least one intestinal site. High SI regions in at least one intestinal region were identified in all 106 patients. Prior to bowel preparation, one collapsed jejunal segment in DWI and DWIBS image series was identified for each patient. After bowel preparation, one distended jejunal segment in DWI and DWIBS image series was identified for each patient. ADC values were measured in three sites per segment using 10–20 mm^2 oval region of interest (ROI), both before and after preparation (Figure 3).

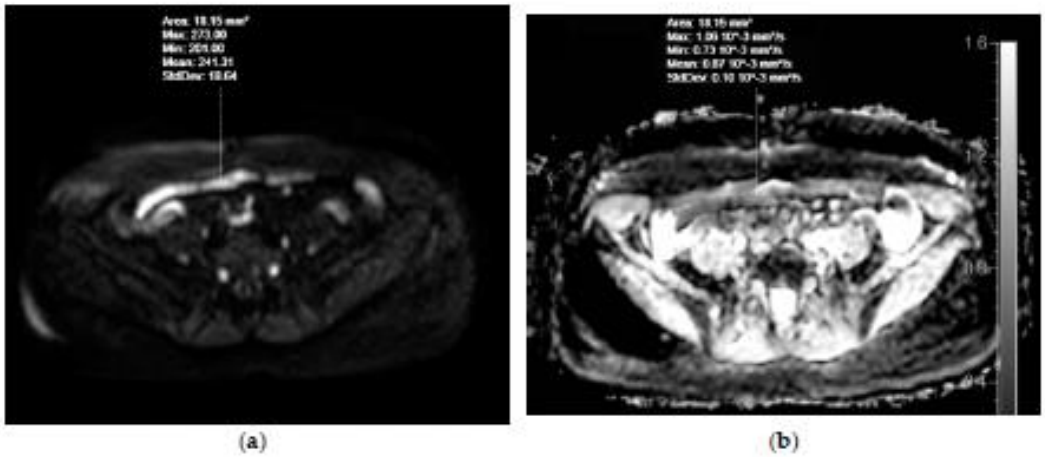

(a) (b)

Figure 3. *Cont.*

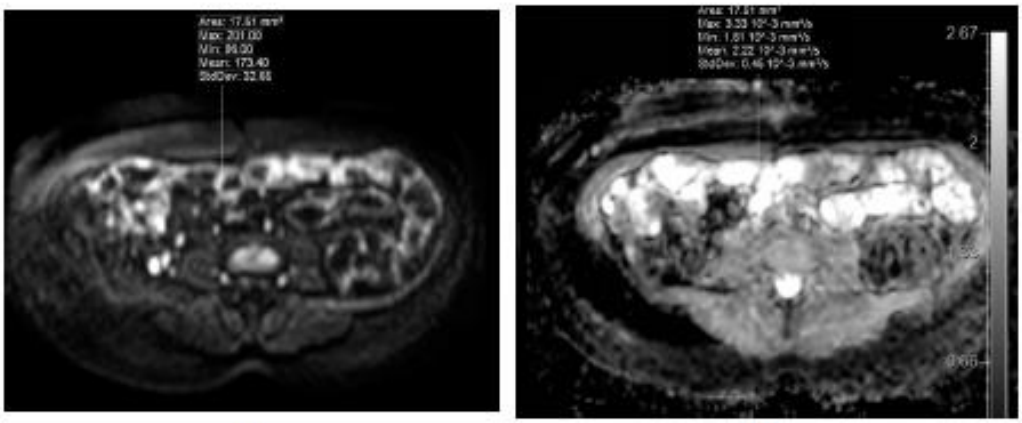

(c) (d)

Figure 3. MRE of a 53-year-old female patient with dyspeptic complaints, with no morphologically verified IBD. Selecting regions of interest (ROIs) for apparent diffusion coefficient (ADC) measurements in DWI images of collapsed (**a**) and distended (**c**) jejunum showing high SI in the DWI tracking images of b = 800 s/mm^2. ADC values appear on the ADC map (**b**, for collapsed jejunum, **d**, for distended jejunum).

2.4. 2nd Cohort

The second cohort was formed of patients in whom high SI bowel walls in DWI tracking images of b = 800 s/mm^2 were identified in at least one colonic site. 78 of the 106 patients were identified to have high SI regions in at least one colonic region. Before bowel preparation in the DWI and DWIBS image series, one caecum or ascending colon segment with presence of intraluminal faeces was identified in each patient. After bowel preparation in the DWI and DWIBS image series, one caecum or ascending colon segment with presence of intraluminal mannitol was identified in each patient. ADC values were measured in three sites per segment using 10–20 mm^2 ROI both before and after preparation (Figure 4).

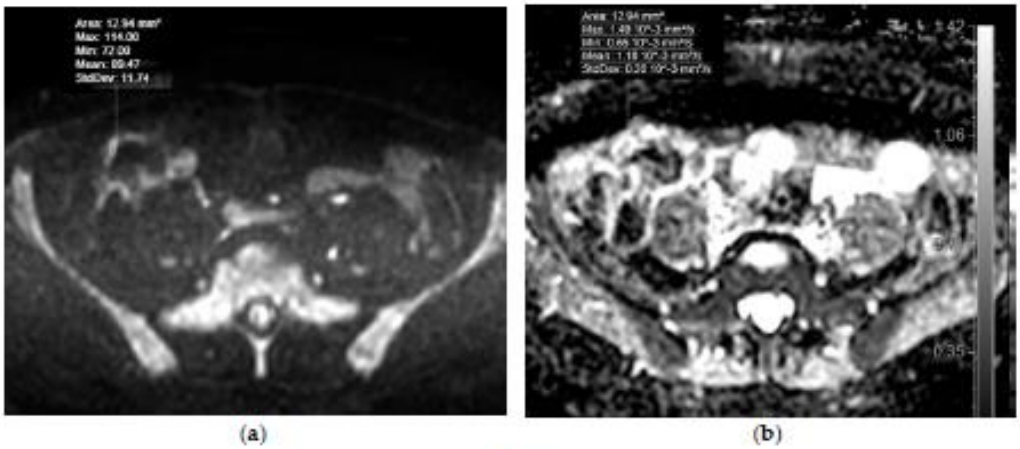

(a) (b)

Figure 4. *Cont.*

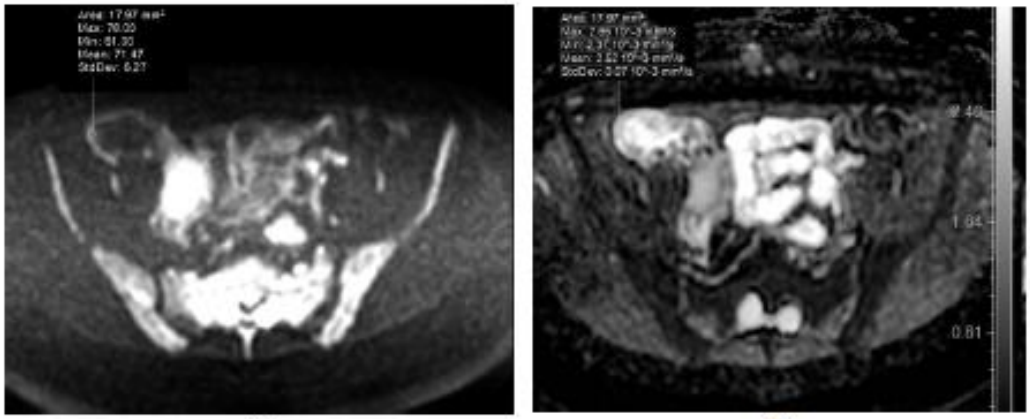

(c) (d)

Figure 4. MRE of a 45-year-old male patient with dyspeptic complaints, with no morphologically verified inflammatory bowel disease (IBD). Selecting ROIs for ADC measurement in DWIBS tracking images (b = 800 s/mm^2) of the ascending colon wall before preparation of patient with mannitol, at presence of intraluminal faeces **(a)** and after preparation, at presence of enteric contrast agent **(b)**, showing high SI. Note the higher SI of colonic wall in presence of mannitol, when compared to the presence of faeces in the colonic lumen. ADC values appear on the ADC map (**b**, for non-prepared colon, **d**, for prepared colon).

2.5. *Statistical Analysis*

Statistical analysis was performed using software Stata/IC (StataCorp LLC, Texas, USA), mean ADC values were compared with paired *t*-test, and 99% confidence intervals (CI) were calculated for differences. The statistical significance of differences between mean values within groups was determined using one-way ANOVA with Bonferroni correction. *P* value of <0.05 was considered to be statistically significant.

3. Results

3.1. *1st Cohort: Comparison of ADC-DWI and ADC-DWIBS Measurements in Non-Prepared and Prepared Intestines*

To perform the ADC measurements amongst the 106 patients, ADC-DWI was measured in 91 collapsed and 106 distended jejunal segments. ADC-DWIBS was measured in 86 collapsed and in 95 distended jejunal segments. Comparisons were drawn by analysis of segment pairs before and after preparation as follows; 88 segment pairs for comparison between ADC-DWI and 83 pairs for ADC-DWIBS. For comparison between ADC-DWI and ADC-DWIBS before preparation 85 segment pairs were analyzed, and 95 pairs were analyzed to compare ADC-DWI and ADC-DWIBS after preparation.

In both DWI and DWIBS sequences, the study found marked significant difference between ADC of non-prepared and prepared bowels. In both DWI and DWIBS ADC, the values of non-prepared jejunum were lower than in prepared jejunum. The ADC difference between non-prepared and prepared bowel was 38.1% in DWI and 48% in DWIBS. The ADC values are shown in Table 2.

Table 2. Comparison of ADC values between DWI and DWIBS in walls of non-prepared and prepared jejunum.

Bowel Preparation State	Non-Prepared (Collapsed) Jejunum	Prepared (Filled) Jejunum	*p* Value	Difference between Mean ADC Values of Filled vs. Collapsed Loops
Mean ADC-DWI value $\times 10^{-3}$ mm^2/s	1.09 (SD = 0.37)	1.76 (SD = 0.41)	<0.0001	0.67 (38.1%)
Mean ADC-DWIBS value $\times 10^{-3}$ mm^2/s	0.91 (SD = 0.47)	1.75 (SD = 0.51)	<0.0001	0.84 (48%)

ADC, apparent diffusion coefficient; SD, standard deviation.

Within the walls of non-prepared jejunum, our data showed a statistically significant ADC difference ($p < 0.0001$) of 16.5% between DWI and DWIBS, being lower in DWIBS. No significant ADC difference ($p = 0.84$) between DWI and DWIBS was observed within walls of prepared jejunum.

3.2. 2nd Cohort: Comparison of ADC-DWI and ADC-DWIBS Measurements in Non-Prepared and Prepared Colon

To perform the ADC measurements amongst the 106 patients, ADC-DWI was measured in 41 non-prepared and in 42 prepared caecum or ascending colon segments. ADC-DWIBS was measured in 25 non-prepared caecum or ascending colon segments and in 18 prepared caecum or ascending colon segments. Forty-one segment pairs were analyzed for comparison between ADC-DWI before and after preparation, and 18 segment pairs were analyzed to compare ADC-DWIBS before and after preparation. For comparison between ADC-DWI and ADC-DWIBS before preparation, 25 segment pairs were analyzed, and 18 pairs were analyzed to compare ADC-DWI and ADC-DWIBS after preparation.

In both DWI and DWIBS sequences, the study found marked significant difference between ADC in non-prepared and prepared bowels. In both DWI and DWIBS ADC, values of the non-prepared colon were lower than in the prepared colon. The ADC difference between non-prepared and prepared bowel was 33.8% in DWI and 50.5% in DWIBS. The ADC values are presented in Table 3.

Table 3. Comparison of ADC values between DWI and DWIBS in walls of non-prepared and prepared colon.

Bowel Preparation State	Non-Prepared (Presence of Faeces) Colon	Prepared (Presence of Mannitol) Colon	*p* Value	Difference between Mean Values in Non-Prepared vs. Prepared Colon
Mean ADC-DWI value $\times 10^{-3}$ mm^2/s	1.41 (SD = 0.31)	2.13 (SD = 0.41)	<0.0001	0.72 (33.8%)
Mean ADC-DWIBS value $\times 10^{-3}$ mm^2/s	1.01 (SD = 0.40)	2.04 (SD = 0.58)	<0.0001	1.03 (50.5%)

By mutually comparing ADC-DWI and ADC-DWIBS values within walls of both non-prepared and prepared colon, the data showed statistically significant ADC difference ($p < 0.0001$) of 28.4% between DWI and DWIBS being lower in DWIBS. No significant ADC difference ($p = 0.58$) between DWI and DWIBS values was found.

4. Discussion

According to the current joint evidence-based guidelines by the European Chron's and Colitis Organization as well as European Society of Gastrointestinal and Abdominal Radiologists, MRE imaging in IBD requires administration of contrast medium giving opportunity to estimate the bowel wall enhancement pattern [5] as well as vasa recta engorgement commonly seen in CD [30]. A significant advantage of using the gadolinium contrast agent is the ability to quantify Crohn's disease

activity [31]. Nevertheless, according to literature data, DWI in detection of bowel inflammatory changes outperforms T1 dynamic series with intravenous gadolinium contrast agent [32,33]. Therefore, DWI could be beneficial in case of diagnostic difficulties, for example, when, in Crohn's disease, the inflamed bowel tissues are covered by intact mucosa [34]. The drawback of DWI is its low specificity [15,16].

In intact bowel walls, high intensity signal resembling inflammation in images of high b factors is a reason for the low specificity of DWI. This pattern is commonly explained with the T2 shine-through effect, where theoretically ADC should be high [35]. Nevertheless, increased DWI signal along with low ADC is observed not only in inflamed but also in disease-free bowel walls [36].

Upon reporting multiple MRE exams, we had several observations regarding the high SI bowel wall at the DWI tracking images of b = 800 s/mm^2. Firstly, we noticed that intestinal SI was markedly higher in bowel wall before preparation, i.e., in totally collapsed bowel, compared to intestinal wall after preparation, i.e., in fully distended bowel. Secondly, in colon, SI was markedly higher in bowel wall after preparation, i.e., in presence of enteric contrast agent, compared to the colonic wall before preparation, i.e., in presence of faeces. In both situations, high SI bowel walls in the ADC map frequently presented low SI. These observations raised a question regarding ADC differences between bowel wall before and after patient preparation, in both intestines and colon.

Results from the 1st cohort comparing ADC of DWI and DWIBS between non-prepared (collapsed) and prepared (distended) intestines showed that ADC values in both DWI and DWIBS in the collapsed bowel sample were markedly lower than in distended bowel samples. As the bowel collapses, the number of cells per volume unit increases; however, the cells itself are not altered. Therefore, the volumes of intracellular and extracellular spaces were still constant, giving no reason for restricted diffusion. The measurement results could be explained by the partial volume effect. In prepared (filled) jejunal wall, the signal of very thin bowel wall was contaminated by the high intensity signal from the massive volume of enteric contrast agent, therefore, ADC value is high. However, in non-prepared (collapsed) bowel samples, the amount of high SI intraluminal content is less, therefore, the contamination of the intestinal wall signal is also less.

A similar explanation applies to the 2nd cohort comparing ADC of DWI and DWIBS between non-prepared (presence of low SI intraluminal faeces) and prepared (presence of mannitol) colon. The results showed that ADC values in both DWI and DWIBS were dependent on colonic intraluminal content and in the presence of low signal intensity faeces were nearly two times lower than in the presence of high signal intensity mannitol.

According to a number of studies, the performance of DWI varied among authors. The range of ADC values in normal bowel wall was 1.18–3.69 mm^2/s whereas in inflamed bowel segments—1.24–1.988 mm^2/s being significantly lower for 0.8–2.4 $\times 10^{-3}$ mm^2/s than in intact bowels. Several authors have also provided their cut-off ADC values for discriminating between inflamed and intact bowel walls. These values are mutually different and lie between ADC ranges of inflamed and intact bowel walls, except in one study where cut-off value lies within the range of the inflamed bowel. According to data from all researchers, ADC ranges of IBD and intact bowel do not mutually overlap [37]. Most of these studies have been performed in prepared bowels. To the best of our knowledge, a team of Kiryu et al. is the only research group reporting ADC values in Crohn's disease patients without patient preparation using free-breathing DWI (i.e., using STIR as fat suppression method). The reported ADC values show a similar trend, with that in prepared bowels being lower in disease-active segments and higher in disease-inactive areas ($1.61 \pm 0.44 \times 10^{-3}$ mm^2/s versus $2.56 \pm 0.51 \times 10^{-3}$ mm^2/s in intestines, respectively) [13]. This difference is high enough to concern the potential benefit of ADC measurements without bowel preparation. If the consistency of differences between ADC values of inflamed and normal bowels applies also in non-prepared bowel samples, this would allow a proper estimation of ADC in patients without preparation. Therefore, assessment of consistency between ADC values of non-prepared and prepared bowel walls was a goal of our research.

Comparing the obtained ADC values of bowel prior preparation and prepared bowel to literature data on ADC values of normal and inflamed bowels, it is obvious that, although the ADC values for the prepared bowels are markedly higher than ADC values in bowel prior to preparation, both ADC values of prepared and non-prepared bowel loops overlap with the ADC range of inflamed bowel provided in literature [37]. Thus, the applicability of ADC in non-prepared bowel samples is still questionable and might be related to scanning conditions and parameters in our institution. to fully compare the extent of overlap in ADC ranges for non-prepared bowel and inflamed bowels, the ADC values for CD have to be obtained in our institution under identical conditions.

A questionable issue is how much mannitol itself changes ADC, by impacting cells due to concentration gradient between bowel epithelium cells of lower and higher osmolarity substance, and the expelling fluid from cells resulting in a lowered packed cell volume [38] and osmotic diarrhoea [6]. Nevertheless, we assume that as the bowel wall filled with mannitol is a very thin (<3 mm), the contribution to signal intensity by osmotic influence of mannitol is negligible.

By mutually comparing ADC-DWI and ADC-DWIBS, we observe no statistically significant difference in the wall of prepared bowels, both regarding intestines and the colon. On the contrary, ADC values in non-prepared bowels and both intestines and colon, is markedly lower than in the prepared bowel samples. In the prepared bowel, the wall signal was influenced with a high large amount of fluid. In the non-prepared bowel, there was a presence of high-viscosity intraluminal content—chime in intestines and faeces in colon. DWI and DWIBS sequences differed when fat suppression techniques were used. In DWI, CHESS (CHEmically Selective Saturation) or SPIR sequences suppress fat selectively. The STIR technique used in DWIBS was based on the T1 relaxation time of tissues [39], and suppressed signals from all substances of short T1 values such as proteinaceous, viscous and mucous substances, including chime and faeces, thus being non-selective [40]. Therefore, ADC-DWIBS values are lower in the presence of the bowel content, comparing to ADC-DWI, and the probability that the ADC-DWIBS range will overlap the ADC range of inflamed bowel is higher. Therefore, based on the findings of this study, we still recommend preferring SPIR-based ADC measurements and using ADC values of STIR-based ADC in non-prepared bowel with caution.

Our study had several limitations. 1) Measurements were performed by one radiologist not assessing inter-observer agreement, and in such a small volume ADC values are reported to be hardly reproducible [37,41] as they rest on subjectivity. Nevertheless, data from ADC measurements in liver imaging suggested better reproducibility of free-breathing DWIBS over respiratory-triggered DWI [26], which could be also proven better for bowel walls, but requires further investigation. 2) Typically, achievable DWI resolution is on the order of $2 \times 2 \times 2$ mm^3 [42]. The pixel size used in our standard protocols (see Table 1) could be large for tiny structures, such as the bowel wall. ADC values are therefore markedly impacted by the partial volume effect being very approximate and can be used only for reference but not as absolute values. 3) In intestines, the most uniform luminal distension was present in jejunum, which was therefore chosen for intestinal measurements, however, ileum is the main location of CD. The terminal loop of ileum also has different morphological patterns—abundance of lymphoid tissues [43]—which also could influence ADC measurements. In the colon, measurements were performed only in walls of the caecum and the ascending colon, since presence or mannitol was mainly observed in these locations. 4) Location of the sites with high SI signal in DWI tracking images of b = 800 s/mm^2 was not consistent among the series, therefore, measurements could not be performed precisely at the same locations. 5) We did not pay special attention to the T2 shine through effect of bowel walls, and measured ADC values in DWI tracking images of b = 800 s/mm^2 regardless of signal appearance in ADC map. 6) Our goal was to observe properties of DWI-ADC and DWIBS-ADC in sites of bowel walls showing high SI at DWI tracking images of b = 800 s/mm^2 resembling bowel inflammation, whereas we did not consider other signs of bowel inflammation like oedema, increased bowel wall thickness, contrast enhancement, etc., which of course were absent in patients with no presence of IBD as required by the study.

5. Conclusions

The study has found that ADC ranges of the non-prepared bowel are significantly lower when compared to the ADC ranges of prepared bowels in both intestines and the colon, potentially overlapping ADC ranges of the inflamed bowel in both DWI and DWIBS sequences. Since ADC values could be related to scanning conditions at a particular institution, ADC values of the intact bowel have to be compared to ADC values obtained from CD patients at our institution, scanned with the same equipment and under identical scanning parameters and conditions.

In prepared bowels, ADC-DWIBS and ADC-DWI measurements are equally useful for bowel wall measurements. In non-prepared bowels, ADC-DWIBS could be disadvantageous over ADC-DWI in revealing IBD, as ADC-DWIBS values are markedly lower than ADC-DWI values, and they potentially overlap ADC ranges of IBD to a greater extent than ADC-DWI.

Author Contributions: Conceptualization, methodology, investigation and writing—original data preparation, I.A.; investigation, M.B. and R.P.; writing—review and editing, J.P. and G.K.; supervision, G.K.

Funding: This research received no external funding.

Acknowledgments: The authors gratefully acknowledge the generosity of Jordi Rimola for the inspiration and valuable ideas to initiate the research, Taro Takahara for his extremely worthy advice regarding this study, Irena Rogovska for support in processing of statistical data, and Peteris Prieditis for tips and constructive criticism in writing this article.

Conflicts of Interest: The authors declare no conflict of interest.

References

1. Molodecky, N.A.; Soon, I.S.; Rabi, D.M.; Ghali, W.A.; Ferris, M.; Chernoff, G.; Benchimol, E.I.; Panaccione, R.; Ghosh, S.; Barkema, H.W.; et al. Increasing Incidence and Prevalence of the Inflammatory Bowel Diseases with Time, Based on Systematic Review. *Gastroenterology* **2012**, *142*, 46–54.e42. [CrossRef] [PubMed]
2. Yoon, K.; Chang, K.; Lee, H.J. MRI for Crohn's Disease: Present and Future. *Biomed. Res. Int.* **2015**, *2015*, 786802. [CrossRef] [PubMed]
3. Cosnes, J.; Gower-Rousseau, C.; Seksik, P.; Cortot, A. Epidemiology and Natural History of Inflammatory Bowel Diseases. *Gastroenterology* **2011**, *140*, 1785–1794. [CrossRef] [PubMed]
4. Lönnfors, S.; Vermeire, S.; Greco, M.; Hommes, D.; Bell, C.; Avedano, L. IBD and health-related quality of life—Discovering the true impact. *J. Crohns Colitis* **2014**, *8*, 1281–1286. [CrossRef] [PubMed]
5. Panes, J.; Bouhnik, Y.; Reinisch, W.; Stoker, J.; Taylor, S.; Baumgart, D.; Danese, S.; Halligan, S.; Marincek, B.; Matos, C.; et al. Imaging techniques for assessment of inflammatory bowel disease: Joint ECCO and ESGAR evidence-based consensus guidelines. *J. Crohns Colitis* **2013**, *7*, 556–585. [CrossRef] [PubMed]
6. Mäkinen, K.K. Gastrointestinal Disturbances Associated with the Consumption of Sugar Alcohols with Special Consideration of Xylitol: Scientific Review and Instructions for Dentists and Other Health-Care Professionals. *Int. J. Dent.* **2016**, *2016*, 1–16. [CrossRef]
7. Kolbe, A.B.; Fletcher, J.G.; Froemming, A.T.; Sheedy, S.P.; Koo, C.W.; Pundi, K.; Bruining, D.H.; Tung, J.; Harmsen, W.S.; Barlow, J.M.; et al. Evaluation of Patient Tolerance and Small-Bowel Distention with a New Small-Bowel Distending Agent for Enterography. *Am. J. Roentgenol.* **2016**, *206*, 994–1002. [CrossRef]
8. Pérez-Rodríguez, J.; Lai, S.; Ehst, B.D.; Fine, D.M.; Bluemke, D.A. Nephrogenic Systemic Fibrosis: Incidence, Associations, and Effect of Risk Factor Assessment—Report of 33 Cases. *Radiology* **2009**, *250*, 371–377. [CrossRef]
9. Gulani, V.; Calamante, F.; Shellock, F.G.; Kanal, E.; Reeder, S.B. Gadolinium deposition in the brain: Summary of evidence and recommendations. *Lancet Neurol.* **2017**, *16*, 564–570. [CrossRef]
10. Wáng, Y.X.; Schroeder, J.; Siegmund, H.; Idée, J.M.; Fretellier, N.; Jestin-Mayer, G.; Factor, C.; Deng, M.; Kang, W.; Morcos, S.K. Total gadolinium tissue deposition and skin structural findings following the administration of structurally different gadolinium chelates in healthy and ovariectomized female rats. *Quant. Imaging Med. Surg.* **2015**, *5*, 534–545.
11. Rogosnitzky, M.; Branch, S.M. Gadolinium-based contrast agent toxicity: A review of known and proposed mechanisms. *BioMetals* **2016**, *29*, 365–376. [CrossRef]

12. Baliyan, V.; Das, C.J.; Sharma, R.; Gupta, A.K.; Baliyan, C.J.D.V. Diffusion weighted imaging: Technique and applications. *World J. Radiol.* **2016**, *8*, 785–798. [CrossRef]
13. Kiryu, S.; Dodanuki, K.; Takao, H.; Watanabe, M.; Inoue, Y.; Takazoe, M.; Sahara, R.; Unuma, K.; Ohtomo, K. Free-breathing diffusion-weighted imaging for the assessment of inflammatory activity in Crohn's disease. *J. Magn. Reason. Imaging* **2009**, *29*, 880–886. [CrossRef]
14. Mentzel, H.-J.; Reinsch, S.; Kurzai, M.; Stenzel, M. Magnetic resonance imaging in children and adolescents with chronic inflammatory bowel disease. *World J. Gastroenterol.* **2014**, *20*, 1180–1191. [CrossRef]
15. Qi, F.; Jun, S.; Qi, Q.Y.; Chen, P.J.; Chuan, G.X.; Jiong, Z.; Rong, X.J. Utility of the diffusion-weighted imaging for activity evaluation in Crohn's disease patients underwent magnetic resonance enterography. *BMC Gastroenterol.* **2015**, *15*, 978. [CrossRef]
16. Choi, S.H.; Kim, K.W.; Lee, J.Y.; Kim, K.J.; Park, S.H. Diffusion-weighted Magnetic Resonance Enterography for Evaluating Bowel Inflammation in Crohn's Disease: A Systematic Review and Meta-analysis. *Inflamm. Bowel Dis.* **2016**, *22*, 669–679. [CrossRef]
17. Takahara, T.; Imai, Y.; Yamashita, T.; Yasuda, S.; Nasu, S.; Van Cauteren, M. Diffusion weighted whole body imaging with background body signal suppression (DWIBS): Technical improvement using free breathing, STIR and high resolution 3D display. *Radiat. Med.* **2004**, *22*, 275–282.
18. Kwee, T.C.; Takahara, T.; Ochiai, R.; Katahira, K.; Van Cauteren, M.; Imai, Y.; Nievelstein, R.A.; Luijten, P.R. Whole-body diffusion-weighted magnetic resonance imaging. *Eur. J. Radiol.* **2009**, *70*, 409–417. [CrossRef]
19. Sanchez-Gonzalez, J.; Lafuente-Martínez, J. Diffusion-Weighted Imaging: Acquisition and Biophysical Basis. In *Diffusion MRI Outside the Brain: A Case-Based Review and Clinical Applications*; Luna, A., Ribes, R., Soto, J.A., Eds.; Springer: Berlin/Heidelberg, Germany, 2012; pp. 1–15.
20. Tomizawa, M.; Shinozaki, F.; Uchida, Y.; Uchiyama, K.; Fugo, K.; Sunaoshi, T.; Ozaki, A.; Sugiyama, E.; Baba, A.; Fukamizu, Y.; et al. Diffusion-weighted whole-body imaging with background body signal suppression/T2 image fusion and positron emission tomography/computed tomography of upper gastrointestinal cancers. *Abdom. Imaging* **2015**, *40*, 3012–3019. [CrossRef]
21. Tomizawa, M.; Shinozaki, F.; Fugo, K.; Sunaoshi, T.; Sugiyama, E.; Kano, D.; Shite, M.; Haga, R.; Fukamizu, Y.; Kagayama, S.; et al. Negative signals for adenomyomatosis of the gallbladder upon diffusion-weighted whole body imaging with background body signal suppression/T2-weighted image fusion analysis. *Exp. Ther. Med.* **2016**, *11*, 1777–1780. [CrossRef]
22. Tomizawa, M.; Shinozaki, F.; Uchida, Y.; Uchiyama, K.; Tanaka, S.; Sunaoshi, T.; Kano, D.; Sugiyama, E.; Shite, M.; Haga, R.; et al. Comparison of DWIBS/T2 image fusion and PET/CT for the diagnosis of cancer in the abdominal cavity. *Exp. Ther. Med.* **2017**, *14*, 3754–3760. [CrossRef]
23. Tomizawa, M.; Shinozaki, F.; Fugo, K.; Tanaka, S.; Sunaoshi, T.; Kano, D.; Sugiyama, E.; Shite, M.; Haga, R.; Fukamizu, Y.; et al. Diagnostic accuracy of diffusion-weighted whole-body imaging with background body signal suppression/T2-weighted image fusion for the detection of abdominal solid cancer. *Exp. Ther. Med.* **2017**, *13*, 3509–3515. [CrossRef]
24. Li, X.-H.; Sun, C.-H.; Mao, R.; Zhang, Z.-W.; Jiang, X.-S.; Pui, M.H.; Chen, M.-H.; Li, Z.-P.; Scalisi, G. Assessment of Activity of Crohn Disease by Diffusion-Weighted Magnetic Resonance Imaging. *Medicine (Baltimore)* **2015**, *94*, e1819. [CrossRef]
25. Dubron, C.; Avni, F.; Boutry, N.; Turck, D.; Duhamel, A.; Amzallag-Bellenger, E. Prospective evaluation of free-breathing diffusion-weighted imaging for the detection of inflammatory bowel disease with MR enterography in childhood population. *Br. J. Radiol.* **2016**, *89*, 20150840. [CrossRef]
26. Kwee, T.C.; Takahara, T.; Koh, D.-M.; Nievelstein, R.A.; Luijten, P.R. Comparison and reproducibility of ADC measurements in breathhold, respiratory triggered, and free-breathing diffusion-weighted MR imaging of the liver. *J. Magn. Reson. Imaging* **2008**, *28*, 1141–1148. [CrossRef]
27. Stone, A.J.; Browne, J.E.; Lennon, B.; Meaney, J.F.; Fagan, A.J. Effect of motion on the ADC quantification accuracy of whole-body DWIBS. *Magn. Reson. Mater. Phys. Biol. Med.* **2012**, *25*, 263–266. [CrossRef]
28. Mazza, M.; Cilluffo, M.G.; Cappello, M. *Crohn's Disease*; Springer: Basel, Switzerland, 2016; pp. 7–8.
29. Tontini, G.E.; Vecchi, M.; Pastorelli, L.; Neurath, M.F.; Neumann, H. Differential diagnosis in inflammatory bowel disease colitis: State of the art and future perspectives. *World J. Gastroenterol.* **2015**, *21*, 21–46. [CrossRef]
30. Amitai, M.M.; Ben-Horin, S.; Eliakim, R.; Kopylov, U. Magnetic resonance enterography in Crohn's disease: A guide to common imaging manifestations for the IBD physician. *J. Crohns Colitis* **2013**, *7*, 603–615. [CrossRef]

31. Rimola, J.; Rodriguez, S.; García-Bosch, O.; Ordás, I.; Ayala, E.; Aceituno, M.; Pellisé, M.; Ayuso, C.; Ricart, E.; Donoso, L.; et al. Magnetic resonance for assessment of disease activity and severity in ileocolonic Crohn's disease. *Gut* **2009**, *58*, 1113–1120. [CrossRef]
32. Oto, A.; Kayhan, A.; Williams, J.T.; Fan, X.; Yun, L.; Arkani, S.; Rubin, D.T. Active Crohn's disease in the small bowel: Evaluation by diffusion weighted imaging and quantitative dynamic contrast enhanced MR imaging. *J. Magn. Reson. Imaging* **2011**, *33*, 615–624. [CrossRef]
33. Sirin, S.; Kathemann, S.; Schweiger, B.; Hahnemann, M.L.; Forsting, M.; Lauenstein, T.C.; Kinner, S. Magnetic Resonance Colonography Including Diffusion-Weighted Imaging in Children and Adolescents with Inflammatory Bowel Disease. *Investig. Radiol.* **2015**, *50*, 32–39. [CrossRef]
34. Surawicz, C.M.; Haggitt, R.C.; Husseman, M.; McFarland, L.V. Mucosal biopsy diagnosis of colitis: Acute self-limited colitis and idiopathic inflammatory bowel disease. *Gastroenterol.* **1994**, *107*, 755–763. [CrossRef]
35. Koh, D.-M.; Blackledge, M.; Padhani, A.R.; Takahara, T.; Kwee, T.C.; Leach, M.; Collins, D.J. Whole-Body Diffusion-Weighted MRI: Tips, Tricks, and Pitfalls. *Am. J. Roentgenol.* **2012**, *199*, 252–262. [CrossRef]
36. Jesuratnam-Nielsen, K.; Løgager, V.B.; Rezanavaz-Gheshlagh, B.; Munkholm, P.; Thomsen, H.S. Plain magnetic resonance imaging as an alternative in evaluating inflammation and bowel damage in inflammatory bowel disease—A prospective comparison with conventional magnetic resonance follow-through. *Scand. J. Gastroenterol.* **2015**, *50*, 519–527. [CrossRef]
37. Dohan, A.; Taylor, S.; Hoeffel, C.; Barret, M.; Allez, M.; Dautry, R.; Zappa, M.; Savoye-Collet, C.; Dray, X.; Boudiaf, M.; et al. Diffusion-weighted MRI in Crohn's disease: Current status and recommendations. *J. Magn. Reson. Imaging* **2016**, *44*, 1381–1396. [CrossRef]
38. Poulton, A.; Winterborn, M.H. Oral mannitol in control of fluid balance. *Arch. Dis. Child.* **1987**, *62*, 729–731. [CrossRef]
39. Del Grande, F.; Santini, F.; Herzka, D.A.; Aro, M.R.; Dean, C.W.; Gold, G.E.; Carrino, J.A. Fat-suppression techniques for 3-T MR imaging of the musculoskeletal system. *Radiographics* **2014**, *34*, 217–233. [CrossRef]
40. Krinsky, G.; Rofsky, N.M.; Weinreb, J.C. Nonspecificity of Short Inversion Time Inversion Recovery (STIR) as a Technique of Fat Suppression: Pitfalls in Image Interpretation. *AJR Am. J. Roentgenol.* **1996**, *166*, 523–526. [CrossRef]
41. Watson, T.; Calder, A.; Barber, J. Quantitative bowel apparent diffusion coefficient measurements in children with inflammatory bowel disease are not reproducible. *Clin. Radiol.* **2018**, *73*, 574–579. [CrossRef]
42. Scherrer, B.; Gholipour, A.; Warfield, S.K. Super-Resolution in Diffusion-Weighted Imaging. *Med. Image Comput. Comput. Assist. Interv.* **2011**, *14*, 1–11.
43. Gullberg, E.; Söderholm, J.D. Peyer's patches and M cells as potential sites of the inflammatory onset in Crohn's disease. *Ann. N. Y. Acad. Sci.* **2006**, *1072*, 218–232. [CrossRef]

Supplement 2

Publication II

diagnostics

MDPI

Article

Comparison between Diffusion-Weighted Sequences with Selective and Non-Selective Fat Suppression in the Evaluation of Crohn's Disease Activity: Are They Equally Useful?

Ilze Apine [1,2,*], Reinis Pitura [2], Ivanda Franckevica [1,3], Juris Pokrotnieks [4] and Gaida Krumina [2]

[1] Children Clinical University Hospital of Riga, LV 1004 Riga, Latvia; ivanda.franckevica@bkus.lv
[2] Department of Radiology, Riga Stradin's University, LV 1004 Riga, Latvia; reinis.pitura@gmail.com (R.P.); gaida.krumina@rsu.lv (G.K.)
[3] Department of Pathology, Riga Stradin's University, LV 1007 Riga, Latvia
[4] Department of Internal Diseases, Riga Stradin's University, LV 1007 Riga, Latvia; pokrot@latnet.lv
* Correspondence: dr.ilze.apine@gmail.com, Tel.: +371-29461616

Received: 28 April 2020; Accepted: 25 May 2020; Published: 27 May 2020

Abstract: *Background*: We compared the efficiency of two MRI diffusion weighted imaging (DWI) techniques: DWI with SPIR (DWI$_{SPIR}$) and DWI with STIR (DWI$_{STIR}$), to estimate their eligibility for quantitative assessment of Crohn's disease activity in children and adults. *Methods*: In inflamed terminal ileum segments (n = 32 in adults, n = 46 in children), Magnetic Resonance Index of Activity (MaRIA) was calculated, ADC values of both DWI techniques were measured, and the corresponding Clermont scores calculated. ADC values of both DWI techniques were compared between both and within each patient group, assessing their mutual correlation. Correlations between MaRIA and the corresponding ADC values, and Clermont scores based on both DWI techniques were estimated. *Results*: No correlation between ADC of DWI$_{SPIR}$ and DWI$_{STIR}$ was observed (rho = 0.27, p = 0.13 in adults, rho = 0.20, p = 0.17 in children). The correlation between MaRIA and Clermont scores was strong in both techniques—in SPIR, rho = 0.93; p < 0.0005 in adults, rho = 0.98, p < 0.0005 in children, and, in STIR, rho = 0.89; p < 0.0005 in adults, rho = 0.95, p < 0.0005 in children. The correlation between ADC and MaRIA was moderate negative for DWI$_{STIR}$ (rho = 0.93, p < 0.0005 in adults, rho = 0.95, p < 0.0005 in children), but, in DWI$_{STIR}$, no correlation between ADC and MaRIA score was observed in adults (rho = −0.001, p = 0.99), whereas children presented low negative correlation (rho = −0.374, p = 0.01). *Conclusions*: DWI$_{STIR}$ is not suitable for quantitative assessment of Crohn's disease activity both in children and adult patients.

Keywords: MR enterography; terminal ileitis; diffusion-weighted imaging; DWI; DWIBS; ADC; MaRIA; Clermont score; DWI fat suppression techniques.

1. Introduction

Crohn's disease (CD) is an idiopathic chronic relapsing inflammatory bowel condition, which manifests itself in fistulae, abscesses and strictures [1]. The chronic inflammation causes progression of intestinal complications, requiring surgery in most cases [2,3]. It is known that active therapy including adjustment of medication reduces the number of complications and the need for surgery [1]. The goal of treatment for CD is either resolution of abdominal complaints and endoscopically confirmed remission, or resolution of inflammatory signs in cross-sectional imaging [4]. Since 2019, according to ECCO-ESGAR Guideline for Diagnostic Assessment in inflammatory bowel diseases, cross-sectional imaging modalities are recognised to be an alternative for the evaluation of the disease activity [5]. Magnetic resonance enterography (MRE) is proven to have a great potential for

evaluating CD activity, due to its high soft tissue resolution, non-invasiveness and lack of ionizing radiation, and ability to obtain findings not only within but also around the bowel wall [6].

To assess CD activity, a number of MRI scoring systems have been developed for standardising the measured outcomes [6]. Among these indices, Magnetic Resonance Index of Activity (MaRIA) is the only approved MRE-based score, having the strongest validation data based on a large population of patients [7]. However, MaRIA score relies on the measurement of enhanced gadolinium contrast media known to be related to systemic nephrogenic fibrosis [8], as well as accumulation of gadolinium deposits in the brain [9] and other body tissues, such as skin, liver and bones [10]. As patients with CD usually require multiple follow-up examinations which expose them to a certain risk of gadolinium accumulation, solutions allowing replacement of the contrast medium administration are of importance.

Diffusion-weighted imaging (DWI) has been shown to have potential as a replacement of the contrast media, by detecting lesions prior their appearance in conventional images [11]. It also outperforms the T1 post-contrast dynamic series [12–15]. DWI is proven to be useful for the detection of inflammation in CD [16,17], and, when added to the MRE protocol, it yields increased sensitivity in diagnostics of CD than conventional MRE alone [18] thus potentially supporting early diagnosis of CD. DWI also has a very important role in evaluating CD activity, which allows assessment of treatment efficacy [7].

DWI can be measured quantitatively with apparent diffusion coefficient (ADC). ADC of DWI is proven to be as useful as the relative contrast enhancement (RCE) used for calculation of MaRIA [19]. A DWI-based MaRIA, or Clermont score, is designed to serve as an alternative to avoid gadolinium administration [17] and is reported to have excellent correlation compared to MaRIA [20]. This index still is to be validated by confirmatory studies.

Due to the low sensitivity to motion-induced phase errors and advantages of short imaging times, DWI normally uses single-shot echo-planar imaging (EPI) acquisition, related to the presence of susceptibility artefacts at tissue interfaces [21] and chemical shift-induced ghosting artefacts deflecting the fat signal several pixels away from the water signal. To avoid these artefacts, DWI protocols should include fat saturation techniques [22,23]. These techniques are simply divided into two categories—fat, or spectral, selective and non-selective ones.

Among fat selective techniques, chemical shift selective fat suppression (CHESS) is a common fat saturation technique in which an excitation pulse with a bandwidth selective to the resonance frequency of fat is applied, followed by a spoiler dephasing gradient [24]. There are also two fat selective hybrid sequences. In spectral attenuated inversion recovery (SPAIR) the fat signal is inverted with an adiabatic spectrally selective pulse, and acquisition starts from the moment of inversion time (TI) that nulls the fat signal. Spectral pre-saturation with inversion recovery (SPIR), in turn, is a hybrid sequence with a spectrally selective inversion pulse is applied tuned to fat frequency [24]. After the TI, a conventional 90° spin-echo pulse is applied to saturate just the fat signal [25]. All these techniques use spectrally selective pulses suppressing signal from only fat protons.

Alongside fat selective saturation techniques, the DWI weighted sequence with Short Tau Inversion Recovery (STIR) fat suppression technique is also used. STIR is an inversion recovery technique based on the difference in relaxation between water and fat tissues, which have a much shorter T1 relaxation time compared to other tissue types. An inversion pulse is applied before the excitation pulse; the spins of all tissues invert and then perform T1 relaxation. By selecting the inversion time (TI) such as the longitudinal magnetisation of fat at that time is zero, fat spins will not participate to the MR signal [26]. STIR-based DWI had been developed in 2004 by the research group of Takahara who named it Diffusion Weighted Imaging with Background Body Signal Suppression (DWIBS). This sequence allows free breathing, permitting multiple slice excitation and signal averaging over an extended period to average motion [27]. When compared to the selective fat saturation techniques, while chemical fat selective saturation techniques are more influenced by magnetic field inhomogeneities [28] the use of DWI with non-selective STIR allows robust and more homogenic fat suppression within large body regions [27,28] including off-center localisations [24], providing a higher contrast-to-noise ratio (CNR) [23], insensitivity to magnetic field inhomogeneities,

and decreased image distortion [29] making it suitable for scanning large areas [23]. It also suppresses the signals from bowel content [29]. DWIBS was initially developed for the whole-body imaging of oncology patients to detect tumour relapse and metastases [27], but it is now used in many other applications including detecting inflammatory lesions, abscesses, intravascular thrombi, and visualisation of the peripheral nerves [23]. DWI with STIR technique is reported to have better image quality and less image artefacts when compared to conventional, or spectral selective, DWI [30]. Regarding ADC analysis, DWI with STIR is proven to be superior over conventional DWI, in the assessment of breast lesions [31]. The American College of Radiologists recommends including DWI with STIR in standard MRE protocols for imaging of the gastrointestinal tract [32]. Using DWI sequence with STIR in MRE examinations is further recommended by a number of authors [33,34]. It is also reported to be used in the assessment of CD activity [35]. The non-selectivity of STIR can be a disadvantage if tissues contain other substances with short T1 time, such as methaemoglobin, mucoid tissue, proteinaceous material, and melanin [24]. Another disadvantage of STIR-based fat suppression, is decreased SNR by partial loss of proton signal during the inversion time [29], causing grainy image appearance. Nevertheless, the free breathing DWIBS as DWI sequence with STIR is one of the most important DWI-related discoveries, allowing whole body imaging [27], and so improving diagnosis in oncology (tumour staging, detection of tumour relapse, monitoring response to therapy) [36]. Despite the reduced SNR, DWIBS contributes in improved detection of subtle lesions due to higher CNR [23]. DWI with STIR is reported to be feasible for the identification and characterisation of lymph nodes in patients with uterine cervical cancer [37]. ADC calculated from DWI_{STIR} (ADC-DWI_{STIR}) tracking images is reported to be superior over ADC of DWI_{SPIR} (ADC-DWI_{SPIR}) in differentiating between malignant and benign breast lesions [31] whilst also being non-dependent on motions [38], important in bowel imaging. However, there have been no studies published on comparison between DWI sequences with non-selective STIR and chemical fat selective DWI techniques for quantitative assessment of CD activity.

The aim of our study was to compare the performance of DWI sequences with fat selective Spectral Presaturation with Inversion Recovery (SPIR) (DWI_{SPIR}) and non-selective STIR, or DWIBS, (DWI_{STIR}), in quantitative assessment of active CD in the terminal ileum through the following measures:

(1) Measuring ADC values of DWI with SPIR (ADC-DWI_{SPIR}) and DWI with STIR (ADC-DWI_{STIR}) in groups of adult and paediatric patients, comparing each individual patient group and assessing their mutual correlation,
(2) comparing ADC- DWI_{SPIR} and ADC-DWI_{STIR} values between the groups of adults and pediatric patients,
(3) estimating correlations of ADC-DWI_{SPIR} and ADC-DWI_{STIR} values with the corresponding MaRIA, calculated from the contrast–enhanced sequences within the same bowel segments,
(4) calculating Clermont scores values based on ADC-DWI_{SPIR} and ADC-DWI_{STIR} and estimating their correlation with MaRIA within the same bowel segments.

2. Materials and Methods

2.1. Patient Population

In this prospective observational cross-sectional study, the patients underwent MRE examination between April 2016 and April 2019. All patients involved in the research had either symptomatic CD, or underwent MRE examination for monitoring the disease course under treatment. The faecal calprotectin levels in all study subjects exceeded 1000 µg/g. The inclusion criteria were: proven active non-stricturing non-penetrating CD in the terminal ileum, presenting with thickened bowel wall (thickness > 3 mm), presence of mural oedema (hyperintensity of the bowel wall in T2-weighted images compared to the psoas muscle) [39], signs of restricted diffusion in both of DWI sequences with SPIR and STIR presenting with high SI in DWI tracking images of $b = 800$ s/mm^2 along with low signal intensity (SI) in the ADC map, and early mucosal hyperenhancement in the post-Gd series [40]. The exclusion criteria were: locations of CD other than

the terminal ileum, bowel thickness less than 3 mm, dynamic blurring in either of the DWI or T1 post-Gd images, inability to locate active bowel wall inflammation in both DWI sequences, with SPIR and STIR, and post-Gd T1 within one and the same segments. The study was performed in accordance with the Declaration of Helsinki and approved by the Ethics committee of Riga Stradin's University on 10 September 2015, its permission number was 6/10.09.2015.

2.2. MRI Technique

All patients fasted for 6 h prior the MRE examination, being allowed to intake only water. No bowel cleansing was carried out. The bowel distension was maintained with 1.000–1.500 mL of 2.5% mannitol solution, consumed slowly before the MRE procedure for 45 min. After that, patients were asked to lie in the right decubitus position, and they received another 250 mL of 2.5% mannitol solution to intake slowly for another 20 min. The MRE examinations were performed with a 1.5T scanner (Ingenia, Philips Medical Systems, Best, The Netherlands) covering the region from the diaphragm to the pelvis with a 16-element phased array body coil. The patients were scanned in the prone position. The MRE protocol included:

(1) coronal bTFE (Balanced Turbo Field Echo) cine sequence for real-time assessment of the bowel peristalsis,
(2) axial DWI sequence with SPIR, using diffusion factors b fixed at 0, 600 and 800 s/mm^2, with corresponding ADC maps,
(3) axial DWIBS sequence (DWI with STIR), using diffusion factors b fixed at 0, 600 and 800 s/mm^2, with corresponding ADC maps,
(4) axial and coronal T2-weighted sequences without fat suppression (T2 TSE),
(5) axial and coronal T2-weighted sequences with fat suppression (T2 SPAIR),
(6) coronal T2 fat suppression magnetic resonance cholangiopancreatography (MRCP) sequence with radial 3D reconstructions,
(7) coronal T1-weighted dynamic postcontrast images e-THRIVE (T1 high-resolution isotropic volume excitation), followed by delayed post-contrast axial e-THRIVE images.

The scanning parameters of the DWI$_{SPIR}$ and DWI$_{STIR}$ (DWIBS) protocols are given in Table 1. To reduce bowel peristalsis, hyoscine butylbromide (Buscopan, Sanofi, Athens, Greece) was intravenously administered, prior to the DWI$_{SPIR}$ and DWI$_{STIR}$ sequences and the coronal dynamic contrast sequences. The dosage was 10 mg in patients under 50 kg and 20 mg in patients 50 kg or above, diluted in 20 mL of saline solution.

Table 1. Scanning parameters of DWI$_{SPIR}$ and DWI$_{STIR}$ techniques included in the MRE protocol.

Scanning Protocol	DWI$_{SPIR}$[1]	DWI$_{STIR}$ (DWIBS)_[2]
Sequence	SE-EPI[3]	STIR-EPI[4]
Mode	Single shot	Single shot
Coil	SENSE[5] body	SENSE body
Slice orientation	Axial	Axial
FOV[6]	RL[7] 400 mm, AP[8] 350 mm, FH[9] 303 mm	RL 400 mm, AP 350 mm, FH 303 mm
ACQ[10] voxel size	RL 3.03 mm × AP 3.57 mm × slice thickness 6 mm	RL 2.50 mm × AP 2.98 mm × slice thickness 6 mm
Reconstruction voxel size	RL 1.79 mm × AP 1.79 mm × slice thickness 6 mm	RL 1.39 mm × AP 1.39 mm × slice thickness 6 mm
Fold-over suppression	No	No
Reconstruction matrix	224	288
SENSE	Yes	Yes
P reduction (AP)	2	2.5
Number of stacks	1	1
Type	Parallel	Parallel

Slices	46	46
Slice gap (mm)	0.6	0.6
Slice orientation	Transverse	Transverse
Fold-over direction	AP	AP
Fat shift direction	A	P
TE[11]	66 ms	78 ms
TR[12]	1426 ms	7055 ms
TI[13]	-	180 ms
Fast imaging mode	EPI[14]	EPI
Flip angle	90°	
Fat suppression	SPIR	STIR
b factors	0, 600, 800 s/mm²	0, 600, 800 s/mm²
Respiratory compensation	Trigger	No
Number of signal averages	3	5
Total scan time	4 min. 12 s	5 min. 56 s

[1] DWI$_{SPIR}$—Diffusion-Weighted imaging with Spectral Presaturation with Inversion Recovery technique. [2] DWI$_{STIR}$—Diffusion-Weighted Imaging with Short-Tau Inversion Recovery. [3] SE-EPI—Spin Echo—Echo Planar Imaging. [4] STIR-EPI—Short T1 Inversion Recovery—Echo Planar Imaging. [5]SENSE—SENSitivity Encoding. [6] FOV—Field of View. [7] RL—Right-Left direction. [8] AP—Anterior-Posterior direction.[9] FH—Foot–Head direction.[10] ACQ—Acquisition. [11] TE—Echo Time. [12] TR—Repetition Time. [13] TI—Inversion Time. [14] EPI—Echo Planar Imaging.

2.3. MR Image Analysis

The altered locations of the terminal ileum were identified and divided into approximately 3 cm long segments. The total number of segments was 78, 32 in adults and 46 in paediatric patients. In each segment, wall thickness was measured in mm, presence of ulcers (present or absent) was estimated, and six measurements of ADC-DWI$_{SPIR}$ and ADC-DWI$_{STIR}$ in the corresponding DWI$_{SPIR}$ and DWI$_{STIR}$ tracking images of b = 800 s/mm² were performed in each segment, in the zone of the highest signal intensity within the bowel wall. Six measurements of the wall signal intensity were taken in the same location both before (WSI-preGd) and after (WSI-postGd) administration of gadolinium contrast medium, in the site with the highest SI in the postcontrast images. Six measurements of standard deviation (SD) representing the image noise were performed outside the body before (SD-preGd) and after (SD-postGd) administration of gadolinium contrast medium [39]. The mean value of all measurements was used for calculations. In each altered bowel segment, MaRIA was calculated using the following formula:

$$\text{MaRIA} = 1.5 \times \text{wall thickness (mm)} + 0.02 \times \text{RCE} + 5 \times \text{oedema} + 10 \times \text{ulcers},$$

where the presence or absence of ulcers and oedema was rated as 1 or 0, accordingly. RCE was calculated as follows:

$$\text{RCE} = (\text{WSI-postGd} - \text{WSI-preGd})/(\text{WSI-preGd})) \times 100 \times (\text{SD-preGd}/\text{SD-postGd}),$$

where the SD-preGd and SD-postGd corresponded to the mean of the six SD values of SI, measured outside of the body before and after gadolinium administration, accordingly [39]. Since oedema was one of the inclusion criteria representing inflammation, it was always present, and its rating was always equal to 1. The Clermont score, or DWI-MaRIA, for both DWI$_{SPIR}$ and DWI$_{STIR}$ sequences, was calculated per formula [20]:

$$\text{DWI-MaRIA} = 1.646 \times \text{bowel thickness} - 1.321 \times \text{ADC} + 5.613 \times \text{oedema} + 8.306 \times \text{ulceration} + 5.039$$

The i/v gadolinium contrast agent used before October 2018 for all adult patients and all but two children was gadodiamide (Omniscan 0.05 mmol/mL, GE Healthcare, Cork, Ireland, dosage 0.2 mL/kg, or 0.1 mmol/kg). Gadobutrol (Gadovist 1 mmol/mL, Bayer, Berlin, Germany, dosage 0.1 mL/kg, or 0.1 mmol/kg) was used for the two paediatric patients examined after October 2018.

The ADC, WSI and SD measurements were performed using 4–9 mm^2 oval region of interest (ROI). The image analysis and the measurements were performed by one radiologist with 19 years' experience in abdominal MRI imaging. The review of images and ADC measurements were performed using a dedicated Philips Intellispace Portal postprocessing server, v. 5.0 (Philips Medical Systems, Best, the Netherlands, 2014). The WSI and image noise measurements were performed using Clear Canvas DICOM Viewer, v. 13.2 (Synaptive Medical, Toronto, ON, Canada, 2019).

2.4. Statistical Analysis

The statistical analysis was performed using software SPSS 20.0 (IBM Corporation, Armonk, NY, USA, 2011). The median values with standard deviations for ADC-DWI$_{SPIR}$ and ADC-DWI$_{STIR}$, MaRIA, DWI$_{SPIR}$-Clermont, and DWI$_{STIR}$-Clermont scores were calculated. 95% CI was calculated for median differences. The statistical significance of differences between the groups was determined using Wilcoxon signed rank test. Spearman's correlation coefficient was used to assess the correlations between quantitative parameters. *P* values of <0.05 (two-tailed) were chosen as a level of statistical significance. The Bonferroni correction was used to control Type 1 error in multiple comparisons.

3. Results

Seventeen patients: five adults (23, 25, 36, 40 and 57 years old) and 12 children (11 years old; n = 2, 12 years old; n = 3, 13 years old; n = 1, 14 years old; n = 4, 17 years old; n = 2) were enrolled in the study. In one adult patient, the duration of medical history prior to the MRE examination was more than two years in three adult patients—from 6 till 12 months, but in one adult patient, CD was asymptomatic, of unknown length, and it was detected upon performing a set of infertility tests. In one paediatric patient, the duration of CD was slightly less than two years, but in the remaining 11 patients the duration of medical history was less than 6 months.

The overview of measured ADC-DWI$_{SPIR}$ and ADC-DWI$_{STIR}$ values, as well as calculated values of MaRIA, DWI$_{SPIR}$-based Clermont score and DWI$_{STIR}$-based Clermont score, is presented in Table 2.

Table 2. Values of ADC-DWI$_{SPIR}$, ADC-DWI$_{STIR}$, MaRIA as well as ADC-DWI$_{SPIR}$ and ADC-DWI$_{STIR}$ - based Clermont scores in the groups of adult and paediatric patients.

Measurement	N	Minimum Value	Maximum Value	Median Value	SD
ADC-DWI$_{SPIR}$ (mm^2/s), adults	32	0.66×10^{-3}	2.16×10^{-3}	1.26×10^{-3}	0.29
ADC-DWI$_{SPIR}$ (mm^2/s), children	46	0.18×10^{-3}	2.23×10^{-3}	1.13×10^{-3}	0.31
ADC-DWI$_{STIR}$ (mm^2/s), adults	32	0.01×10^{-3}	2.37×10^{-3}	1.15×10^{-3}	0.49
ADC-DWI$_{STIR}$ (mm^2/s), children	46	0.20×10^{-3}	2.74×10^{-3}	1.16×10^{-3}	0.44
MaRIA, adults	32	10.65	36.65	24.43	5.31
MaRIA, children	46	9.96	37.67	22.08	6.67
DWI$_{SPIR}$-based Clermont score, adults	32	12.85	39.23	26.23	4.76
DWI$_{SPIR}$-based Clermont score, children	46	13.59	40.74	23.53	5.42
DWI$_{STIR}$-based Clermont score, adults	32	5.92	38.78	24.28	4.65
DWI$_{STIR}$-based Clermont score, children	46	8.25	39.52	24.39	5.77

There was a statistically significant difference of 10.32% (p = 0.02) between the median values of ADC-DWI$_{SPIR}$ in adults and children, appearing lower in children than in adults; no statistically significant difference (p = 0.38) between ADC-DWI$_{STIR}$ in adults and children was detected. There was statistically significant difference of 8% (p = 0.03) between ADC-DWI$_{SPIR}$ and ADC-DWI$_{STIR}$ values in

adults, appearing lower in DWI$_{STIR}$, but no statistically significant difference ($p = 0.97$) between ADC-DWI$_{SPIR}$ and ADC-DWI$_{STIR}$ values in children. The graphical comparative distribution of the ADC-DWI$_{SPIR}$ and ADC-DWI$_{STIR}$ values between both patient groups is shown in Figure 1a,b. The graphical comparative distribution of the ADC-DWI$_{SPIR}$ and ADC-DWI$_{STIR}$ values within each of the patient groups is shown in Figure 2a,b.

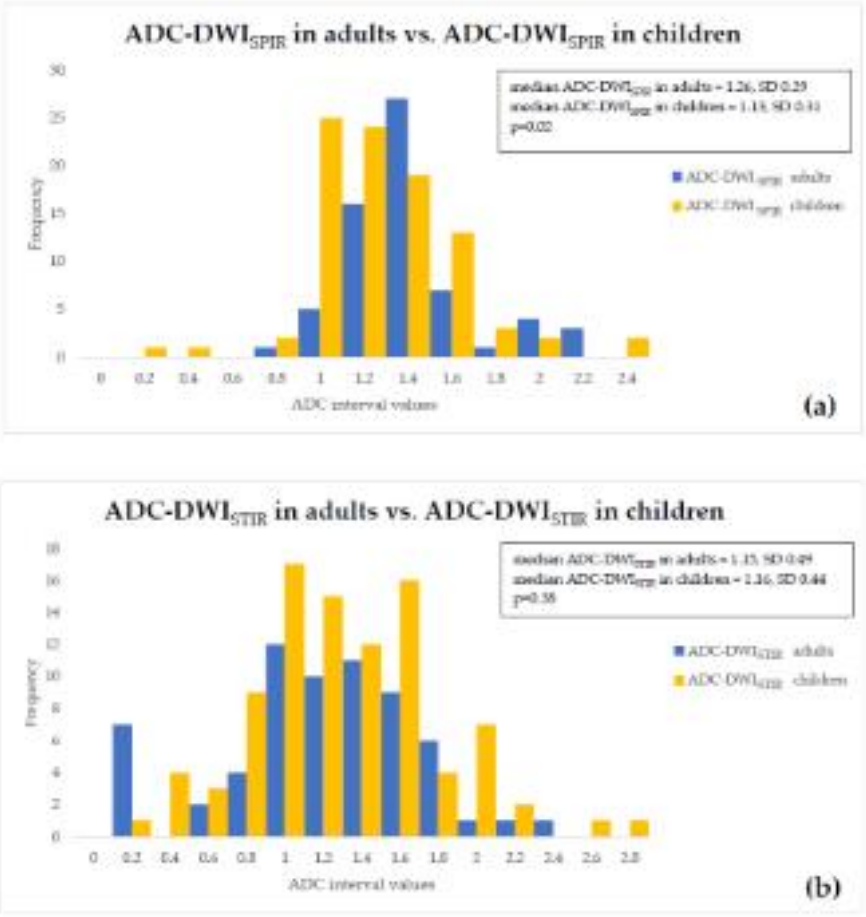

Figure 1. Comparison of (**a**) ADC-DWI$_{SPIR}$ values, and (**b**) ADC-DWI$_{STIR}$ values between adults and children.

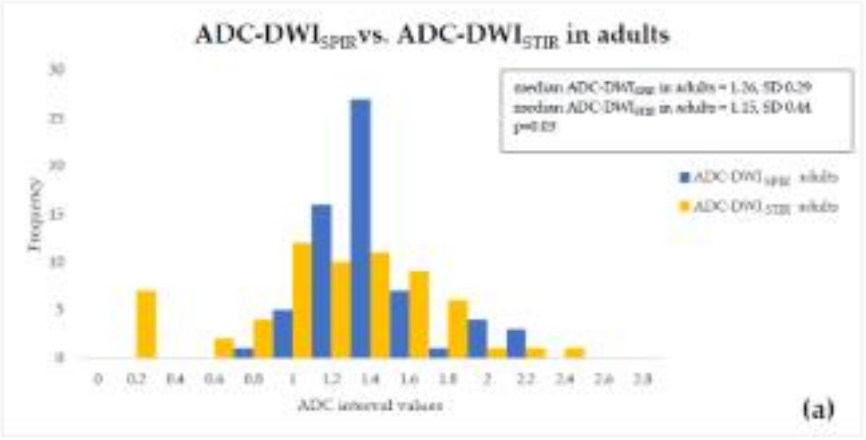

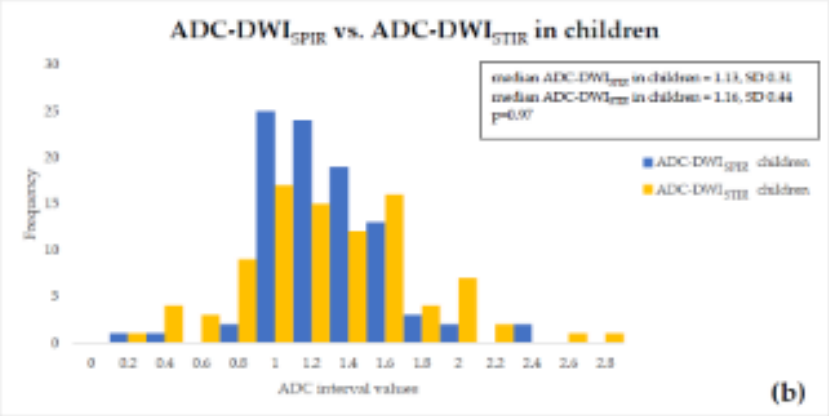

Figure 2. Comparison between ADC-DWI$_{SPIR}$ and ADC-DWI$_{STIR}$ values in the (**a**) adult group and (**b**) in children.

In all patients of both groups, the MaRIA value corresponded to active disease (i.e., ≥7) [6]. Excluding one patient with the score value of 10.65, MaRIA score values in all adult patients also corresponded to severe disease (i.e., ≥11). In the paediatric group, in all but three patients, with the values of 9.95, 10.25 and 10.66, MaRIA values exceeded 11 thus corresponding to severe disease [6].

In all patients of both groups, the DWI$_{SPIR}$-based Clermont score value corresponded not only to active disease (i.e., >8.4) but severe disease (i.e., ≥12.5). In two adult patients, the DWI$_{STIR}$-based Clermont score values (i.e., 5.92 and 8.20) were below the threshold of 8.4 for active disease, however the values of all other patients corresponded both to active and to severe disease. In one paediatric patient, the DWI$_{STIR}$-based Clermont score value (i.e., 8.24) was slightly below the threshold of 8.4 for active disease; two patients with values of 11.26 and 12.38 corresponded to active disease, and all other patients corresponded to severe disease [6].

The correlation between ADC-DWI$_{SPIR}$ and ADC-DWI$_{STIR}$ was weak and statistically unreliable in both adults (rho = 0.27; $p = 0.13$) (Figure 3a) and children (rho = 0.22; $p = 0.15$) (Figure 3b).

There was a strong and statistically significant correlation between MaRIA and ADC-DWI$_{SPIR}$-based Clermont score in both adults (rho = 0.93; $p < 0.0001$) (Figure 4a) and in children (rho = 0.98; $p < 0.0001$) (Figure 4b). There was also a strong and statistically significant correlation between MaRIA and ADC-DWI$_{STIR}$-based Clermont score in adults (r = 0.89; $p < 0.0001$) (Figure 5a) and in children (rho = 0.95; $p < 0.0001$) (Figure 5b). The correlation between ADC-DWI$_{SPIR}$ and MaRIA was moderate negative and statistically reliable in both adults (r = −0.50, $p = 0.004$) (Figure 6a) and children (r = −0.54, $p < 0.0001$) (Figure 6b). There was no correlation between ADC-DWI$_{STIR}$ and MaRIA (rho = −0.001, $p = 0.99$) in adults (Figure 7a), and low negative statistically reliable correlation (rho = −0.374, $p = 0.01$) in children (Figure 7b).

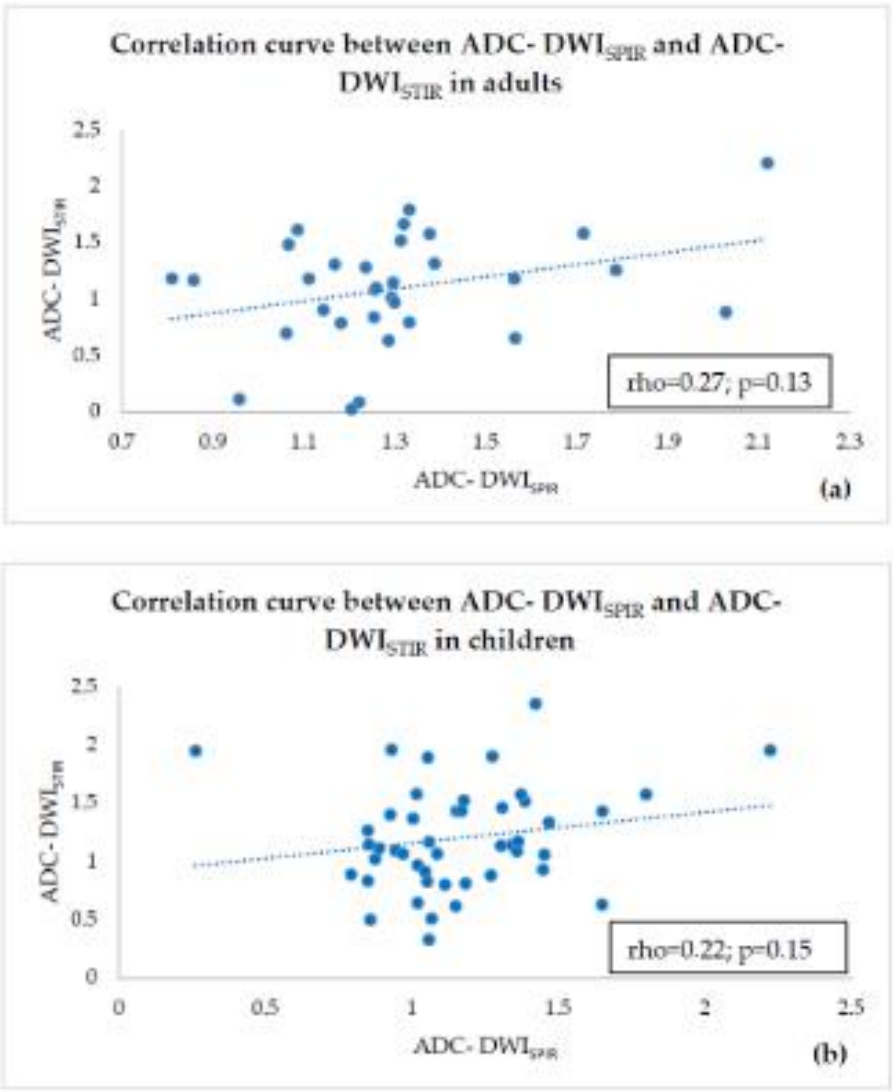

Figure 3. Correlation curve between ADC-DWI$_{SPIR}$ and ADC-DWI$_{STIR}$ in adults (**a**) and children (**b**) showing no correlation.

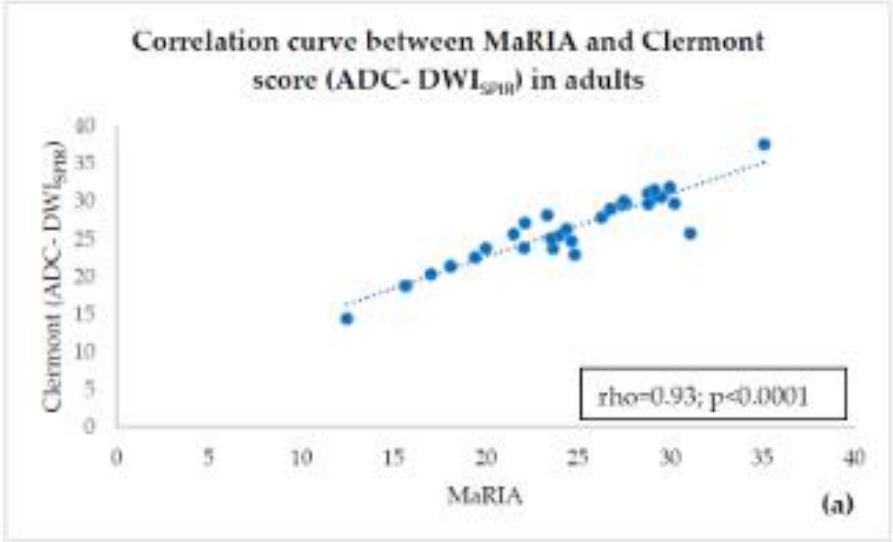

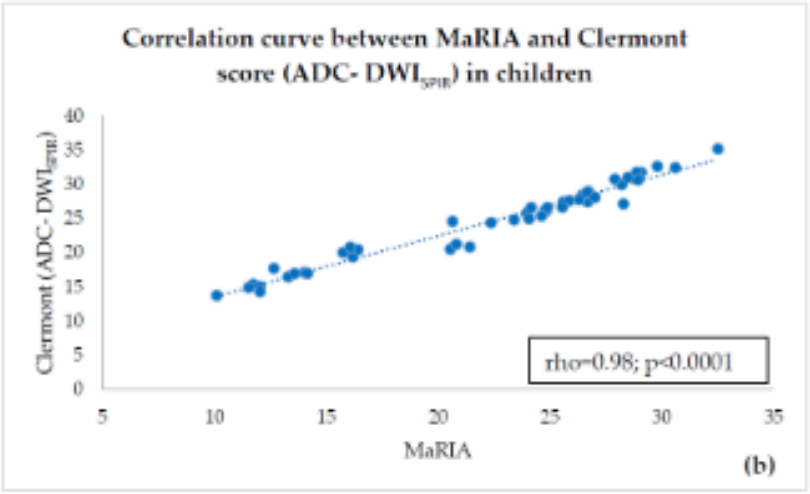

Figure 4. Correlation curve between MaRIA and ADC-DWI$_{SPIR}$—based Clermont score in adults (**a**) and children (**b**) showing high correlation.

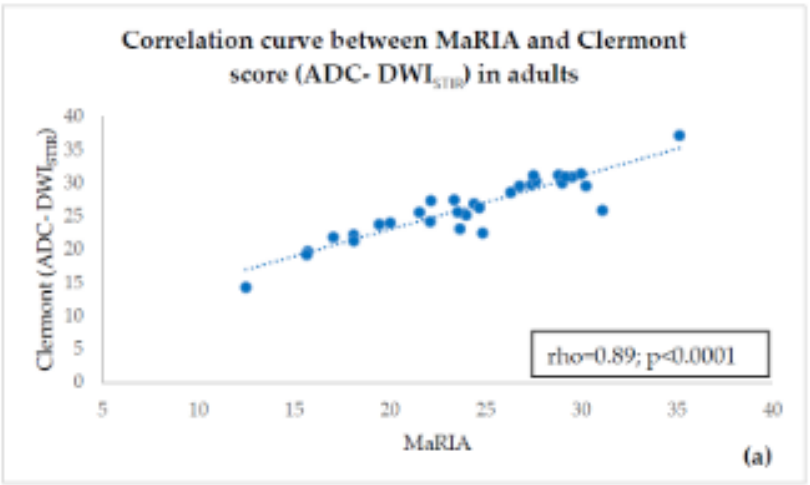

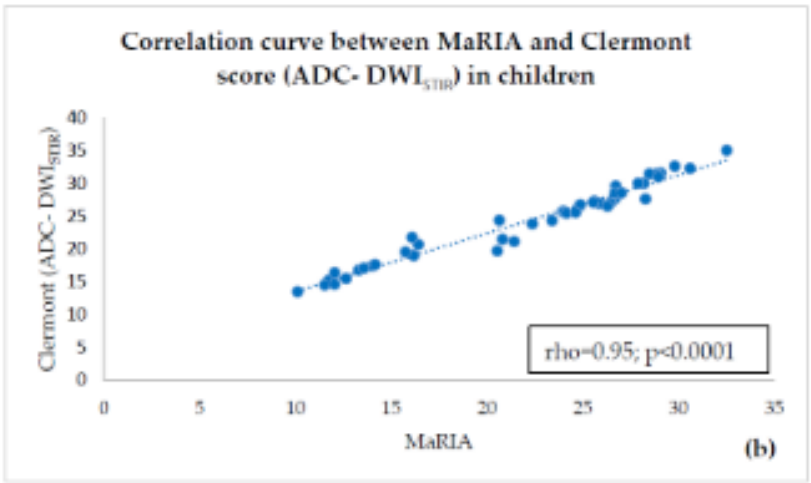

Figure 5. Correlation curve between MaRIA and ADC-DWI$_{STIR}$—based Clermont score in adults (**a**) and children (**b**) showing high correlation.

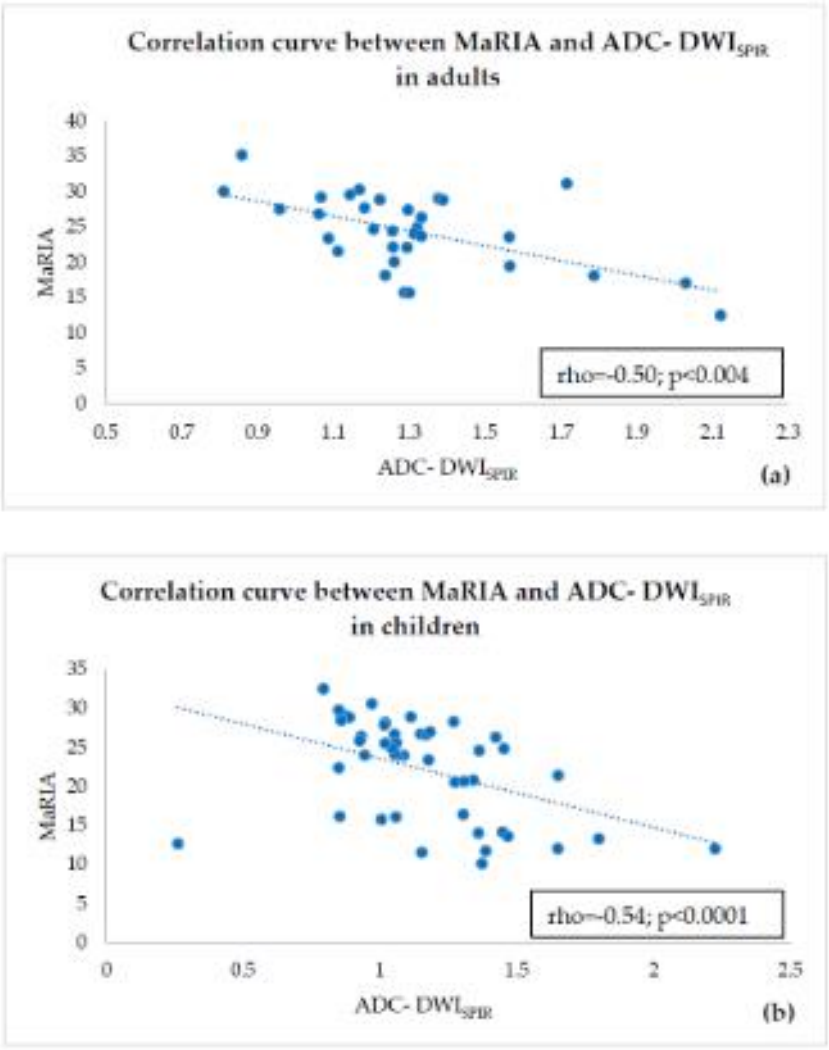

Figure 6. Correlation curve between ADC-DWI$_{SPIR}$ and MaRIA in adults (**a**) and children (**b**) showing moderate negative correlation.

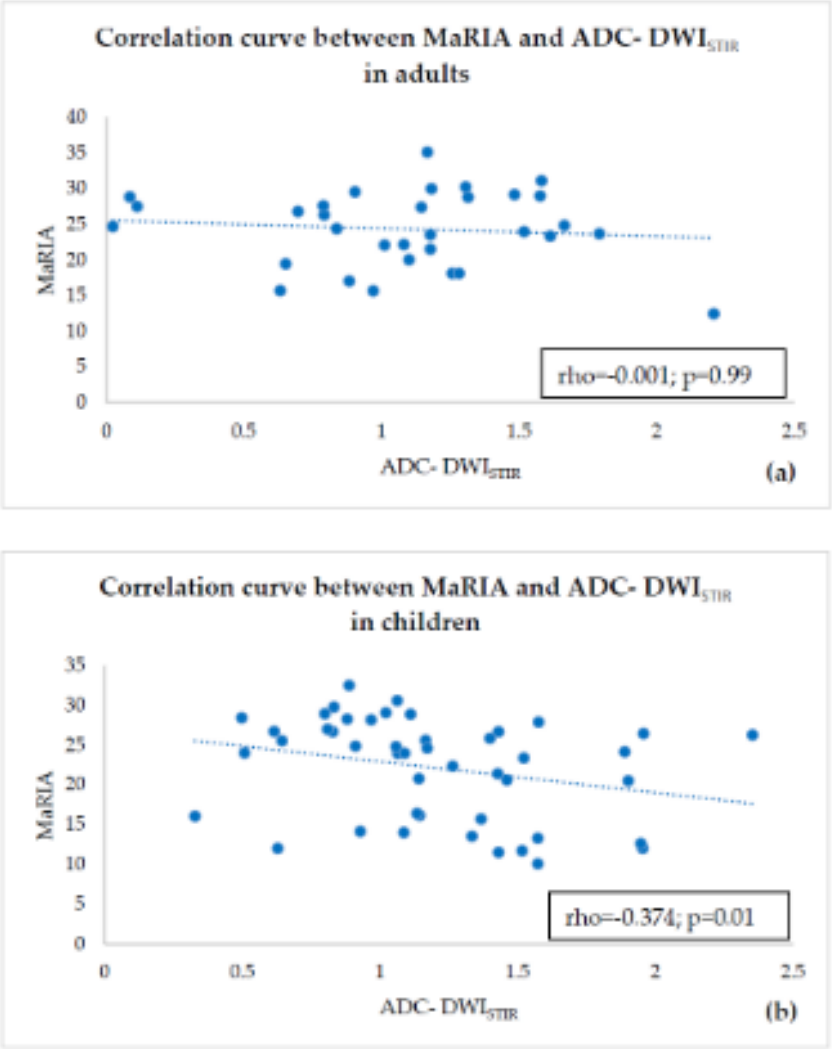

Figure 7. Correlation curve between ADC-DWI$_{STIR}$ and MaRIA in adults (**a**) showing no correlation and in children (**b**) showing low negative correlation.

4. Discussion

The primary goal of treatment for CD is to achieve remission. Although the primary endpoint of treatment has long been endoscopic remission i.e., mucosal healing [5,39,40], CD is a transmural inflammation. Even in patients with sustained mucosal healing, transmural inflammation may persist [41–43]. It is proven that compared to mucosal healing, transmural healing is related to improved long-term outcomes, including sustained long-term steroid-free clinical remission, less need for rescue therapy, less CD-related hospitalisations and CD-related surgery [44]. Therefore, transmural healing has recently been proposed as a new target for CD treatment [45]. To assess transmural changes, imaging techniques are required allowing evaluation of the altered intestinal wall along its entire length and thickness. MRE, being an informative non-invasive radiation-free cross-sectional imaging modality providing high soft tissue resolution, is proven to have a potential to replace endoscopy in assessment of inflammatory activity [39].

MaRIA score, developed by the Rimola research team [39], is the only validated index for measuring inflammatory activity in the ileum distal loop, tested in large patient populations [7] and multicenter research [46]. However, multiple gadolinium contrast injections should be avoided, due to related adverse effects [9–11]. In 2019, this same research group also published a report on the simplified MaRIA (sMaRIA), based on data from 98 patients, accounting fat stranding, instead of RCE

[46]. However, this novelty approach requires larger validation studies. The London index measures the wall thickness and presence of edema [47], providing an accurate assessment of inflammatory activity, however cannot be used in estimating disease severity, and thus is not applicable in the evaluation of therapeutic response upon follow-up examinations [46]. The Clermont score is based on DWI (therefore called DWI-MaRIA), and it was derived by the research group of Clermont-Ferrand university as an alternative for MaRIA, replacing RCE with ADC, thus avoiding administration of gadolinium contrast media. The authors of the Clermont score state it is not only useful in estimation of ileal CD activity, with excellent correlation with RCE-based MaRIA [20], but also in the detection of ulcers [48] and prediction of remission after biological therapy [49]. However, the performance of the Clermont score still should be validated.

In DWI, which the Clermont score is based on, tissue contrast relies on differences of motions of water molecules among various tissues [50]. In each MRI system, there are several choices of fat saturation techniques for use with DWI. At our institution, the MR protocol repository for abdominal imaging contains two types of DWI sequences—DWI with SPIR fat suppression technique and DWIBS sequence using STIR; their scanning parameters are given in Table 1. When compared to the DWI with SPIR, bowel walls in DWIBS visually look sharper and contours of structures are better delineated (Figure 8). Precise delineation of inflammatory lesions could be very important in diagnosis of CD, which can be subject to delay for up to several years [51], especially in locations not assessible by endoscope, where cross-sectional imaging could be the only solution to reveal inflammation. Therefore, due to better delineation of bowel walls in DWI with STIR, our goal was to assess the reliability of ADC-DWI$_{STIR}$ measurements to be used in calculating the Clermont score, when compared to the ADC-DWI$_{SPIR}$ values.

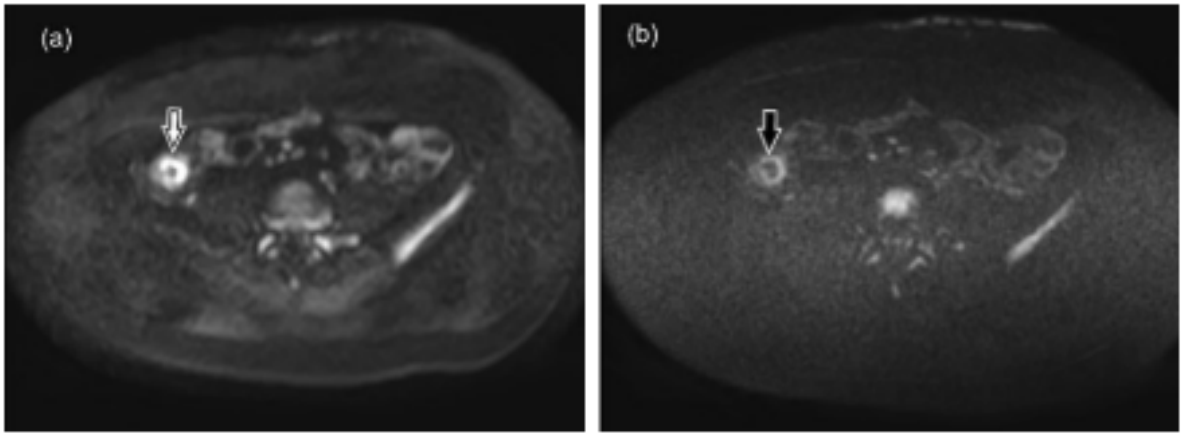

Figure 8. DWI$_{SPIR}$ (**a**) and DWI$_{STIR}$ (**b**) tracking images of b = 800 s/mm^2 images of 40 years old male patient with active CD. Inflamed bowel walls present high signal intensity. Despite decreased SNR causing graininess in the images, the resolution of inflamed bowel and delineation of contours is better in DWI$_{STIR}$ image (black arrow) as compared to the DWI$_{SPIR}$ image (white arrow).

In the current literature, there are no strictly defined recommendations regarding the best fat suppression techniques to be used in DWI for evaluation of CD activity. Singha et al. and Park recommend using DWI sequence with STIR within protocols for assessment of gastrointestinal tract mentioning the role of ADC measurement [33,34]. The American College of Radiologists recommends that DWI sequence with STIR should be included within the MRE protocol [32]. The free-breathing technique affords multiple averages, thus leading to better SNR, so probably having advantages in performing measurements of ADC [29]. To our knowledge of using ADC in the assessment of bowel inflammation, Kiryu et al. and Caruso et al. are the only research teams reporting DWI with STIR used in ADC measurements for quantitative assessment of bowel information [35,52]. The Caruso team also used this ADC exactly to calculate the Clermont score. However, several other authors emphasise using free breathing techniques [13,14,18–20,53–55], without specifying the fat saturation method used with DWI. Therefore, there is a chance that researchers consider navigator

triggered DWI sequences with SPIR, SPAIR, and CHESS requiring less signal averaging than free breathing techniques, however, in some of these studies, the related fat saturation technique could theoretically be STIR. Consequently, if the article does not explicitly state the technique of fat saturation, it is impossible to judge exactly which one is used.

Initially, we calculated the correlation between ADC-DWI$_{SPIR}$ and ADC-DWI$_{STIR}$ with the expectation of a good correlation. To our surprise, although ADC-DWI$_{SPIR}$ and ADC-DWI$_{STIR}$ visually seemed to be comparable, we observed almost no correlation between ADC-DWI$_{SPIR}$ and ADC-DWI$_{STIR}$ measured in one and the same bowel segments in both adults (rho = 0.27; p = 0.13) and children (rho = 0.22; p = 0.15). Although DWI$_{STIR}$ is performed under free breathing, and availability of both repeated stimulations and acquisitions contributes to improved SNR and both spatial and temporal resolution [30] the allowance of respiratory motion in DWI$_{STIR}$, means that slice levels of images obtained with different b-values may not be identical. Since DWIBS employs multiple slice excitations, slice levels of images obtained with the same b-value may be different [29]. The weak correlation between ADC-DWI$_{SPIR}$ and ADC-DWI$_{STIR}$ values may also be impacted by the conceptually different fat suppression mechanisms of SPIR and STIR, on ADC values of the intestinal wall in relation to histopathological characteristics of bowel inflammation, due to differences in gut wall histopathology in adults and children. This issue will be discussed further in the article.

Within the study, the ADC-DWI$_{SPIR}$ and ADC-DWI$_{STIR}$ values were analysed in two dimensions:

(1) ADC values of both adults and children were compared within a single fat suppression technique, and we observed statistically significant ADC-DWI$_{SPIR}$ difference between adults and children (1.31×10^{-3} mm^2/s, SD 0.29, vs. 1.16×10^{-3} mm^2/s, SD 0.31; p = 0.02), with 12.12% lower ADC values in children compared to adults, but no statistically significant difference between the ADC-DWI$_{STIR}$ values in adults and children (1.09×10^{-3} mm^2/s, SD 0.49, vs. 1.20 mm^2/s $\times 10^{-3}$, SD 0.44; p = 0.38);

(2) both DWI$_{SPIR}$ and DWI$_{STIR}$ techniques were compared within one patient group, both in adults and children. In this case, the analysis showed difference of 16.73% between ADC-DWI$_{SPIR}$ and ADC-DWI$_{STIR}$ values in adults, being lower in DWI$_{STIR}$ (1.31×10^{-3} mm^2/s, SD 0.29, vs. 1.09×10^{-3} mm^2/s, SD 0.49; p = 0.03), but did not show difference between ADC-DWI$_{SPIR}$ and ADC-DWI$_{STIR}$ values in the children's group (1.16 mm^2/s $\times 10^{-3}$, SD 0.31, vs. 1.20 $\times 10^{-3}$ mm^2/s, SD 0.44, p = 0.97).

These observations raise questions about why ADC-DWI$_{SPIR}$ values are lower in paediatric patients than in adults whilst no difference in ADC-DWI$_{STIR}$ between adult and paediatric patients is observed, and why the ADC-DWI$_{STIR}$ values are lower than ADC-DWI$_{SPIR}$ in adults, whilst there is no difference between ADC-DWI$_{SPIR}$ and ADC-DWI$_{STIR}$ values in pediatric patients. In answering these questions, either a differing histopathological pattern in adult and paediatric CD, or differences between the fat suppression mechanism of DWI$_{SPIR}$ and DWI$_{STIR}$ techniques influences ADC values, or combination of both factors must be taken into account.

To interpret our results, it is necessary to consider the pathophysiological characteristics of the tissue, the physical basis of both DWI sequences and the duration of CD history. Although the exact cause of the restricted diffusion in CD still remains unknown, the three ruling theories considered are as follows: (1) narrowing of extracellular space in active CD (caused by presence of oedema and increased cell density due to migration of inflammatory cells, mostly lymphocytes), formation of lymphoid aggregates into the lamina propria and submucosa of the inflamed wall segments (Figure 9a), presence of dilated lymphatic vessels and epithelioid granulomas, and formation of micro-abscesses) [56–59], (2) increased perfusion, and (3) mural fibrosis [56,57]. Although the morphological pattern of CD is generally similar in adult and pediatric patients [59], the main difference between the histopathology of pediatric and adult CD, is the more frequent appearance of epithelioid granulomas in the inflamed bowel wall of children [58,60,61] (Figure 9b).

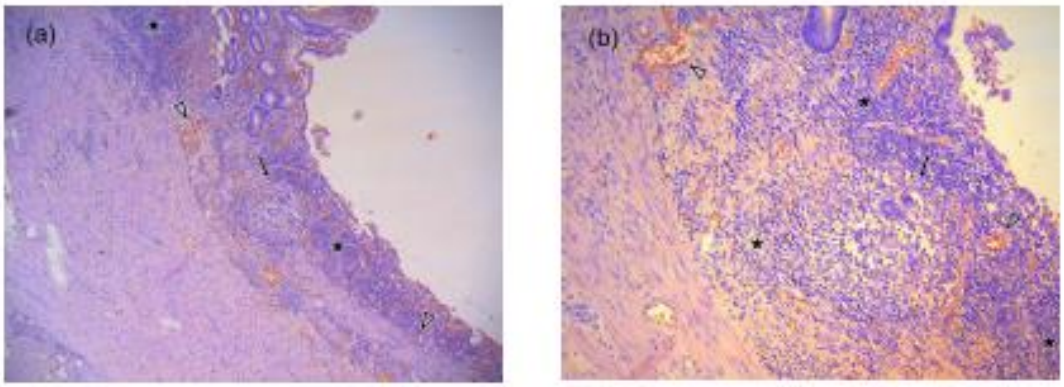

Figure 9. Inflammation of the ileal wall in active chronic CD in 14 y.o. boy, hematoxylin-eosin staining (courtesy of Dr. Ivars Melderis), (**a**) at magnification × 40, (**b**) at magnification × 100. Infiltration by plasma cells, neutrophils and abundant number of lymphocytes is present in the mucosal part of the bowel (star), along with epithelioid granuloma (arrow) in the lamina muscularis mucosae providing additional contribution for restricted diffusion signal in DWI images in children CD. Due to granulation process, there are unaltered red blood cells (arrowheads) in the capillaries of intestinal mucosa. The presence of blood degradation products is not detectable in any of the intestinal wall layers.

Whenever analysing the performance of ADC-DWI$_{STIR}$, the non-selectivity of STIR fat suppression must be considered. Unlike the SPIR technique which uses spectral selective radiofrequency pulse suppressing solely the fat signal, STIR technique uses an inversion recovery technique based on the T1 relaxation time of the tissues examined. Apart from fat having a short T1 time, STIR technique suppresses other substances of short T1 time, thus adding to decrease of ADC value by suppression of signal from methaemoglobin, melanin, mucoid tissue, and proteinaceous fluid [24]. When considering the presence of methaemoglobin, although early mucosal lesions in CD can be associated with the damage of small capillaries [58], no data on haemorrhagic changes in the blood vessels has been found in literature. An exception to this is angiitis in the outer part of the bowel wall, which manifests through the infiltration of inflammatory cells into vascular adventitia, or formation of granulomas alongside blood vessels. There is no evidence of haemorrhagic lesions [62] containing the products of methaemoglobin. The deposition of melanin (along with lipofuscin) in the intestinal wall is characteristic of colonic melanosis, related with the chronic use of laxatives [63], and there is limited data on its association with CD [64,65]. Given its extremely rare occurrence, the chance of intestinal melanosis occurring in the patients included in the study is unlikely. The inflammatory bowel wall tends to contain crypt abscesses, the contents of which could be considered as both mucoid and protein-rich tissues. However they are occasional, and are only observed in 19% of patients [62]. However, an additional very important consideration influencing the signal intensity of fine and thin structures, such as the bowel wall, is the partial volume effect [66], where the voxel is influenced not only by the properties of the same structure but also by the nature of the adjacent tissues. Typically, achievable DWI resolution is in the order of 2 mm × 2 mm × 2 mm [67]. In our DWIBS protocol, the acquisition voxel size is 2.50 mm (RL) × 2.98 AP (AP) × 6 mm (slice thickness) therefore, within the single voxel, there will be signal contamination from the adjacent media. Since the bowel lumen contains the viscous and proteinaceous chyme, and occasionally fecal admixture, the ADC-DWI$_{STIR}$ values will be influenced not only by suppression of the mesenterial fat tissue, but also by saturation of signal from the bowel content with short T1 relaxation time. Therefore, when measured at a short distance from the intestinal lumen as carried out in the group of adults, ADC-DWI$_{STIR}$ values are artificially lower, compared to ADC values of DWI with selective fat suppression, i.e., DWI$_{SPIR}$.

ADC-DWI$_{SPIR}$ values are lower in paediatric patients than in adults. This is explained by differences in medical history. Although all adult patients had active CD, their medical history prior

the study. However, the literature provides a broad picture of the correlation not only between MRE and endoscopic findings, but also between MRE and surgery specimens of resected intestinal segments with certain defined criteria, along with the conclusion that MRI is an informative and sufficiently accurate method to assess altered bowel wall. Based on these observations, for several years now, when referring patients for MRE examinations, clinicians do not duplicate their results with the invasive endoscopy that is also cumbersome for patients. Consequently, in 2019, for the first time, the ECCO-ESGAR guidelines came up with a revolutionary statement that radiological cross-sectional imaging methods (and, therefore, MR) can be used as an alternative to endoscopy to assess CD activity [5]. Therefore, although CD had been endoscopically confirmed in all patients included in our study, the results of the MRE examination were not duplicated by the endoscopic and histopathological findings in any cases. It would have been useful to correlate the MR finding with the histopathological picture of the surgical resection specimens. However, surgical resection with subsequent histopathological analysis of the specimen, which would provide the most complete picture of intestinal wall changes, was performed in only one pediatric patient.

In another related research project, our study team assessed the intra-observer agreement of measurements of ADC-DWI$_{SPIR}$ values, ADC-DWI$_{STIR}$ values, and other components of MaRIA and Clermont scores—bowel thickness, presence of ulcers and RCE composed from WSE-preGd and WSI-postGd. The data was recently published. According to our results, there was a systematic difference in the assessment of ulcers, however, no difference was observed between the measurements of the bowel wall thickness, ADC values of DWI with SPIR, ADC values of DWI with STIR as well as measurements performed for assessment of WSI-preGd and WSI post-Gd [70].

In our opinion, the strengths of our research were as follows: (1) the prospective study design, (2) accurate location-by-location comparison in one and the same bowel segment, (3) explicit ROI size not being defined in the previous studies on MaRIA and Clermont score, except for when conducted by the Caruso's team using the ROI size between 12 and 20 mm^2. However, our study also faced several limitations: (1) the relatively low number of participants in the study groups, (2) the study population could be subject to selection bias, as both adult and paediatric study groups were not homogenous regarding the duration of the disease. Paediatric patients included in our study had a relatively shorter history than the adult patients; (3) in both post-Gd and DWI images, the ROIs were placed on the site of the maximum SI. After administration of gadolinium contrast media, in some cases the most intense contrast enhancement was predominantly observed in ileal mucosa, however in other cases the enhancement was evenly distributed throughout the intestinal wall. In contrast, in both types of DWI techniques, bowel wall layers were indistinguishable as the diffusion restriction throughout the intestinal walls was equally intense, which could result in differences of positioning ROI between the T1 post-contrast and DWI sequences; (4) the MaRIA studies are based on a comparison of the visual image with the CDEIS—CD endoscopic activity index in adult patients. Unlike adults, estimation of inflammatory activity in children does not rely on endoscopy findings due to its invasiveness, but rather on the Pediatric Crohn's Disease Activity Index (PCDAI), which correlates poorly with the MaRIA index ($r = 0.42$, $p = 0.016$) [6]. Its correlation with Clermont score has not yet been estimated, so, in children, the utility of Clermont score is still unclear.

5. Conclusions

In Crohn's disease, DWI MRI sequence with STIR, when compared to DWI MRI sequence with SPIR, is less reliable and is not suitable for quantitative bowel inflammatory activity assessment to be used in Clermont score, in both adult and paediatric patients. DWI MRI sequence with STIR is advisable to provide qualitative visual identification of bowel inflammation foci in adults as well as paediatric patients.

Author Contributions: Conceptualization, methodology, investigation and writing—original data preparation, I.A.; investigation, data curation R.P.; resources, writing—review and editing I.F., writing—review and editing, J.P. and G.K.; supervision, G.K. All authors have read and agreed to the published version of the manuscript.

Funding: This research received no external funding.

to the MRE examination was at least six months long (except for one patient whose duration of illness was unknown), whereas all children (except one with an almost 2-year history of CD) were examined no longer than six months after the onset of symptoms. Therefore, the edema component in the pediatric bowel wall was more pronounced, resulting in a greater diffusion restriction when compared to the adult patients. The presence of epithelioid granulomas may further limit diffusion in the inflamed wall.

The explanation of non-difference between ADC-DWI$_{STIR}$ values in adults and children is more complex. In children, there is expressive oedema. The ROI was positioned at the site with the highest signal intensity (within the submucosal layer of the bowel wall), therefore the distance to the intestinal lumen was sufficient to prevent the signal contamination caused by the partial volume effect. Since the history of the disease is longer in the group of adult patients, apart from oedema, fibrosis is also present. In these locations, the bowel wall is thinner, and ADC-DWI STIR values are influenced by the partial volume effect from the bowel content with short T1 time, which artificially lowers the ADC values.

The absence of difference between ADC-DWI$_{SPIR}$ and ADC-DWI$_{STIR}$ values in the children's group could also be explained with the predominance of the edematous component, which, by increasing the thickness of the intestinal wall, does not allow the partial volume effect to affect the ADC-DWI$_{STIR}$ values measured in the middle of the submucosal layer of the intestinal wall.

The correlation between ADC-DWI$_{SPIR}$ and MaRIA was moderately negative in both adults ($r = -0.50$, $p = 0.004$) and children ($r = -0.54$, $p < 0.0005$) being worse than reported by the study group of the Clermont-Ferrand university showing excellent correlation [19,20]. However, in the systematic review and meta-analysis on using diffusion-weighted MRE for evaluating bowel inflammation in CD, Choi et al. states that ADC demonstrates a moderate strength of correlation at best and Clermont score performs better [68]. This is also consistent with our results, since like the studies by the research group from Clermont-Ferrand university, we also observed excellent correlation between DWI-based Clermont score and MaRIA in both adults (rho = 0.93; $p < 0.0005$) and children (rho = 0.98; $p < 0.0005$). However, there might a methodological error in using correlation between MaRIA and Clermont score, as the data to be correlated should be mutually independent, and should not be used if they include more than one observation in any individual [69]. Apart from RCE used in MaRIA and ADC used in the Clermont score, all other three variables (wall thickness, presence of edema and presence of ulcerations), are used in both equations. The use of correlation analysis opposes the conditions in which correlation can be applied, and in the instances of highest probability, could lead to an overestimation of the similarity between MaRIA and Clermont score. The correctness of this statement is supported by the contradiction between correlation of ADC-DWI$_{STIR}$ and the ADC-DWI$_{STIR}$-based Clermont Index with MaRIA, as despite no apparent correlation between ADC-DWI$_{STIR}$ and MaRIA ($r = -0.001$, $p = 0.99$) in the adult group, and low negative correlation between ADC-DWI$_{STIR}$ and MaRIA in the paediatric group ($r = -0.37$, $p = 0.01$), the correlation between DWI$_{STIR}$-based Clermont score and MaRIA remained strong in both adults ($r = 0.89$; $p < 0.0005$) and in children (rho = 0.95; $p < 0.0005$).

For scanning of the study patients, we used DWI$_{STIR}$ and DWI$_{SPIR}$ (DWIBS) sequences included in the MRE protocol, obtained from the repository provided by the manufacturer. DWI$_{STIR}$ sequence differs from DWI$_{SPIR}$ with the inversion recovery pulse applied. The sharpness of contours in DWI$_{STIR}$ images always outperforms the DWI$_{SPIR}$ series, due to better suppression of background signal and less T2 "shine through" effect, provided that all scanning parameters (number of signal averages, voxel size, slice thickness, FOV and DWI directions parameters) are the same. As the voxel size and number of signal averages does not influence the DWI outcome including the ADC value and these sequences are designed to provide the best possible performance, we did not modify or harmonise the scanning parameters used in the protocol.

In our study, we did not use endoscopy as the reference standard but selected the study groups exclusively by visual MRE findings of CD, i.e., thickened, oedematous bowel wall and markedly increased SI in the DWI tracking images of b = 800 s/mm^2 along with the low SI in the ADC map. Of course, the lack of correlation with the endoscopic picture could be considered to be a limitation of

Acknowledgments: The authors gratefully acknowledge the generosity of Taro Takahara for his advices regarding this study, Irena Rogovska for support in processing of statistical data and Rihards Rumnieks for help with processing of images.

Conflicts of Interest: The authors declare no conflict of interest.

References

1. Dulai, P.S.; Singh, S.; Cesarini, M.; Bouguen, G.; Nelson, S.A.; Peyrin-Biroulet, L.; Feagan, B.G.; Ordas, I.; Sandborn, W.J.; Santillan, C.; et al. Cochrane Database of Systematic Reviews MRI scoring indices for evaluation of disease activity and severity in Crohn ′ s disease (Methodology Protocol). *Cochrane Database Syst. Rev.* **2015**, *4*, 1–8.
2. Cosnes, J.; Gowerrousseau, C.; Seksik, P.; Cortot, A. Epidemiology and natural history of inflammatory bowel diseases. *Gastroenterology* **2011**, *140*, 1785–1794.
3. Sakuraba, H.; Ishiguro, Y.; Hasui, K.; Hiraga, H.; Fukuda, S.; Shibutani, K.; Takai, Y. Prediction of maintained mucosal healing in patients with Crohn's disease under treatment with infliximab using diffusion-weighted magnetic resonance imaging. *Digestion* **2014**, *89*, 49–54.
4. Peyrin-Biroulet, L.; Sandborn, W.; Sands, B.E.; Reinisch, W.; Bemelman, W.; Bryant, R.V.; D'Haens, G.; Dotan, I.; Dubinsky, M.; Feagan, B.; et al. Selecting Therapeutic Targets in Inflammatory Bowel Disease (STRIDE): Determining Therapeutic Goals for Treat-to-Target. *Am. J. Gastroenterol.* **2015**, *110*, 1324–1338.
5. Maaser, C.; Sturm, A.; Vavricka, S.R.; Kucharzik, T.; Fiorino, G.; Annese, V.; Calabrese, E.; Baumgart, D.C.; Bettenworth, D.; Borralho Nunes, P.; et al. ECCO-ESGAR Guideline for Diagnostic Assessment in IBD Part 1: Initial diagnosis, monitoring of known IBD, detection of complications. *J. Crohn's Colitis* **2019**, *13*, 144–164K.
6. Rozendorn, N.; Amitai, M.M.; Eliakim, R.A.; Kopylov, U.; Klang, E. A review of magnetic resonance enterography-based indices for quantification of Crohn's disease inflammation. *Therap. Adv. Gastroenterol.* **2018**, *11*, 1756284818765956
7. Dohan, A.; Taylor, S.; Hoeffel, C.; Barret, M.; Allez, M.; Dautry, R.; Zappa, M.; Savoye-Collet, C.; Dray, X.; Boudiaf, M.; et al. Diffusion-Weighted MRI in Crohn's Disease: Current Status and Recommendations. *J. Magn. Reson. Imaging* **2016**, *44*, 1381–1396.
8. Perez-Rodriguez, J.; Lai, S.; Ehst, B.D.; Fine, D.M.; Bluemke, D.A. Nephrogenic Systemic Fibrosis: Incidence, Associations, and Effect of Risk Factor Assessment—Report of 33 Cases. *Radiology* **2009**, *250*, 371–377.
9. Gulani, V.; Calamante, F.; Shellock, F.G.; Kanal, E.; Reeder, S.B. Gadolinium deposition in the brain: Summary of evidence and recommendations. *Lancet Neurol.* **2017**, *16*, 564–570.
10. Quattrocchi, C.C.; van der Molen, A.J. Gadolinium Retention in the Body and Brain: Is It Time for an International Joint Research Effort? *Radiology* **2017**, *282*, 12–16.
11. Baliyan, V.; Das, C.J.; Sharma, R.; Gupta, A.K. Diffusion weighted imaging: Technique and applications. *World J. Radiol.* **2016**, *8*, 785–798.
12. Oto, A.; Kayhan, A.; Williams, J.T.B.; Fan, X.; Yun, L.; Arkani, S.; Rubin, D.T. Active Crohn's disease in the small bowel: Evaluation by diffusion weighted imaging and quantitative dynamic contrast enhanced MR imaging. *J. Magn. Reson. Imaging* **2011**, *33*, 615–624.
13. Sirin, S.; Kathemann, S.; Schweiger, B.; Hahnemann, M.L.; Forsting, M.; Lauenstein, T.C.; Kinner, S. Magnetic resonance colonography including diffusion-weighted imaging in children and adolescents with inflammatory bowel disease: Do we really need intravenous contrast? *Investig. Radiol.* **2015**, *50*, 32–39.
14. Dubron, C.; Avni, F.; Boutry, N.; Turck, D.; Duhamel, A.; Amzallag-Bellenger, E. Prospective evaluation of free-breathing diffusion weighted imaging for the detection of inflammatory bowel disease with MR enterography in childhood population. *Br. J. Radiol.* **2016**, *89*, 2–10.
15. Neubauer, H.; Pabst, T.; Dick, A.; MacHann, W.; Evangelista, L.; Wirth, C.; Köstler, H.; Hahn, D.; Beer, M. Small-bowel MRI in children and young adults with Crohn disease: Retrospective head-to-head comparison of contrast-enhanced and diffusion-weighted MRI. *Pediatr. Radiol.* **2013**, *43*, 103–114.
16. Oto, A.; Zhu, F.; Kulkarni, K.; Karczmar, G.S.; Turner, J.R.; Rubin, D. Evaluation of diffusion-weighted MR imaging for detection of bowel inflammation in patients with Crohn's disease. *Acad. Radiol.* **2009**, *16*, 597–603.
17. Buisson, A.; Joubert, A.; Montoriol, P.F.; Ines, D.D.; Hordonneau, C.; Pereira, B.; Garcier, J.M.; Bommelaer, G.; Petitcolin, V. Diffusion-weighted magnetic resonance imaging for detecting and assessing ileal inflammation in Crohn's disease. *Aliment. Pharmacol. Ther.* **2013**, *37*, 537–545.

18. Kim, K.-J.; Lee, Y.; Park, S.H.; Kang, B.-K.; Seo, N.; Yang, S.-K.; Ye, B.D.; Park, S.H.; Kim, S.Y.; Baek, S.; et al. Diffusion-weighted MR Enterography for Evaluating Crohn's Disease: How Does It Add Diagnostically to Conventional MR Enterography? *Inflamm. Bowel Dis.* **2015**, *21*, 101–109.
19. Kopylov, U.; Klang, E.; Yablecovitch, D.; Lahat, A.; Avidan, B.; Neuman, S.; Levhar, N.; Greener, T.; Rozendorn, N.; Beytelman, A.; et al. Magnetic resonance enterography versus capsule endoscopy activity indices for quantification of small bowel inflammation in Crohn's disease. *Therap. Adv. Gastroenterol.* **2016**, *9*, 655–663.
20. Hordonneau, C.; Buisson, A.; Scanzi, J.; Goutorbe, F.; Pereira, B.; Borderon, C.; Da Ines, D.; Montoriol, P.F.; Garcier, J.M.; Boyer, L.; et al. Diffusion-weighted magnetic resonance imaging in ileocolonic Crohn's disease: Validation of quantitative index of activity. *Am. J. Gastroenterol.* **2014**, *109*, 89–98.
21. Drake-Pérez, M.; Boto, J.; Fitsiori, A.; Lovblad, K.; Vargas, M.I. Clinical applications of diffusion weighted imaging in neuroradiology. *Insights Imaging* **2018**, *9*, 535–547.
22. Javier Sánchez-González, J.L.-M. Diffusion-Weighted Imaging: Acquisition and Biophysical Basis. In *Diffusion MRI Outside the Brain: A Case-Based Review and Clinical Applications*; Springer: Berlin/Heidelberg, Germany, 2012; pp. 1–15.
23. Kwee, T.C.; Takahara, T.; Ochiai, R.; Katahira, K.; Van Cauteren, M.; Imai, Y.; Nievelstein, R.A.J.; Luijten, P.R. Whole-body diffusion-weighted magnetic resonance imaging. *Eur. J. Radiol.* **2009**, *70*, 409–417.
24. Del Grande, F.; Santini, F.; Aro, M.R.; Gold, G.E.; Carrino, J.A. Fat-Suppression Techniques for 3-T MR Imaging of the Musculoskeletal system. *Radiographics* **2014**, *34*, 217–233.
25. Indrati, R. Comparing SPIR and SPAIR Fat Suppression Techniques in Magnetic Resonance Imaging (MRI) of Wrist Joint. *J. Med. Sci. Clin. Res.* **2017**, *05*, 23180–23185.
26. Horger, W. Fat Suppression in the Abdomen (Siemens). *MAGNETOM Flash* **2007**, *3*, 114–119.
27. Takahara, T.; Imai, Y.; Yamashita, T.; Yasuda, S.; Nasu, S.; Van Cauteren, M. Diffusion weighted whole body imaging with background body signal suppression (DWIBS): Technical improvement using free breathing, STIR and high resolution 3D display. *Radiat. Med.* **2004**, *22*, 275–282.
28. Moore, W.A.; Khatri, G.; Madhuranthakam, A.J.; Sims, R.D.; Pedrosa, I. Added value of diffusion-weighted acquisitions in MRI of the abdomen and pelvis. *Am. J. Roentgenol.* **2014**, *202*, 995–1006.
29. Ouyang, Z.; Ouyang, Y.; Zhu, M.; Lu, Y.; Zhang, Z.; Shi, J.; Li, X.; Ren, G. Diffusion-weighted imaging with fat suppression using short-tau inversion recovery: Clinical utility for diagnosis of breast lesions. *Clin. Radiol.* **2014**, *69*, e337–e344.
30. Kwee, T.C.; Takahara, T.; Ochiai, R.; Nievelstein, R.A.J.; Luijten, P.R. Diffusion-weighted whole-body imaging with background body signal suppression (DWIBS): Features and potential applications in oncology. *Eur. Radiol.* **2008**, *18*, 1937–1952.
31. Stadlbauer, A.; Salomonowitz, E.; Bernt, R.; Haller, J.; Gruber, S.; Bogner, W.; Pinker, K.; van der Riet, W. Diffusion-weighted MR imaging with background body signal suppression (DWIBS) for the diagnosis of malignant and benign breast lesions. *Eur. Radiol.* **2009**, *19*, 2349–2356.
32. "American College of Radiology, WWW.ACR.ORG," ACR–SAR–SPR Practice Parameter for the Performance of Magnetic Resonance (MR) Enterography. Available online: https://www.acr.org/-/media/ACR/Files/Practice-Parameters/MR-Enterog.pdf (accessed on 1 March 2020).
33. Sinha, R.; Rajiah, P.; Ramachandran, I.; Sanders, S.; Murphy, P.D. Diffusion-weighted MR imaging of the gastrointestinal tract: Technique, indications, and imaging findings. *Radiographics* **2013**, *33*, 655–676.
34. Park, S.H. Bowel Inflammation in Crohn Disease. *Am. J. Roentgenol.* **2016**, *207*, 40–48.
35. Kiryu, S.; Dodanuki, K.; Takao, H.; Watanabe, M.; Inoue, Y.; Takazoe, M.; Sahara, R.; Unuma, K.; Ohtomo, K. Free-breathing diffusion-weighted imaging for the assessment of inflammatory activity in Crohn's disease. *J. Magn. Reson. Imaging* **2009**, *29*, 880–886.
36. Kwee, T.C.; Takahara, T.; Koh, D.M.; Nievelstein, R.A.J.; Luijten, P.R. Comparison and reproducibility of ADC measurements in breathhold, respiratory triggered, and free-breathing diffusion-weighted MR imaging of the liver. *J. Magn. Reson. Imaging* **2008**, *28*, 1141–1148.
37. Jeong, K.K.; Kyoung, A.K.; Park, B.W.; Kim, N.; Cho, K.S. Feasibility of diffusion-weighted imaging in the differentiation of metastatic from nonmetastatic lymph nodes: Early experience. *J. Magn. Reson. Imaging* **2008**, *28*, 714–719.
38. Stone, A.J.; Browne, J.E.; Lennon, B.; Meaney, J.F.; Fagan, A.J. Effect of motion on the ADC quantification accuracy of whole-body DWIBS. *Magn. Reson. Mater. Phys. Biol. Med.* **2012**, *25*, 263–266.

39. Rimola, J.; Rodriguez, S.; García-Bosch, O.; Ordás, I.; Ayala, E.; Aceituno, M.; Pellisé, M.; Ayuso, C.; Ricart, E.; Donoso, L.; et al. Magnetic resonance for assessment of disease activity and severity in ileocolonic Crohn's disease. *Gut* **2009**, *58*, 1113–1120.
40. Moy, M.P.; Sauk, J.; Gee, M.S. The role of MR enterography in assessing Crohn's disease activity and treatment response. *Gastroenterol. Res. Pract.* **2016**, *2016*, 8168695.
41. Nardone, O.M.; Iacucci, M.; Cannatelli, R.; Zardo, D.; Ghosh, S. Can advanced endoscopic techniques for assessment of mucosal inflammation and healing approximate histology in inflammatory bowel disease ? **2019**, *12*, 1756284819863015.
42. Zorzi, F.; Stasi, E.; Bevivino, G.; Scarozza, P.; Biancone, L.; Zuzzi, S.; Rossi, C.; Pallone, F.; Calabrese, E. A Sonographic Lesion Index for Crohn's Disease Helps Monitor Changes in Transmural Bowel Damage During Therapy. *Clin. Gastroenterol. Hepatol.* **2014**, *12*, 2071–2077.
43. Civitelli, F.; Nuti, F.; Oliva, S.; Messina, L.; La Torre, G.; Viola, F.; Cucchiara, S.; Aloi, M. Looking beyond Mucosal Healing: Effect of Biologic Therapy on Transmural Healing in Pediatric Crohn's Disease. *Inflamm. Bowel Dis.* **2016**, *22*, 2418–2424.
44. Serban, E.D. Treat-to-target in Crohn's disease: Will transmural healing become a therapeutic endpoint? *World J. Clin. Cases* **2018**, *6*, 501–513.
45. Castiglione, F.; Imperatore, N.; Testa, A.; De Palma, G.D.; Nardone, O.M.; Pellegrini, L.; Caporaso, N.; Rispo, A. One-year clinical outcomes with biologics in Crohn's disease: Transmural healing compared with mucosal or no healing. *Aliment. Pharmacol. Ther.* **2019**, *49*, 1026–1039.
46. Ordás, I.; Rimola, J.; Alfaro, I.; Rodríguez, S.; Castro-Poceiro, J.; Ramírez-Morros, A.; Gallego, M.; Giner, À.; Barastegui, R.; Fernández-Clotet, A.; et al. Development and Validation of a Simplified Magnetic Resonance Index of Activity for Crohn's Disease. *Gastroenterology* **2019**, *157*, 432–439.
47. Steward, M.J.; Punwani, S.; Proctor, I.; Adjei-Gyamfi, Y.; Chatterjee, F.; Bloom, S.; Novelli, M.; Halligan, S.; Rodriguez-Justo, M.; Taylor, S.A. Non-perforating small bowel Crohn's disease assessed by MRI enterography: Derivation and histopathological validation of an MR-based activity index. *Eur. J. Radiol.* **2012**, *81*, 2080–2088.
48. Buisson, A.; Hordonneau, C.; Goutte, M.; Boyer, L.; Pereira, B.; Bommelaer, G. Diffusion-weighted magnetic resonance imaging is effective to detect ileocolonic ulcerations in Crohn's disease. *Aliment. Pharmacol. Ther.* **2015**, *42*, 452–460.
49. Buisson, A.; Hordonneau, C.; Goutorbe, F.; Allimant, C.; Goutte, M.; Reymond, M.; Pereira, B.; Bommelaer, G. Bowel wall healing assessed using magnetic resonance imaging predicts sustained clinical remission and decreased risk of surgery in Crohn's disease. *J. Gastroenterol.* **2018**, *54*, 312–320.
50. Chilla, G.S.; Tan, C.H.; Xu, C.; Poh, C.L. Diffusion weighted magnetic resonance imaging and its recent trend-a survey. *Quant. Imaging Med. Surg.* **2015**, *5*, 407–422.
51. Novacek, G.; Gröchenig, H.P.; Haas, T.; Wenzl, H.; Steiner, P.; Koch, R.; Feichtenschlager, T.; Eckhardt, G.; Mayer, A.; Kirchgatterer, A.; et al. Diagnostic delay in patients with inflammatory bowel disease in Austria. *Wien. Klin. Wochenschr.* **2019**, *131*, 104–112.
52. Caruso, A.; D'Incà, R.; Scarpa, M.; Manfrin, P.; Rudatis, M.; Pozza, A.; Angriman, I.; Buda, A.; Sturniolo, G.C.; Lacognata, C. Diffusion-weighted magnetic resonance for assessing ileal Crohn's disease activity. *Inflamm. Bowel Dis.* **2014**, *20*, 1575–1583.
53. Kinner, S.; Blex, S.; Maderwald, S.; Forsting, M.; Gerken, G.; Lauenstein, T.C. Addition of diffusion-weighted imaging can improve diagnostic confidence in bowel MRI. *Clin. Radiol.* **2014**, *69*, 372–377.
54. Ninivaggi, V.; Missere, M.; Restaino, G.; Gangemi, E.; Di Matteo, M.; Pierro, A.; Sallustio, G.; Bonomo, L. MR-enterography with diffusion weighted imaging: ADC values in normal and pathological bowel loops, a possible threshold ADC value to differentiate active from inactive Crohn's disease. *Eur. Rev. Med. Pharmacol. Sci.* **2016**, *20*, 4540–4546.
55. Tielbeek, J.A.W.; Ziech, M.L.W.; Li, Z.; Lavini, C.; Bipat, S.; Bemelman, W.A.; Roelofs, J.J.T.H.; Ponsioen, C.Y.; Vos, F.M.; Stoker, J. Evaluation of conventional, dynamic contrast enhanced and diffusion weighted MRI for quantitative Crohn's disease assessment with histopathology of surgical specimens. *Eur. Radiol.* **2014**, *24*, 619–629.
56. Zhu, J.; Zhang, F.; Liu, F.; He, W.; Tian, J.; Han, H.; Cao, P. Identifying the inflammatory and fibrotic bowel stricture: MRI diffusion-weighted imaging in Crohn's disease. *Radiol. Infect. Dis.* **2015**, *2*, 128–133.
57. Morani, A.C.; Smith, E.A.; Ganeshan, D.; Dillman, J.R. Diffusion-Weighted MRI in Pediatric Inflammatory Bowel Disease. *Am. J. Roentgenol.* **2015**, *204*, 1269–1277.

58. Geboes, K. Histopathology of Crohn's Disease and Ulcerative Colitis. In *Inflammatory Bowel Diseases*; Satsangi, J.S.L., Ed.; Churchill-Livingstone Elsevier: Edinburgh, Scotland; London, UK; Melbourne, Australia, 2003; Volume 18, pp. 255–276.
59. Feakins, R.M. Inflammatory bowel disease biopsies: Updated British Society of Gastroenterology reporting guidelines. *J. Clin. Pathol.* **2013**, *66*, 1005–1026.
60. Magro, F.; Langner, C.; Driessen, A.; Ensari, A.; Geboes, K.; Mantzaris, G.J.; Villanacci, V.; Becheanu, G.; Nunes, P.B.; Cathomas, G.; et al. European consensus on the histopathology of inflammatory bowel disease. *J. Crohn's Colitis* **2013**, *7*, 827–851.
61. Roger, M.; Feakins, N.A.S. An update on the pathology of chronic inflammatory bowel disease. In *Recent Advances in Histopathology 23*; Massimo Pignatelli, P.G., Ed.; JP Medical Ltd.: London, UK, 2014; pp. 117–134, ISBN 9781907816857.
62. Robert Riddell, D.J. *Gastrointestinal Pathology and its Clinical Implications*, 2nd ed.; Lippincott Williams & Wilkins, Ed.; Wolters Kluwer: Philadelphia, PA, USA, 2014; Volume II, ISBN 9780781722162.
63. Li, X.A.; Zhou, Y.; Zhou, S.X.; Liu, H.R.; Xu, J.M.; Gao, L.; Yu, X.J.; Li, X.H. Histopathology of melanosis coli and determination of its associated genes by comparative analysis of expression microarrays. *Mol. Med. Rep.* **2015**, *12*, 5807–5815.
64. Lambert, J.R.; Luk, S.C.; Pritzker, K.P. Brown bowel syndrome in Crohn' disease. *Arch. Pathol. Lab. Med.* **1980**, *104*, 201–205.
65. Liu, Z.H.; Fooo, D.C.C.; Law, W.L.; Chan, F.S.Y.; Fan, J.K.M.; Peng, J.S. Melanosis coli: Harmless pigmentation? A case-control retrospective study of 657 cases. *PLoS ONE* **2017**, *12*, e0186668.
66. González Ballester, M.Á.; Zisserman, A.P.; Brady, M. Estimation of the partial volume effect in MRI. *Med. Image Anal.* **2002**, *6*, 389–405.
67. Scherrer, B.; Gholipour, A.; Warfield, S.K. Super-Resolution in Diffusion-Weighted Imaging Benoit. *Med. Image Comput. Comput. Assist. Interv.* **2011**, *14*, 124–132.
68. Choi, S.H.; Kim, K.W.; Lee, J.Y.; Kim, K.J.; Park, S.H. Diffusion-weighted Magnetic Resonance Enterography for Evaluating Bowel Inflammation in Crohn's Disease: A Systematic Review and Meta-analysis. *Inflamm. Bowel Dis.* **2016**, *22*, 669–679.
69. Aggarwal, R.; Ranganathan, P. Common pitfalls in statistical analysis: The use of correlation techniques. *Perspect. Clin. Res.* **2016**, *7*, 187–190.
70. Apine, I.; Pirksta, I.; Pitura, R.; Pokrotnieks, J.; Puíte, I.; Krûmiòa, G. Repeatability of Magnetic Resonance Measurements Used for Estimating Crohn's Disease Activity. *Proc. Latv. Acad. Sci. Sect. B. Nat. Exact Appl. Sci.* **2020**, *74*, 75–82.

Publication III

sciendo

PROCEEDINGS OF THE LATVIAN ACADEMY OF SCIENCES. Section B, Vol. 74 (2020), No. 2 (725), pp. 75–82.

DOI: 10.2478/prolas-2020-0012

REPEATABILITY OF MAGNETIC RESONANCE MEASUREMENTS USED FOR ESTIMATING CROHN'S DISEASE ACTIVITY

Ilze Apine[1,#], Ieva Pirksta[2], Reinis Pitura[3], Juris Pokrotnieks[4], Ieva Puķīte[1], and Gaida Krūmiņa[3]

[1] Children Clinical University Hospital, 45 Vienības Av., Riga, LV-1004, LATVIA

[2] Riga Stradiņš University, 16 Dzirciema Str., Riga, LV-1007, LATVIA

[3] Department of Radiology, Riga Stradiņš University, Dzirciema iela 16, Riga, LV-1007, LATVIA

[4] Department of Internal Diseases, Riga Stradiņš University, 16 Dzirciema Str., Riga, LV-1007, LATVIA

[#] Corresponding author, dr.ilze.apine@gmail.com

Communicated by Ilze Konrāde

The MR activity indices used for quantification and follow-up of Crohn's disease are composed of a number of subjectively determinable components with equivocal repeatability. The purpose of this article was to assess the repeatability of measurements used for quantitative estimation of Crohn's disease activity in the terminal ileum. In five adults (23–57 y.o.) and 12 children (10–17 y.o.) with active terminal ileitis, the inflamed bowel was divided into 3 cm segments (n = 32 in adults, n = 46 in children), and measurements for the calculation of MaRIA and Clermont scores were performed. Parameters included apparent diffusion coefficients (ADC) for diffusion-weighted imaging (DWI) sequences with selective and non-selective fat suppression, wall signal enhancement before (WSI-preGd) and after (WSI-preGd) gadolinium enhancement, bowel thickness, and presence of ulcers. The measurements were standardised (accurate site-to-site comparison, exact ROI size, where applicable) and repeated by the same researcher after two months. Intra-observer agreement for ADC, WSI-preGd and WSI-postGd, bowel thickness was assessed with a paired t-test, and the significant difference in presence/absence of ulcers was assessed by the Pearson ^{2} test. Absolute difference was not found between the 1st and 2nd measurements of ADC, WSI-preGd, WSI-postGd and wall thickness. There was systematic difference in the presence of bowel ulcers. In standardised conditions the repeatability of ADC, WSI-preGd and WSI-postGd is high. Efforts must be made to precisely define the size and appearance of ulcers that may be included in the index calculation.

Key words: *Terminal ileitis, magnetic resonance enterography, Clermont score, MaRIA, activity indices, intra-observer agreement.*

INTRODUCTION

Crohn's disease (CD) is a chronic relapsing inflammatory bowel disease affecting any part of the gastrointestinal tract, but most commonly, the terminal ileum (Horsthuis *et al.*, 2008). The overall goal of CD treatment is to achieve and maintain remission. Therefore, monitoring disease activity is crucial during the course of the disease. Ileocolonoscopy with histopathological sampling is the method of choice in assessment of IBD. However, apart from causing general patient discomfort (Buisson *et al.*, 2017), visualisation rendered by endoscopy is limited to the terminal ileum and colon, and only superficial tissues from the luminal side can be viewed and sampled (Van Rheenen *et al.*, 2010). Wireless capsule endoscopy allows an advance beyond the reach of a conventional endoscope by visualising intestinal mucosa throughout its entire length in case of a non-stricturing disease (Triester *et al.*, 2006). Nevertheless, this modality, like conventional endoscopy, does not allow assessment of bowel wall tissue beyond mucosa. Therefore, cross-sectional imaging is the only solution to assess the bowel wall throughout its entire thickness.

When considering the superior soft-tissue resolution, non-invasiveness and ability to obtain findings within entire bowel wall thickness and around the bowel, and lack of ion-

ising radiation, magnetic resonance enterography (MRE) has been shown to be an informative imaging modality, capable of evaluating disease activity in IBD (Foti *et al*., 2015). Numerous attempts have been made to develop scoring systems for less invasive but informative quantification of disease activity in the intestines. Examples of these scoring systems include: Magnetic Resonance Index of Activity (MaRIA), Clermont score, Crohn's disease MRI index (CDMI), Magnetic Resonance Enterography Global Score (MEGS), Lemann index (Rozendorn *et al*., 2018), as well as London index (Steward *et al.,* 2012). Presently, the MaRIA score is the only validated radiological CD activity index tested in large patient populations (Dohan *et al.,* 2016), which has high and significant correlation with the Chron's Disease Endoscopic Activity Index. The MaRIA score is composed of values of intestinal wall thickness and relative contrast enhancement (RCE), as well as rating of presence of oedema and ulcers in the bowel wall. RCE is calculated from wall signal intensity (WSI) series before (WSI-preGd) and after (WSI-postGd) administration of gadolinium contrast agent (Rimola *et al*., 2009). However, gadolinium administration is related to potentially severe adverse reactions like systemic nephrogenic fibrosis (Broome *et al.,* 2008) and accumulation of gadolinium deposits in the brain (Gulani *et al*., 2017) and other body tissues (Quattrocchi *et al.,* 2017). The Clermont score, an alternative MRI index of activity, has been developed on the basis of diffusion weighted imaging (DWI) by replacing RCE with the apparent diffusion coefficient (ADC), which is a numerical measurement of diffusion restriction and is calculated from DWI images (Hordonneau *et al*., 2014). The Clermont score is, therefore, also called DWI-MaRIA. It is reported to have an excellent correlation with the MaRIA score (Rimola *et al*., 2009) and a moderate correlation with CDEIS (Buisson *et al.,* 2017), but further confirmatory studies are needed to validate the Clermont score.

There is equivocal data available on the repeatability of measurements used for calculation of MaRIA and Clermont scores. No standardised technique of performing measurements and assessment of ulcers is described in most of the available publications, possibly influencing repeatability. The goal of our study was therefore to assess intra-observer agreement on measurements performed for calculation of MaRIA and Clermont scores. Measurements such as ADC-DWI, wall signal intensity (WSI) before (WSI-preGd) and after (WSI-postGd) administration of gadolinium contrast medium contributing in relative contrast enhancement (RCE), were performed to define the proper size of region of interest (ROI) and to provide accurate site-to-site comparison. Intra-observer variability of the wall thickness and detection of presence of ulcers was also analysed.

MATERIALS AND METHODS

This prospective observational cross-sectional study was conducted in accordance with the Declaration of Helsinki. Before inclusion in the study, written informed consent was received from all patients or their legal representatives. Approval (permission number 6/10.09.2015) was obtained from the Ethics Committee of Rīga Stradiņš University.

Table 1. Demographic data of patients included in the study

Data	Adult group	Paediatric group
Gender	Males, n = 4; females, n = 1	Males; n = 9, females; n = 3
Age	23 y.o.; n = 1, 25 y.o.; n = 1, 36 y.o.; n = 1, 40 y.o.; n = 1, 57 y.o.; n = 1	11 y.o.; n = 2, 12 y.o.; n = 3, 13 y.o.; n = 1, 14 y.o.; n= 4, 17 y.o.; n = 2

Patients. The study involved 17 patients (five adults, 23–57 y.o., and 12 children, 10–17 y.o.; see Table 1 for details) with faecal calprotectin levels over 1000 μg/mg and histologically proven active Crohn's non-stricturising and non-penetrating disease in the terminal ileum, and signs of active Crohn's disease in MRE examination. These signs included: 1) small bowel wall thickness > 3 mm, 2) presence of mural oedema — hyperintensity of the bowel wall in T2-weighted images compared to that in the psoas muscle (Rimola *et al.,* 2009), 3) signs of active inflammation in conventional DWI sequence — high SI in DWI tracking images of b = 800 s/mm^2, 4) low signal intensity (SI) in the ADC map, and 5) early mucosal hyperenhancement in the series following administration of gadolinium contrast agent (post-Gd) (Moy *et al.,* 2016). CD located outside the terminal ileum, areas of bowel thickness less than 3 mm, lack of signs of active bowel wall inflammation in DWI, DWIBS and post-Gd T1 series within one and the same segments, and dynamic blurring in either of the DWI or T1 post-Gd images were not accepted for performing measurements.

According to the Montreal and Paris classification of CD (Moon, 2019), the phenotype of 10 patients was A1 L1 B1; the phenotype of the remaining seven patients was A2 L1 B1.

MRI technique. All patients were examined without prior bowel cleansing. Fasting was required six hours prior to MRE procedures. Patients were asked to slowly intake 1.000–1.500 ml of 2.5% peroral mannitol solution 45 minutes prior to the MRI procedure, and then to lie in the right decubitus position, drinking extra 250 ml of 2.5% mannitol solution for another 20 minutes. The MRE examinations were performed with a 1.5T MRI scanner (Ingenia, Philips Medical Systems, Best, the Netherlands) covering the region from the diaphragm to the pelvis with a 16-channel body coil. All patients were scanned in the prone position.

The MRE protocol included:

1) coronal breath-hold balanced turbo field echo (bTFE) cine sequence for real-time assessment of the bowel peristalsis,

2) axial and coronal breath-hold Turbo Spin Echo, T2-weighted sequences without fat suppression (T2 TSE),

3) axial and coronal breath-hold Spectral Attenuated Inversion Recovery T2-weighted sequences with fat suppression (T2 SPAIR),

4) axial respiratory triggered Spectral Presaturation Inversion Recovery (SPIR) based DWI sequence using diffusion factors b fixed at 0, 600 and 800 s/mm^2 with the corresponding ADC map,

5) axial free-breathing Short Tau Inversion Recovery (STIR)-based DWI sequence using diffusion factors b fixed at 0, 600 and 800 s/mm^2 with the corresponding ADC map,

6) coronal respiratory triggered T2 fat suppression magnetic resonance cholangiopancreatography (MRCP) sequence with radial 3D reconstructions,

7) coronal breath-hold dynamic T1-weighted High-Resolution Isotropic Volume (THRIVE), where scanning was started simultaneously with intravenous administration of gadolinium contrast media. Gadodiamide (Omniscan) 0.05 mmol/ml, GE Healthcare, dosage 0.2 ml/kg, or 0.1 mmol/kg was used in patients before October 2018, except in two children examined after October 2018, who received gadobutrol (Gadovist) 1 mmol/ml, Bayer, dosage 0.1 ml/kg, or 0.1 mmol/kg.

To stop intestinal peristalsis, hyoscine butylbromide (Buscopan, Sanofi) was administered in slow intravenous injection prior to SPIR-DWI and STIR-based DWI sequences as well as the dynamic contrast sequences. A dosage of 10 mg was used in patients under 50 kg, increased to 20 mg in patients of 50 kg or above, and the dose was diluted in 20 ml of saline solution.

MRI image analysis. The measurements were performed by one radiologist with 19 years of experience in gastrointestinal MRI imaging, and repeated by the same radiologist after two months.

The measurement approach was standardised. Prior to measurements, the whole parts of the inflamed terminal ileum were divided into approximately 3 cm long segments (n = 32 in adult patients, n = 46 in children), and the below process was performed when taking measurements in each of the segments: 1) one measurement of bowel wall thickness was performed in the location of the largest thickness; 2) presence/absence of ulcers was defined (1 – yes, 0 – no); 3) three measurements of ADC of the SPIR-based DWI (Fig. 1a), and ADC of the STIR-based DWI (Fig. 2a) were performed at the site of the maximum signal intensity (SI) within the inflamed bowel wall. The ADC value along with the chosen region of interest (ROI) was automatically propagated on the corresponding ADC map (Figure 1b for STIR- based DWI and 2.b for STIR-based DWI); 4) three measurements of wall signal intensity (WSI) were taken before (WSI-preGD) and after (WSI-postGd) administration of gadolinium contrast medium in exactly the same locations of the highest SI in the bowel wall in both DWI sequences, 5) three measurements of the image noise — standard deviation (SD) were performed outside the patient's body before (SD-preGd) and after (SD-postGd) administration of the contrast medium (Rimola *et al.*, 2009). The ADC, WSI and SD measurements were performed using the

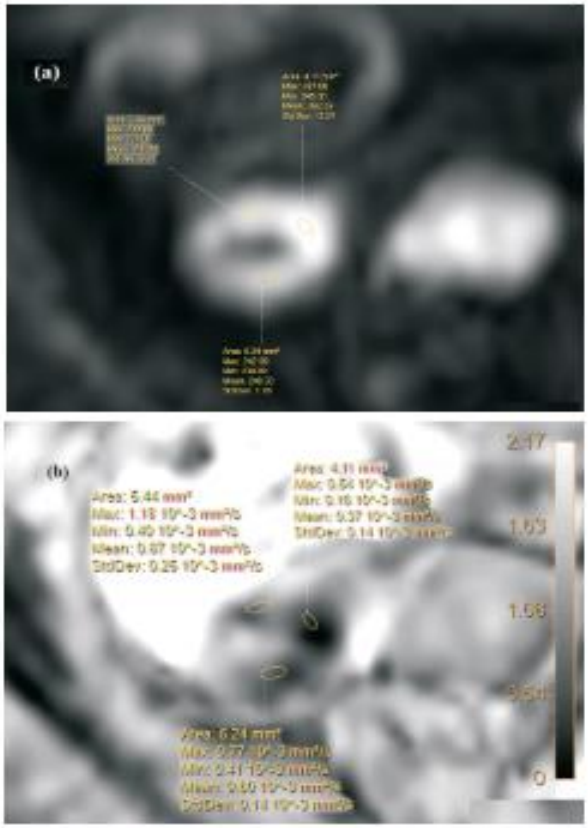

Fig. 1. Selecting the ROI in SPIR-based DWI images (b = 800 s/mm2) of 56 y.o. female (a). On the corresponding ADC map (b), the chosen ROI appears automatically.

4–9 mm^2 oval region of interest (ROI). The average values of the three measurements of ADC, WSI and SD were used for further calculations.

In each inflamed segment, the segmental MaRIA score was calculated per equation:

1.5 × bowel thickness(mm) + 0.02 × RCE + 5 × oedema + 10 × ulceration.

The presence of ulcers was rated as 1 and absence of ulcers – as 0. RCE was calculated as: RCE = (WSI-postGd – WSI-preGd)/(WSI-preGd)) × 100 × (SD-preGd/SD-postGd), where the SD-preGd and SD-postGd corresponded to the mean of the three SD values of the SI. This was measured outside of the body before and after administration of gadolinium contrast medium, accordingly (Rimola *et al.*, 2009). Since oedema was a criterion of inclusion in the study, it was present in all patients and was always equal to 1.

The Clermont score, or DWI-MaRIA, for both SPIR- and STIR-based DWI sequences, was calculated as:

DWI-MaRIA = 1.646 × bowel thickness - 1.321 × ADC + 5.613 × oedema + 8.306 × ulceration + 5.039 (Hordonneau *et al.*, 2014).

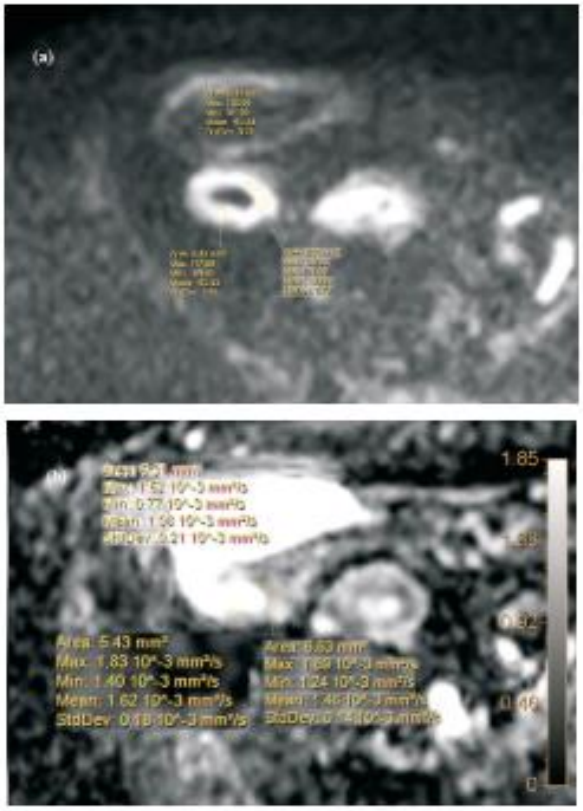

Fig. 2. Selecting the ROI in STIR-based DWI images of 56 y.o. female (b = 800 s/mm2) (a). On the corresponding ADC map (b), the chosen ROI appears automatically.

Similar to the calculation of the MaRIA score, presence of ulcers was rated as 1, absence of ulcers as 0, and presence of oedema was rated as 1.

The assessment of images and measurements of ADC values was performed using a dedicated post-processing server Philips Intellispace Portal 5.0 (Philips Medical Systems, Best, The Netherlands). WSI and image noise measurements were performed using a Clear Canvas DICOM Viewer, v. 13.2 (Synaptive Medical, Toronto, Canada, 2019).

Statistical analysis. Statistical analysis was performed using software Stata/IC (StataCorp LLC, Texas, USA). The mean values and standard deviations were calculated for SPIR- and STIR-based ADC, as well as RCE, MaRIA and Clermont scores. The mean values of the first and second measurement were compared, and statistical significance of the differences was tested using a paired t-test; 95% confidence intervals (CI) were calculated for differences. The statistical significance of differences was determined using one-way ANOVA with Bonferroni correction. A p value of < 0.05 was considered as statistically significant. Differences in the presence/absence of ulcers was evaluated with the Pearson's χ^2 test.

RESULTS

No statistically significant difference was observed between the two measurements performed by a single observer neither in the measurement of the bowel wall thickness ($p = 0.42$), nor in the assessment of ADC values of SPIR-based DWI ($p = 0.65$) and ADC values of STIR-based DWI ($p = 0.23$). There was also no statistically significant difference between the two measurements performed by a single observer in assessment of WSI-preGd ($p = 0.06$) or WSI post-Gd ($p = 0.57$). The highest absolute difference between two measurements was observed for WSI-preGd measurements (8%), and the lowest absolute difference for SPIR-based ADC measurements (1%). The results of measurements, along with absolute differences between the two measurements, are presented in the Table 2.

For the assessment of presence of bowel ulcers between the 1st and the 2nd assessment, the Pearson χ^2 was 13.70 ($p < 0.0005$), indicating a systemic difference between the two assessments for presence of ulcers. The results of the assessment of presence/absence of ulcers are presented in Table 3.

DISCUSSION

The therapeutic endpoint of CD treatment is to achieve and maintain remission. Therefore, assessment of disease activity is crucial for guiding therapeutic decisions in treatment of patients with CD. Apart from the resolution of symptoms as the primary target (Shi *et al*., 2018), different grades of activity such as clinical, biochemical and histopathological activity, are considered. The concept of mucosal healing has been under discussion for decades (Rogler *et al*., 2013) being associated with lower demand for steroids, reduced admissions to hospital, and reduced need for surgical treatment in case of complicated CD (D'Haens *et al*., 2008).

Table 2. Numerical values of the 1st and 2nd measurements of the bowel wall thickness SPIR- and STIR-based ADC, WSI-preGd, and WSI-postGd

Measurement	First assessment (mean)	Second assessment (mean)	Difference	
			Difference (%)	p
Wall thickness (mm)	6.4	6.6	0.2 (5%)	0.42
ADC of SPIR-based DWI (mm^2/s)	1.219 (SD 0.320)	1.227 (SD 0.321)	0.008 (1%)	0.65
ADC of STIR-based (mm^2/s)	1.180 (SD 0.505)	1.132 (SD 0.478)	0.048 (4%)	0.23
WSI-preGd	162.925 (SD 127.57)	150.305 (SD 99.68)	12.61 (8%)	0.06
WSI-post Gd	336.39 (SD 235.35)	316.11 (SD 212.90)	20.33 (6%)	0.57

ADC, apparent diffusion coefficients; WSI, wall signal intensity

Table 3. Evaluation of 1st and 2nd measurements of the presence/absence of ulcers

Evaluation	Ulceration	No. of segments	%	Pearson χ^2	*p*-value
First	Absence	43	55.13	13.70	< 0.0005
	Presence	35	44.87		
Second	Absence	26	33.33		
	Presence	52	66.67		

Mucosal healing has been accepted as an optimal therapeutic target in clinical practice for many years; however, in patients with sustained mucosal healing, transmural inflammation may persist (Nardone *et al*., 2019). Transmural healing is associated with better long-term outcomes than mucosal healing, therefore transmural healing has recently been proposed as a new target for CD treatment (Castiglione *et al*., 2019). Since endoscopy does not provide transmural evaluation even in the accessible regions of the gastrointestinal tract, cross-sectional imaging studies (MR) have become the mainstay of intestinal wall evaluation (Buisson *et al*., 2019). Both mucosal and transmural healing can be assessed with MRI (Panes *et al*., 2013; Maaser *et al*., 2019), and according to the newest joint guidelines by European Crohn's and Colitis Organisation (ECCO) and the European Society of Gastrointestinal and Abdominal Radiologists (ESGAR), MRI can be used as alternative for assessment of disease activity (Maaser *et al*., 2019).

Calculations of MaRIA and Clermont indices include several variables that are common to both indices, such as the presence of ulcers and bowel wall oedema, and the thickness of the gut wall. In the Clermont index, also called as DWI-MaRIA, gadolinium contrast medium administration is replaced by DWI (Rimola *et al*., 2009; Hordonneau *et al*., 2014). Since 2009, this has been proven to be effective for assessment of bowel inflammation. It has potential benefits in the assessment of disease activity (Dohan *et al*., 2016) and is used to replace contrast medium (Neubauer *et al*., 2013). DWI reflects both anatomical and functional information, providing data on diffusion restriction in the intestinal wall that characterises an active inflammation (Dohan *et al*., 2016), and is proven to be capable of detecting lesions before their appearance in conventional images (Baliyan *et al*., 2016). The DWI technique is however very sophisticated, since it requires ideal magnetic field homogeneity, very strong gradients and infinitively fast acquisition that is not achievable with existing MRI machines. The quality of DWI images is therefore lesser than that of conventional MR images, due to low resolution, noise, distortions, and limited morphological interpretability (Chilla *et al*., 2015); therefore, DWI provides functional rather than anatomical information. Opinions on reproducibility of ADC-DWI measurements used in the Clermont score varies among authors, and despite good to excellent repeatability reported from certain authors (Yu *et al*., 2019), contrary concerns on low reproducibility based on research data also exist (Watson *et al*., 2018). Due to equivocal data on repeatability of measurements the form the MaRIA and Clermont score, our interest was to assess the repeatability of measurements contributing to both of these indices — WSI-preGd and WSI-postGD forming RCE in MaRIA, ADC-DWI used in the Clermont score, as well as bowel thickness and estimation of presence of bowel ulcers, which are common to both MaRIA and Clermont scores.

There are numerous DWI techniques, all of which are based on fat suppression, which is necessary for artefact reduction (Takahara *et al*., 2004). These techniques can be classified into fat, or spectral, selective and non-selective ones, based on different behaviour among lipid protons and hydrogen protons from water during MR imaging. In selective fat suppression, protons of proper resonance frequency of fat are suppressed, whereas in non-selective fat suppression the difference in T1 between protons in water and fat tissue is used to suppress the fat signal with inversion-recovery technique (Delfaut *et al*., 1999). In our institution, apart from selective SPIR-based DWI, a non-selective STIR-based fat suppression technique was evaluated in the study due to better image quality (Ouyang *et al*., 2014), i.e. visually sharper images and more clearly differentiated contours of structures (Fig. 3), and superiority of ADC measurements over DWI with selective fat suppression in assessment of other tissues, such as breast lesions (Stadlbauer *et al*., 2009). This technique could theoretically improve the accuracy of the assessment of disease activity in the intestinal wall. In our study, intra-observer reproducibility of both SPIR- and

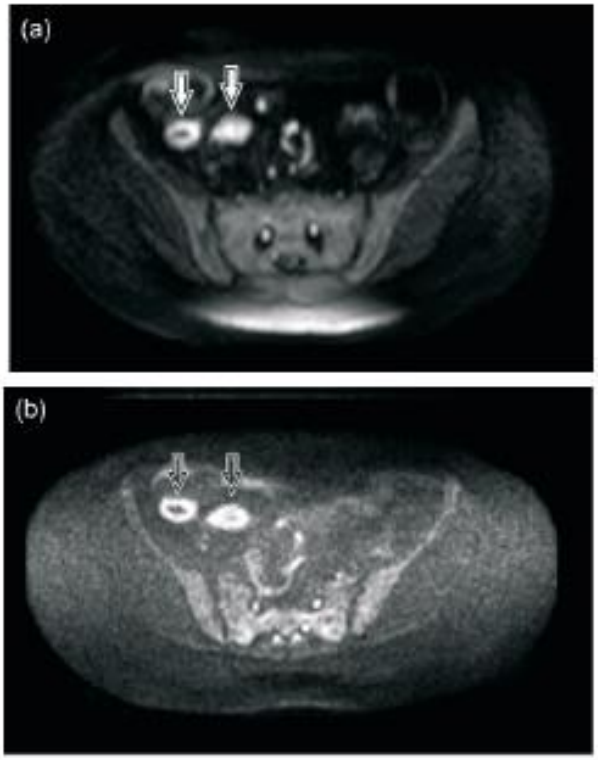

Fig. 3. DWI (a) and DWIBS (b) images of high diffusion gradient b value = 800 mm^2/s in a 56-year-old female patient with active Crohn's disease. Inflamed bowel walls present high signal intensity. The resolution of inflamed bowel and delineation of contours is better in the STIR-based DWI image (black arrows) than in the DWI image (white arrows).

STIR-based DWI techniques was good, since no statistically significant difference was found between mean values in both ADC of SPIR-based DWI ($p = 0.65$), as well as ADC of STIR-based DWI ($p = 0.23$), and difference between mean values of ADC was only 1% in SPIR-based DWI and 4% in STIR-based DWI (Table 1). However, unlike breast tissue, ADC measurements of STIR-based DWI quantitative may not be of practical importance in assessment of bowel walls, due to non-selectivity of fat suppression; not only signals from fat, but other media of short T1 time, such as proteinaceous, viscous and mucous substances, methaemoglobin products (Grande *et al*., 2014), as well as chime and faeces (Kwee *et al*., 2008) are suppressed. Since DWI has a strong partial volume effect (Scherrer *et al*., 2011), the measured ADC values in STIR-based images could be artificially lower in the presence of these substances (Apine *et al*., 2019).

Several authors found poor repeatability of RCE measurements (Sharman *et al*., 2009; Tielbeek *et al*., 2013). We found no statistically significant difference in WSI-preGd ($p = 0.06$), or in WSI post-Gd ($p = 0.57$) values used in calculating of RCE. We believe that a strict definition of ROI size and accurate site-by-site WSI-preGd and post-Gd measurement in one and the same bowel segment, would result in good inter-observer agreement. It has however to be noted that our results show high standard deviations in both WSI-preGD (SD 127.57 for the 1st assessment and SD 99.68 for the 2nd assessment) and WSI-post-Gd measurements (SD 235.35 for the 1st assessment and SD 212.9 for the 2nd assessment) covering 66–78% of the WSI values. Our observations suggest that, if WSI-preGd values were in the tens, the WSI-post Gd values would also be in the tens; if WSI-preGd values were in the hundreds, this would also be replicated in the WSI-post Gd values. We explain this observation through individual tissue characteristics of patients, magnetic field inhomogeneity and linearity of gradients yielding wide distribution of WSI values. Detailed analysis of this finding, however, is beyond the scope of our current research.

Tielbeek *et al.* (2013) reported moderate repeatability of bowel thickness measurements and excellent repeatability when the thickness measurements were performed by an experienced radiologist. In our study, no statistically significant difference was found between the 1st and the 2nd measurements. It should, however, be noted that wall thickness differed within one and the same bowel segment, and the maximum thickness was always chosen for the calculations. However, identifying the same exact location of the maximum thickness often was not possible in DWI images due to their low spatial resolution. Similarly, in the pre- and post-contrast series, bowel thickness was always measured in the axial images but pre- and post-T1 images were acquired in the coronal plane.

In our study, there was a systematic difference in the assessment of ulcers. The inconsistency of ulcer detection in our study could be associated with lack of strict consensus regarding standardised MR definition of an ulcer. Developers of the MaRIA index defined ulcers as deep depressions in the mucosal surface (Rimola *et al*., 2009). However, MRI reveals a wide range of ulcers. Even small aphthous ulcers can be seen in MRI images (Ram *et al*., 2016), and there is no clear definition of the size and appearance of ulcers that should be included in calculation of disease activity indices or excluded from it. Intra-observer agreement of the ulcer rating could be improved with a 3T MR scanner, as this provides better spatial and temporal resolution, and literature data indicates that the resolution of 3T MR in ulcer diagnosis is superior compared to that of the 1.5T device (Fiorino *et al*., 2013).

Due to lack of data, histopathological findings were not used as the reference standard in our study. The patients were enrolled in the study only by visual MRE signs of Crohn's disease, i.e. thickened, oedematous bowel wall and significantly increased SI in the DWI images with diffusion gradient value of b = 800 s/mm^2, and low SI on the ADC map. However, the aim of our study was not to investigate the relationship of visual findings with histological findings, but rather whether repeated measurements, based on certain defined MRE criteria for the evaluation of Crohn's disease activity, produced comparable results. Literature provides a broad picture of the correlation not only between MRE and endoscopic findings, but also between MRE and surgical specimens of resected intestinal segments, with certain defined criteria, along with conclusion that MRI is an informative and sufficiently accurate method to assess altered bowel wall. Based on these observations, for several years now when referring patients for MRE examinations, clinicians do not duplicate its results with invasive endoscopy, which is cumbersome for patients. Consequently, in 2019, for the first time, the ECCO-ESGAR guidelines (Maaser *et al*., 2019) came up with a revolutionary statement that radiological cross-sectional imaging methods, including MR, can be used as an alternative to endoscopy to assess Crohn's disease activity. Therefore, although all patients in our study had endoscopically confirmed Crohn's disease, the results of the MRE examination were not duplicated by the endoscopic findings in any cases. Consequently, the correlation of the MR activity indices with the histopathological and endoscopic activity indices was not possible. It should also be noted that the correlation of the MR findings with the endoscopic image is still relative. The endoscopical and histopathological findings, including endoscopically obtained tissue specimens, reflect changes in the intestinal mucosa, whereas the MR activity indices include not only mucosal but also transmural components. Both literature data and the experience from our hospital indicate situations when intact intestinal mucosa is observed endoscopically in active Crohn's disease. The correlation of histopathological-radiological findings could be most accurately reflected in the resection specimen after bowel surgery. Resection of the altered intestinal segment was performed only in one of the patients enrolled in our study.

There may be a methodological error in using correlation between MaRIA and Clermont score, since these indices

mostly contain the same components, except that RCE is used in MaRIA and ADC value in Clermont score, leading to overestimation of actual correlation. However, the goal of this study was to assess the repeatability of all necessary measurements without analysing the shortcomings of methodology of assessment of their correlation. A wider discussion on the application of the correlation coefficient, with references to literature sources, will be discussed in another publication currently awaiting approval.

In our opinion, the strengths of our study were: 1) the prospective study design, 2) exact site-by-site comparison in the same bowel segment, and 3) exact ROI size that was not defined in studies on MaRIA and Clermont scores. The limitations of our research were as follows: 1) the relatively low number of participants in the study groups, 2) the study group included both adults and paediatric patients causing lack of homogeneity regarding the length of the disease or treatment status. However, a mixed data poll of adult and paediatric patients was chosen because the methodology of all measurements (bowel wall thickness, WSI-preGd, WSI-postGd, ADC of SPIR-based DWI, ADC of STIR-based DWI and estimation of ulcers) was identical for both adults and children. Therefore, the estimations of intra- observer agreement were not influenced by the age of patients. Unlike adults, estimation of disease activity in children does not rely on endoscopy findings due to its invasiveness, but rather on the Paediatric Crohn's Disease Activity Index (PCDAI) (Rozendorn *et al*., 2018). In children, the utility of MaRIA and Clermont score is still unclear, and accordingly, the relationship of RCE and DWI-based ADC with actual Crohn's disease activity is unclear.

CONCLUSIONS

The reproducibility of ADC-DWI, WSI-preGd and WSI-post Gd measurements used in calculation of MRE-based indices for quantification of Crohn's disease inflammation is high when standardised conditions, such as proper ROI size and exact site-to site comparison are clearly defined and observed. Effort still needs to be made in defining the size and appearance of ulcers that should either be included in the calculation of Crohn's disease activity indexes, or excluded from it.

ACKNOWLEDGEMENTS

The authors gratefully acknowledge the generosity of Dr. med. Irēna Rogovska for support in processing of statistical data and for constructive criticism in writing this article.

REFERENCES

Apine, I., Baduna, M., Pitura, R., Pokrotnieks, J., Krumina, G. (2019). The influence of bowel preparation on ADC measurements: Comparison between conventional DWI and DWIBS sequences. *Medicina*, **55** (7), 394.

Baliyan, V., Das, C. J., Sharma, R., Gupta, A. K. (2016). Diffusion weighted imaging: Technique and applications. *World J. Radiol.*, **8** (9), 785–798.

Broome, D. R. (2008). Nephrogenic systemic fibrosis associated with gadolinium-based contrast agents: A summary of the medical literature reporting. *Eur. J. Radiol.*, **66** (2), 230–234.

Buisson, A., Gonzalez, F., Poullenot, F., Nancey, S., Sollellis, E., Fumery, M., Pariente, B., Flamant, M., Trang-Poisson, C., Bonnaud, G. *et al.* (2017). Comparative acceptability and perceived clinical utility of monitoring tools: A nationwide survey of patients with inflammatory bowel disease. *Inflamm. Bowel Dis.*, **23** (8), 1425–1433.

Buisson, A., Pereira, B., Goutte, M., Reymond, M., Allimant, C., Obritin-Guilhen, H., Bommelaer, G., Hordonneau, C. (2017). Magnetic resonance index of activity (MaRIA) and Clermont score are highly and equally effective MRI indices in detecting mucosal healing in Crohn's disease. *Digest. Liver Dis.*, **49** (11), 1211–1217.

Buisson, A., Hordonneau, C., Goutorbe, F., Allimant, C., Goutte, M., Reymond, M., Pereira, B., Bommelaer, G. (2019). Bowel wall healing assessed using magnetic resonance imaging predicts sustained clinical remission and decreased risk of surgery in Crohn's disease. *J. Gastroenterol.*, **54** (4), 312–320.

Castiglione, F., Imperatore, N., Testa, A., De Palma, G. D., Nardone, O. M., Pellegrini, L., Caporaso, N., Rispo, A. (2019). One-year clinical outcomes with biologics in Crohn's disease: Transmural healing compared with mucosal or no healing. *Alimentary Pharmacol. Ther.*, **49** (8),1026–1039.

Chilla, G. S., Tan, C. H., Xu, C., Poh, C. L. (2015). Diffusion weighted magnetic resonance imaging and its recent trend-a survey. *Quantitative Imaging in Medicine and Surgery*, 5 (3), 407–422.

D'Haens, G., Baert, F., van Assche, G., Caenepeel, P., Vergauwe, P., Tuynman, H., De Vos, M., van Deventer, S., Stitt, L., Donner, A. *et al.* (2008). Early combined immunosuppression or conventional management in patients with newly diagnosed Crohn's disease: An open randomised trial. *The Lancet*, **371**, 660–667.

Del Grande, F., Santini, F., Herzka, D. A., Aro, M. R., Dean, C. W., Gold, G. E., John, A. (2014). Fat-suppression techniques for 3-T MR imaging of the musculoskeletal system. *Radiographics*, **34** (1), 217–233.

Delfaut, E. M., Beltran, J., Johnson, G., Rousseau, J., Marchandise, X., Cotten, A. (1999). Fat suppression in MR imaging: Techniques and pitfalls. *Radiographics*, **19** (2), 373–382.

Dohan, A., Taylor, S., Hoeffel, C., Barret, M., Allez, M., Dautry, R., Zappa, M., Savoye-Collet, C., Dray, X., Boudiaf, M., Reinhold, C., Soyer, P. (2016). Diffusion-weighted MRI in Crohn's disease: Current status and recommendations. *J. Magn. Reson. Imag.*, **44** (6), 1381–1396.

Fiorino, G., Bonifacio, C., Padrenostro, M., Sposta, F.M., Spinelli, A., Malesci, A., Balzarini, L., Peyrin-Biroulet, L., Danese, S. (2013). Comparison between 1.5 and 3.0 Tesla Magnetic Resonance Enterography for the assessment of disease activity and complications in ileo-colonic Crohn's disease. *Digest. Dis. Sci.*, **58** (11), 3246–3255.

Foti, P. V., Farina, R., Coronella, M., Palmucci, S., Ognibene, N., Milone, P., Conti Bellocchi, C., Samperi, L., Inserra, G., Laghi, A., Ettorre, G. C. (2015). Crohn's disease of the small bowel: evaluation of ileal inflammation by diffusion-weighted MR imaging and correlation with the Harvey-Bradshaw index. *Radiol. Med.*, **120** (7), 585–594.

Gulani, V., Calamante, F., Shellock, F. G., Kanal, E., Reeder, S. B. (2017). Gadolinium deposition in the brain: Summary of evidence and recommendations. *The Lancet Neurol.*, **16** (7), 564–570.

Hordonneau, C., Buisson, A., Scanzi, J., Goutorbe, F., Pereira, B., Borderon, C., Da Ines, D., Montoriol, P. F., Garcier, J. M., Boyer, L., Bommelaer, G. Petitcolin, V. (2014). Diffusion-weighted magnetic resonance imaging in ileocolonic Crohn's disease: Validation of quantitative index of activity. *Amer. J. Gastroenterol.*, **109** (1), 89–98.

Horsthuis, K., Stokkers, P. C., Stoker, J. (2008). Detection of inflammatory bowel disease: Diagnostic performance of cross-sectional imaging modalities. *Abdom. Imaging*, **33** (4), 407–416.

Kwee, T. C., Takahara, T., Ochiai, R., Nievelstein, R. A. J., Luijten, P. R. (2008). Diffusion-weighted whole-body imaging with background body signal suppression (DWIBS): Features and potential applications in oncology. *Eur. Radiol.*, **18** (9), 1937–1952.

Maaser, C., Sturm, A., Vavricka, S. R., Kucharzik, T., Fiorino, G., Annese, V., Calabrese, E., Baumgart, D. C., Bettenworth, D., Borralho Nunes, P., *et al.* (2019). ECCO-ESGAR Guideline for Diagnostic Assessment in IBD

Part 1: Initial diagnosis, monitoring of known IBD, detection of complications. *J. Crohn's Colitis*, **13** (2), 144–164.

Moon, J. Clinical aspects and treatments for pediatric inflammatory bowel disease. *Intestinal Res.*, **17** (1), 17–23.

Moy, M. P., Sauk, J., Gee, M. S. (2016). The role of MR enterography in assessing Crohn's disease activity and treatment response. *Gastroenterol. Res. Practice*, 8168695.

Nardone, O. M., Cannatelli, R., Zardo, D., Ghosh, S., Marietta, I. (2019). Can advanced endoscopic techniques for assessment of mucosal inflammation and healing approximate histology in inflammatory bowel disease? *Ther. Adv. Gastroenterol.*, **12**, 1–17.

Neubauer, H., Pabst, T., Dick, A., MacHann, W., Evangelista, L., Wirth, C., Köstler, H., Hahn, D., Beer, M. (2013). Small-bowel MRI in children and young adults with Crohn disease: Retrospective head-to-head comparison of contrast-enhanced and diffusion-weighted MRI. *Pediatr. Radiol.*, **43** (1), 103–114.

Ouyang, Z., Ouyang, Y., Zhu, M., Lu, Y., Zhang, Z., Shi, J., Li, X., Ren, G. (2014). Diffusion-weighted imaging with fat suppression using short-tau inversion recovery: Clinical utility for diagnosis of breast lesions. *Clin. Radiol.*, **69** (8), e337–e344.

Panes, J., Bouhnik, Y., Reinisch, W., Stoker, J., Taylor, S. A., Baumgart, D. C., Danese, S., Halligan, S., Marincek, B., Matos, C. *et al.* (2013). Imaging techniques for assessment of inflammatory bowel disease: Joint ECCO and ESGAR evidence-based consensus guidelines. *J. Crohn's Colitis*, **7** (7), 556–585.

Quattrocchi, C. C., Van Der Molen, A. J. (2017). Gadolinium retention in the body and brain: Is it time for an international joint research effort? *Radiology*, **282** (1), 12–16.

Ram, R., Sarver, D., Pandey, T., Guidry, C. L., Jambhekar, K. R. (2016). Magnetic resonance enterography: A stepwise interpretation approach and role of imaging in management of adult Crohn's disease. *Ind. J. Radiol. Imag.*, **26** (2), 173–184.

Rimola, J., Rodriguez, S., Garcia-Bosch, O., Ordjs, I., Ayala, E., Aceituno, M., Pellisé, M., Ayuso, C., Ricart, E., Donoso, L., Panés, J. (2009). Magnetic resonance for assessment of disease activity and severity in ileocolonic Crohn's disease. *Gut*, **58** (8), 1113–1120.

Rogler, G., Vavricka, S., Schoepfer, A., Lakatos, P. L. (2013). Mucosal healing and deep remission: What does it mean? *World J. Gastroenterol.*, **19** (43), 7552–7560.

Rozendorn, N., Amitai, M. M., Eliakim, R. A., Kopylov, U., Klang, E. (2018). A review of magnetic resonance enterography-based indices for quantification of Crohn's disease inflammation. *Ther. Adv. Gastroenterol.*, **11**, 1–21.

Scherrer, B., Gholipour, A., Warfield, S. K. (2011). Super-resolution in diffusion-weighted imaging. *Med. Image Comput. Comput Assist. Interv.*, **14** (Pt 2), 124–132.

Sharman, A., Zealley, I. A., Greenhalgh, R., Bassett, P., Taylor, S. A. (2009). MRI of small bowel Crohn's disease: Determining the reproducibility of bowel wall gadolinium enhancement measurements. *Eur. Radiol.*, **19** (8), 1960–1967.

Shi, H. Y., Ng, S. C. (2018). The state of the art on treatment of Crohn's disease. *J. Gastroenterol.*, **53** (9), 989–998.

Stadlbauer, A., Salomonowitz, E., Bernt, R., Haller, J., Gruber, S., Bogner, W., Pinker, K., van der Riet, W. (2009). Diffusion-weighted MR imaging with background body signal suppression (DWIBS) for the diagnosis of malignant and benign breast lesions. *Eur. Radiol.*, **19** (10), 2349–2356.

Steward, M. J., Punwani, S., Proctor, I., Adjei-Gyamfi, Y., Chatterjee, F., Bloom, S., Novelli, M., Halligan, S., Rodriguez-Justo, M., Taylor, S. A. (2012). Non-perforating small bowel Crohn's disease assessed by MRI enterography: Derivation and histopathological validation of an MR-based activity index. *Eur. J. Radiol.*, **81** (9), 2080–2088.

Takahara, T., Imai, Y., Yamashita, T., Yasuda, S., Nasu, S., Van Cauteren, M. (2004). Diffusion weighted whole body imaging with background body signal suppression (DWIBS): Technical improvement using free breathing, STIR and high resolution 3D display. *Radiat. Med.*, **22** (4), 275–282.

Tielbeek, J. A. W., Makanyanga, J. C., Bipat, S., Pendse, D. A., Nio, C. Y., Vos, F. M., Taylor, S. A., Stoker, J. (2013). Grading Crohn disease activity with MRI: Interobserver variability of MRI features, MRI scoring of severity, and correlation with Crohn disease endoscopic index of severity. *Amer. J. Roentgenol.*, **201** (6), 1220–1228.

Triester, S. L., Leighton, J. A., Leontiadis, G. I., Gurudu, S. R., Fleischer, D. E., Hara, A. K., Heigh, R. I., Shiff, A. D., Sharma, V. K. (2006). A meta-analysis of the yield of capsule endoscopy compared to other diagnostic modalities in patients with non-stricturing small bowel Crohn's disease. *Amer. J. Gastroenterol.*, **101** (5), 954–964.

Van Rheenen, P. F., Van De Vijver, E., Fidler, V. (2010). Faecal calprotectin for screening of patients with suspected inflammatory bowel disease: Diagnostic meta-analysis. *Brit. Med. J.*, **341**, 188.

Watson, T., Calder, A., Barber, J. L. (2018). Quantitative bowel apparent diffusion coefficient measurements in children with inflammatory bowel disease are not reproducible. *Clin. Radiol.*, **73** (6), 574–579.

Yu, H., Shen, Y. Q., Tan, F. Q., Zhou, Z. L., Li, Z., Hu, D. Y., Morelli, J. N. (2019). Quantitative diffusion-weighted magnetic resonance enterography in ileal Crohn's disease: A systematic analysis of intra and interobserver reproducibility. *World J. Gastroenterol.*, **25** (27), 3619–3633.

Received 14 January 2020
Accepted in the final form 7 April 2020

KRONA SLIMĪBAS AKTIVITĀTES IZVĒRTĒŠANĀ IZMANTOTO MAGNĒTISKĀS REZONANSES MĒRĪJUMU ATKĀRTOJAMĪBA

Pētījuma mērķis bija izvērtēt ileum distālajā cilpā lokalizētas Kroina slimības aktivitātes noteikšanas parametru atkārtojamību. Pētījumā tika iekļauti 5 pieaugušie (23-57 g.v.) un 12 bērni (11-17 g.v.) ar aktīvu terminālo ileītu. Iekaisuma skartā zarnas siena tika sadalīta 3 cm garos segmentos (n = 32 pieaugušiem, n=46 bērniem), un veikti MaRIA indeksa un Klērmontas indeksa aprēķināšanai nepieciešamie mērījumi: acīmredzamās difūzijas koeficienti (ADC) difūzijas uzsvērto attēlu (DWI) sekvencēs ar selektīvu un neselektīvu tauku nospiešanu, zarnas sieniņu signāla intensitāte (WSI - *Wall Signal intensity*) pirms (WSI-preGd) un pēc (WSI-post-Gd) i/v gadolinijas kontrastvielas ievades, zarnu sieniņas biezums, kā arī noteikta čūlu klātbūtne. Mērījumus, veicot precīzu segmentu salīdzināšanu noteiktās lokalizācijās un definējot noteiktu izpētes apgabala (ROI - *Region of Interest*) lielumu, standartizēja un pēc 2 mēnešiem atkārtoja viens un tas pats radiologs. ADC, WSI-preGd un WSI-postGd, zarnu sieniņu biezuma, mērījumu atkārtojamība viena novērotāja robežās tika izvērtēta ar pāru t-testu. Čūlu klātbūtnes vērtējuma atkārtojamība tika izvērtēta ar Pearson χ^2 testu. Starp 1. un 2. mērījumu netika konstatēta statistiski ticama ADC, WSI-preGd, WSI-postGd un sienas biezuma mērījumu atšķirība. Konstatēta statistiski nozīmīga atšķirība čūlu klātbūtnes izvērtēšanā. Standartizētos apstākļos ADC, WSI-preGd un WSI-postGd atkārtojamība ir augsta. Nepieciešami tālāki pētījumi, lai noteiktu kritērijus čūlu lieluma un izskata definējumam.

Ethical permision

Veidlapa Nr. E-9 (2)

RSU ĒTIKAS KOMITEJAS LĒMUMS NR. 6 / 10.09.2015.

Rīga, Dzirciema iela 16, LV-1007
Tel. 67061596

	Komitejas sastāvs	Kvalifikācija	Nodarbošanās
1.	Profesors Olafs Brūvers	Dr.theo.	teologs
2.	Profesore Vija Sīle	Dr.phil.	filozofs
3.	Asoc.prof. Santa Purviņa	Dr.med.	farmakologs
4.	Asoc.prof. Voldemārs Arnis	Dr.biol.	rehabilitologs
5.	Profesore Regīna Kleina	Dr.med.	patalogs
6.	Profesors Guntars Pupelis	Dr.med.	ķirurgs
7.	Asoc.prof. Viesturs Liguts	Dr.med.	toksikologs
8.	Docente Iveta Jankovska	Dr.med.	
9.	Docents Kristaps Circenis	Dr.med.	

Pieteikuma iesniedzējs: **Ilze Apine**
Medicīnas fakultāte, doktorantūra

Pētījuma nosaukums: „ Magnētiskās rezonanses enterogrāfija iekaisīgo zarnu slimību diagnostikās, izmantojot difūzijas uzsvērto attēlu ar ķermeņa fona signāla supresiju (MR DWIBS) sekvenci"

Iesniegšanas datums: 09.09.2015.

Pētījuma protokols: Izskatot augstāk minētā pētījuma pieteikuma materiālus (protokolu) ir redzams, ka pētījuma mērķis tiek sasniegts veicot pacientu medicīniskās dokumentācijas (medicīnas vēstures) izpēti, iegūto datu apstrādi un analīzi, kā arī izsakot priekšlikumus. Personu (pacientu, dalībnieku) datu aizsardzība un konfidencialitāte tiek nodrošināta. Līdz ar to pieteikums atbilst pētījuma ētikas prasībām.

Izskaidrošanas formulārs: nav nepieciešams

Piekrišana piedalīties pētījumā: nav nepieciešama

Komitejas lēmums: **piekrist** pētījumam

Komitejas priekšsēdētājs Olafs Brūvers Tituls: Dr. miss., prof.

Paraksts

RĪGAS STRADIŅA UNIVERSITĀTES ĒTIKAS KOMITEJA

Ētikas komitejas sēdes datums: 10.09.2015.

Informed consent form

Piekrišanas veidlapa dalībai zinātniski pētnieciskajā darbā „ Magnētiskās rezonanses enterogrāfija iekaisīgo zarnu slimību diagnostikā, izmantojot difūzijas uzsvērto attēlu ar ķermeņa fona signāla supresiju (MR DWIBS) sekvenci"

Mēs uzaicinām Jūs kā pacientu/pacienta vecāku piedalīties zinātniski pētnieciskā projektā. Svarīgi, lai Jūs izlasītu šo pētījuma aprakstu un uzzinātu, kāda būs jūsu loma tajā, ja izlemsiet piedalīties.

Iekaisīgo zarnu slimību pacientu skaits pēdējās desmitgadēs strauji turpina pieaugt. Savu klīnisko izpausmju dēļ zarnu iekaisumi rada diagnostiskas problēmas, pasliktina dzīves kvalitāti un to progresēšanas rezultātā var būt nepieciešama ārstēšana ar dārgiem medikamentiem vai pat ķirurģiska operācija, ko var novērst, slimību diagnosticējot savlaicīgi. Kā iekaisīgas zarnu slimības diagnosticēt agrīnāk? Uz šo jautājumu pētnieki nenogurstoši meklē atbildi.

Izvēles metode zarnu iekaisumu diagnostikā ir endoskopiskā izmeklēšana – videokolonoskopija vai kapsulas endoskopija; šo metožu trūkumi ir iespēja izvērtēt tikai zarnu gļotādu un ierobežotas zarnas daļas, tādēļ, paļaujoties tikai uz endoskopiskajām metodēm, diagnostikas process var būt nepilnīgs. Vienkārša metode iespējama zarnu iekaisuma diagnostikai ir kalprotektīna līmeņa noteikšana izkārnījumos. Kalprotektīns ir olbaltumviela, kas atrodama iekaisuma šūnās, un tā līmeņa pieaugums palīdz atklāt iekaisīgās izmaiņas, tomēr nereti ir sastopamas situācijas, kad kalprotektīna līmenis ir paaugstināts, taču iekaisīgas izmaiņas zarnās netiek konstatētas vai pretēji – pie iekaisīgām izmaiņām kalprotektīna līmenis izkārnījumos nav paaugstināts.

Magnētiskā rezonanse (MR) ir informatīva metode zarnu sieniņu un tām apkārtesošo audu izvērtēšanai visā zarnu trakta garumā. MR izmeklējuma laikā attēli tiek iegūti vairākos režīmos, ko sauc par sekvencēm. Līdz šim lietotās populārākās sekvences nebija piemērotas agrīnai iekaisuma konstatēšanai zarnās, turklāt atbilstoši starptautiskajām vadlīnijām, lai diagnosticētu iekaisumu, izmeklējuma laikā vēnā ir nepieciešams ievadīt kontrastvielu, kas uzkrājas iekaisuma skartajās vietās. Gadolīnija kontrastviela retos gadījumos pacientiem ar nieru funkciju traucējumiem var izraisīt komplikāciju, ko sauc par sistēmisko nefrogēno fibrozi. Tā izpaužas kā ādas un iekšējo orgānu audu sabiezēšanās, kas var pasliktināt šo orgānu darbību. Tomēr pēdējos gados, attīstoties magnētiskās rezonanses tehnoloģijām, ir izstrādātas jaunas sekvences, kas pašreiz šķiet perspektīvas iekaisīgu zarnu slimību diagnostikā un, iespējams, ļaus veikt izmeklējumus bez nepieciešamības vēnā ievadīt kontrastvielu.

Mūsu pētījuma mērķis ir izvērtēt viena no šiem režīmiem, ko sauc par DWIBS, iespējas un piemērotību agrīna zarnu iekaisuma atklāšanā. DWIBS ir sekvence, kas izmeklējuma standarta procedūras ietvaros tiek veikta visiem pacientiem ar aizdomām uz iekaisīgu zarnu slimību.

Kas notiks ar Jums, ja Jūs piedalīsities pētījumā?

Pētījuma ietvaros Jums/Jūsu bērnam tiks veikts standarta magnētiskās rezonanses izmeklējums, izmeklējuma režīmu kopumā ietverot kā DWIBS sekvenci, tā arī sekvenci ar kontrastvielas ievadi vēnā. Šāds izmeklējums tiek veikts pilnīgi visiem pacientiem – arī tādiem, kas nepiedalās pētījumā.

Piekrītot piedalīties šajā pētījumā:

- izjautāsim Jūs par agrākiem kuņģa – zarnu trakta darbības traucējumiem, tagadējo veselības stāvokli,
- izmantosim ar Jūsu un Jūsu ārstējošā ārsta piekrišanu veikto kalprotektīna analīžu un endoskopijas (kolonoskopijas vai kapsulas endoskopijas) izmeklējuma rezultātus.

Pētījuma ietvaros Jums/Jūsu bērnam tiks veikts magnētiskās rezonanses izmeklējums – Jūs/Jūsu bērnu stāvoklī guļus uz vēdera ievietos magnētiskās rezonanses iekārtas tunelī un uz muguras uzliks magnētiskās rezonanses spoli. Tā izmeklējuma laikā izstaros un uztvers radioviļņus, kas ir MR

attēla informācijas avots. Atšķirībā no rentgena stariem, radioviļņi nekaitē audiem un izmeklējums ir veselībai drošs. Izmeklējuma laikā Jūs/Jūsu bērns iekārtā dzirdēs dažādus trokšņus, kas ir normāla parādība.

Riska faktori un neērtības

Jums jāņem vērā, ka MR izmeklējums var ietvert zināmus un nezināmus riska faktorus.

1. **Sagatavošana ar 2,5% mannīta šķīdumu**

Pirms izmeklējuma Jums/Jūsu bērnam būs nepieciešams 30-60 minūšu laikā lēni izdzert 1 l mannīta šķīduma. Tas nepieciešams lai izvērstu zarnu sieniņas padarītu tās labāk izvērtējamas. Mannīta šķīdums var izraisīt caureju, kas parasti gan nav mokoša un pēkšņa.

2. **Buskopāna ievadīšana vēnā**

Lai zarnu sieniņas varētu izvērtēt, tām izmeklējuma laikā ir jābūt nekustīgām. Šim nolūkam neilgi pēc izmeklējuma sākuma vēnā tiek ievadīts medikaments buskopāns, kas apstādina zarnu kustības. Buskopāna darbības ilgums ir apmēram 7 minūtes un izmeklējuma laikā to ievada divas reizes – izmeklējuma sākumā un beigās - pirms kontrastvielas ievades vēnā. Buskopāna iedarbības rezultātā īslaicīgi var pavājināties vai migloties redze, iespējamas urinēšanas grūtības. Šīs reakcijas parasti pāriet pusstundas laikā.

3. **Kontrastvielas ievade vēnā**

Izmeklējuma laikā, neilgi pirms tā beigām, vēnā tiek ievadīta gadolīniju saturoša kontrastviela, kas parasti nevēlamas blakusparādības neizraisa. Tomēr pacientiem ar nieru funkciju traucējumiem kontrastviela retos gadījumos var izraisīt komplikāciju, ko sauc par sistēmisko nefrogēno fibrozi, kas izpaužas kā ādas un iekšējo orgānu audu sabiezēšanās, kas var pasliktināt šo orgānu darbību. Gadolīnija kontrastviela var izraisīt arī alerģiskas reakcijas un sliktu dūšu.

4. **Klaustrofobija**

Magnētiskās rezonanses izmeklējuma laikā Jūs/Jūsu bērns tiks ievietots/-ta MR iekārtas tunelī – gentrijā; tas var izraisīt stresu pacientiem, kuriem bail no noslēgtām telpām. Lai izmeklējuma laikā Jūs/Jūsu bērns justos mierīgāk, nepieciešamības gadījumā izmeklējuma telpā Jums blakus drīkst atrasties cits cilvēks – pacientu pavadoša persona vai medicīniskais personāls. Ja Jums/Jūsu bērnam ir bailes no noslēgtām telpām vai nepārvaramas bailes sajūtat stresa laikā, informējiet MR kabineta personālu.

5. **Stāvoklis guļus uz vēdera**

Izmeklējuma laikā Jūs/Jūsu bērns tiks noguldīts/-ta uz MR iekārtas galda stāvoklī uz vēdera ar rokām uz galvas, kas var radīt diskomforta sajūtu; tomēr izmeklējums, kura ilgums ir līdz 1 stundai, ir labi panesams.

Tā kā pētījumā tiek veikta izpēte, iespējamas blaknes un neērtības, par kurām līdz šim nav zināms.

Ieguvumi

Jūsu/Jūsu bērna dalība pētījumā ārstiem sniegs vairāk informācijas, izvērtējot Jūsu/Jūsu bērna zarnu stāvokli, atklājot iekaisuma skartās vietas vai – pretēji tam – konstatējot, ka iekaisīgi izmainītu vietu nav. Pētījuma rezultātā iespējama iekaisīgas zarnu slimības agrīna atklāšana, precīzāka raksturošana un līdz ar to arī savlaicīga ārstēšana, kas nākotnē var palīdzēt izvairīties no komplikācijām un nepieciešamības veikt ķirurģisku operāciju. Informācija, kas tiks iegūta šajā pētījumā, var palīdzēt nākotnē diagnosticēt iekaisumu zarnās agrīnāk, iespējams, pat neveicot pacientam nepatīkamo kolonoskopijas vai dārgo kapsulas endoskopijas izmeklējumu, kā arī bez nepieciešamības sagatavot pacientu ar mannītu, kā arī ievadīt vēnā kontrastvielu.

Tomēr ir iespējams arī, ka Jūs/Jūsu bērns no šī pētījuma negūs nekādu labumu.

Alternatīva diagnostika

Tā kā pacientiem – pētījuma dalībniekiem tiek veikts standarta MR izmeklējums pilnā apjomā, tad gadījumā, ja Jūs/Jūsu bērns izlemsit nepiedalīties pētījumā, Jums/Jūsu bērnam tiks veikts tieši tāds pats MR izmeklējums kā pētījumā iekļautajiem pacientiem, taču Jūsu/Jūsu bērna dati pētījumā netiks izmantoti.

Ja esat sieviete produktīvā vecumā

Šajā pētījumā nevar piedalīties grūtnieces vai sievietes, kuras baro bērnu bērnu ar krūti.

Ierobežojumi un pienākumi

Ja Jūs/Jūsu bērns piekrītat piedalīties pētījumā, Jums/Jūsu bērnam būs nepieciešams informēt MR kabineta personālu par savu kalprotektīna analīzes rezultātu un endoskopijas izmeklējumu – fibrokolonoskopijas un/vai kapsulas endoskopijas – rezultātiem.

Pirms MR izmeklējuma Jums/Jūsu bērnam jāievēro šādi nosacījumi:

- MR izmeklējuma laikā Jums/Jūsu bērnam jābūt tukšā dūšā, taču ūdeni drīkst lietot bez ierobežojuma, Tā kā Jums/Jūsu bērnam izmeklējums paredzēts pēcpusdienā, izmeklējuma dienas rītā Jūs/Jūsu bērns drīkst paēst vieglas brokastis un pēc tam dzert tikai ūdeni. Ūdens uzņemšana jāpārtrauc 2 stundas pirms norādītā laika, kurā jāierodas slimnīcā.
- pirms izmeklējuma MR kabineta personāls Jums/Jūsu bērnam izsniegs 1-1,5 l mannīta šķīduma, ko nepieciešams izdzert **pa malciņam, lēni**, stundas laikā.
- Izmeklējuma ietvaros Jums/Jūsu bērnam magnētiskās rezonanses skenēšana tiks veikta divas reizes – pirms zarnu sagatavošanas ar mannīta šķīdumu (šis skenēšanas posms ilgs aptuveni 10 minūtes), un pēc skenēšanas ar mannīta šķīdumu – šis skenēšanas posms ilgs līdz 45 minūtēm. Taču, tā kā izmeklējumam nepieciešamā sagatavošanās ar mannīta šķīdumu ir laikietilpīga, kopējais izmeklējumam nepieciešamais laiks, ko Jūs/Jūsu bērns varētu pavadīt slimnīcā, ir līdz 3-4 stundām.

Brīvprātīga piedalīšanās

Piedalīšanās šajā pētījumā ir brīvprātīga. Jums/Jūsu bērnam ir tiesības pārtraukt piedalīšanos pētījumā jebkurā brīdī bez soda sankcijām un nezaudējot ieguvumus, kuri Jums/Jūsu bērnam pienāktos pretējā gadījumā. Ja Jūs/Jūsu bērns pārtrauc savu dalību pētījumā, tas neietekmēs Jūsu/Jūsu bērna medicīniskās aprūpes kvalitāti, nedz arī Jūsu/Jūsu bērna dalību turpmākos pētījumos un izmeklējumos. Bez

tam Jūsu/Jūsu bērna dalību pētījumā var pārtraukt pētījuma ārsts, neņemot vērā Jūsu piekrišanu, ja ir pētījuma plāna pārkāpumi, konstatēti ar pētījumu saistīti veselības traucējumi, kā arī administratīvu iemeslu dēļ.

Atļauja izmantot medicīnisko informāciju

Parakstot šo informētās piekrišanas veidlapu, Jūs piekrītat, ka pētnieki izskata Jūsu/Jūsu bērna medicīnisko dokumentāciju. Jūsu/Jūsu bērna personas dati būs konfidenciāli un Jūs/Jūsu bērna u personas identitāte bez Jūsu atļaujas netiks atklāta nevienā ziņojumā vai publikācijā par šo pētījumu.

Piekrišanas apliecinājums dalībai pētījumā:

Es izlasīju minēto informāciju, pirms parakstīju šo piekrišanas veidlapu, guvu atbildes uz visiem man neskaidrajiem jautājumiem. Mana/mana bērna piedalīšanās pētījumā ir brīvprātīga.

_____	_____	_____
Vārds, uzvārds (drukātiem burtiem)	Paraksts	Datums

Pētniecisko darbu doktorantūras studiju ietvaros veic Bērnu klīniskās universitātes slimnīcas ārste radioloģe Ilze Apine.

Paraksts:_____